Universitat Autònoma de Barcelona

GENOMIC AND FUNCTIONAL GENOMIC ANALYSIS OF FATTY ACID COMPOSITION IN SWINE

Manuel Revilla Sánchez

UNIVERSITAT AUTÒNOMA DE BARCELONA

Departament de Ciència Animal i dels Aliments

Facultat de Veterinària

CENTRE DE RECERCA EN AGRIGENÒMICA

Grup de Recerca de Genòmica Animal

GENOMIC AND FUNCTIONAL GENOMIC ANALYSIS OF FATTY ACID COMPOSITION IN SWINE

Manuel Revilla Sánchez

Doctoral thesis to obtain the PhD degree in Animal Production of the Universitat Autònoma de Barcelona, May 2017

Supervisors

Dr. Josep Maria Folch Albareda

Dr. Maria Ballester Devis

El Dr. Josep Maria Folch Albareda, professor titular del Departament de Ciència Animal i dels Aliments de la Universitat Autònoma de Barcelona, i la Dra. Maria Ballester Devis, investigadora del Departament de Genètica i Millora Animal del Institut de Recerca i Tecnologia Agroalimentàries (IRTA),

fan constar

que el treball de recerca i la redacció de la memòria de la tesi doctoral titulada "*Genomic and functional genomic analysis of fatty acid composition in swine*" han estat realitzats sota la seva direcció per
MANUEL REVILLA SÁNCHEZ i

certifiquen

que aquest treball s'ha dut a terme al Departament de Ciència Animal i del Aliments de la Facultat de Veterinària de la Universitat Autònoma de Barcelona i a la unitat de Genòmica Animal del Centre de Recerca en Agrigenòmica,

considerant

que la memòria resultant es apta per optar al grau de Doctor en Producció Animal per la Universitat Autònoma de Barcelona.

I perqué quedi constància, signen aquest document a Bellaterra,
a 18 de maig de 2017.

Dr. Josep Maria Folch Albareda Dra. Maria Ballester Devis Manuel Revilla Sánchez

This work was funded by the Spanish Ministry of Economy and Competitiveness (grant numbers: AGL2011-29821-C02 and AGL2014-56369-C2). We acknowledge the support of the Spanish Ministry of Economy and Competitiveness for the *Centre of Excellence Severo Ochoa 2016–2019* (SEV-2015-0533) grant awarded to the Centre for Research in Agricultural Genomics.

Manuel Revilla Sánchez was funded by the "Formació i contractació de personal investigador novell (FI-DGR)" fellowship provided by the "Agència de Gestió d'Ajuts Universitaris i de Recerca (AGAUR)" from Generalitat de Catalunya (2014-2017). The pre-doctoral stay at the Institut National de la Recherche Agronomique (INRA), Génétique Animale et Biologie Intégrative (GABI) department was financed by a grant from the Erasmus+ PhD Learning Mobility.

A mis padres y hermana, mi norte,
mi abrigo, mi refugio.
El lugar donde siempre vuelvo,
de donde nunca me he ido.

CONTENT

SUMMARY

Pork is one of the main sources of human-consumed meat and consumer's preference towards high quality meat is increasing. Hence, understanding the molecular mechanisms affecting meat production and quality would help in the selection of these traits. Meat quality is determined largely by its fatty acid (FA) composition and understanding the underlying molecular processes of FA composition is the general objective of this thesis.

We analyzed quantitative trait *loci* (QTL) on porcine chromosome 8 (SCC8) for FA composition in backfat, identifying two trait-associated SNP regions at 93 Mb and 119 Mb. The strongest statistical signals for both regions were observed for palmitoleic acid and, C18:0/C16:0 and C18:1(n-7)/C16:1(n-7) elongation ratios. *MAML3* and *SETD7* genes were analyzed as positional candidate genes in the 93 Mb region. The two novel microsatellites analyzed in the *MAML3* gene, and the *SETD7:c.700G>T* SNP in the *SETD7* gene did not show the strongest signal in this region, discarding these polymorphisms as the causal mutations. Furthermore, in the 119 Mb region, the *ELOVL6:c.-533C>T* SNP showed a strong association with the percentage of palmitic and palmitoleic acids and elongation ratios in backfat. These results for *ELOVL6* gene, support the hypothesis that it has a pleiotropic effect in backfat and muscle for the 119 Mb QTL, and reinforce this gene as a strong candidate for the SSC8 QTL for FA composition.

Moreover, whole genome sequence (WGS) data from Iberian and Landrace pigs were used to identify 1,279 copy number variations (CNVs), merging into 540 swine CNV regions (CNVRs). The impact of four of them in growth and FA composition in intramuscular fat and backfat was studied. Association with carcass length and FA composition in backfat and intramuscular fat was showed for the CNVR112, containing the *GPAT2* gene which catalyse the biosynthesis of triglycerides and glycerophospholipids. These results underline the importance of CNVRs affecting economically important traits in pigs.

Finally, the adipose tissue mRNA expression of 44 candidate genes related with lipid metabolism was analyzed in 115 animals. The expression genome-wide association (eGWAS) identified 193 eSNPs located in 19 expression QTLs (eQTLs). Three out of 19 eQTLs corresponding to *ACSM5*, *FABP4*, and *FADS2* were classified as *cis*-acting eQTLs, whereas the remaining 16 eQTLs had *trans*-regulatory effects. These findings and the polymorphisms evaluated for some of these genes provide new data to further understand the functional mechanisms implicated in the variation of meat quality traits in pigs.

RESUMEN

El cerdo es una de las principales fuentes de carne consumida por el hombre y las preferencias de los consumidores hacia productos de alta calidad han aumentado durante los últimos años. Por lo tanto, conocer los mecanismos moleculares que afectan a la producción y a la calidad de esta carne ayudaría a la selección de estos caracteres. La calidad de la carne está determinada en gran medida por la composición de los ácidos grasos (AG) y la comprensión de los procesos moleculares subyacentes a éstos son el objetivo general de esta tesis.

En este trabajo, se han identificado QTLs en el cromosoma 8 porcino (SSC8) para la composición de AG en grasa dorsal (GD) y se han identificado dos regiones cromosómicas con SNPs asociados, localizadas a 93 y 119 Mb. Las señales estadísticamente más significativas para ambas regiones se observaron para el ácido palmitoleico y los índices C18:0/C16:0 y C18:1(n-7)/C16:1(n-7). Los genes *MAML3* y *SETD7* fueron estudiados como genes candidatos posicionales para la región localizada a 93 Mb. Los dos nuevos microsatélites analizados en el gen *MAML3* y el SNP del gen *SETD7* (*SETD7:c.700G>T*) no mostraron las asociaciones más significativas en esta región, descartando estos polimorfismos como las mutaciones causales. Además, en la región localizada a 119 Mb, el SNP *ELOVL6:c.-533C>T* mostró la asociación más significativa con el porcentaje de los ácidos palmítico y palmitoleico y los índices de elongación en GD. Los resultados obtenidos para el gen *ELOVL6,* gen candidato posicional del QTL localizado a 119 Mb refuerzan la hipótesis de su efecto pleiotrópico sobre la composición de AG en GD y en músculo, y su papel en la determinación del QTL del SSC8 para el perfil de AG.

Por otra parte, se utilizaron datos del genoma completo de cerdos ibéricos y landrace para identificar 1.279 variaciones en el número de copias (CNV), las cuales se fusionaron en 540 regiones de CNVs (CNVRs). El impacto de cuatro de ellas fue estudiado para caracteres de crecimiento y composición de AG. Se encontró asociación con la longitud de la canal y la composición de AG en grasa intramuscular y GD para el CNVR112. Este CNVR contiene el gen *GPAT2* que cataliza la biosíntesis de triglicéridos y glicerofosfolípidos. Los resultados obtenidos subrayan la importancia de los CNVRs en la determinación de caracteres económicamente importantes en el cerdo.

Finalmente, se analizó la expresión de 44 genes candidatos relacionados con el metabolismo lipídico en 115 animales. El estudio de asociación genómico con los datos de expresión (eGWAS) identificó 193 eSNPs localizados en 19 eQTLs. Tres de los eQTLs correspondientes a los genes *ACSM5*, *FABP4* y *FADS2* se clasificaron como *cis*-eQTLs; mientras que los 16 eQTLs restantes mostraron efectos reguladores en *trans*. Estos hallazgos, junto con los polimorfismos evaluados para alguno de estos genes, mejoran nuestro conocimiento sobre los mecanismos funcionales implicados en la variación de los caracteres relacionados con la calidad de la carne porcina.

LIST OF TABLES

GENERAL INTRODUCTION

PAPER I

PAPER II

PAPER III

GENERAL DISCUSSION

ANNEXES: Paper I

ANNEXES: Paper II

ANNEXES: Paper III

LIST OF FIGURES

GENERAL INTRODUCTION

PAPER I

PAPER II

PAPER III

GENERAL DISCUSSION

ANNEXES: Paper I

ANNEXES: Paper II

ANNEXES: Paper III

LIST OF PUBLICATIONS

The present thesis is based on the work contained in the list of articles below:

- Paper I. **Revilla M**, Ramayo-Caldas Y, Castelló A, Corominas J, Puig-Oliveras A, Ibáñez-Escriche N, Muñoz M, Ballester M, Folch JM (2014). New insight into the SSC8 genetic determination of fatty acid composition in pigs. *Genetics Selection Evolution* 46:28. http://doi.org/10.1186/1297-9686-46-28

- Paper II. **Revilla M**, Puig-Oliveras A, Castelló A, Crespo-Piazuelo D, Paludo E, Fernández AI, Ballester M, Folch JM (2017). A global analysis of CNVs in swine using whole genome sequence data and association analysis with fatty acid composition and growth traits. *PLoS One* 12(5):e0177014. http://doi.org/10.1371/journal.pone.0177014

- Paper III. **Revilla M**, Ballester M, Puig-Oliveras A, Castelló A, Fernández AI, Folch JM. Expression analysis in adipose tissue of candidate genes for fatty acid composition and identification of eGWAS regions. (*Manuscript in preparation*)

RELATED PUBLICATIONS BY THE AUTHOR

(Not included in the thesis)

- Ballester M, Puig-Oliveras A, Castelló A, **Revilla M**, Fernández AI, Folch JM (2017). Analysis of *FABP4* and *FABP5* gene expression affecting pig fatness. *Animal Genetics* (*submitted*).

- Ballester M, Ramayo-Caldas Y, **Revilla M**, Corominas J, Castelló A, Estellé J, Fernández AI, Folch JM (2017). Integration of liver gene co-expression networks and eGWAs analyses highlighted candidate regulators implicated in lipid metabolism in pigs. *Scientific Reports* 7:46539. http://doi.org/10.1038/srep46539

- Ballester M, **Revilla M**, Puig-Oliveras A, Marchesi JA, Castelló A, Corominas J, Fernández AI, Folch JM (2016). Analysis of the porcine *APOA2* gene expression in liver, polymorphism identification and association with fatty acid composition traits. *Animal Genetics* 47(5):552-9. http://doi.org/10.1111/age.12462

- Puig-Oliveras A, **Revilla M**, Castelló A, Fernández AI, Folch JM, Ballester M (2016). Expression-based GWAS identifies variants, gene interactions and key regulators affecting intramuscular fatty acid content and composition in porcine meat. *Scientific Reports* 6:31803. http://doi.org/10.1038/srep31803

- Corominas J, Marchesi JA, Puig-Oliveras A, **Revilla M**, Estellé J, Alves E, Folch JM, Ballester M (2015). Epigenetic regulation of the *ELOVL6* gene is associated with a major QTL effect on fatty acid composition in pigs. *Genetics Selection Evolution* 47:20. http://doi.org/10.1186/s12711-015-0111-y

- Puig-Oliveras A, Ballester M, Corominas J, **Revilla M**, Estellé J, Fernández AI, Ramayo-Caldas Y, Folch JM (2014). A co-association network analysis of the genetic determination of pig conformation, growth and fatness. *PLoS One* 9(12):e114862. http://doi.org/10.1371/journal.pone.0114862

ABBREVIATIONS

ACACA	Acetyl-CoA carboxylase 1
aCGH	Array comparative genome hybridization
ACSM5	acyl-CoA synthetase medium-chain family member 5
AGPAT	1-acylglycerol-3-phospate acyltransferase
ANK2	Ankyrin 2
AWM	Association weight matrix
BAC	Bacterial artificial chromosome
BC1_DU	25% Iberian x 75% Duroc backcross
BC1_LD	25% Iberian x 75% Landrace backcross
BC1_PI	25% Iberian x 75% Pietrain backcross
C16:0	Palmitic acid
C16:1(n-7)	Palmitoleic acid
C18:0	Stearic acid
C18:1(n-7)	Vaccenic acid
C18:1(n-9)	Oleic acid
CNV	Copy number variation
CNVRs	CNV regions
CRISPR	Clustered regulatory interspaced short palindromic repeats
CRISPR/Cas	CRISPR in combination with Cas9 protein
DGATs	Diacylglycerol acyltransferases
eGWAS	Expression genome-wide association study
ELF1	E74 like ETS transcription factor 1
ELOVL	Elongase enzymes
EP300	E1A binding protein p300
eQTLs	Expression quantitative trait *loci*
eSNP	Expression-associated SNP
ESR1	Estrogen receptor 1
EU	European Union
FA	Fatty acid
FABP2	Fatty acid binding protein 2
FABP4	Fatty acid binding protein 4
FADS1	Fatty acid desaturase 1
FADS2	Fatty acid desaturase 2
FAS	Fatty acid synthase
FHL2	Four and a half LIM domains 2
GLUT4	Glucose transporter 4
GPAT	Glycerol-3-phosphate acyltransferase
GWAS	Genome-wide association studies
HTO	High-throughput omics
IBMAP	Iberian x Landrace animal material
IFC	Integrated fluidic circuits
IMF	Intramuscular fat
indels	Insertions and deletions
KIT	KIT proto-oncogene receptor tyrosine kinase

LD	Linkage disequilibrium
LDLA	Linkage disequilibrium and linkage analysis
LPL	Lipoprotein lipase
MAML3	Mastermind-like 3
MAS	Marker-assisted selection
MTTP	Microsomal triglyceride transfer protein
MUFA	Monounsaturated fatty acids
NCOA2	Nuclear receptor coactivator 2
NGS	Next-generation sequencing
NR3C1	Nuclear receptor subfamily 3 group C member 1
PA	Phosphatidic acid
PIGMaP	Pig gene mapping project
PPAR	Peroxisome proliferator activated receptor
PPARG	Peroxisome proliferator activated receptor gamma
PRDM16	PR/SET domain 16
PRKAG3	Protein kinase AMP-activated non-catalytic subunit gamma 3
PUFA	Polyunsaturated fatty acids
qPCR	Real-time quantitative PCR
QTL	Quantitative trait *loci*
RNA-Seq	RNA sequencing
RYR1	Ryanodine receptor 1
SCD	Stearoyl-CoA desaturase
SETD7	SET domain containing lysine methyltransferase 7
SFA	Saturated fatty acids
SGSC	Swine genome sequencing consortium
SLC27A4	Solute carrier family 27 member 4
SNP	Single nucleotide polymorphism
SREBF	Sterol regulatory element binding transcription factor
SSC	*Sus scrofa* chromosome
TAS	Trait-associated SNPs
TBCK	TBC1 domain containing kinase
VLDLs	Very low-density lipoproteins
WGS	Whole genome sequence

General Introduction

Chapter 1

1.1. Current situation of porcine meat production

Domesticated animal species such as cattle, pigs and poultry are the most common sources of meat, being the main sources of animal protein for humans. Meat derived from pigs is known as pork, and is the most widely eaten meat in the world, accounting for over 36% of the world meat intake [FAO 2014; http://www.fao.org/; accessed January 2017]. The quality of animals slaughtered has a big effect on the standard of meat produced. The most important factors are feeding, age, genetics and health status. Efforts have been made to improve meat production and quality by breeding, or to combine the key characteristics by means of crossbreeding. The improvements in the pig breeding technologies have facilitated the extension of pork production worldwide, reaching approximately a billion animals produced in 2014 (Figure 1.1). Asia is so far the major producer worldwide, accounting for 57.7% of the pork production, followed by Europe (23.8%) and America (16.8%) [FAO 2014; http://www.fao.org/; accessed January 2017]. In Europe, the two main producers are Spain and Germany (Figure 1.2); Spain produced 19.10% of the EU-28's (European Union) pork production in 2015, while Germany produced 18.59% [Eurostat 2015; http://ec.europa.eu/eurostat/; accessed January 2017].

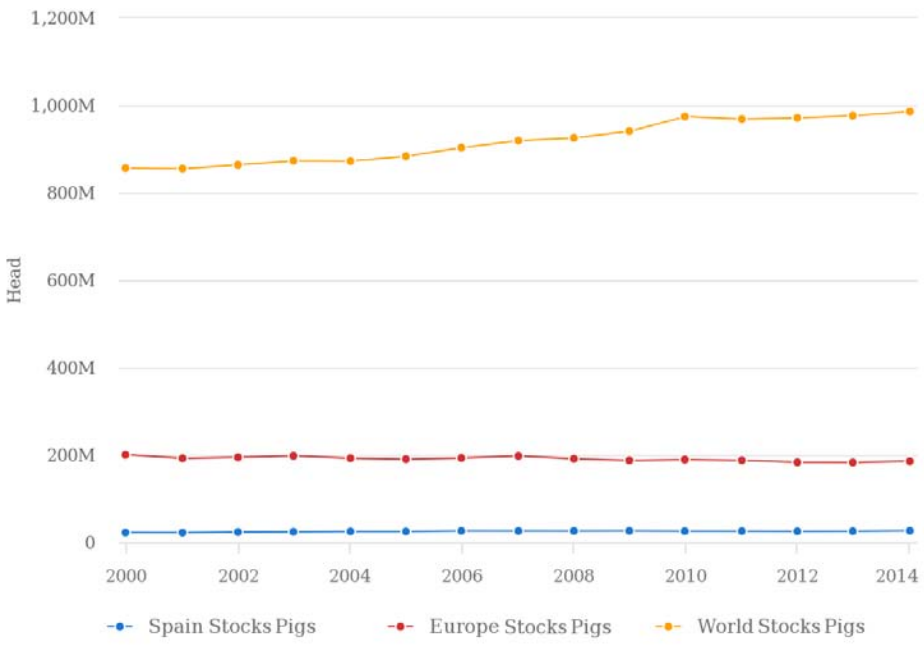

Figure 1.1. Pig heads production in the World, Europe and Spain from 2000 to 2014 [FAO 2014; http://www.fao.org/; accessed January 2017].

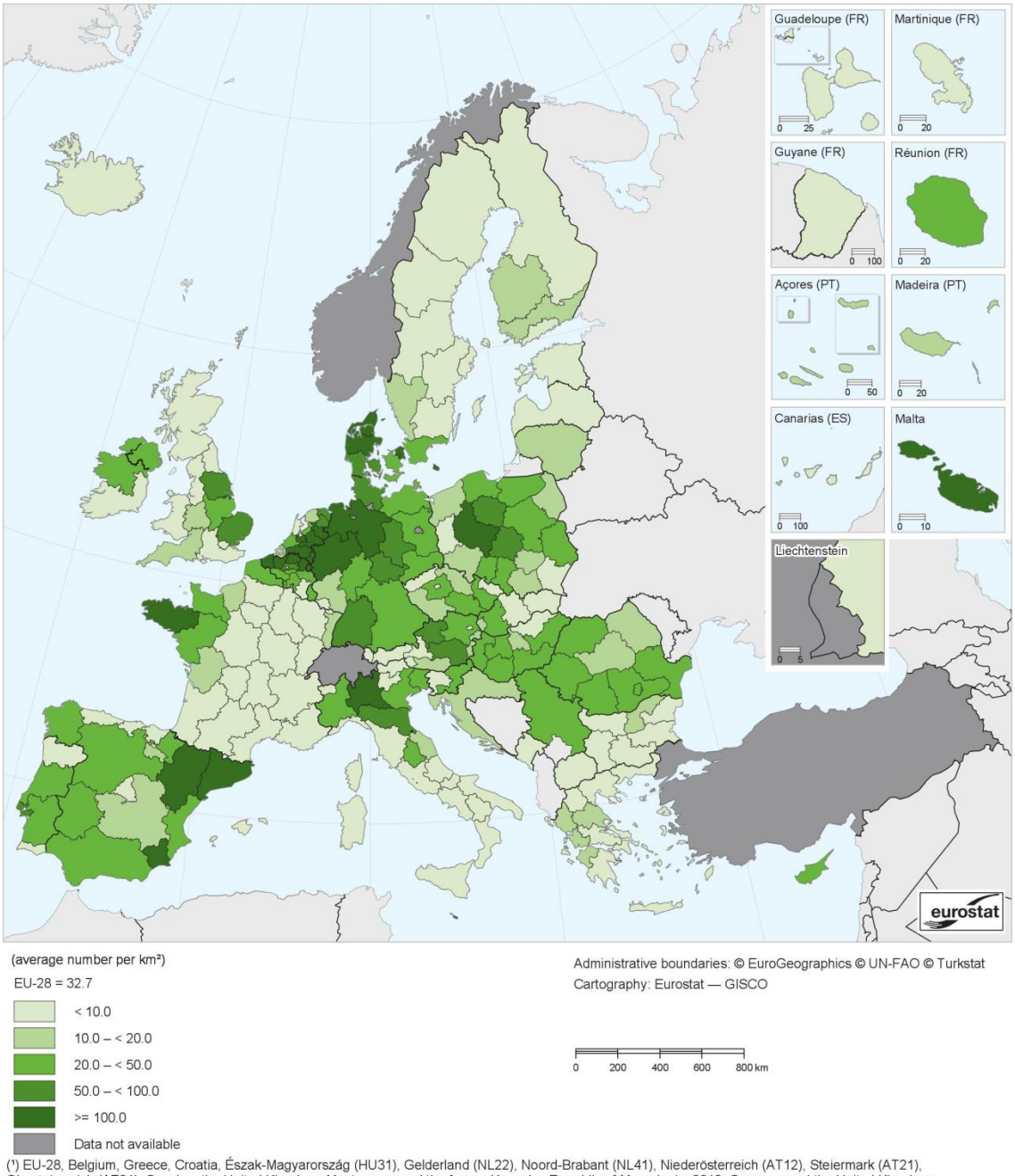

Figure 1.2. Average number of pigs per km² produced by European regions in 2015 [Eurostat 2015; http://ec.europa.eu/eurostat/; accessed January 2017].

1.2. Main traits of interest in porcine meat production

Pig breeding programmes have selected measurable, attainable and realistic goals to improve breeds according to the needs of producers, processors and consumers. With the main objective to satisfy demand of consumers, these pig breeding goals have been in permanent revision over the years (Dekkers *et al.*, 2011). Traditionally, swine breeding

programs have focused on the genetic improvement of economically important production traits, such as growth rate, meat percentage, feed efficiency, and piglet production (Table 1.1). However, the strong selection process focused on increasing the percentage of lean meat in carcass, had led to a dramatic reduction of intramuscular fat (IMF) content in some breeds, negatively affecting meat quality, and therefore, leading to detrimental changes in taste and tenderness of the meat produced (Wood & Whittemore 2007). Many factors (Table 1.1) affect meat quality and its definition, however it is normally defined by the compositional quality (lean to fat ratio) and the palatability factors such as visual appearance, smell, firmness, juiciness, tenderness, and flavor. From the technological point of view, aspects such as pH, water-holding capacity, cooking loss and firmness have a clear importance (Bidner *et al.*, 2004; Boler *et al.*, 2010; Ciobanu *et al.*, 2011). Furthermore, the sensorial aspects such as texture, flavor, juiciness, color and marbling are determinant for consumer meat acceptance (Font-i-Furnols & Guerrero 2014). In addition, this meat quality is also determined by nutritional, and safety and hygienic factors. One aspect, which is common for all the definitions received for this trait, is that consumers play a key role in the assessment of quality since their personal preferences drive the market demands. As a consequence, during the last decade the genetics of pig meat quality has been included as part of pig selection programmes to satisfy the increasing consumer demand for high quality meat.

Usually, heritabilities of meat quality traits show great variation (Ciobanu *et al.*, 2011) and the genetic background of each population have a great impact on this variation. In general, the heritability related to meat quality index range between 0.11 to 0.33 (Ciobanu *et al.*, 2011). Heritabilities for technological factors of meat quality, such as pH (h^2= 0.04-0.41), water-holding capacity (h^2= 0.01-0.43) and cooking loss (h^2= 0.00-0.51), and sensorial aspects of meat quality traits such as, flavor (h^2= 0.01-0.16), juiciness (h^2= 0.00-0.28), and color (h^2= 0.15-0.57) varied from low to medium values (Ciobanu *et al.*, 2011).

Table 1.1. Schematic representation of the main traits of interest in the porcine industry.

Growth	Average daily gain Age at slaughter Feed efficiency	
Carcass quality	Loin muscle area Primary cut weights	
Fatness	Backfat thickness Abdominal fat	
Fertility	Litter size Piglet weight and viability	
Disease resistance	Immune capacity	
Behaviour	Stress susceptibility Welfare	
Meat quality traits	Technological factors	pH Water-holding capacity Cooking loss Firmness
	Sensorial aspects	Texture Flavor Juiciness Color Marbling
	Nutritional factors	Fat content Lipid composition Digestibility
	Safety & Hygiene factors	

1.2.1. Intramuscular fat content

Quality characteristics that play an integral role in consumer acceptance, such as IMF, have decreased as breeders have intensely selected for increased leanness (Barton-Gade 1990; Cameron 1990). IMF, can be defined as the amount of fat within muscles (Hocquette *et al.*, 2010), and differs from intermuscular fat which is the fat located between muscles.

Muscle lipids are composed of polar lipids (mainly phospholipids) located in the cell membrane and neutral lipids (mostly triacylglycerol) located in the adipocytes along the muscle fibers and in the interfascicular area (De Smet *et al.*, 2004). The content of phospholipids in the muscle varies between 0.2 and 1%, and it is relatively independent of the total fat content. However, the triacylglycerol content varies from 0.2% to more than 5%, and is closely related to the total fat content (Fernandez *et al.*, 1999a).

The role of IMF is of particular interest in pigs because of its importance in eating quality and overall consumer acceptance (Goodwin & Burroughs 1995). It has been demonstrated

that IMF positively influences flavor, juiciness, tenderness and/or firmness. In this sense, when IMF levels increase above approximately 2.5% in fresh pork meat, the flavor and juiciness are significantly enhanced (Hodgson *et al.*, 1991; Fernandez *et al.*, 1999b; Huff-Lonergan *et al.*, 2002). On the other hand, IMF has only a small effect on the perceived pork tenderness and texture (Lonergan *et al.*, 2007).

The quantity of IMF can be accurately measured on muscle samples by various analytical methods (e.g. Folch *et al.*, 1957) or estimated *in vivo* by real-time ultrasound (e.g. Hassen *et al.*, 2001; Newcom *et al.*, 2002) and nuclear magnetic resonance (e.g. García-Olmo *et al.*, 2012) techniques. The ideal concentration of IMF has been estimated to be between 2 and 3% (Bejerholm & Barton-Gade 1986; DeVol *et al.*, 1988; Barton-Gade 1990), and this trait has become important in the genetic improvement of pork quality. Different studies have described a moderate-high heritability ranging from 0.39 to 0.53 regarding the IMF content (Cameron *et al.*, 1990; Suzuki *et al.*, 2005).

1.2.2. Fatty acid composition

Selection for increased percent lean meat in pigs has also produced a decrease in adipose quality and overall firmness of fat. Adipose tissue, body fat, or simple fat is composed of adipocytes embedded in a matrix of connective tissue with a highly developed vascular system and is one of the main energy reserves in animals. The quality of this fat is determined by its fatty acid (FA) composition (Gatlin *et al.*, 2003; Wood *et al.*, 2004). It should be noted that FA composition differs between various tissues, including intra- and intermuscular, as well as subcutaneous adipose tissue. Another factor with a significant effect on fatness is sex (Nürnberg *et al.*, 1998), as well as differences in maturity, age and/or live weight at slaughter. In addition, the genetic variability observed for this trait consists of differences between breeds, differences due to the crossing of these breeds, and differences between animals within breeds (De Smet *et al.*, 2004).

FAs influence technological and organoleptic characteristics of meat quality in several aspects. The melting point of specific FAs differs widely; therefore, FA composition directly affects the firmness and/or softness of adipose tissue (Pitchford *et al.*, 2002). Moreover, the nutritional profile of meat fat has been extensively studied because it is a major source of dietary lipids, and has an important influence not only in meat quality but also on human health.

FAs are made up of carbon and hydrogen molecules. There are three types: saturated fatty acids (SFA), monounsaturated fatty acids (MUFA) and polyunsaturated fatty acids (PUFA). The basic difference between each of these is the number of carbon atoms with or without two hydrogen atoms bonded to them. In a SFA, each carbon atom has bonded with two hydrogen atoms. This saturation makes the FA very stable, which means it can withstand more heat. However, SFAs are associated with human diseases like various cancers, obesity and especially coronary heart diseases (Chizzolini *et al.*, 1999).

In a MUFA, one pair of carbon atoms forms a double bond with each other that replaces the bond each would have with one hydrogen atom. This means that MUFA are less stable than SFA, and contribute to a better taste and lower oxidation rate of meat.

A PUFA has two or more carbon pairs that have bonded together rather than with a hydrogen atom. This means that PUFAs are quite unstable. Furthermore, PUFA, mainly n-3, have been considered beneficial for human health due to their effect in the reduction of total cholesterol concentration and the modulation of immune functions and inflammatory processes (Rudel *et al.* 1995; Poudyal *et al.*, 2011).

It has been described that MUFA and SFA increase in subcutaneous fat and muscle with age, while the content of PUFA decrease (Bosch *et al.*, 2012). Additionally, the concentrations of MUFA, SFA and PUFA differ among breeds and within fat (Cameron & Enser 1991). Raj *et al.* (2010) also described a higher concentration of PUFA/SFA ratio in backfat in comparison to IMF.

Heritabilities for FA composition have been estimated by several studies using different genetic backgrounds, ranging from 0.15 to 0.57 (Ntawubizi *et al.*, 2010; Casellas *et al.*, 2010).

1.3. Fatty acid metabolism

FAs are essential for life as they constitute a major source of energy and are structural components of membranes. In addition, FAs are crucial in key biological functions, such as regulation of lipid metabolism, cell division and inflammation. They are included in a broad variety of compounds including oils, waxes, sterols, glycerophospholipids, sphingolipids and triacylglycerols. A large percentage of lipids are synthesized from dietary glucose (Nafikov & Beitz 2007). The main tissues for fat synthesis in animals are liver, adipose tissue and muscle (Duran-Montgé *et al.*, 2009). The adipose tissue is a highly active

metabolic and endocrine organ that acts as a fat storage depot, and is essential for circulating free FA and regulation of lipid metabolism (Xing *et al.*, 2016).

The transformations that lipids undergo are produced mainly by two reactions, lipolysis or β-oxidation and lipogenesis or *de novo* FA synthesis.

Lipolysis is the enzymatic process by which triacylglycerol, stored in cellular lipid droplets, is hydrolytically cleaved to generate glycerol and free FAs. The free FAs can be subsequently used as energy substrates, essential precursors for lipid and membrane synthesis, or mediators in cell signaling processes. The complete oxidation of free FAs to generate ATP occurs in the mitochondria. It involves the sequential degradation of FAs to multiple units of acetyl-CoA which can then be completely oxidized.

Lipogenesis is the process by which glycerol is esterified with free FAs to form triglycerides and the main organ for *de novo* fat synthesis is the adipose tissue (O'Hea & Leveille 1969; Bergen & Mersmann 2005). Dietary fat (triglycerides), when ingested with food, is absorbed by the gut and triglycerides are transported in the form of plasma-lipoproteins. Lipids are released from their carrier lipoproteins through the local activity of lipoprotein lipase (LPL) and subsequently split into their constituent FAs and glycerol. These are taken up by adipose tissue where the triglycerides are resynthesized and stored in cytoplasmic lipid droplets. Lipogenesis also includes the anabolic process by which triglycerides are formed in the liver from excess glucose. Here FAs of varying length are synthesised by the sequential addition of two-carbon units derived from acetyl-CoA. FAs generated by lipogenesis in the liver, are subsequently esterified with glycerol to form triglycerides that are packaged, in very low-density lipoproteins (VLDLs) and secreted into the circulation. Once in the circulation, VLDLs come in contact with LPL in the capillary beds in the body (adipose, cardiac, and skeletal muscle) where LPL releases the triglycerides for intracellular storage or energy production. The predominant products of *de novo* lipogenesis are palmitic (C16:0), stearic (C18:0), oleic (C18:1(n-9)) and palmitoleic (C16:1(n-7)) acids, which are formed through procedures of elongation and/or desaturation.

Dietary FAs require the presence of enzymes, transporters, and chaperone proteins to facilitate their absorption, transport, and uptake by cells in the body (Figure 1.3). Normally, mammals obtain SFA from either the diet or endogenous synthesis from glucose or amino acids (Volpe & Vagelos 1976) and MUFA can be converted from SFA by the stearoyl-CoA desaturase (*SCD*) gene (Paton & Ntambi 2009) or can also be obtained from the diet. On

the other hand, PUFA are mainly acquired through the diet (Leonard *et al.*, 2004). The process of storing energy from carbohydrate-derived carbon precursors occurs in the cytosol of cells and is performed by a series of enzymes beginning with the production of acetyl-CoA by ATP citrate lyase. Acetyl-CoA is then metabolized by the rate-limiting enzyme of the FA synthesis pathway, acetyl-CoA carboxylase 1 (ACACA) to produce the limiting reagent, malonyl-CoA (Figure 1.3). The multifunctional enzyme, fatty acid synthase (FAS) then produces saturated, short (C14:0) to medium (C18:0) chain FAs by sequentially adding malonyl-CoA to the growing acyl chain through a series of biochemical reactions, with palmitic acid (C16:0) representing about 80-90% of its total product (Jayakumar *et al.*, 1995; Kuhajda *et al.*, 1994). Various elongation and desaturase enzymes can further modify FAs. These *de novo* synthesized FAs can then be esterified and converted into triglyceride molecules for storage.

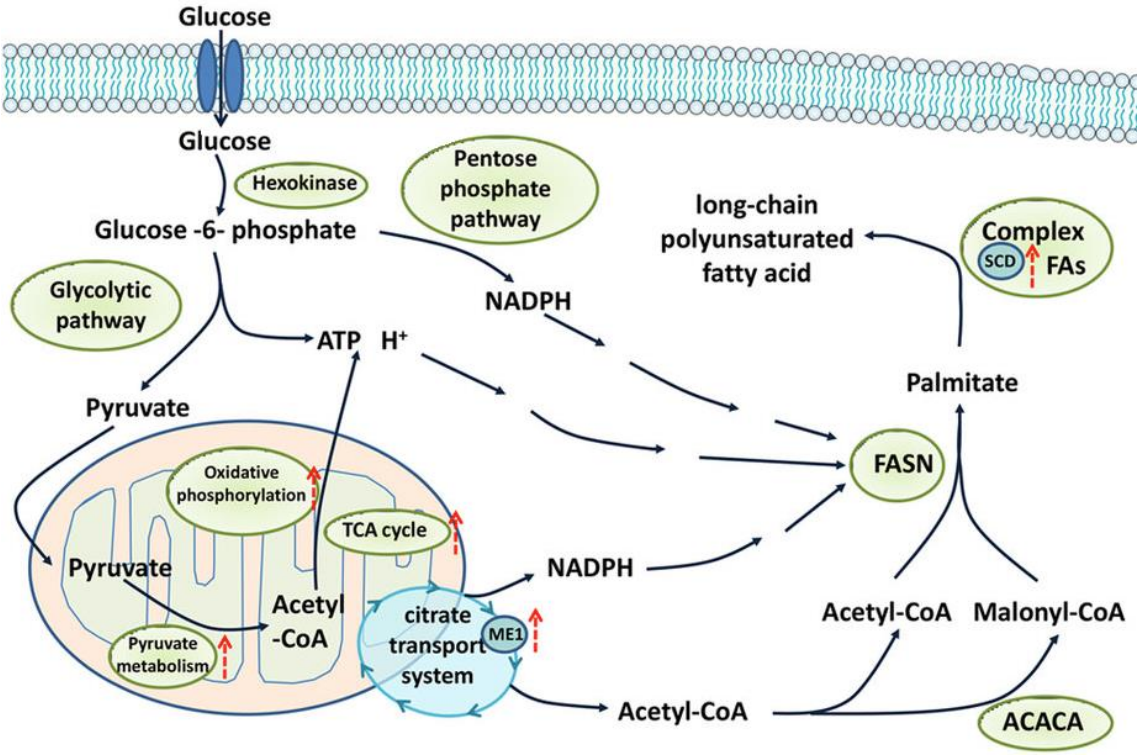

Figure 1.3. Schematic pathway in *de novo* fatty acid synthesis (Xing *et al.*, 2016).

The metabolism of *de novo* and dietary FAs can differ greatly, but they may also compete as substrates for the same elongation and desaturation enzymes. Mammals possess seven known elongase enzymes (ELOVL1-7) with various substrate specificities that mediate the elongation of FAs through the addition of malonyl-CoA (Guillou *et al.*, 2010).

Introduction of double bonds into FAs is mediated by the activity of the desaturase enzymes, SCD (also known as, delta 9 desaturase), fatty acid desaturase 1 (FADS1), and fatty acid desaturase 2 (FADS2), each of which insert a double bond at specific locations in the FA carbon chain. SCD is specific for the conversion of SFA to MUFA, while FADS1 (delta 5 desaturase) and FADS2 (delta 6 desaturase) are specific to PUFA (Guillou *et al.*, 2010); hence, SCD can metabolize both *de novo* and dietary FAs, while dietary intake influences the activities of desaturase enzymes. Enzymes known to be strictly responsible for *de novo* FA metabolism include FAS, ELOVL1, ELOVL3, and ELOVL6, while enzymes that metabolize only dietary FAs include ELOVL2, ELOVL5, FADS1, and FADS2.

Furthermore, several transcription factors are known to play an essential role in the regulation of the expression of genes involved in FA metabolism. These transcription factors, according to the stimulus (i.e. nutrients, hormones, etc.), have the ability to bind on target-sequences of the genes and promote or supress transcription (Laliotis *et al.*, 2010). Two of the transcription factors that have been reported to modulate and control the transcription of genes involved in lipogenesis are: sterol regulatory element binding transcription factor (SREBF) and peroxisome proliferator activated receptor (PPAR).

SREBFs are considered one of the most important transcription factors that can mediate the expression of lipogenic genes, and can be divided into two transcription factors, SREBF1 and SREBF2. The regulation of lipid homeostasis is directly regulated by SREBF1 by activating lipogenic genes, which are involved in the production of palmitate (Jump 2004). On the other hand, SREBF2 is associated with genes involved in cholesterol metabolism.

PPARs are part of the adipocyte differentiation program regulating adipogenesis (Rosen *et al.*, 2000) and are considered as monitors of the oxidized lipids.

Furthermore, members of the nuclear receptor family such as HNF4, RAR, ROR, and RXR have been described to be involved in the transcriptional regulation of lipogenic genes (Chawla *et al.*, 2001; Tarling *et al.*, 2004).

In addition, lipid metabolism is under the regulation of hormones (peptides or lipids), cofactors and nuclear receptors that are tissue specific. In order to manipulate meat FA composition, we have to understand the genetic architecture involved in this biological process.

1.4. Pig genomics

Classical genetic evaluation approaches have had a huge impact on the improvement of the efficiency of pork production and on carcass quality. Genetic progress can be made by measurement the interest trait, if this is heritable, on the selection candidates.

Genomics can help in the selection of relevant traits by increasing the accuracy of the prediction of the breeding value and by obtaining earlier evaluations. This is particularly valuable for sow prolificacy traits, which tend to have low heritability and which are only expressed in the mature females. Genomics will be also valuable for traits which can not be evaluated in breeding animals, like meat quality traits.

The pig (*Sus scrofa*) was the first livestock species whose scientific community decided to map its genome in the early 1990s with the EU-funded Pig Gene Mapping Project (PIGMaP; Haley *et al.*, 1990). This PIGMaP project data allowed the implementation of linkage analysis for the identification of quantitative trait *loci* (QTLs) (Andersson *et al.*, 1994). Years later, in September 2003, the Swine Genome Sequencing Consortium (SGSC) was established to sequence the pig genome (Schook *et al.*, 2005), following the successful generation of genetic (Groenen *et al.*, 2011) and physical (Raudsepp *et al.*, 2011) maps of the pig. The strategy by the SGSC was based on hierarchical shotgun Sanger sequencing of bacterial artificial chromosome (BAC) clones representing a minimal tile path across the genome (Humphray *et al.*, 2007), which was later supplemented with *Illumina* next-generation sequencing (NGS) data (Archibald *et al.*, 2010). These efforts resulted in the assembly and publication of a draft reference genome sequence of *Sus scrofa* in 2012 (Groenen *et al.*, 2012). This assembly, which is in constant improvement, came from a female domestic Duroc pig and comprised 2.60 Gb assigned to chromosomes and more than 212 Mb in unplaced scaffolds. The most recent upgraded version of the pig genome sequence is called *Sscrofa10.2*, and the last upgraded annotation available for this sequence in the *Ensembl* database is the release 87 [Ensembl; http://www.ensembl.org, accessed January 2017], which comprises a total of 21,640 genes encoding 30,585 transcripts, 3,124 non-coding genes and 568 pseudogenes. Moreover, there is information about more than 60 million short variants, including single nucleotide polymorphisms (SNPs), insertions and deletions (indels), and 85 structural variants.

Apart from the availability of the pig genome, another important genomic tool was the development of a first commercial SNP panel for high-throughput genotyping (Ramos *et*

al., 2009). This SNP panel was commercially available from *Illumina* (*PorcineSNP60 BeadChip*; San Diego, CA) and contains about 60K SNPs that cover all autosomal and X chromosomes (Ramos *et al.*, 2009). In addition to this SNP panel, low-density SNP panels have been developed in several studies with the purpose of reducing genotyping costs. A commercial low-density SNP chip was developed by *GeneSeek/Neogen* (Lincoln, NE) to face the need of an economic SNP chip to the market (*GeneSeek/Neogen GPP-Porcine LD Illumina Bead Chip panel*). Recently, *GeneSeek/Neogen* also prepared a higher density SNP panel including about 70K SNPs. A high-density SNP panel (Groenen 2015), containing ~650,000 SNPs and including a large percentage of the SNPs present in the *Illumina PorcineSNP60 v2 BeadChip*, has been recently released by *Affymetrix* (Santa Clara, CA) (Table 1.2).

Table 1.2. Commercially available SNP genotyping panels for the pig (adapted from Samorè & Fontanesi 2016).

Chip name	SNPs	Company	Technology
PorcineSNP60 v2 BeadChip	64,232	*Illumina*	Illumina Infinium chemistry
GeneSeek® Genomic Profiler for Porcine LD (GGP-Porcine LD)	10,241	*GeneSeek/Neogen*	Illumina Infinium chemistry
GeneSeek® Genomic Profiler for Porcine HD (GGP-Porcine HD)	70,231	*GeneSeek/Neogen*	Illumina Infinium chemistry
Axiom® Porcine Genotyping Array	658,692	*Affymetrix*	Axiom assay

The SNP chips have improved the ability to detect QTL for different relevant traits for pig production. Furthermore, the high-density SNP panels can provide significant insights into the molecular basis of phenotypic variation of production traits and assist breeders in pig selection (Plastow *et al.*, 2005) and are the base of genomic selection.

Recent technological advances have created new opportunities to study complex traits in pigs considering a more holistic view of the biological system under study. Instead of focusing only on the discovery of a single gene or DNA markers that co-segregate with a trait, researchers focused their interests in the detection of large-scale molecular gene-expression profiles, gene clusters, and networks, that are characteristics of a biological process or of a specific phenotype. Thanks to the development of high-throughput techniques (Figure 1.4) such as genomic (high-density genotyping and DNA sequencing), epigenomic (DNA methylation), transcriptomic (microaarays, RNA sequencing 'RNA-Seq', and high-throughput real-time quantitative PCR 'qPCR' microfluidic systems), proteomic (tandem mass spectophotometry), and metabolome approaches (gas chromatography and

high-performance liquid chromatography-mass spectrophotometry), it is now possible to add functional genomics to the range of approaches available for understanding the molecular basis of pork meat quality (Schena *et al.*, 1995; Bendixen *et al.*, 2005; Tuggle *et al.*, 2006; Weis 2005).

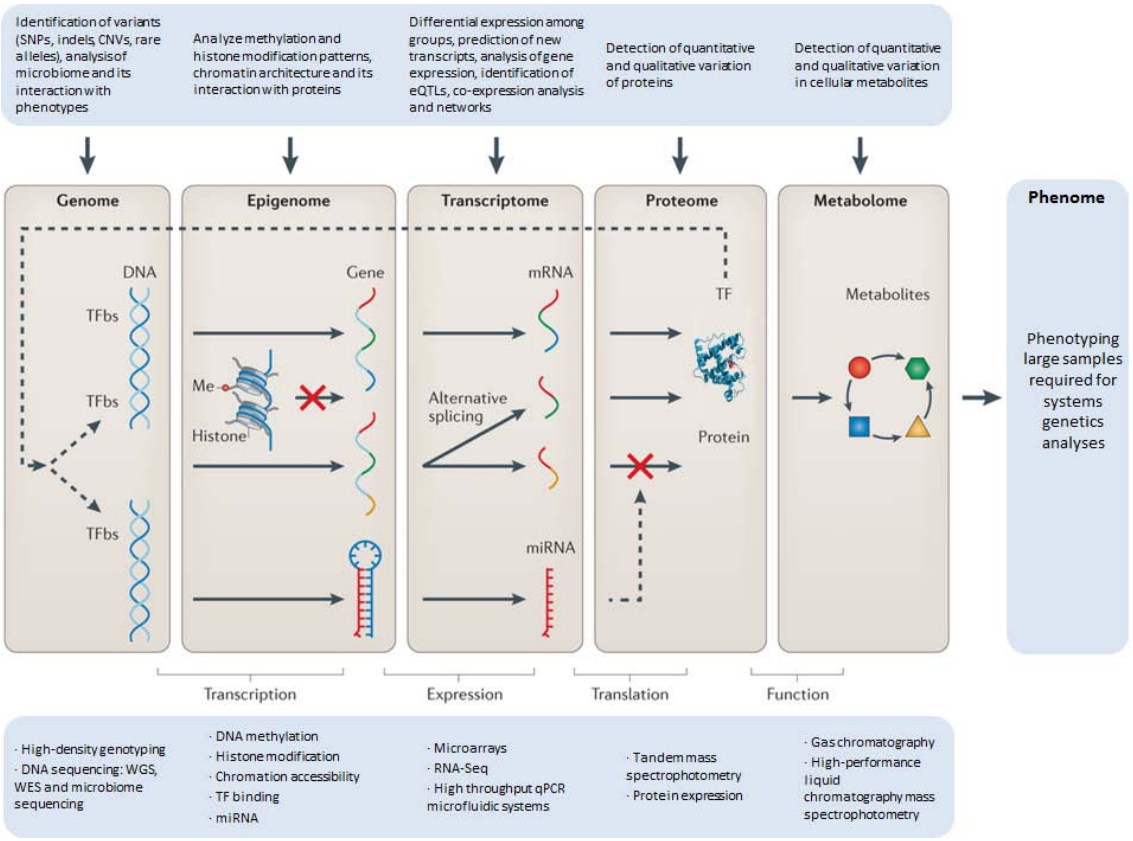

Figure 1.4. Biological systems multi-omics from the genome, epigenome, transcriptome, proteome and metabolome to the phenome. Abbreviations used: copy number variation (CNV), expression quantitative trait *loci* (eQTLs), messenger RNA (mRNA), micro RNA (miRNA), real-time quantitative PCR (qPCR), single nucleotide polymorphism (SNP), transcription factor (TF), transcription factor-binding site (TFbs), whole exome sequence (WES) and whole genome sequence (WGS). Arrows indicate the flow of genetic information from the genome level to the phenome level; red crosses indicate inactivation of transcription or translation (adapted from Ritchie *et al.*, 2015).

The application of these new genomic tools has the advantage of generating information in parallel on multiple genes and gene products, which in turn provides the opportunity to identify pathways and interacting genes (Andersson & Georges 2004; Tuggle *et al.*, 2006; Hocquette 2005). In this way, the approach is providing insight into the relationships of genes that can further improve our understanding of the genetic component of complex traits.

1.4.1. NGS technologies

Next-generation sequencing describe a DNA sequencing technology which is set to revolutionize the way complex trait genetics research is carried out. Since their introduction into the market in 2005, NGS technologies offer the scientific community the opportunity to explore the whole genome, transcriptome or epigenome of an organism in a cost-effective manner (Morozova & Marra 2008). Several massively parallel platforms are in widespread use by sequencing centres or laboratories at present (Table 1.3).

Table 1.3. Comparison of most used next-generation sequencing platforms (adapted from Goodwin *et al.*, 2016).

Platform	Read length (bp)	Throughput	Reads	Runtime
2nd Next-generation sequencing (PCR based)				
454 GS Junior+	700 avg (SE, PE)*	70 Mb*	~0.1 M*	18 h*
454 GS FLX Titanium XL+	700 avg (SE, PE)*	700 Mb*	~1 M*	23 h*
Ion PGM 318	200 (SE)	600 Mb–1 Gb	4–5.5 M*	4 h
	400 (SE)*	1–2 Gb*		7.3 h*
Ion Proton	Up to 200 (SE)	Up to 10 Gb*	60–80 M*	2–4 h*
Illumina MiSeq v3	75 (PE)	3.3–3.8 Gb	44–50 M (PE)*	21–56 h*
	300 (PE)*	13.2–15 Gb*		
Illumina HiSeq2500 v4	36 (SE)	64–72 Gb	2 B (SE)	29 h
	50 (PE)	180–200 Gb	4 B (PE)*	2.5 d
	100 (PE)	360–400 Gb		5 d
	125 (PE)*	450–500 Gb*		6 d*
Illumina NextSeq 500/550 High output	75 (SE)	25–30 Gb	400 M (SE)*	11 h
	75 (SE)	50–60 Gb	800 M (PE)*	18 h
	150 (PE)*	100–120 Gb*		29 h*
Illumina HiSeq X	150 (PE)*	800–900 Gb*	2.6–3 B (PE)*	<3 d*
3rd generation sequencing (Single molecule)				
Pacific BioSciences RS II	~20 Kb	500 Mb–1 Gb*	~55,000*	4 h*
Oxford Nanopore MK 1 MinION	Up to 200 Kb	Up to 1.5 Gb	>100,000	Up to 48 h

avg, average; B, billion; bp, base pairs; d, days; Gb, gigabase pairs; h, hours; Kb, kilobase pairs; M, million; Mb, megabase pairs; PE, paired-end sequencing; SE, single-end sequencing. *Manufacture's data.

These NGS platforms differ in many parameters, such as instrument used, sequencing enzyme/method used, and read length generated. The first NGS technology to be released was the pyrosequencing method by *454 Life Sciences* (now *Roche*) (Margulies *et al.*, 2005), generating relatively long reads in a short run time. In 2006, the *Solexa/Illumina* sequencing platform was commercialized (*Illumina* acquired *Solexa* in 2007). Currently, *Illumina*, which offers the highest throughput and the lowest per-base cost, is the leading NGS platform.

The *Illumina* sequencers generated very high-throughput at a very balanced price per-base pair. One of the disadvantages is the relative long run time and that the sequence quality decreases towards the end. In 2010, *Ion Torrent* (now *Life Technologies*) released the Personal Genome Machine, which uses semiconductor technology and does not rely on the optical detection of incorporated nucleotides using fluorescence and camera scanning.

A few years ago, in 2010, *Pacific BioSciences* developed a third generation method allowing the real-time sequencing of a single molecule. This methodology (Menlo Park, CA, USA) offers longer read lengths than the previous generation sequencing technologies, making it well-suited for unsolved problems in genome, transcriptome, and epigenetic research. However, other promising technologies are starting to appear. In 2014, the first consumer prototype of a nanopore sequencer, the *MinION* from *Oxford Nanopore* technologies, became available. This technology is based on the transit of a DNA molecule through a pore while the sequence is read out through the effect on an electric current or optical signal (Clarke *et al.*, 2009). The major advantage is that the library preparation or sequencing reagents are not necessary due to the fact that the DNA or RNA molecules are directly sequenced.

Several studies had used whole genome sequence (WGS) data to identify selective sweeps in pigs and numerous methods have been developed to identify such signatures of selection (Vitti *et al.*, 2013). One of the first studies that used NGS data from pig populations to identify selection footprints across domesticated genomes was performed by Amaral *et al.* in 2011. The results from this study suggested the selection in domestic pigs on genes that affect coat color, growth, muscle development, olfaction, immunity, and brain development. However, this study lacked sufficient resolution to identify unequivocally specific genes due to the low-coverage of the sequence data. Rubin *et al.* (2012) compared the whole genome of pools of European domestic and European wild boars, revealing the staggering complexity of multiple duplications around the KIT proto-oncogene receptor tyrosine kinase (*KIT)* gene and its potential regulatory sequences, which are responsible for different coat color phenotypes, such as dominant white, patch, and belt. After the study performed by Rubin *et al.*, many analyses have been performed using WGS data, by sequencing different *Sus* species and *Sus scrofa* subspecies, with the objective of understanding the signatures of selection and speciation process (Ramírez *et al.*, 2015; Moon *et al.*, 2015; Paudel *et al.*, 2015; Choi *et al.*, 2015), and to study breed variability

(Groenen *et al.*, 2012; Bosse *et al.*, 2012; Esteve-Codina *et al.*, 2013; Veroneze *et al.*, 2013; Ai *et al.*, 2015; Bianco *et al.*, 2015).

Moreover, whole genome transcriptome shotgun sequencing technology or RNA-Seq has been developed to fulfill different biological purposes. RNA-Seq (Mortazavi *et al.*, 2008; Wang *et al.*, 2009) is used to exploit NGS technologies to sequence cDNAs from RNA samples and is being used for quantitative gene-expression studies (Blow 2009). However, accurate gene-expression estimation requires accurate genome annotation (Roberts *et al.*, 2011). By utilizing complete or nearly completely annotated reference genomes, RNA-Seq can assist researchers in identifying differentially-expressed genes and novel transcripts for agricultural animals in a quantitative and efficient way. In this regard, different RNA-Seq studies have been performed in swine to identify differentially-expressed genes between samples under different condition(s) that could be crucial for production traits. In this way, the expression patterns of porcine liver, muscle (*longissimus dorsi*) and abdominal fat were examined in two full-sib hybrid pigs with extreme phenotypes for growth and fatness traits (Chen *et al.*, 2011). Furthermore, in previous works of our group the RNA-Seq transcriptome profiling of liver (Ramayo-Caldas *et al.*, 2012a), backfat (Corominas *et al.*, 2013a), muscle (Puig-Oliveras *et al.*, 2014a), and hypothalamus (Pérez-Montarelo *et al.,* 2014) were performed by using extreme animals for intramuscular FA composition (liver, backfat and muscle) or for growth and fatness (hypothalamus) of Iberian x Landrace pigs. Similarly, a recent analysis analyzed also the RNA-Seq transcriptome profile of muscle (*biceps femoris*) by comparing Iberian and Iberian x Duroc early extreme pigs for IMF (Ayuso *et al.*, 2015). More recently, Szostak *et al.* (2016) used this approach to identify changes in the pig liver transcriptome induced by a diet enriched with linoleic acid (omega-6 family) and α-linoleic acid (omega-3). These authors revealed that the transcriptomic profile of the pig liver is altered when a diet enriched with omega-6 and omega-3 FAs is provided.

Regarding the transcriptome of porcine adipose tissue, several studies have focused on differences in breeding growth phases (Li *et al.*, 2012a; Sodhi *et al.*, 2014), phenotype (Chen *et al.*, 2011; Corominas *et al.*, 2013a; Xing *et al.*, 2015, 2016), developmental period (Jiang *et al.*, 2013), and adipose depots (Wang *et al.*, 2013a), underlying the importance of this technique for the identification of candidate genes for livestock production traits.

1.5. Genomic studies of porcine meat quality traits

1.5.1. QTLs, GWAS and candidate genes

Most economically important traits in pigs are complex or quantitative and, thus, are influenced by multiple genes. The development of molecular markers and genome maps have facilitated the application of molecular genetic approaches to identify genes and polymorphisms controlling variation in traits of interest. The hunt for QTL in pigs has been ongoing for nearly two decades, beginning with the first publication of a QTL for fatness on *Sus scrofa* chromosome 4 (SSC4) in 1994 (Andersson *et al.*, 1994). Since then, hundreds of publications have documented thousands of QTLs for a wide variety of traits. The Pig QTLdb (Hu *et al.*, 2013) [http://www.animalgenome.org/cgi-bin/QTLdb/SS/index; accessed January 2017] includes information for 16,516 QTLs from 566 publications representing 626 different traits, and this total is conservative, given that it does not include all publishes pig QTL studies. From the total QTLs reported, 2,358 are associated with fatness traits, 1,328 are related to growth traits, and 1,311 and 841 to fat composition and conformation traits, respectively (Figure 1.5). The populations in the majority of these studies involved experimental crosses, using pig breeds exhibiting extreme phenotypes for traits of interest, with the expectation that alleles for QTL controlling these phenotypes would be segregating.

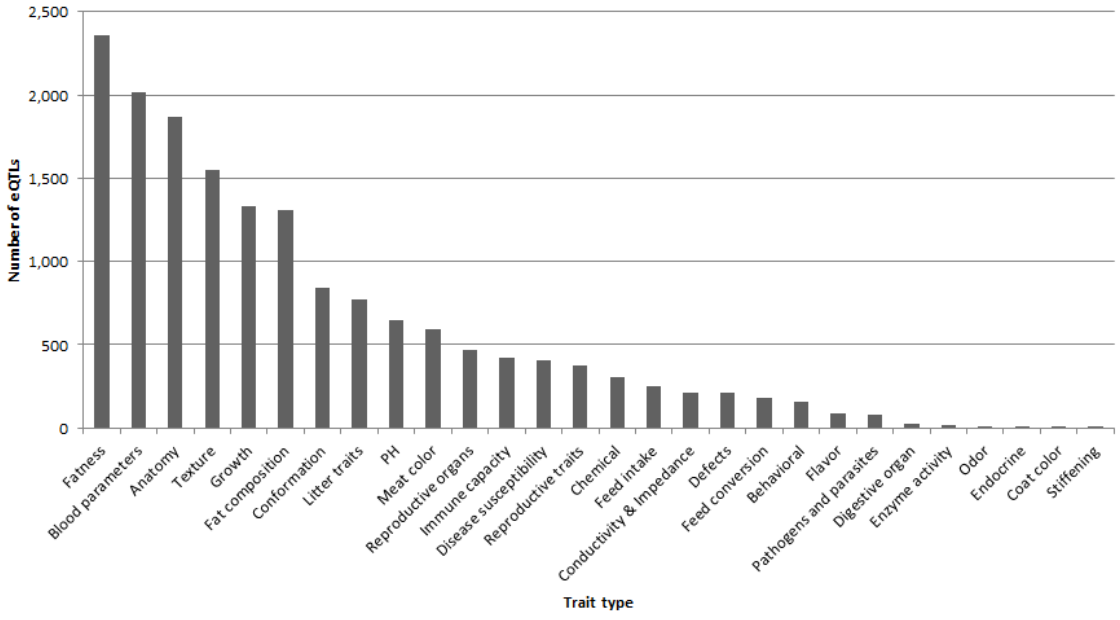

Figure 1.5. Distribution of porcine QTLs among the different trait types in the Pig QTLdb [Pig QTLdb; http://www.animalgenome.org/cgi-bin/QTLdb/SS/index; accessed January 2017].

QTL identification have been greatly enhanced in recent years with the development of high-density SNP panels for pig genotyping. These panels have been initially used to perform genome-wide association studies (GWAS) to identify QTLs for various traits. Association testing exploits population-wide linkage disequilibrium (LD), as well as linkage, and provides more resolution to map QTLs compared with using only within-family linkage information. In addition, GWAS have made a substantial progress in identifying genomic locations and genetic factors underlying or associated with complex traits. This success has been possible by a change in technology. Microarray technologies enable fast and accurate genotyping of thousands of SNPs in a short time. In contrast, genome-wide family-based linkage studies had much lower resolution, with standard panels including only hundreds of microsatellite markers. An overview of the general design of a GWAS analysis is shown in Figure 1.6.

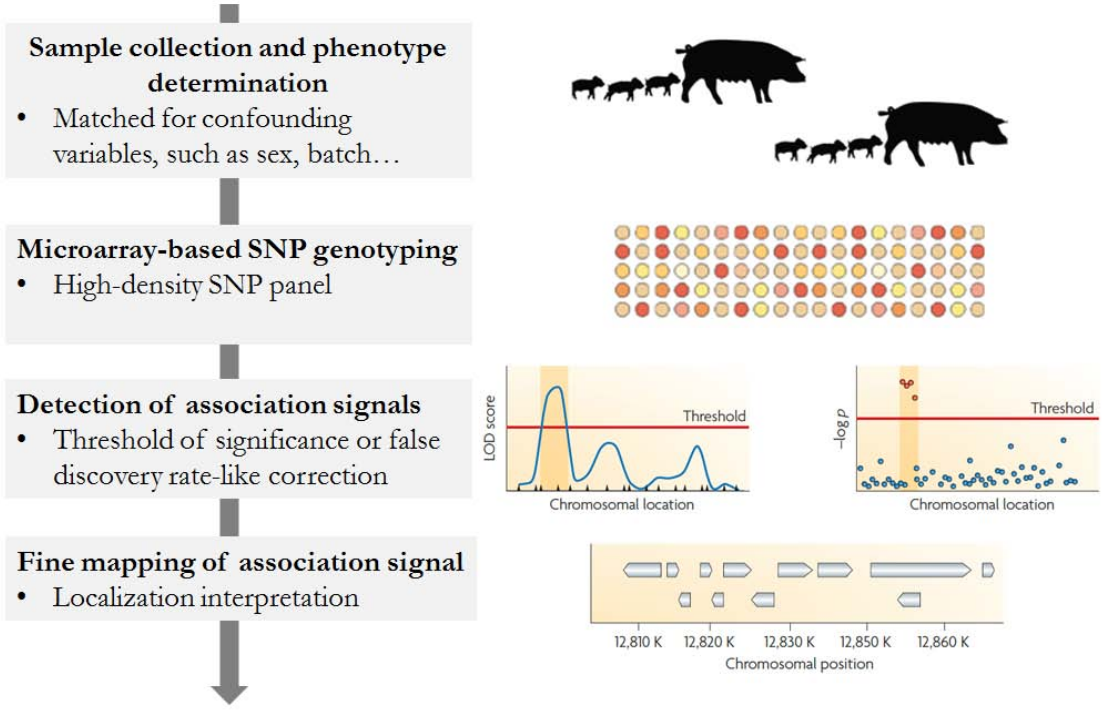

Figure 1.6. Overview of the general design and workflow of a GWAS analysis (adapted from Kingsmore *et al.*, 2008; Albert & Kruglyak 2015).

In comparison with the classical QTL mapping, GWAS has the advantage of using all recombination events after the mutations occur and, therefore, increases the precision of the QTL position estimates and reduces their confidence intervals (Meuwissen & Goddard 2000; Goddard & Hayes 2009). In pigs, GWAS have detected a large number of *loci* for a variety of traits in divergent populations, including a list of significant *loci* for FA

composition in pork (Ramayo-Caldas *et al.*, 2012b; Yang *et al.*, 2013; Muñoz *et al.*, 2013; Zhang *et al.*, 2016a,b).

Candidate genes have been selected based on both their expected physiological function on the trait and/or their map location near QTLs for the trait. Despite the large number of QTLs that have been identified in pigs, relatively few genes have been evaluated for the identification of segregating polymorphisms and allelic associations with trait phenotypes, some of which are highlighted in Table 1.4. In addition, few studies have succeeded in identifying causal mutations mainly due to (1) limited statistical power due to relatively small sample sizes, (2) production traits are complex and difficult to measure, (3) genetic variants tend to explain a reduced amount of the genetic variation, (4) several QTL studies are conducted in experimental crosses with large QTL intervals due to linkage between markers, and (5) marker associations may be influenced by the genetic background of the animals and, thus, the magnitude of the observed effect may be population specific. For instance, the estrogen receptor 1 (*ESR1*) which has been demonstrated to be associated with litter size in some genetic lines, but not in others (Rothschild *et al.*, 1996; Noguera *et al.*, 2003; Muñoz *et al.*, 2010). Several pig candidate gene markers have been applied in marker-assisted selection (MAS) in the pig breeding industry, most notably with *KIT*, Protein kinase AMP-activated non-catalytic subunit gamma 3 (*PRKAG3*), and Ryanodine receptor 1 (*RYR1*). MAS is a process whereby a marker (based on DNA variation) is used for indirect selection of a trait of interest.

Table 1.4. Examples of candidate genes with reported association for pig production traits identified in QTL or GWAS analyses (adapted from Ernst & Steibel 2013).

Gene name	Gene Symbol	Trait(s)	Reference(s)
Calpastatin	*CAST*	Meat quality	Ciobanu *et al.*, 2004; Nonneman *et al.*, 2011
Carbonic anhydrase 3	*CA3*	Meat quality	Wimmers *et al.*, 2007
ELOVL fatty acid elongase 6	*ELOVL6**	Meat quality	Corominas *et al.*, 2013b
Estrogen receptor 1	*ESR1**	Litter size	Rothschild *et al.*, 1996; Noguera *et al.*, 2003; Muñoz *et al.*, 2010
Fatty acid binding protein 4	*FABP4*	Meat quality	Ojeda *et al.*, 2006
Fatty acid binding protein 5	*FABP5*	Meat quality	Estellé *et al.*, 2006
Follicle stimulating hormone beta subunit	*FSHB*	Litter size	Onteru *et al.*, 2009
Fucosyltransferase 1	*FUT1*	Disease resistance	Wang *et al.*, 2012a
Insulin like growth factor 2	*IGF2**	Growth and carcass composition	Van Laere *et al.*, 2003; Aslan *et al.*, 2012; Estellé *et al.*, 2005a
KIT proto-oncogene receptor tyrosine kinase	*KIT*	Coat color	Johansson Moller *et al.*, 1996
Leptin	*LEP*	Growth and carcass composition	de Oliveira Peixoto *et al.*, 2006
Leptin receptor	*LEPR*	Growth and carcass composition	Ovilo *et al.*, 2005
Melanocortin 1 receptor	*MC1R**	Coat color	Kijas *et al.*, 2001
Melanocortin 4 receptor	*MC4R**	Growth and carcass composition	Kim *et al.*, 2000; Bruun *et al.*, 2006; Fan *et al.*, 2009
Myopalladin	*MYPN*	Carcass composition	Wimmers *et al.*, 2007
Phosphoenolpyruvate carboxykinase 1	*PCK1**	Meat quality	Latorre *et al.*, 2016
POU class 1 homeobox 1	*POU1F1*	Growth and carcass composition	Kuryl & Pierzchala 2001; Song *et al.*, 2007
Protein kinase AMP-activated non-catalytic subunit gamma 3	*PRKAG3**	Meat quality	Milan *et al.*, 2000; Ciobanu *et al.*, 2001
Prolactin receptor	*PRLR**	Litter size and boar reproduction	Kmieć & Terman 2006; Tomás *et al.*, 2006
Retinal binding protein 4	*RBP4*	Litter size	Muñoz *et al.*, 2010; Rothschild *et al.*, 2000
Ryanodine receptor 1	*RYR1**	Stress susceptibility, leanness, and meat quality	Fujii *et al.*, 1991; O'Brien & MacLennan 1992
Stearoyl-CoA desaturase	*SCD**	Meat quality	Estany *et al.*, 2014
Titin	*TTN*	Meat quality	Wimmers *et al.*, 2007

*Detected polymorphism is in LD with causal genetic variation within particular populations

1.5.2. eQTL mapping approach

The analysis of variants in the context of gene-expression measured in cells or tissues has spawned a field in animal genetics studying expression quantitative trait *loci* (eQTLs). An eQTL is a *locus* that explains a fraction of the genetic variance of a gene-expression phenotype, and standard analysis involves associations between genetic markers with gene-expression levels measured in animals of interest. The polymorphic regulators may be protein coding regions, microRNAs, or other functional nucleotide sequences (Michaelson *et al*., 2009). In order to detect such genomic regions it is necessary to genotype genetically diverse individuals and measure their expression pattern by using, for example microarrays, qPCR or deep sequencing technologies. One of the distinctive features of this approach is the ability to discriminate between *cis*- and *trans*- acting influences on gene-expression and elucidate complex regulatory networks (Li *et al*., 2005). The first, termed *cis*-acting, results from DNA polymorphisms of a gene that directly influences transcript levels of the same gene. The second variety, termed *trans*-acting, where the genetic variant is located further away from the affected gene, or on a completely different chromosome. *Cis*-acting genes, which are generally easier to detect by linkage, explain a large fraction of the variance of gene expression and have more interest as positional candidate genes for QTLs (Doss *et al*., 2005). Besides this, *trans*-eQTLs, generally associated with lesser statistical significance, are often detected as clusters reflecting coordinated regulation of many genes (Yvert *et al*., 2003). In general, studies performed in animals have identified regulatory hotspot and *trans*-eQTL in a higher ratio that those performed in humans (Gilad *et al*., 2008; Cheung & Spielman 2009). Furthermore, Petretto *et al*. (2006) reported that the median heritabilities range from a minimum of 0.14 for the *trans*-eQTLs to a maximum of 0.37 for the *cis*-eQTLs.

The concept of eQTL mapping and the first studies in humans, plants, and model organisms were published during the early 2000s (Jansen & Nap 2001; Schadt *et al*., 2003). However, due to the high-cost of eQTL projects and the complexity of conducting eQTL analyses, few studies have been conducted in agricultural animal species, with only a reduced number performed on pigs. To date, few groups have reported genome-wide eQTL studies in pigs (Table 1.5), with initial studies focusing on transcriptional profiling of skeletal muscle tissue.

Table 1.5. Reported eQTL/eGWAS studies in pigs for production traits.

Related trait type	Reference(s)
Growth	Steibel *et al.*, 2011; Ponsuksili *et al.*, 2012
Fatness	Steibel *et al.*, 2011; Ponsuksili *et al.*, 2011; Cánovas *et al.*, 2012
Meat quality and FA composition	Ponsuksili *et al.*, 2008; Ponsuksili *et al.*, 2010; Wimmers *et al.*, 2010; Steibel *et al.*, 2011; Heidt *et al.*, 2013; Muñoz *et al.*, 2013; Pena *et al.*, 2013; Manunza *et al.*, 2014; Ponsuksili *et al.*, 2014; Puig-Oliveras *et al.*, 2016; Ballester *et al.*, 2017; González-Prendes *et al.*, 2017
Blood metabolite profile	Chen *et al.*, 2013
Disease susceptibility and disorders	Liaubet *et al.*, 2011; Reiner *et al.*, 2014

Regarding FA composition traits in pigs, the combination of traditional QTL mapping with eQTL mapping have provided crucial information about the nature of this trait (Table 1.5). In recently published studies of our group, an analysis of the muscle (Puig-Oliveras *et al.*, 2016) and liver (Ballester *et al.*, 2017) mRNA expression of several candidate genes related with lipid metabolism was performed. Remarkably, a list of candidate genes, regulatory polymorphisms and genetic networks have been described, and the PI3K-Akt pathway has been identified as a central pathway in the genetic determination of FA composition traits.

1.5.3. Genomic structural variants

The availability of genome sequence data from individuals within a species enables the investigation of a range of inherited genetic variations at a high-resolution. Genomic analysis of DNA variants has focused on the identification of SNPs, and indels. However, in recent years, other forms of genomic variation have also begun to receive attention. One such form is copy number variation (CNV), defined as a type of genetic structural variation which corresponds to a genomic region (typically larger than 1 kb) that has been deleted or duplicated, giving different number of copies of a DNA fragment (Freeman *et al.*, 2006). Although their role in genetic susceptibility to a variety of production traits have been predicted to be important, they have not been explicitly examined in most association analyses in the past. With the development of improved methods for CNV detection, this particular type of genetic variation has gained increasing attention throughout the last years.

Benefitting from the achievements of pioneering CNV studies in humans, substantial progress has been made in the discovery and characterization of CNVs in livestock genomes. In the past few years, a significant amount of research on genome-wide CNV identification was conducted in pigs (Fadista *et al.*, 2008; Ramayo-Caldas *et al.*, 2010; Wang *et al.*, 2012b; Li *et al.*, 2012b). Remarkably, Ramayo-Caldas *et al.* (2010) performed the first whole genome identification of CNVs in pigs using SNP arrays. Moreover, a suite of genes with copy number alteration were analyzed contributing to variation of either Mendelian phenotypes (Giuffra *et al.*, 2002; Salmon Hillbertz *et al.*, 2007; Fontanesi *et al.*, 2009) or complex traits (Seroussi *et al.*, 2010). However, potential issues in the majority of previous CNV studies in livestock species are a lack of power and accuracy for CNV identification, due to the technical limitations of the two most frequently used detection platforms, SNP chips and array comparative genome hybridization (aCGH) (Alkan *et al.*, 2011). This highlights the need to develop more powerful tools for construction of high-resolution CNV maps. Nowadays, NGS technologies provide a sensitive and accurate alternative approach for detecting genomic variations. The quality and speed give NGS a significant advantage over microarrays (Hurd & Nelson 2009; Su *et al.*, 2011). Taking these advantages into account, a diverse set of tools has been developed to detect CNVs based on different features that can be extracted from NGS data. So far, the NGS based CNV detection methods can be categorized into five different strategies (Figure 1.7), including: (1) Paired-end mapping strategy which detects CNVs through discordantly mapped reads. A discordant mapping is produced if the distance between two ends of a read pair is significantly different from the average insert size. (2) Split read-based methods use incompletely mapped reads from each read pair to identify small CNVs. (3) Read depth-based approach detects CNVs by counting the number of reads mapped to each genomic region. (4) *De novo* assembly of a genome detects CNVs by mapping contigs to the reference genome. And (5) a combination of the above approaches to detect CNVs: read depth and paired-end mapping information.

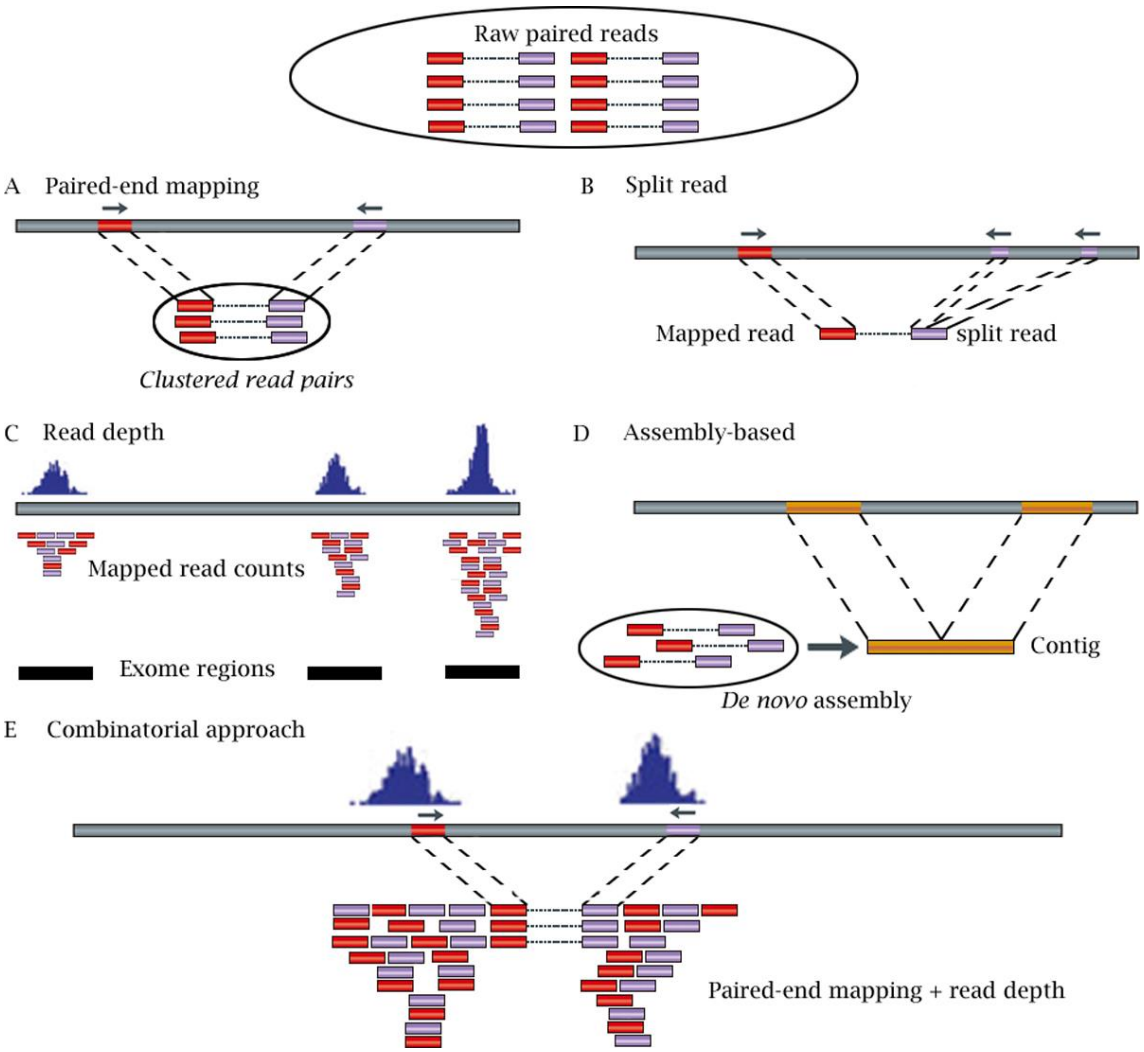

Figure 1.7. Approaches to detect CNVs from NGS data (Zhao *et al.*, 2013).

In pig species, much effort has been made to detect CNVs using NGS technologies (Fernández *et al.*, 2014; Paudel *et al.*, 2015; Wiedmann *et al.*, 2015), but little is known about how CNVs contribute to normal phenotypic variation (Rubin *et al.*, 2012; Schiavo *et al.*, 2014; Wang *et al.*, 2015a) and to disease susceptibility.

1.6. The IBMAP cross

The IBMAP consortium, created in 1996, was a collaboration between UAB (*Universitat Autònoma de Barcelona;* Barcelona, Spain), INIA (*Instituto Nacional de Investigación y Tecnología Agraria y Alimentaria;* Madrid, Spain), and IRTA (*Institut de Recerca i Tecnologia Agroalimentàries;* Lleida, Spain) which made possible the generation of an initial Iberian x Landrace F_2 cross and several subsequent crosses (Figure 1.8).

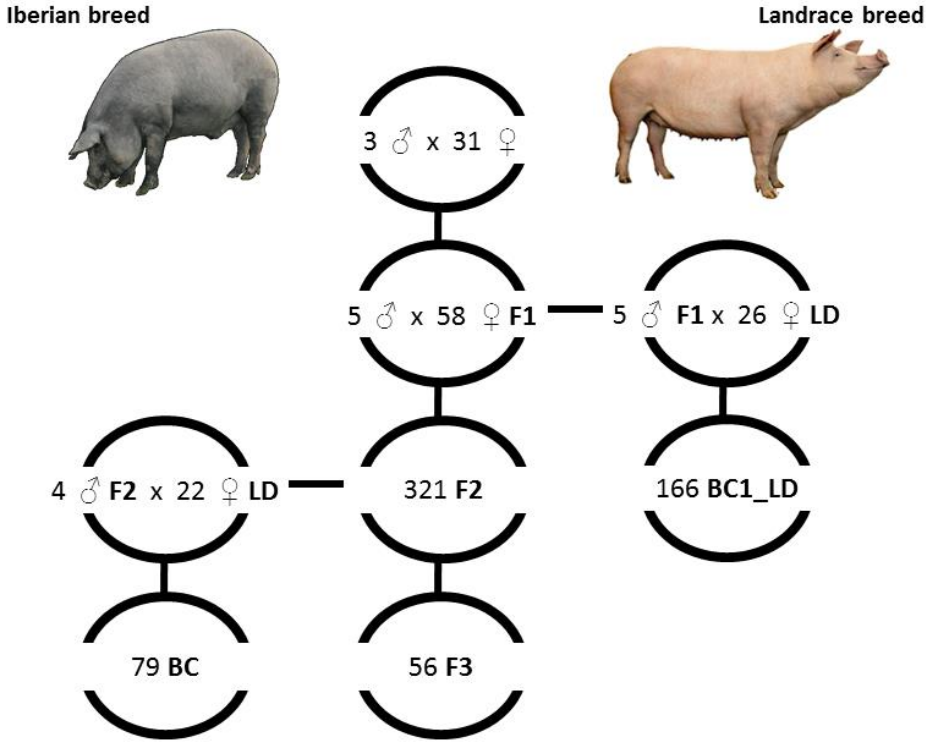

Figure 1.8. Schematic representation of the Iberian by Landrace cross (IBMAP).

Experimental populations derived from two lines differing widely for traits of interest have been successfully used in livestock to detect QTL (Andersson *et al.*, 1994). In this context, Iberian and Landrace breeds were selected for being divergent pig lines for meat quality, growth, fatness, fertility, and feed efficiency traits. The Iberian pig is a racial grouping of native pigs originating from *Sus scrofa meridionalis* which has been maintained for centuries in large areas of the southwestern Iberian Peninsula. They constitute the largest of the surviving populations of the Mediterranean type, which is one of the three ancient types of domestic pigs (the others are the European/Celtic and Asian types). Its excellent meat quality and cured products, with a higher content of SFA and MUFA, make them a highly appreciated animal. In this sense, the Guadyerbas line stands out for its slow-growth, very low prolificacy and high fat (Serra *et al.*, 1998), and is an Iberian pig strain that has remained isolated on an experimental farm since 1945 (Toro *et al.*, 2000). By comparison, Landrace is

a lean international breed that has undergone a strong selection for production, lean meat content, muscularity, and enhanced reproduction traits (Porter 1993). Nonetheless, the Landrace meat has lower levels of fat, less IMF, higher content of PUFA, and lower content of MUFA and SFA (Serra *et al.*, 1998).

In this thesis the main population studied descends from crossing three Iberian Guadyerbas boars (*Dehesón del Encinar*; Toledo, Spain) with 31 Landrace sows (*Nova Genètica S.A.*; Lleida, Spain), obtaining an F_1 generation. From this F_1 generation, different generations were created as shown in Figure 1.8, including F_2, F_3, and different backcrosses with Pietrain (BC1_PI; 25% Iberian x 75% Pietrain backcross) and Duroc breeds (BC1_DU; 25% Iberian x 75% Duroc backcross). The analyses performed in this thesis were main focused on the 166 BC1_LD animals (25% Iberian x 75% Landrace backcross) created by crossing 5 F_1 boars with 26 Landrace sows.

1.6.1. QTLs identified in the IBMAP cross

The first QTL studies performed in the IBMAP cross were based on microsatellite markers and identified significant associated regions for carcass quality, growth, fatness and FA composition in chromosomes SSC2, SSC3, SSC4, SSC6, SSC7, SSC8, SSC10, SSC12, and SSCX (Ovilo *et al.*, 2000; Pérez-Enciso *et al.*, 2000; Ovilo *et al.*, 2002; Pérez-Enciso *et al.*, 2002; Varona *et al.*, 2002; Clop *et al.*, 2003; Mercadé *et al.*, 2005a; Ovilo *et al.*, 2005; Pérez-Enciso *et al.*, 2005; Mercadé *et al.*, 2006a; Muñoz *et al.*, 2007). More recently, QTL and GWAS approaches using high-density SNP markers allowed in general a higher resolution in QTL intervals and the identification of new genomic regions with the analysed traits (Fernández *et al.*, 2012; Ramayo-Caldas *et al.*, 2012b; Corominas *et al.*, 2013b; Muñoz *et al.*, 2013).

A few QTLs for FA composition have been reported on SSC8 in the IBMAP population. Clop *et al.* (2003) performed the first report of a genome scan for QTLs affecting FA composition in pigs of the IBMAP cross. In this study, using F_2 generation animals, a QTL was identified on SSC8 for percentages of palmitic (C16:0) and palmitoleic acids (C16:1(n-7)) and for average chain length of FA in backfat (Clop *et al.*, 2003). Recently, a GWAS study conducted in BC1_LD animals of the IBMAP cross led to the identification of five genomic regions on SSC8 associated with intramuscular FA composition in *Longissimus dorsi* muscle (Ramayo-Caldas *et al.*, 2012b). Furthermore, Muñoz *et al.* (2013) found two relevant

regions on SSC8 for palmitic (C16:0) and palmitoleic acids (C16:1(n-7)) in backfat and IMF. The QTLs described, suggest a pleitropic effect of both FA QTLs in IMF and backfat (Ramayo-Caldas *et al.*, 2012b; Muñoz *et al.*, 2013).

1.6.2. Positional candidate genes of QTLs analyzed in the IBMAP cross

The final goal of complex traits dissection is to identify the genes involved and to decipher their cellular role and functions. Within the described QTLs, several positional and functional candidate genes for growth, fatness, and meat quality traits have been identified in the IBMAP consortium, and are summarized in Table 1.6.

Table 1.6. Main positional candidate genes analyzed in the IBMAP cross.

Chr	QTL associated trait(s)	Candidate gene(s)	Reference
SSC2	Growth and fatness	*IGF2*	Estellé *et al.*, 2005a
SSC4	Growth, FA composition and form	*APOA2*	Ballester *et al.*, 2016
		DECR	Clop *et al.*, 2002
		DGAT1	Mercadé *et al.*, 2005b
		FABP4	Mercadé *et al.*, 2006b
		FABP5	Estellé *et al.*, 2006
SSC6	Fatness and IMF	*ACADM*	Kim *et al.*, 2006
		FABP3	Ovilo *et al.*, 2002
		LEPR	Ovilo *et al.*, 2005 Muñoz *et al.*, 2009
SSC8	FA composition	*CDS1*	Mercadé *et al.*, 2007
		ELOVL6	Corominas *et al.*, 2013b, 2015
		FABP2	Estellé *et al.*, 2009a
		MAML3 *SETD7*	Revilla *et al.*, 2014
		MTTP	Estellé *et al.*, 2005b Estellé *et al.*, 2009b
SSC12	FA composition	*ACACA* *FASN* *GIP*	Muñoz *et al.*, 2007
SSCX	FA composition, growth, fatness and IMF	*ACSL4*	Mercadé *et al.*, 2006a Corominas *et al.*, 2012

To date, there is still a lot to discover regarding the number of genes that control meat quality, but the QTLs detected for FA composition on SSC8 in the IBMAP population show the importance of studying this chromosomal region. Different studies of our group (Estellé *et al.*, 2005b; Mercadé *et al.*, 2007; Estellé *et al.*, 2009a: Estellé *et al.*, 2009b;

Corominas *et al.*, 2013b; Corominas *et al.*, 2015) have analyzed genes for this genomic region in order to unravel the molecular basis of phenotypic variations with important effects on meat quality traits.

One of the genes studied with more detail has been de *ELOVL6* (Corominas *et al.* 2013b) The coincidence between the biological function of *ELOVL6* and the observed QTL effect on FA composition on SSC8 (Clop *et al.*, 2003; Ramayo-Caldas *et al.*, 2012b) strengthens the interest of the *ELOVL6* as the positional gene for this QTL. The characterization of the coding and proximal promoter regions of the porcine *ELOVL6* gene allowed the identification of several mutations, especially the *ELOVL6:c.-533C>T* polymorphism strongly associated with muscle and backfat percentages of palmitic (C16:0) and palmitoleic (C16:1(n-7)) acids (Corominas *et al.*, 2013b). Furthermore, this SNP was found to be in full LD with SNP *ELOVL6:c.-394G>A*, which was associated with an increase in methylation levels of the promotor of this gene and with a decrease of *ELOVL6* expression (Corominas *et al.*, 2015).

1.6.3. New genomic tools in the IBMAP cross

NGS technologies are allowing the mass sequencing of genomes and transcriptomes, which are producing a vast array of genomic information. The IBMAP consortium has directly benefited from these developments, and have used several of these new genomic approaches to reveal the mechanisms involved in lipid metabolism. RNA-Seq have been used to quantify gene expression in the main tissues affecting lipid metabolism: liver (Ramayo-Caldas *et al.*, 2012a), backfat (Corominas *et al.*, 2013a) and muscle (Puig-Oliveras *et al.*, 2014a). These transcriptomic analyses have been performed in two divergent groups of animals: a group of animals showing a higher proportion of SFA and MUFA and another group with a higher content of PUFA. The results revealed a decreased FA oxidation in liver (Ramayo-Caldas *et al.*, 2012a), an increase of *de novo* lipogenesis in adipose tissue (Corominas *et al.*, 2013a), and also an increase of FA and glucose uptake and enhanced lipogenesis in muscle (Puig-Oliveras *et al.*, 2014a) in the animals with higher proportion of SFA and MUFA. Interestingly, common pathways related with LXR/RXR activation, PPARs and β-oxidation were identified in the three RNA-Seq studies. Thus, the RNA-Seq method has helped in the selection of candidate genes and pathways related to important meat quality traits such as FA composition. Moreover, RNA-Seq technology has

been exploited as a method to detect polymorphisms in transcribed regions in an efficient and cost-effective way (Martínez-Montes *et al.*, 2017a).

A co-association network analysis was performed to study FA composition and growth. Ramayo-Caldas *et al.* (2014) used the Association Weight Matrix (AWM) methodology (Fortes *et al.*, 2010; Reverter & Fortes 2013) to build a network of genes associated with intramuscular FA composition. This analysis pointed to three transcription factors that explain the majority of the network topology of FA metabolism: nuclear receptor coactivator 2 (*NCOA2*), four and a half LIM domains 2 (*FHL2*) and E1A binding protein p300 (*EP300*). Furthermore, Puig-Oliveras *et al.* (2014b) also used this methodology to decipher gene interactions and pathways affecting pig conformation, growth and fatness traits. Three transcription factors were identified: the peroxisome proliferator activated receptor gamma (*PPARG)*, E74 like ETS transcription factor 1 (*ELF1*) and PR/SET domain 16 (*PRDM16*), as key transcription factors regulating growth traits.

The expression of a selection of potential candidate genes was analyzed in muscle (Puig-Oliveras *et al.*, 2016) and liver (Ballester *et al.*, 2017) by qPCR in a large number of animals. Remarkably, in the muscle gene-expression analyses (Puig-Oliveras *et al.*, 2016), the nuclear receptor subfamily 3 group C member 1 (NR3C1) transcription factor was pointed as a strong candidate gene to be involved in the regulation of the analyzed genes, and several genes were identified as potential regulators co-localizing with QTLs for fatness and growth traits. The NR3C1 was also identified in the liver gene-expression analyses (Ballester *et al.*, 2017), and also a hotspot on SSC8 associated with the gene expression of eight genes was identified underlying the TBC1 domain containing kinase *(TBCK)* gene as a potential candidate gene to regulate it. In another study, Muñoz *et al.* (2013) also combined QTL and eQTL mapping to identify candidate genes with potential effect on backfat thickness and intramuscular FA composition. More recently, Martínez-Montes *et al.*, (2017b) also used this approach to detect genomic regions regulating the gene expression of genes whose expression is correlated with growth, fat deposition, and premium cut yield measures. A long non-coding RNA (ALDBSSCG0000001928) was identified, whose expression is correlated with premium cut yield.

In summary, the use of new genomic tools is of great value for the genetic dissection and knowledge in the functional regulatory mechanisms involved in the analyzed complex traits.

Objectives

Chapter 2

This PhD thesis was done under the framework of the IBMAP Project funded by the Spanish Ministry of Economy and Competitiveness (grant numbers: AGL2011-29821-C02 and AGL2014-56369-C2). The present research has been performed using the animal material generated by the IBMAP Project, a coordinated project involving INIA, IRTA and UAB research groups.

The general objective of this thesis was to increase the knowledge of the genetic basis determining fatty acid composition in pigs.

More specifically, the objectives were:

1. To deepen the study of the QTL architecture of pig chromosome 8 for fatty acid composition and to evaluate positional candidate genes.

2. To identify copy number variation regions from porcine whole genome sequence data on autosomal chromosomes, validate a selection of them in a large number of animals, and study their association with growth and meat quality traits.

3. To study the expression in adipose tissue of a set of candidate genes for fatty acid composition and to identify and characterize the genomic regions regulating the expression of these genes.

Papers and Studies

Chapter 3

PAPER I

New insight into the SSC8 genetic determination of fatty acid composition in pigs

Revilla M[1], Ramayo-Caldas Y[1,2], Castelló A[1,2], Corominas J[1,2], Puig-Oliveras A[1,2], Ibáñez-Escriche N[3], Muñoz M[4], Ballester M[1,2], Folch JM[1,2*]

[1] Centre de Recerca en Agrigenòmica (CRAG), Consorci CSIC-IRTA-UAB-UB, Campus UAB, Bellaterra, 08193, Spain

[2] Departament de Ciència Animal i dels Aliments, Facultat de Veterinària, Universitat Autònoma de Barcelona, Bellaterra 08193, Spain

[3] Genètica i Millora Animal, IRTA, Av Rovira Roure 191, Lleida 25198, Spain

[4] Departamento Mejora Genética Animal, SGIT-INIA, Ctra. Coruña Km 7.5, Madrid 28040, Spain

[*] Corresponding author

Genetics Selection Evolution (2014). 46:28.
http://doi.org/10.1186/1297-9686-46-28

Abstract

Background: Fat content and fatty acid composition in swine are becoming increasingly studied because of their effect on sensory and nutritional quality of meat. A QTL (quantitative trait locus) for fatty acid composition in backfat was previously detected on porcine chromosome 8 (SSC8) in an Iberian x Landrace F_2 intercross. More recently, a genome-wide association study detected the same genomic region for muscle fatty acid composition in an Iberian x Landrace backcross population. *ELOVL6*, a strong positional candidate gene for this QTL, contains a polymorphism in its promoter region (*ELOVL6:c.-533C < T*), which is associated with percentage of palmitic and palmitoleic acids in muscle and adipose tissues. Here, a combination of single-marker association and the haplotype-based approach was used to analyze backfat fatty acid composition in 470 animals of an Iberian x Landrace F_2 intercross genotyped with 144 SNPs (single nucleotide polymorphisms) distributed along SSC8.

Results: Two trait-associated SNP regions were identified at 93 Mb and 119 Mb on SSC8. The strongest statistical signals of both regions were observed for palmitoleic acid (C16:1(n-7)) content and C18:0/C16:0 and C18:1(n-7)/C16:1(n-7) elongation ratios. *MAML3* and *SETD7* are positional candidate genes in the 93 Mb region and two novel microsatellites in *MAML3* and nine SNPs in *SETD7* were identified. No significant association for the *MAML3* microsatellite genotypes was detected. The *SETD7:c.700G > T* SNP, although statistically significant, was not the strongest signal in this region. In addition, the expression of *MAML3* and *SETD7* in liver and adipose tissue varied among animals, but no association was detected with the polymorphisms in these genes. In the 119 Mb region, the *ELOVL6:c.-533C > T* polymorphism showed a strong association with percentage of palmitic and palmitoleic fatty acids and elongation ratios in backfat.

Conclusions: Our results suggest that the polymorphisms studied in *MAML3* and *SETD7* are not the causal mutations for the QTL in the 93 Mb region. However, the results for *ELOVL6* support the hypothesis that the *ELOVL6:c.-533C > T* polymorphism has a pleiotropic effect on backfat and intramuscular fatty acid composition and that it has a role in the determination of the QTL in the 119 Mb region.

Background

One of the main sources of human-consumed meat is pork, which represents more than 40% of the meat produced worldwide [1]. The success of pig production is strongly related to improvements in growth and carcass yield. Meat-quality traits are essential for the processing industry and end-consumer acceptance [2], and, as a result, these qualitative traits have been the subject of many studies in breeding programs. Fat content and fatty acid (FA) composition in swine are becoming increasingly studied because of their effect on sensory and nutritional quality of meat. They determine important sensory and technological aspects of pork and meat products because of their influence on the melting point and oxidative status of porcine tissues [3]. In addition, the amount and type of fat in the diet have a major impact on human health. The high consumption of saturated fatty acids (SFA) raises plasma LDL-cholesterol, which is a major risk factor for arteriosclerosis and coronary heart disease (CHD) [4-6]. However, recent studies suggest that individual SFA have different physiological effects. Indeed, lauric acid (C12:0), myristic acid (C14:0) and palmitic acid (C16:0) raise LDL and HDL cholesterol plasma levels, whereas stearic acid (C18:0) is considered neutral [7,8], although some epidemiologic evidence suggests that stearic acid (C18:0) is associated with CHD [9]. In contrast, cis-monounsaturated fatty acids (MUFA) and polyunsaturated fatty acids (PUFA) are beneficial for human health. PUFA have been shown to protect against CHD [10], whereas MUFA are also considered to have a hypocholesterolemic effect [11] and, in addition, to have a beneficial effect on insulin sensitivity [12].

A few QTL (quantitative trait loci) for FA composition have been reported on porcine chromosome 8 (SSC8) in F_2 Duroc x Large White [13], F_2 White Duroc x Erhualian [14] and Duroc [15] populations. Using an Iberian x Landrace F_2 intercross (IBMAP) [16], a QTL was identified on SSC8 for percentages of palmitic (C16:0) and palmitoleic (C16:1(n-7)) FA and for average length of FA in backfat (BF). Recently, a genome-wide association study (GWAS) conducted in a backcross population (BC1_LD; 25% Iberian and 75% Landrace) led to the identification of five genomic regions on SSC8 associated with intramuscular fat in *longissimus dorsi* (IMF) FA composition [17]. In addition, a study that combined a linkage QTL scan and a GWAS on the same backcross revealed significant pleiotropic regions with effects on palmitic (C16:0) and palmitoleic (C16:1(n-7)) FA in both IMF and BF tissues [18].

The main goals of this work were: (1) to study the QTL architecture for FA composition on SSC8 in the F_2 generation of the IBMAP cross using a panel of 144 informative SNPs, and (2) to analyze additional positional candidate genes.

Methods

Animal samples

Animals used in this study belong to the IBMAP experimental population [19]. Two Iberian (Guadyerbas line) boars were crossed with 30 Landrace sows to generate the F_1 generation. Six F_1 boars were coupled with 67 F_1 sows to obtain 470 F_2 animals. In addition, gene-expression analyses were carried out on 56 females from a backcross (BC1_LD) generated by crossing five F_1 (Iberian x Landrace) boars with 23 Landrace sows. All animals were maintained under intensive conditions and feeding was *ad libitum* with a cereal-based commercial diet. The experiments were performed in Europe following national and institutional guidelines for the ethical use and treatment of animals in experiments. In addition, the protocol was approved by the Ethical Committee of the Institution (IRTA Institut de Recerca i Tecnologia Agroalimentàries). F_2 animals were slaughtered at an average age of 175.5 ± 0.3 days. However, tissues for RNA extraction were not isolated from animals of the F_2 generation. Backcross animals were slaughtered at an average age of 179.8 ± 2.6 days, and samples of liver and adipose tissue were collected, snap-frozen in liquid nitrogen and stored at -80°C until analysis.

Genomic DNA was extracted from blood samples of all animals by the phenol-chloroform method, as described elsewhere.

Traits analyzed

The composition of 10 FA in IMF and BF (taken between the third and the fourth ribs) tissues was determined by gas chromatography as described in [16,17,19]. Subsequently, the percentage of each FA, relative to the total FA, was calculated as well as the global percentages of SFA, MUFA, PUFA and related indices, including desaturation and elongation indices.

Genotyping and quality control

A total of 470 animals were genotyped for 144 SNPs located on SSC8; these include a selection of 142 informative SNPs derived from the Porcine SNP60K BeadChip [20] and two SNPs that corresponded to the previously detected polymorphisms in the *FABP2* [21] and *MTTP* [22] genes. These SNPs [See Additional file 1: Table S1] were included in a custom-generated panel,

genotyped using a Veracode Golden Gate Genotyping Kit (Illumina Inc.) and analyzed with a Bead Xpress Reader (Illumina Inc.). SNP positions were based on the whole-genome sequence assembly 10.2 build of *Sus scrofa* (http://www.animalgenome.org/repository/pig/). All genotypes were assigned using the GenomeStudio software (Illumina Inc.). Markers that had a minor allele frequency (MAF) lower than 5% and missing genotypes that had a frequency greater than 5% were removed using PLINK [23] software. In total, 133 SNPs (92%) passed this quality-threshold filter and were used in the subsequent analysis. Genotypes of all the parents were obtained with the 60 K SNP chip (Illumina) [17] or by pyrosequencing [21,22].

SNPs *SETD7:c.-1034T > G*, *SETD7:c.700G > T* and *ELOVL6:c.-533C > T* were genotyped using the KASP SNP genotyping system platform (http://www.lgcgenomics.com/genotyping/). Besides these, two new microsatellites in the *MAML3* gene were genotyped by PCR amplification and capillary electrophoresis and fluorescent detection using an ABI Prism 3730 DNA Analyzer (Applied Biosystems).

Fifty-six animals of the BC1_LD were genotyped for SNPs *SETD7:c.-1034T > G* and *SETD7:c.700G > T* and the two *MAML3* microsatellites for gene-expression studies. In addition, a subset of 168 F_2 animals were genotyped for SNPs *ELOVL6:c.-533C > T*, *SETD7:c.700G > T* and the two *MAML3* microsatellites for association studies. All parents and grandparents of these animals were also genotyped in the same way.

Association analysis

Association analysis was performed for FA composition and indices of FA metabolism in 470 F_2 animals. A mixed model that accounts for additive effects was performed using Qxpak 5.0 [24]:

$$y_{ijlkm} = Sex_i + Batch_j + \beta c_l + \lambda_l a_k + u_l + e_{ijlkm},$$

where y_{ijlkm} is the l^{th} individual record, sex (two levels) and batch (five levels) are fixed effects, ß is a covariate coefficient with *c* being carcass weight, λ_l is a -1, 0, +1 indicator variable depending on the l^{th} individual genotype for the k^{th} SNP, a_k represents the additive effect associated with SNP, u_l represents the infinitesimal genetic effect treated as random and distributed as $N(0, \mathbf{A}\sigma_u)$ where **A** is a numerator of the kinship matrix and e_{ijlkm} is the residual. A similar model that fitted different QTL effects was used to test the hypothesis of the presence of two QTL located in the studied regions with effects a_1 and a_2 on the same FA:

$$y_{ijlkm} = Sex_i + Batch_j + \beta c_l + \lambda_l a_{1k} + \lambda_l a_{2k} + u_l + e_{ijlkm},$$

The R package q-value [25] was used to calculate the false-discovery rate (FDR), and the cut-off of the significant association at the whole-genome level was set at the q-value ≤ 0.05. Version 2.15.2 of R [26] was used to calculate the descriptive statistics for the 10 analyzed traits and their related indices.

For linkage and linkage disequilibrium (LDLA) analysis, haplotypes were reconstructed using DualPHASE software [27], which exploits population (linkage disequilibrium) and family information (Mendelian segregation and linkage) in a Hidden Markov Model setting. Then, QTL fine-mapping was performed for the most significant traits C16:1(n-7), C18:0/C16:0, C16:1(n-7)/C18:1(n-7), and the FA average chain-length (ACL) by applying the mixed model:

$$\mathbf{y} = \mathbf{Xb} + \mathbf{Z_h h} + \mathbf{Z_u u} + \mathbf{e},$$

in which **b** is a vector of fixed effects (sex and batch), **h** is the vector of random QTL effects corresponding to the K cluster defined by the Hidden State, **u** is the vector of random individual polygenic effects and **e** is the vector of individual error.

Amplification and sequencing of the pig *MAML3* and *SETD7* genes

Genomic DNA samples from 10 individuals of the BC1_LD and two Iberian boars were used to amplify and sequence the proximal promoter and exon 1 of the *MAML3* and *SETD7* genes.

A 931-bp region of the *MAML3* gene was amplified and sequenced in two overlapping fragments of 517 bp and 663 bp. Primers [See Additional file 2: Table S2] were designed based on a SSC8 sequence of a *Sus scrofa* mixed breed [ENSSSCG00000009060] available from the *Sscrofa10.2* database and conserved with the human *MAML3* gene [ENSG00000196782].

For the *SETD7* gene, two overlapping fragments of 473 bp and 478 bp were amplified and sequenced. Primers [See Additional file 2: Table S2] were designed based on a SSC8 sequence of a *Sus scrofa* mixed breed [ENSSSCG00000030396] available from the *Sscrofa10.2* database and conserved with the human *SETD7* gene [ENSG00000145391].

All primers were designed using the PRIMER3 software [28] and were validated using the PrimerExpress 2.0 software (Applied Biosystems).

PCR (polymerase chain reactions) were carried out in a total volume of 25 μL containing 0.6 units of AmpliTaq Gold (Applied Biosystems), 1.5 to 2.5 mM $MgCl_2$ depending on the primers [See Additional file 2: Table S2], 0.2 mM of each dNTP, 0.5 μM of each primer and 20 ng of genomic DNA. The temperature profile was 94°C for 10 min and 35 cycles at 94°C for 1 min,

58°C to 62°C depending on the primers [See Additional file 2: Table S2] for 1 min and 72°C for 1.5 min, including a final step of 7 min at 72°C. Gradient parameters were determined based on size and GC content of the amplicon. The samples were then analyzed on 1.5% agarose gels. Purification was performed using an Exonuclease I and FastAP™ Thermosensitive Alkaline Phosphatase [29]. For the sequencing reaction, we used the Big Dye Terminator v.3.1 Cycle Sequencing Kit and an ABI Prism 3730 DNA analyzer was employed (Applied Biosystems). Polymorphisms were checked through the Seq scape v2.1.1 program (Applied Biosystems).

Detection of microsatellite polymorphisms

Based on the sequencing results of the promoter region and exon 1 of the *MAML3* gene, two new microsatellites were identified. Both microsatellites were independently amplified using fluorescent primers [See Additional file 2: Table S2]. PCR were performed in a 25-μL reaction mix containing 20 ng of genomic DNA, 0.2 mM of each dNTP, 2.5 mM $MgCl_2$, 0.5 μM of each PCR primer and 0.6 units of AmpliTaq Gold (Applied Biosystems). PCR were run as follows: 94°C for 10 min, 35 cycles of 94°C for 1 min, 58°C for 1 min, 72°C for 1.5 min and a final extension step at 72°C for 7 min. The two amplicons were mixed at a ratio of 1:3 (HEX: FAM) and analyzed using capillary electrophoresis on an ABI Prism 3730 DNA analyzer (Applied Biosystems) and the ROX-500 GeneScan Size Standard. The peak height of each product was determined using Peak Scanner 2 software (Applied Biosystems).

RNA isolation and cDNA synthesis

Total RNA was extracted from liver and BF tissues using the RiboPure kit (Ambion), according to the manufacturer's recommendations. RNA was then quantified using a NanoDrop ND-1000 spectrophotometer (NanoDrop products) and RNA integrity was assessed with an Agilent Bioanalyzer-2100 (Agilent Technologies). One μg of total RNA of each sample was reverse-transcribed using the High-Capacity cDNA Reverse Transcription kit (Applied Biosystems) in a reaction volume of 20 μL.

Gene-expression quantification

Fifty-six females of the BC1_LD were used to quantify gene expression. The expression of *MAML3* and *SETD7* was analyzed using the 48.48 microfluidic dynamic array IFC chip (Fluidigm) according to the manufacturer's instructions. Briefly, 2 μL of 1:5 diluted cDNA was pre-amplified using 2X Taqman PreAmp Master Mix (Applied Biosystems) and 50 nM of each primer pair in 5 μL reaction volume. The cycling program consisted of an initial step of 10 min

at 95°C followed by 16 cycles of 15 s at 95°C and 4 min at 60°C. At the end of this pre-amplification step, the reaction products were diluted 1:5 (diluted pre-amplification samples). RT-qPCR on the dynamic array chips was conducted on the BioMarkTM system (Fluidigm). A 5-μL pre-mix sample containing 2.5 μL of SsoFast EvaGreen Supermix with Low ROX (Bio-Rad), 0.25 μL of DNA Binding Dye Sample Loading Reagent (Fluidigm) and 2.25 μL of diluted pre-amplification samples (1:16 or 1:64 from the diluted pre-amplification samples from liver and BF samples, respectively), as well as a 5-μL assay mix containing 2.5 μL of Assay Loading Reagent (Fluidigm), 2.25 μL of DNA Suspension Buffer (Teknova) and 0.25 μL of 100 μM primer pairs (500 nM in the final reaction) were mixed inside the chip using the IFC controller MX (Fluidigm). The cycling program consisted of an initial step of 60 s at 95°C followed by 30 cycles of 5 s at 96°C and 20 s at 60°C. A dissociation curve was also drawn for each primer pair.

Data were collected using the Fluidigm Real-Time PCR analysis software 3.0.2 (Fluidigm) and analyzed with the DAG expression software 1.0.4.11 [30] using standard curves for relative quantification. Relative standard-curves with a four-fold dilutions series (1/4, 1/16, 1/64, 1/256, 1/1024) of a pool of 10 cDNA samples were constructed for each gene to extrapolate the value of the quantities of each studied sample. Of the four endogenous genes tested (*ACTB*, *B2M*, *HPRT1*, *TBP*), *ACTB* and *TBP* had the most stable expression [31] in both tissues. The normalized quantity values of each sample and assay were used to compare our data.

PCR primer sequences [See Additional file 2: Table S2] were designed using PrimerExpress 2.0 software (Applied Biosystems).

Mean values between genotypes were compared using a linear model implemented in R, which performs a single stratum analysis of variance considering sex and batch as fixed effects. Differences were considered statistically significant at a p-value of 0.05.

Results and discussion

Association studies and combined linkage disequilibrium and linkage analyses

A custom panel of 144 SNPs located on SSC8 was used to genotype 470 F_2 animals. Association analyses for the BF FA composition in the C14:0 to C22:0 ranges were performed with genotypes from a subset of 133 SNPs (call rate > 0.99). Statistically significant associations were found (Table 1) for the SFA myristic (C14:0), palmitic (C16:0) and stearic acids (C18:0). Among MUFA, palmitoleic acid (C16:1(n-7)) and oleic acid (C18:1(n-9)) were associated, whereas for

PUFA only eicosadienoic acid (C20:2(n-6)) was significant. Similarly, the ACL metabolic ratio showed a significant association. A strong association signal was found for the C16:1(n-7)/C16:0 desaturation ratio and two elongation ratios: C18:0/C16:0 and C18:1(n-7)/C16:1(n-7).

Table 1. Significant SNPs affecting BF FA composition (FDR = 0.05) in an association study with 470 animals of the F_2 generation

Trait	Chromosomal region (Mb)	SNP	LR	*P*-value	*a* (SE)
C14:0	93.79	ALGA0048597	17.2127	3.34E-05	0.042 (0.019)
	117.55	ALGA0049135	18.7843	1.46E-05	0.055 (0.016)
C16:0	93.72	ALGA0048594	32.4610	1.22E-08	0.573 (0.881)
	117.66	ALGA0049139	48.1404	3.97E-12	0.599 (0.871)
C18:0	91.56	H3GA0025111	11.7215	6.18E-04	-0.254 (0.630)
	119.85[1]	INRA0030422	20.6040	5.65E-06	-0.366 (0.616)
C16:1(n-7)	91.56	H3GA0025111	42.9598	5.59E-11	0.163 (0.082)
	119.85[1]	INRA0030422	71.7870	1.11E-18	0.223 (0.082)
C18:1(n-9)	93.66	ALGA0048589	22.4009	2.21E-06	-0.651 (1.589)
	117.66	ALGA0049139	33.1059	8.73E-09	-0.672 (1.571)
C20:2(n-6)	94.73	MARC0097057	23.1170	1.52E-06	-0.032 (0.017)
	117.55	ALGA0049135	23.9259	1.00E-06	-0.039 (0.017)
ACL	93.72	ALGA0048594	46.5350	9.00E-12	-0.020 (0.001)
	117.66	ALGA0049139	71.4236	1.11E-16	-0.021 (0.001)
C16:1(n-7)/C16:0	91.56	H3GA0025111	22.7521	1.84E-06	0.006 (0.000)
	119.85[1]	INRA0030422	37.4524	9.37E-10	0.008 (0.000)
C18:0/C16:0	91.56	H3GA0025111	47.8703	4.55E-12	-0.023 (0.002)
	119.85[1]	INRA0030422	76.1635	1.11E-16	-0.032 (0.002)
C18:1(n-7)/C16:1(n-7)	93.72	ALGA0048594	32.8062	1.02E-08	-0.076 (0.016)
	119.85[1]	INRA0030422	61.0692	5.55E-15	-0.089 (0.015)
C20:2(n-6)/C18:2(n-6)	120.99	ALGA0049254	13.8456	1.98E-04	-0.003 (0.000)

LR = Likehood ratio test values; *a* (SE): additive effect (standard error); [1]SNPs SIRI0000509 (119.73 Mb) and H3GA0025321 (119.89 Mb) showed the same *P*-value.

Two regions that contain trait-associated SNPs (TAS) were clearly visualized in the association plots at around 93 Mb and 119 Mb for all of the above-mentioned FA and indices with the exception of the C20:2(n-6)/C18:2(n-6) elongation ratio, which showed only one significant TAS region at 120.99 Mb (Table 1). For all significant traits, the 119 Mb TAS region showed a stronger signal than the 93 Mb region. The strongest effects of both TAS regions were found for palmitoleic acid (C16:1(n-7)) content and C18:0/C16:0 and C18:1(n-7)/C16:1(n-7) elongation ratios.

A combination of linkage disequilibrium and linkage analysis (LDLA) was then performed for the most significantly associated traits [See Additional file 2: Table S3]. With this haplotype-based approach, it is possible to simultaneously exploit linkage analysis and linkage disequilibrium. Several studies have shown the usefulness of this strategy for fine-mapping and QTL interval reduction [27,32]. The LDLA study identified the two TAS regions by association analysis, with the 119 Mb region showing the strongest statistical signal for all analyzed traits. Figure 1 shows the two genomic regions identified for the C18:0/C16:0 elongation ratio. Plots of the other three traits analyzed are shown in Additional file 3: Figure S1.

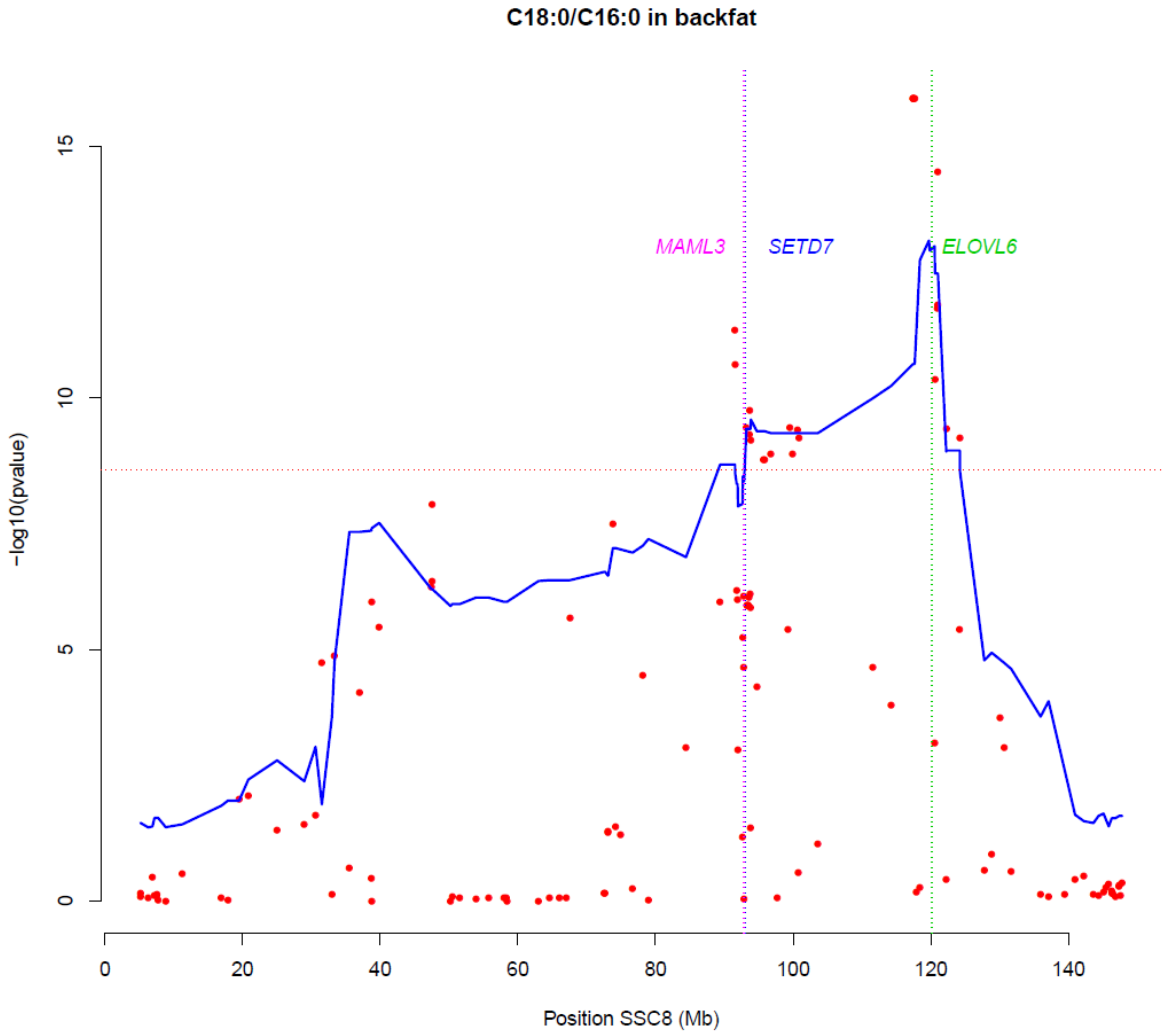

Figure 1. Association study and LDLA of the C18:0/C16:0 elongation ratio in BF. Plot of association study (red points) and LDLA patterns (blue line) for the stearic/palmitic ratio; the X-axis represents positions in Mb on SSC8, and the Y-axis shows the –log10 (p-value); vertical, the pink line represents the position of the *MAML3* gene, the blue line represents the position of the *SETD7* gene and the green line represents the position of the *ELOVL6* gene on SSC8; horizontal, dashed lines mark the association study significance level (FDR-based q-value ≤ 0.05); positions in Mb are relative to the *Sscrofa10.2* assembly of the pig genome.

In order to determine whether one or two QTL were segregating on SSC8 for the BF FA and their indices, models fitting one QTL against a model considering two different QTL were tested. Results of the LR test indicated that the model with two QTL was the most likely for the 10 traits analyzed [See Additional file 2: Table S4].

Previously, a QTL scan for BF FA composition was performed with 369 animals from the same F_2 generation [16], but only six microsatellite markers were genotyped. A clear effect of SSC8 markers was observed only for percentages of palmitic (C16:0) and palmitoleic (C16:1(n-7)) FA and ACL. A suggestive effect on percentage of oleic acid (C18:1(n-9)) was also observed. However, the confidence interval for this QTL was greater than 30 cM. Two other studies of our group analyzed positional candidate genes for this QTL, i.e. *FABP2* [21] and *MTTP* [22], but the

localization of the QTL was not refined. In addition, QTL for IMF palmitic (C16:0) FA composition have been reported in a Duroc x Large White F_2 cross [13] and for stearic (C18:0) FA in a White Duroc x Erhualian F_2 cross [14].

A GWAS for IMF FA composition [17] with genotypes from the 60 K SNP chip (Illumina) was carried out using 144 animals from a related backcross population (BC1_LD). The strongest signals on SSC8 were observed for the palmitoleic (C16:1(n-7)) FA content and the C18:1(n-7)/C16:1(n-7) ratio for SNPs ALGA0048684 and SIRI0000509, which in the *Sscrofa10.2* assembly are located at 99.2 Mb and 119.7 Mb, respectively. Furthermore, two significant pleiotropic regions (at 93.3 Mb - 99.5 Mb and 110.9 Mb - 126.9 Mb) with effects on palmitoleic (C16:1(n-7)) FA in both IMF and BF tissues have been identified in the same backcross [18]. For palmitic (C16:0) FA, a large (83.8 Mb - 130.6 Mb) chromosomal interval was significant for both BF and IMF [18].

Here, two QTL at approximately 93 Mb and 119 Mb were detected and affected the BF composition of the six FA and the four indices mentioned above in the 470 F_2 animals. The palmitoleic (C16:1(n-7)) FA QTL on SSC8 have been shown to be segregating in different crosses of the IBMAP population, and both QTL have a pleiotropic effect on BF and IMF FA deposits.

Gene annotation and identification of polymorphisms in positional candidate genes

Gene annotation of the two TAS genomic regions allowed us to identify genes related to FA metabolism. In the first region, the genes *mastermind-like 3* (*MAML3*) (at position 92.67 Mb) and *SET domain containing lysine methyltransferase 7* (*SETD7*) (at position 93.13 Mb) were found. Both genes have recently been reported in a predicted co-association gene network for intramuscular FA composition in pigs (Ramayo *et al.*, 2013; unpublished observations).

MAML3 is a member of the *Mam* gene family, which plays an essential role in the stabilization of Notch transcriptional activation complexes [33]. This Notch signaling pathway mediates short-range communication between cells, and it has recently been associated with the regulation of lipogenesis and gluconeogenesis in liver [34]. A 931-bp fragment of the pig *MAML3* gene that covers part of the promoter region and part of exon 1, was amplified from genomic DNA and sequenced. Two novel microsatellites were found: *MAML3_MS1,* a $(CA)_n$ tandem repeat located in the promoter region and *MAML3_MS2,* a $(CGG)_n$ tandem repeat identified in exon 1. The variability of both microsatellites is described in Table 2.

Table 2. Microsatellites identified in the *MAML3* gene

SSR locus	Repeat	5' fluorescent label	Number of alleles	Size of alleles
MAML3_MS1	(CA)n	HEX	8	233,239,243,245, 247,251,257,259
MAML3_MS2	(CGG)n	FAM	2	135,138

The product of the *SETD7* gene is a histone methyltransferase that specifically monomethylates Lys-4 of histone H3 [35] and, thus, it is involved in the epigenetic transcriptional regulation of genes, activating genes such as *collagenase* or *insulin* [36]. To identify polymorphims in the porcine *SETD7* gene, a 839-bp fragment of the *SETD7* promoter and exon 1 was amplified from genomic DNA and sequenced. In addition, the identification of polymorphisms in the entire coding region of the *SETD7* gene was performed using *RNA-Seq* data [37] with the Integrative Genomics Viewer (IGV) software (http://www.broadinstitute.org/igv/). Alignment and analysis of these sequences led to the identification of nine polymorphisms (Table 3). Two of these polymorphisms were used to genotype BC1_LD animals, one located in the promoter region (*SETD7:c.-1034T > G*) and one non-synonymous polymorphism in exon 6 (*SETD7:c.700G > T*), which determines an amino-acid change of valine to leucine. Apart from the fact that these SNPs are located in the *SETD7* gene, they were selected because they showed divergent allelic frequencies between the Iberian and Landrace IBMAP founders i.e. the *SETD7:c.-1034 T* and *SETD7:c.700 T* alleles were fixed in the Iberian boars. Complete linkage disequilibrium between the two SNPs was observed in the genotyped BC1_LD animals and, thus, only *SETD7:c.700G > T* was further genotyped in 168 animals belonging to the F_2 generation.

Table 3. Polymorphisms identified in the proximal promoter and coding regions of the *SETD7* gene

Gene localization	Position (bp)	Ref[4]	Pol[5]	Aminoacid change
Promoter[1]	-1300	A	G	
	-1034[3]	T	G	
	-980	C	A	
	-632	T	C	
Exon 4[2]	462	C	T	
Exon 6[2]	700[3]	G	T	VAL/LEU
	708	G	A	
Exon 7[2]	807	C	T	
Exon 8[2]	960	C	T	

[1]Positions relative to the transcription start-site using, as reference, the GenBank ENSSSCG00000030396 sequence; [2]referring to the coding region, using RNA-Seq data; [3]SNPs genotyped; [4]Ref = nucleotide in the reference sequence; [5]Pol = polymorphisms found.

In the second region, the *ELOVL6* gene was identified at position 120.12 Mb. The *ELOVL6* gene is a strong positional and functional candidate gene involved in *de novo* lipogenesis and acts on the elongation of SFA and MUFA. A polymorphism in the promoter region of this gene (*ELOVL6:c.-533C> T*) has previously been associated with percentages of palmitic and palmitoleic FA in muscle and backfat in the BC1_LD population [38]. In addition, expression of the *ELOVL6* gene was lower in the backfat of animals with the Iberian allele in comparison to those with the Landrace allele. As expected from the elongation function of this gene, a lower *ELOVL6* expression was associated with a higher percentage of palmitic and palmitoleic FA in muscle and adipose tissue [38].

Based on our results, the observed effects on FA composition and indices are concordant with a lower expression of the *ELOVL6* gene in animals with the Iberian allele [38] for both TAS regions (Figure 2). *ELOVL6* elongates palmitic (C16:0) to stearic (C18:0), and palmitoleic (C16:1(n-7)) to vaccenic (C18:1(n-7)) FA. Thus, a lower ELOVL6 activity associated with the Iberian allele will directly decrease these elongation ratios. Moreover, as observed, a lower ELOVL6 activity will result in the accumulation of palmitic (C16:0) and palmitoleic (C16:1(n-7)) FA and a reduction in stearic (C18:0) FA content (Figure 2).

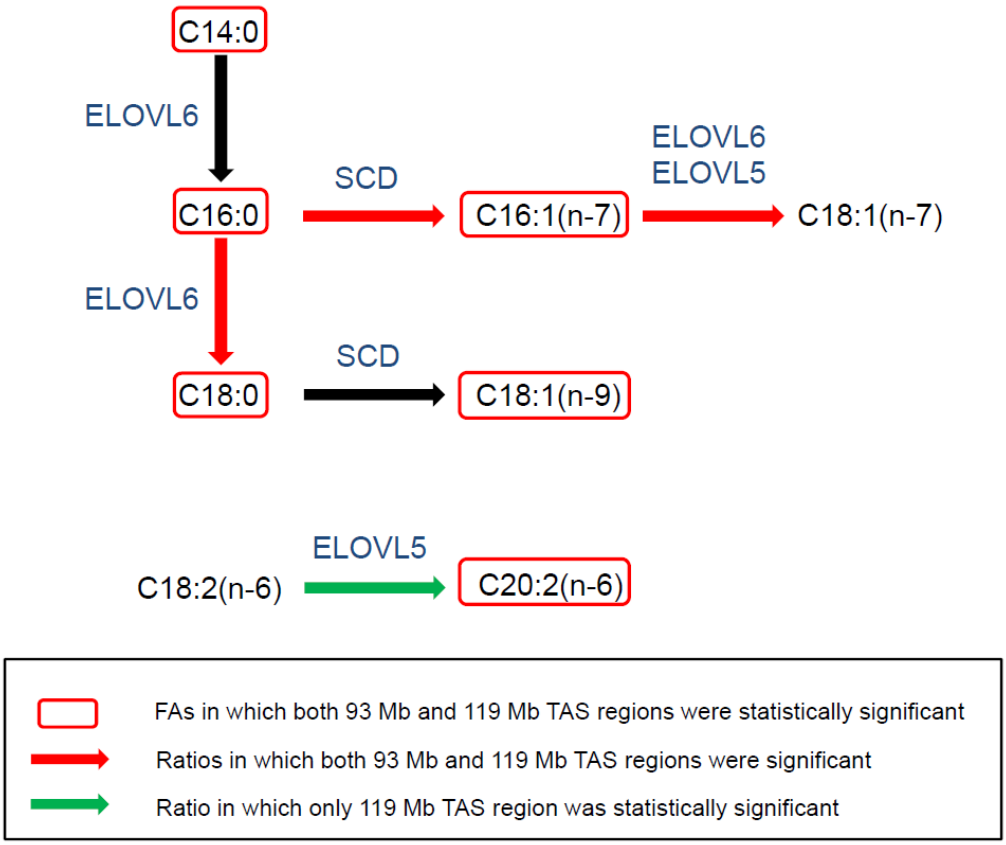

Figure 2. Schematic representation of the elongation pathway of 16 and 18 carbon FAs. Statistically significant FA (red square) and ratios of elongation and desaturation (colored arrows) are shown for BF FA composition in the F_2 generation.

Regarding oleic FA (C18:1(n-9)), the main dietary FA, its content in BF was decreased in animals with the Iberian allele for the TAS regions on SSC8. It must be noted that the opposite effect was observed in the major SSC4 and SSC6 TAS regions for oleic (C18:1(n-9)) IMF content [17].

Effect of the *SETD7:c. 1034T > G* and *SETD7:c.700G > T* SNPs and *MAML3* microsatellites on gene expression

The expression profiles of the pig *MAML3* and *SETD7* genes were studied in liver and BF tissues of 56 BC1_LD females by RT-qPCR. The analysis of gene expression in the F_2 generation was not possible because tissues for RNA isolation were not available. Differences in the expression of *MAML3* among animals were observed, with coefficients of variation (CV) of 35% and 42% in liver and BF, respectively. The *SETD7* gene expression was less variable, with CV values of 18% and 33% in liver and BF tissue, respectively. However, no significant differences in expression of *SETD7* were detected among animals classified according to the *SETD7* genotypes (either *SETD7:c.-1034T > G* or *SETD7:c.700G > T*) in either tissue. Similarly, no differences in expression of *MAML3* were observed among animals classified according to

the *MAML3_MS1* and *MS2* microsatellites. In addition, no significant correlation was found between expression levels of *MAML3* or *SETD7* in the liver and adipose, which suggests that different and tissue-specific mechanisms control the liver and adipose tissue expression of *MAML3* and *SETD7*.

Association study for BF FA composition with markers located in positional candidate genes

Two microsatellites in the *MAML3* gene (*MAML3_MS1* and *MAML3_MS2*), one SNP in the *SETD7* gene (*SETD7:c.700G > T*), and one SNP in the *ELOVL6* gene (*ELOVL6:c.-533C > T*) were used to genotype 168 animals of the F_2 generation. An association analysis with these markers and the SSC8 genotypes from the 133 SNPs of our custom porcine SNP panel was performed.

For the first region (93 Mb), polymorphisms in the *SETD7* and *MAML3* genes were studied. For *SETD7*, the *SETD7:c.700G > T* polymorphism did not show the most significant association (Table 4). In addition, *MAML3* gene microsatellites showed no significant associations for any of the traits studied. However, the SNPs showing the strongest signals (Table 4) were located within a 2 Mb interval of the *SETD7* and *MAML3* genes. These results suggest that other non-genotyped polymorphisms may cause the observed effects on FA composition in the 93-Mb region.

Table 4. Significant SNPs affecting BF FA composition (FDR = 0.05) in 168 F_2 animals

Trait	Chromosomal region (Mb)	SNP	LR	*P*-value	*a* (SE)
C16:0	93.29	MARC0024098	14.3307	1.53E-04	0.645 (0.828)
	120.01	*ELOVL6:c.533C > T*	16.9446	3.85E-05	0.652 (0.818)
C16:1(n-7)	93.62	MARC0005229	23.5897	1.19E-06	0.181 (0.049)
	120.01	*ELOVL6:c.533C > T*	33.1038	8.74E-09	0.221 (0.045)
C18:1(n-9)	93.29	MARC0024098	23.7323	1.11E-06	-0.838 (0.810)
	117.44	ASGA0039595	24.0369	9.45E-07	-0.827 (0.809)
C18:1(n-7)	142.23	ALGA0106925	13.3222	2.62E-04	0.174 (0.049)
ACL	93.29	MARC0024098	19.4268	1.05E-05	-0.021 (0.001)
	120.01	*ELOVL6:c.533C > T*	24.7173	6.64E-07	-0.022 (0.001)
MUFA	117.44	ASGA0039595	13.8134	2.02E-04	-0.724 (1.108)
C16:1(n-7)/C16:0	93.62	MARC0005229	16.2984	5.41E-05	0.007 (0.000)
	127.78	MARC0087394	20.5866	5.70E-06	0.007 (0.000)
C18:0/C16:0	93.29	MARC0024098	17.2826	3.22E-05	-0.027 (0.001)
	120.01	*ELOVL6:c.533C > T*	28.3700	1.00E-07	-0.032 (0.001)
C18:1(n-7)/C16:1(n-7)	93.77	MARC0020530	26.6172	2.48E-07	-0.092 (0.009)
	120.01	*ELOVL6:c.533C > T*	36.7487	1.34E-09	-0.101 (0.008)
C20:2(n-6)/C18:2(n-6)	91.93	ALGA0048544	17.4256	2.99E-05	0.009 (0.000)
	93.62	MARC0005229	15.8393	6.90E-05	-0.004 (0.000)

LR = Likehood ratio test values; *a* (SE) = additive effect (standard error).

For the second region (119 Mb), a polymorphism in the *ELOVL6* gene was studied. The *ELOVL6:c.-533C > T* polymorphism showed the highest association with percentage of palmitic and palmitoleic FA, ACL, and C18:0/C16:0 and C18:1(n-7)/C16:1(n-7) ratios (Table 4). Hence, these results are consistent with those found in the IMF FA composition of the BC1_LD generation [38]. The clear association of the *ELOVL6:c.-533C > T* polymorphism with percentage of FA in IMF and BF indicates a pleiotropic effect of this gene in both tissues.

Analysis of the additive value of SNPs *SETD7:c.700G > T* and *ELOVL6:c.-533C > T* showed a higher contribution of *ELOVL6:c.-533C > T* SNP for all studied FA and indices. Furthermore, the additive value of the two SNPs [See Additional file 2: Table S5] showed an effect in the same direction. For instance, the Iberian alleles of both QTL increased palmitic and palmitoleic FA content and reduced the elongation ratios. These results are in accordance with the reported Iberian-Landrace breed differences in BF FA composition [39].

Conclusions

In summary, two TAS regions at 93 Mb and 119 Mb on SSC8 affect BF FA composition. Both regions showed a strong effect on palmitoleic acid content and C18:0/C16:0 and C18:1(n-7)/C16:1(n-7) elongation ratios. The *MAML3* and *SETD7* genes were analyzed as positional candidate genes of the 93-Mb TAS region. Two novel microsatellites were identified in the *MAML3* gene, and nine SNPs in the *SETD7* gene. However, the association analysis did not reveal any significant association between the *MAML3* microsatellite genotypes and the traits studied, and the *SETD7:c.700G > T* SNP did have not the strongest signal in the 93-Mb region. Although the expression of *MAML3* and *SETD7* genes in liver and adipose tissue varied among animals, it was not associated with any of the genotyped polymorphisms in these genes. These results suggest that the polymorphisms studied in *MAML3* and *SETD7* are not the causal variants of the 93-Mb QTL. Conversely, for the 119-Mb region, the *ELOVL6:c.-533C > T* SNP was strongly associated with percentage of palmitic and palmitoleic FA, ACL, and C18:0/C16:0 and C18:1(n-7)/C16:1(n-7) elongation ratios. These results suggest pleiotropic effects of *ELOVL6:c.-533C > T* on BF and IMF FA composition.

Competing interests

The authors declare that they have no competing interests.

Authors' contributions

JMF, MB and YRC conceived and designed the experiment. JMF was the principal investigator of the project. NI, MM and JMF collected samples. APO, JC, MB and MR performed the DNA and RNA isolation. MR, AC, JC and MB identified the polymorphisms and performed the genotyping. MR, YRC and JC performed the association analysis. MR, AC, APO and MB performed the gene-expression analysis. MR and JMF wrote the manuscript. All authors read and approved the final manuscript.

Acknowledgments

This work was funded by MICINN AGL2008-04818-C03/GAN and MINECO AGL2011-29821-C02 and the Innovation Programme Consolider-Ingenio 2010 (CSD2007-00036). M. Revilla is a Master's student of Animal Breeding and Biotechnology of Reproduction (Polytechnical University of Valencia and Autonomous University of Barcelona). Y. Ramayo-Caldas was funded by a FPU grant (AP2008-01450), J. Corominas by a FPI scholarship from the Ministry of Education (BES-2009-018223) and A. Puig-Oliveras by a PIF scholarship (458-01-1/2011). This manuscript has been proofread by Chuck Simons, a native English speaking university instructor in English.

References

1. Rothschild MF, Ruvinsky A: *The Genetics of the Pig.* 2nd edition. Wallingford: CABI; 2011.
2. Park GB, Moon SS, Ko YD, Ha JK, Lee JG, Chang HH, Joo ST: **Influence of slaughter weight and sex on yield and quality grades of Hanwoo (Korean native cattle) carcasses.** *J Anim Sci* 2002, **80:**129–136.
3. Ventanas S, Tejeda JF, Estévez M: **Chemical composition and oxidative status of tissues from Iberian pigs as affected by diets: extensive feeding v.oleic acid- and tocopherol-enriched mixed diets.** *Animal* 2008, **2:**621–630.
4. Clarke R, Frost C, Collins R, Appleby P, Peto R: **Dietary lipids and blood cholesterol: quantitative meta-analysis of metabolic ward studies.** *BMJ* 1997, **314:**112–117.
5. Mensink RP, Katan MB: **Effect of dietary fatty acids on serum lipids and lipoproteins. A meta-analysis of 27 trials.** *Arterioscler Thromb* 1992, **12:**911–919.
6. Wolfram G: **Dietary fatty acids and coronary heart disease.** *Eur J Med Res* 2003, **8:**321–324.

7. Hunter JE, Zhang J, Kris-Etherton PM: **Cardiovascular disease risk of dietary stearic acid compared with trans, other saturated, and unsaturated fatty acids: a systematic review.** *Am J Clin Nutr* 2010, **91:**46–63.
8. Astrup A, Dyerber J, Elwood P, Hermansen K, Hu FB, Jakobsen MU, Kok FJ, Krauss RM, Lecerf JM, LeGrand P, Nestel P, Risérus U, Sanders T, Sinclair A, Stender S, Tholstrup T, Willet WC: **The role of reducing intakes of saturated fat in the prevention of cardiovascular disease: where does the evidence stand in 2010?** *Am J Clin Nutr* 2011, **93:**684–688.
9. Hu FB, Stampfer MJ, Manson JE, Ascherio A, Colditz GA, Speizer FE, Hennekens CH, Willett WC: **Dietary saturated fats and their food sources in relation to the risk of coronary heart disease in women.** *Am J Clin Nutr* 1999, **70:**1001–1008.
10. Harris WS, Poston WC, Haddock CK: **Tissue n-3 and n-6 fatty acids and risk for coronary heart disease events.** *Atherosclerosis* 2007, **193:**1–10.
11. López-Huertas E: **Health effects of oleic acid and long chain omega-3 fatty acids (EPA and DHA) enriched milks. A review of intervention studies.** *Pharmacol Res* 2010, **61:**200–207.
12. Ros E: **Dietary cis-monounsaturated fatty acids and metabolic control in type 2 diabetes.** *Am J Clin Nutr* 2003, **78:**617S–625S.
13. Sanchez MP, Iannuccelli N, Basso B, Bidanel JP, Billon Y, Gandemer G, Gilbert H, Larzul C, Legault C, Riquet J, Milan D, Le Roy P: **Identification of QTL with effects on intramuscular fat content and fatty acid composition in a Duroc x Large White cross.** *BMC Genet* 2007, **8:**55.
14. Guo T, Ren J, Yang K, Ma J, Zhang Z, Huang L: **Quantitative trait loci for fatty acid composition in longissimus dorsi and abdominal fat: results from a White Duroc x Erhualian intercross F2 population.** *Anim Genet* 2009, **40:**185–191.
15. Uemoto Y, Soma Y, Sato S, Ishida M, Shibata T, Kadowaki H, Kobayashi E, Suzuki K: **Genome-wide mapping for fatty acid composition and melting point of fat in a purebred Duroc pig population.** *Anim Genet* 2012, **43:**27–34.
16. Clop A, Ovilo C, Pérez-Enciso M, Cercos A, Tomas A, Fernandez A, Coll A, Folch JM, Barragan C, Diaz I, Oliver MA, Varona L, Silio L, Sanchez A, Noguera JL: **Detection of QTL affecting fatty acid composition in the pig.** *Mamm Genome* 2003, **14:**650–656.
17. Ramayo-Caldas Y, Mercadé A, Castelló A, Yang B, Rodríguez C, Alves E, Díaz I, Ibáñez-Escriche N, Noguera JL, Pérez-Enciso M, Fernández AI, Folch JM: **Genome-wide**

association study for intramuscular fatty acid composition in an Iberian x Landrace Cross. *J Anim Sci* 2012, **90:**2883–2893.

18. Muñoz M, Rodríguez MC, Alves E, Folch JM, Ibañez-Escriche N, Silió L, Fernández AI: **Genome-wide analysis of porcine backfat and intramuscular fat fatty acid composition using high-density genotyping and expression data.** *BMC Genomics* 2013, **14:**845.
19. Pérez-Enciso M, Clop A, Noguera JL, Ovilo C, Coll A, Folch JM, Babot D, Estany J, Oliver MA, Díaz I, Sánchez A: **A QTL on pig chromosome 4 affects fatty acid metabolism: evidence from an Iberian by Landrace intercross.** *J Anim Sci* 2000, **78:**2525–2531.
20. Ramos AM, Crooijmans RP, Affara NA, Amaral AJ, Archibald AL, Beever JE, Bendixen C, Churcher C, Clark R, Dehais P, Hansen MS, Hedegaard J, Hu ZL, Kerstens HH, Law AS, Megens HJ, Milan D, Nonneman DJ, Rohrer GA, Rothschild MF, Smith TP, Schnabel RD, Van Tassell CP, Taylor JF, Wiedmann RT, Schook LB, Groenen MA: **Design of a high density SNP genotyping assay in the pig using SNPs identified and characterized by next generation sequencing technology.** *PLoS ONE* 2009, **4:**e6524.
21. Estellé J, Mercadé A, Pérez-Enciso M, Pena RN, Silió L, Sánchez A, Folch JM: **Evaluation of *FABP2* as candidate gene for a fatty acid composition QTL in porcine chromosome 8.** *J Anim Breed Genet* 2009, **126:**52–58.
22. Estellé J, Fernández AI, Pérez-Enciso M, Fernández A, Rodríguez C, Sánchez A, Noguera JL, Folch JM: **A non-synonymous mutation in a conserved site of the *MTTP* gene is strongly associated with protein activity and fatty acid profile in pigs.** *Anim Genet* 2009, **40:**813–820.
23. Purcell S, Neale B, Todd-Brown K, Thomas L, Ferreira MA, Bender D, Maller J, Sklar P, de Bakker PI, Daly MJ, Sham PC: **PLINK: a tool set for whole-genome association and population-based linkage analyses.** *Am J Hum Genet* 2007, **81:**559–575.
24. Pérez-Enciso M, Misztal I: **Qxpak.5: Old mixed model solutions for new genomics problems.** *BMC Bioinforma* 2011, **12:**202.
25. Storey JD, Tibshirani R: **Statistical significance for genomewide studies.** *Proc Natl Acad Sci U S A* 2003, **100:**9440–9445.
26. Ihaka R, Gentleman R: **R: A language for data analysis and graphics.** *J Comput Graph Stat* 1996, **5:**299–314.
27. Druet T, Georges M: **A hidden Markov model combining linkage and linkage disequilibrium information for haplotype reconstruction and quantitative trait locus fine mapping.** *Genetics* 2010, **184:**789–798.

28. Rozen S, Skaletsky H: **Primer3 on the WWW for general users and for biologist programmers.** *Methods Mol Biol* 2000, **132:**365–386.
29. Werle E, Schneider C, Renner M, Völker M, Fiehn W: **Convenient single-step, one tube purification of PCR products for direct sequencing.** *Nucleic Acids Res* 1994, **22:**4354–4355.
30. Ballester M, Cordón R, Foch JM: **DAG expression: high-throughput gene expression analysis of real-time PCR data using standard curves for relative quantification.** *PLoS ONE* 2013, **8:**e80385.
31. Vandesompele J, De Preter K, Pattyn F, Poppe B, Van Roy N, De Paepe A, Speleman F: **Accurate normalization of real-time quantitative RT-PCR data by geometric averaging of multiple internal control genes.** *Genome Biol* 2002, **3:**RESEARCH0034.
32. Karim L, Takeda H, Lin L, Druet T, Arias JA, Baurain D, Cambisano N, Davis SR, Farnir F, Grisart B, Harris BL, Keehan MD, Littlejohn MD, Spelman RJ, Georges M, Coppieters W: **Variants modulating the expression of a chromosome domain encompassing PLAG1 influence bovine stature.** *Nat Genet* 2011, **43:**405–413.
33. Oyama T, Harigaya K, Sasaki N, Okamura Y, Kokubo H, Saga Y, Hozumi K, Suganami A, Tamura Y, Nagase T, Koga H, Nishimura M, Sakamoto R, Sato M, Yoshida N, Kitagawa M: **Mastermind-like 1 (MamL1) and mastermind-like 3 (MamL3) are essential for Notch signaling in vivo.** *Development* 2011, **138:**5235–5246.
34. Pajvani UB, Qiang L, Kangsamaksin T, Kitajewski J, Ginsberg HN, Accili D: **Inhibition of Notch uncouples Akt activation from hepatic lipid accumulation by decreasing mTorc1 stability.** *Nat Med* 2013, **19:**1054–1060.
35. Syreeni A, El-Osta A, Forsblom C, Sandholm N, Parkkonen M, Tarnow L, Parving HH, McKnight AJ, Maxwell AP, Cooper ME, Groop PH, Finn Diane Study Group: **Genetic examination of *SETD7* and *SUV39H1/H2* methyltransferases and the risk of diabetes complications in patients with Type 1 diabetes.** *Diabetes* 2011, **60:**3073–3080.
36. Chakrabarti SK, Francis J, Ziesmann SM, Garmey JC, Mirmira RG: **Covalent histone modifications underlie the developmental regulation of insulin gene transcription in pancreatic beta cells.** *J Biol Chem* 2003, **278:**23617–23623.
37. Ramayo-Caldas Y, Mach N, Esteve-Codina A, Corominas J, Castello A, Ballester M, Estelle J, Ibañez-Escriche N, Fernandez AI, Perez-Enciso M, Folch JM: **Liver transcriptome profile in pigs with extreme phenotypes of intramuscular fatty acid composition.** *BMC Genomics* 2012, **13:**547.

38. Corominas J, Ramayo-Caldas Y, Puig-Oliveras A, Pérez-Montarelo D, Noguera JL, Folch JM, Ballester M: **Polymorphism in the *ELOVL6* gene is associated with a major QTL effect on fatty acid composition in pigs.** *PLoS ONE* 2013, **8:**e53687.
39. Serra X, Gil F, Pérez-Enciso M, Oliver MA, Vázquez J, Gispert M, Díaz I, Moreno F, Latorre R, Noguera JL: **A comparison of carcass, meat quality and histochemical characteristics of Iberian (Guadyerbas line) and Landrace pigs.** *Livest Prod Sci* 1998, **56:**215–223.

Additional files

Additional file 1: Table S1. List of SNPs genotyped. List of 144 SNPs located on SSC8 genotyped and genotyping statistics.

Additional file 2: Table S2. Primers for *SETD7* and *MAML3* promoter sequencing (P), promoter and exon 1 sequencing (PE), microsatellite genotyping (MS), and RT-qPCR (RT) study. **Table S3.** Significant SNPs affecting BF FA composition (FDR = 0.05) in LDLA analyses in the F_2 generation. **Table S4**. Analysis of a two QTL model on SSC8 for the most significant regions affecting BF FA composition. **Table S5.** Additive value affecting BF FA composition in 168 F_2 animals for the *SETD7:c.700G > T* and *ELOVL6:c.533C > T* SNPs.

Additional file 3: Figure S1. Association study and LDLA of the C16:1(n-7), ACL and C18:1(n-7)/C16:1(n-7) elongation ratio in BF. Plot of association study (red points) and LDLA patterns (blue line) for palmitoleic acid, ACL and vaccenic/palmitoleic ratio; the X-axis represents positions in Mb on SSC8, and the Y-axis shows the –log10 (p-value); vertical, the pink line represents the position of the *MAML3* gene, the blue line represents the position of the *SETD7* gene and the green line represents the position of the *ELOVL6* gene on SSC8; horizontal, dashed lines mark the association study significance level (FDR-based q-value ≤ 0.05); positions in Mb are relative to the *Sscrofa10.2* assembly of the pig genome.

PAPER II

A global analysis of CNVs in swine using whole genome sequence data and association analysis with fatty acid composition and growth traits

Revilla M[1,2*], Puig-Oliveras A[1,2], Castelló A[1,2], Crespo-Piazuelo D[1,2], Paludo E[3], Fernández AI[4], Ballester M[5], Folch JM[1,2]

[1] Departament de Ciència Animal i dels Aliments, Facultat de Veterinària, Universitat Autònoma de Barcelona (UAB), Bellaterra, Spain

[2] Plant and Animal Genomics, Centre de Recerca en Agrigenòmica (CRAG), Consorci CSIC-IRTA-UAB-UB, Campus UAB, Bellaterra, Spain

[3] Department of Animal Science, Santa Catarina State University, Lages, Santa Catarina, Brazil

[4] Departamento de Genética Animal, Instituto Nacional de Investigación y Tecnología Agraria y Alimentaria (INIA), Madrid, Spain

[5] Departament de Genètica i Millora Animal, Institut de Recerca i Tecnologia Agroalimentàries (IRTA), Torre Marimon, Caldes de Montbui, Spain

[*] Corresponding author

PLoS ONE (2017). 12(5):e0177014.
http://doi.org/10.1371/journal.pone.0177014

Abstract

Copy number variations (CNVs) are important genetic variants complementary to SNPs, and can be considered as biomarkers for some economically important traits in domestic animals. In the present study, a genomic analysis of porcine CNVs based on next-generation sequencing data was carried out to identify CNVs segregating in an Iberian x Landrace backcross population and study their association with fatty acid composition and growth-related traits. A total of 1,279 CNVs, including duplications and deletions, were detected, ranging from 106 to 235 CNVs across samples, with an average of 183 CNVs per sample. Moreover, we detected 540 CNV regions (CNVRs) containing 245 genes. Functional annotation suggested that these genes possess a great variety of molecular functions and may play a role in production traits in commercial breeds. Some of the identified CNVRs contained relevant functional genes (e.g., *CLCA4, CYP4X1, GPAT2, MOGAT2, PLA2G2A* and *PRKG1*, among others). The variation in copy number of four of them (*CLCA4*, *GPAT2, MOGAT2* and *PRKG1*) was validated in 150 BC1_LD (25% Iberian and 75% Landrace) animals by qPCR. Additionally, their contribution regarding backfat and intramuscular fatty acid composition and growth–related traits was analyzed. Statistically significant associations were obtained for CNVR112 (*GPAT2*) for the C18:2(n-6)/C18:3(n-3) ratio in backfat and carcass length, among others. Notably, GPATs are enzymes that catalyze the first step in the biosynthesis of both triglycerides and glycerophospholipids, suggesting that this CNVR may contribute to genetic variation in fatty acid composition and growth traits. These findings provide useful genomic information to facilitate the further identification of trait-related CNVRs affecting economically important traits in pigs.

Introduction

The pig (*Sus scrofa*) is one of the most economically important livestock animals worldwide, and one of the main sources of animal meat for humans. The pig is also a valuable animal model for human diseases and nutrition. In recent years, genomic structural variations have received considerably more attention, as they represent the major source of genetic variation in mammalian genomes in terms of number of nucleotides involved [1]. Copy number variations (CNVs) are a type of genetic structural variation which corresponds to relatively large regions of the genome (typically larger than 1 kb) that have been deleted or duplicated, giving different numbers of copies of a DNA fragment [2]. CNVs can affect both gene expression and regulation, with potentially large phenotypic effects [3]. In humans, several studies on CNVs showed association with Mendelian diseases and complex genetic disorders, such as schizophrenia [4], cancer [5,6], and various congenital defects [7]. In pigs, CNVs have been associated with several phenotypes such as coat color [8], backfat (BF) thickness [3] and meat quality [9], demonstrating that CNVs can be considered as promising biomarkers for some economically important traits in domestic animals. Fat content and fatty acid (FA) composition determine important sensory and technological aspects of pork and meat products because of their influence on the melting point and oxidative status of porcine tissues [10]. Artificial selection to increase meat production in pigs has caused a reduction of intramuscular fat (IMF) and changes in meat FA composition in some breeds. Pork quality is important to the meat-processing industry, therefore a higher IMF content and a better FA profile, while maintaining a reduced amount of BF, is a main selection objective [11,12].

In the past few years, different approaches have been used to detect CNVs in pig genomes: array comparative genomic hybridization (aCGH) [13,14], high-density single nucleotide polymorphisms genotyping [3, 15-19] and next-generation sequencing (NGS) of whole genomes [20-23]. Ramayo-Caldas *et al.* [15] reported the first whole genome description of CNVs in the pig genome using genotypes from the 60K SNP chip (*Illumina*). Fernández *et al.* [24] also applied the SNP array method on 217 highly inbred Iberian pigs, and then used high-throughput sequencing on four of those pigs for validation. Bickhart *et al.* [20] demonstrated that the NGS has superiority over the SNP chip and aCGH in CNV detection in livestock genomes. The aCGH and SNP arrays have been extensively used for CNV screens, however, these techniques are often affected by low probe density and cross-hybridization of repetitive sequences [20]. The influence and utilization of NGS and

complementary analysis programs have provided better approaches to detect CNVs at the genome-wide level [25].

The goal of this study is to identify CNV regions (CNVRs) from whole genome sequence (WGS) data on autosomal chromosomes, using an Iberian x Landrace (IBMAP) cross, validate a selection of them in a larger number of animals and study their association with growth and meat quality traits.

Materials and Methods

Ethics Statement

All animal procedures were performed according to the Spanish Policy for Animal Protection RD1201/05, which meets the European Union Directive 86/609 concerning the protection of animals used in experimentation. Animals were sacrificed in a commercial slaughterhouse following national and institutional guidelines for the Good Experimental Practices and approved by the Ethical Committee of the Institution (IRTA- Institut de Recerca i Tecnologia Agroalimentàries).

Animal samples

Seven founders of the IBMAP experimental population [26], two Iberian boars (Guadyerbas line) and five Landrace sows, were used to identify CNVs by NGS of whole genomes. Furthermore, thirty-two individuals of different backcrosses: BC1_LD (25% Iberian and 75% Landrace; n=10), BC1_PI (25% Iberian and 75% Pietrain; n=10), and BC1_DU (25% Iberian and 75% Duroc; n=12) were used to test the variability of six computationally-predicted CNVs. Finally, association analyses between CNVs and FA composition and growth traits were performed in 150 BC1_LD individuals from the IBMAP population. All animals were maintained under intensive conditions and feeding was *ad libitum* with a cereal-based commercial diet. Backcross animals were slaughtered at an average age of 179.8±2.6 days, and samples of diaphragm tissue were collected, snap-frozen in liquid nitrogen and stored at -80°C until analysis. Genomic DNA was extracted from diaphragm tissue samples of all animals by the phenol-chloroform method [27].

NGS Data

The whole genomes of seven founders of the IBMAP population (two Iberian boars and five Landrace sows) were sequenced with the *Illumina* Hi-Seq 2000 platform (*Illumina*; San

Diego, CA, USA) in the CNAG institution (Centro Nacional de Análisis Genómico; Barcelona, Spain), obtaining 100 bp paired-end reads. The reads were mapped using Burrows-Wheeler Aligner software [28] to the reference genome (*Sscrofa10.2*), having a mean coverage of 13.1x. Sequencing information is provided in the Results section.

Detection of CNV

Control-FREEC software [29,30] was used to detect CNVs in the genomes of all individuals. This software uses GC-content to normalize read counts, and lower mappability regions can be excluded from the analysis using provided mappability tracks [29,30]. The mapped paired-end reads files were used to calculate read count in non-overlapping windows by a sliding-window approach. An optimal windows size was selected by the program for each sample (Table 1). Then, normalization of read counts was performed by GC content in the same set of windows. At the end, the software analyzed the prediction regions for gains and losses in order to assign copy numbers to these regions. The program was run using the default parameters without any control sample. Following the recommendations of Derrien *et al.* [31] to limit the number of false positives, we used a GEM mappability file created by the GEM (Genome Multi-tool) mappability program. Then, *p*-values to the predicted CNVs were added by running the "rtrackplayer" R package [32], which adds both Wilcoxon test and Kolmogorov-Smirnov test *p*-values to each Control-FREEC prediction.

The CNVRs were determined by merging CNVs identified in two or more animals when the overlap is of at least 1 bp, according to the criteria proposed by Redon *et al.* [1]. This merging was performed by CNVRuler software [33]. Regions of very low density of overlapping (recurrence parameter<0.1) were not used in the analyses for a more robust definition of the beginning and end regions.

Gene content and functional annotation

Based on the *Sscrofa10.2* sequence assembly, pig gene annotations within the identified CNVRs were retrieved from the Ensembl Genes 84 Database using the BioMart tool of Ensembl (http://ensembl.org/biomart). Pathway analysis of these genes was performed with DAVID bioinformatics resources 6.7 (http://david.abcc.ncifcrf.gov/). Considering the limited number of genes annotated in the pig genome, we first converted the pig Ensembl gene IDs to homologous human Ensembl gene IDs by BioMart, and then carried

out the pathway analysis. The *P* value and Benjamini correction for multiple testing were assessed for statistical significance.

Real-time quantitative PCR

Real-time quantitative PCR (qPCR) was used to analyze CNVRs. Thirty-two individuals of different backcrosses: BC1_LD (n=10), BC1_PI (n=10) and BC1_DU (n=12) were used to validate CNVRs. Furthermore, 150 individuals of the BC1_LD were used to perform the association analysis between CNVRs and FA composition and growth traits. The $2^{-\Delta\Delta Ct}$ method [34] for relative quantification (RQ) of CNVRs was used as previously described in Ramayo-Caldas *et al.* [15].

Primers (S1 Table) were designed using the Primer Express 2.0 software (Applied Biosystems). qPCRs were carried out using SYBR® Select Master Mix in an ABI PRISM® 7900HT instrument for primer testing (Applied Biosystems, Inc.; Foster City, CA) and a QuantStudio™ 12K Flex Real-Time PCR System (Applied Biosystems, Inc.; Foster City, CA) for the CNV quantification, following the manufacturer's guidelines. The reactions were carried out in a 96-well plate for the ABI PRISM® 7900HT instrument in a 20µl volume containing 10 ng of genomic DNA. For the QuantStudio™ 12K Flex Real-Time PCR instrument, the reactions were carried out in a 384-well plate in 15µl volume containing 7.5 ng of genomic DNA. All primers were used at 300 nM. The thermal cycle was: 10 min at 95°C, 40 cycles of 15 sec at 95°C and 1 min at 60°C. Each sample was analyzed in triplicate. One sample without CNV for each of the genomic regions analyzed was used as reference. The control region was determined within the region of the glucagon gene [EMBL:GCG]. Results for the standard curve were analyzed by DAG Expression software [35] and all samples were analyzed with Thermo Fisher Cloud software 1.0 (Applied Biosystems). For each CNVR to be validated, a value from the $2x2^{-\Delta\Delta Ct}$ formula was calculated for each individual.

Traits analyzed

For this study, phenotypic records were used from 150 animals belonging to the IBMAP BC1_LD backcross. The composition of 15 FA of both *Longissimus dorsi* muscle and BF (taken between the third and the fourth ribs) tissues was determined by gas chromatography as described in Pérez-Enciso *et al.* [26]. Subsequently, the percentage of each FA relative to the total FA was calculated as well as the global percentages of

saturated fatty acids (SFA), monounsaturated fatty acids (MUFA), polyunsaturated fatty acids (PUFA) and related indices, including desaturation and elongation indices.

In addition, 16 phenotypic growth and carcass traits were used in the analysis, corresponding to body weight measured at 125, 155 and 180 days (BW125, BW155, and BW180, respectively), backfat thickness (BFT) at the level of the fourth rib at 4 cm of the midline measured by ultrasounds at 125, 155 and 180 days (BFT125, BFT155 and BFT180, respectively) and measured with a ruler at slaughter (BFT), carcass length (CRCL) and carcass weight (CW), ham weight (HW), shoulder weight (SW), belly weight (BLW) and the IMF percentage, which was measured in the *Longissimus dorsi* muscle by Near Infrared Transmittance (NIT; Infratec 1625, Tecator Hoganas). Additionally pH was measured at 45 min in *semimembranosus* muscle (pH45SM) and at 24 h (pH24LD) and 45 min in the *Longissimus dorsi* muscle (pH45LD).

Statistical analysis

Associations of RQ values of the CNVRs with phenotypic records were analyzed with a multiplicative effect model in the CNVassoc R package [36]. The CNVassoc function incorporates calls by using a latent class model as described in González *et al.* [37]. Association analyses were performed with the copy number status inferred with the CNV function of the CNVassoc R package. The qPCR data and the composition of FA in IMF and BF were normalized and corrected both by gender and batch (five levels) effects, and the composition of FA also for CW, using glm R package [38]. Different corrections were used for the analysis of phenotypic growth records. Carcass weight was corrected by gender, batch and slaughter age. Also, gender, batch and CW were used to correct pH45SM, pH45LD, pH24LD, CRCL, BLW, BFT, HW, SW and IMF. For BFT125, BFT155 and BFT180, the corrections used were gender, batch and the body weight at their respective days. Meanwhile, for the body weight, the corrections used were gender, batch and the animal age. The R package *q*-value [39] was used to calculate the false-discovery rate (FDR), and the cut-off of the significant association was set at the *q*-value ≤ 0.05.

Results and Discussion

Genome-wide detection of CNVs

Based on the *Illumina* platform (Hi-Seq 2000, *Illumina*; San Diego, CA, USA), WGS data of seven founders of the IBMAP population (two Iberian boars and five Landrace sows) were

obtained. These animals were selected because they were founders with a large progeny contribution to the IBMAP population. The sequences were 100 bp paired-end reads with a coverage per animal ranging from 12.1 to 13.8x, with an average of 13.1x, which is sufficient for genome-wide CNV detection using the Read Depth method according to previous studies [20].

A total number of 1,279 CNVs, after removing false positives, were predicted from all seven individuals in autosomal chromosomes. The number of CNV events ranged from 106 to 235 CNVs across samples, with an average of 183 CNVs per sample. The size of these CNVs ranged from 3.22 to 2,237.31 kb per sample, with a median size of 3.42 kb (Table 1). The minimum CNV size is limited by the window size selected by the Control-FREEC program and, hence, the minimum size value includes all the CNVs with smaller sizes. The CNV median size is equal to the minimum size in six of the seven analyzed animals, indicating that most of the CNVs have sizes smaller or equal to the minimum sizes. When comparing the frequency of CNVs, duplications showed a higher average frequency than did deletions (106 versus 77). This proportion may be related to natural selection, as it is assumed that the genome is more tolerant of duplications than of deletions [40]. The overall profile of these CNVs across the genome for each individual is detailed in S2 Table.

Table 1. Summary of CNVs of the seven analyzed pigs

Sample	Breed	No. of total calls	No. of duplications	No. of deletions	Window size for CNV detection (kb)	Median size and (range), in kb
Ib1	Iberian	235	117	118	3.39	3.39 (3.39-1,008.02)
Ib2	Iberian	189	101	88	3.34	3.34 (3.34-2,237.31)
Ld1	Landrace	106	76	30	3.39	6.78 (3.39-416.85)
Ld2	Landrace	203	117	86	3.42	3.42 (3.42-855.75)
Ld3	Landrace	172	104	68	3.22	3.22 (3.22-366.62)
Ld4	Landrace	208	122	86	3.64	3.64 (3.64-563.58)
Ld5	Landrace	166	101	65	3.24	3.24 (3.24-447.67)
On average		**183**	**106**	**77**	**3.38**	**3.42 (3.22-2,237.31)**

All detected CNV segments were further merged into 540 unique CNVRs (S3 Table) across all experimental animal genomes following the criteria that the union of overlapping CNVs across individuals is considered as a CNVR [1].

Although CNVRs were found on all chromosomes, the number and the total size of CNVRs per chromosome were not correlated with chromosome length. The majority (428 out of 540; 79.26%) of the CNVRs identified were smaller than 10 kb (Fig 1).

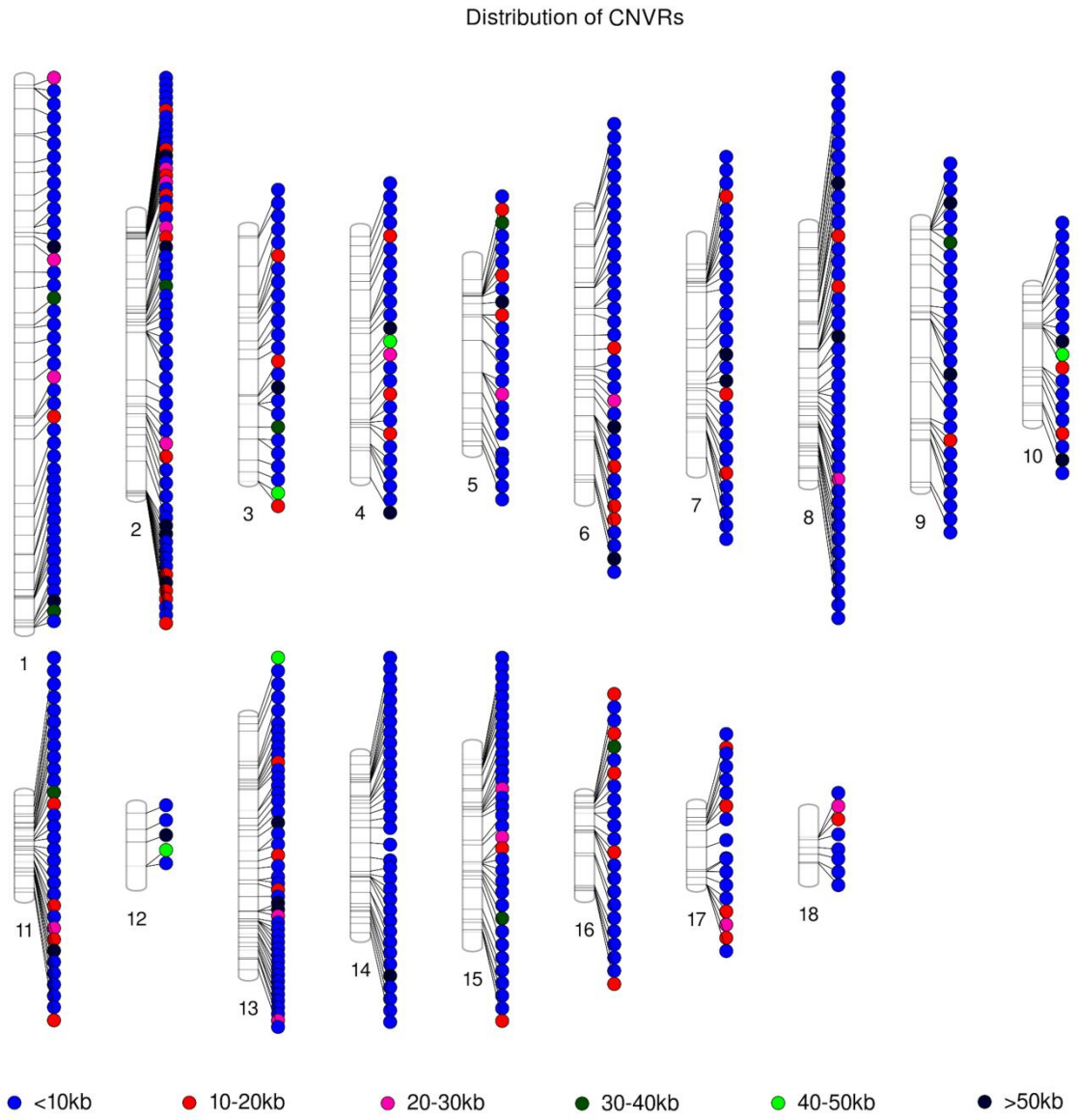

Fig 1. Distribution of CNVRs on the different chromosomes of the porcine genome. Each CNVR is represented by a circle and colors correspond to the different sizes explained in the legend.

Comparison with CNVRs identified in previous reports

The quality of CNVR calls was assessed by a comparison against a previously reported porcine CNV dataset identified in the IBMAP population with the Porcine SNP60 BeadChip [15]. After remapping the position of the CNVRs identified in Ramayo-Caldas *et al.* [15] to the *Sscrofa10.2* (http://www.ncbi.nlm.nih.gov/dbvar/studies/nstd44/#varianttab), we found 32 CNVRs that overlapped with CNVRs in that dataset, accounting for 65% of their CNVR calls. Another comparison was performed against the work published by Fernández *et al.* [24] using 223 Guadyerbas Iberian pigs and based on whole genome SNP genotyping data, obtaining seven CNVRs that overlapped (S3 Table).

Potential reasons for the differences between our results and these studies may be: (i) there was a difference in population size and genetic background between our study and others; (ii) call algorithms to detect CNVs are different, and (iii) our results were based on the *Sscrofa10.2* genome assembly, while previous works were based on *Sscrofa9.0*. This discrepancy between works also occurred in CNV studies of other mammals [41-43].

Gene annotation and functional analysis of the CNVRs

In total, 245 genes within or partially inside of the identified CNVRs were retrieved from the Ensembl Genes 84 Database using the BioMart data management system, including 227 protein-coding genes, 13 pseudogenes, 2 miRNA, 1 miscRNA and 2 snRNA (S3 Table).

In order to provide insight into the functional enrichment of the CNVRs, pathway analysis was performed with the DAVID bioinformatics resource. The pathway analysis revealed that genes in CNVRs mainly participated in olfactory transduction, retinol metabolism and also in metabolism of xenobiotics by cytochrome P450 and arachidonic acid metabolism, among others (S4 Table). Olfactory transduction was the most overrepresented pathway, including 48 genes, which is consistent with the study of Paudel *et al.* [23]. These authors suggested that inter-specific CNV of olfactory receptors (ORs) facilitated rapid adaptation to different environments during the diversification of the genus *Sus*. The genes involved in retinol and arachidonic acid metabolism pathways are components of the cytochrome P450 superfamily of enzymes, which catalyzes a high variety of chemical reactions mainly involved in detoxification and hormone and lipid metabolism [44]. Together with ORs,

CNV in cytochrome P450 (*CYP450*) genes suggests a relevant role of these genes in the organism's adaptation to rapid changes in the environment [23].

Interestingly, one gene of this family: Cytochrome P4502 C32 Fragment gene (*CYP2C32*; ENSSSCG00000010488), was identified in a previous study using BC1_LD animals of the IBMAP population [15], suggesting a possible role of this structural variation in determining androsterone levels. Differential expression of genes of the *CYP450* family has been correlated with androsterone levels in pigs from Duroc and Landrace breeds [45].
In addition, other genes related to this family were identified: *CYP1A1* (ENSSSCG00000001906), *CYP19A1* (ENSSSCG00000030168), *CYP2B6* (ENSSSCG00000003006), *CYP4A24* (ENSSSCG00000024778), and *CYP4X1* (ENSSSCG00000024129), which could affect arachidonic acid metabolism. In this sense, Ramayo-Caldas *et al.* [46] demonstrated some members of this family differentially-expressed in the liver transcriptome of pigs with extreme phenotypes for intramuscular FA composition.

Also, the excess of CNVRs in intergenic regions implies that a major part of these variations are likely to be neutral [47].

Identification of candidate genes for growth and FA composition traits in CNVRs

The overlapping was analyzed between the CNVRs identified in this study and the Genome-Wide Association Study (GWAS) regions described in Ramayo-Caldas *et al.* [48] using BC1_LD animals of the IBMAP population. After remapping these regions using the Assembly Converter tool of Ensembl, 19 regions co-localized among these works (S3 Table). The overlapping between the CNVRs and QTLs for growth and body composition traits described in Fernández *et al.* [49], which use a genome QTL scan based on linkage-mapping analyses with three generations of the IBMAP population, was also analyzed, identifying five co-localized regions (S3 Table). Finally, Muñoz *et al.* [50] also performed an analysis of the genetic basis of the FA composition of BF and IMF in the IBMAP population to identify significant QTLs for these traits using linkage-mapping and GWAS methods. A total of 24 overlapping regions were identified between both studies (S3 Table). In addition, we found 10 genes located in CNVRs that have been reported as differentially-expressed in the liver [46], muscle [51] or adipose tissue [52] of BC1_LD animals phenotypically extreme for intramuscular FA composition (S3 Table).

After compiling this information and taking into consideration the functional analysis of the genes within or partially inside of these CNVRs, six genes were selected as potential candidate genes related to growth and FA composition traits (Table 2).

Table 2. Selected CNVRs for validation and association studies

CNVR ID	Chr	CNVR Start	CNVR End	Length (bp)	CNVR gene	Gene Start	Gene End	Gene region	Function	Overlapping with previous reports		
										CNVs	GWAS	DE studies[a]
112	3	48,486,060	48,496,968	10,908	*GPAT2*	48,487,404	48,497,055	All gene	Esterifies acyl-group from acyl-ACP to the sn-1 position of glycerol-3-phosphate, an essential step in glycerolipid biosynthesis			
157	4	141,944,876	142,127,882	183,006	*CLCA4*	142,080,450	142,110,266	All gene	Mediates calcium-activated chloride conductance	[15]	[48]	
198	6	72,514,368	72,520,800	6,432	*PLA2G2A*	72,517,360	72,520,303	All gene	Catalyzes the hydrolysis of the sn-2 fatty acid acyl ester bond of phosphoglycerides, releasing free fatty acids and lysophospholipids			
214	6	151,988,436	151,995,708	7,272	*CYP4X1*	151,954,326	152,007,678	I6-7/E7/I7-8/E8/I8-9	Catalyzes many reactions involved in synthesis of cholesterol, steroids and other lipids			[46]
298	9	11,128,173	11,133,432	5,259	*MOGAT2*	11,119,062	11,132,962	I2-3/E3/I3-4/E4/I4-5/E5/I5-6/E6	Absorption of dietary fat in the small intestine			[46, 52]
447	14	106,486,107	106,491,408	5,301	*PRKG1*	106,253,479	106,707,670	I2-3	Serine/threonine protein kinase that acts as key mediator of the nitric oxide (NO)/cGMP signaling			[51]

[a]Differentially-expressed genes analysis using RNA-Seq data in IBMAP animals.

These six CNVRs represent different predicted statues of copy numbers (duplication/deletion) and are located on different chromosomes (SSC3, SSC4, SSC6, SSC9 and SSC14):

1. CNVR112 contains the *GPAT2* gene (ENSSSCG00000008121), encoding the mitochondrial glycerol-3-phosphate acyl-transferase 2, which plays a key role in phospholipid and triacylglycerol biosynthesis by catalyzing the addition of fatty acylCoA at the sn1 position of glycerol-3-phosphate to form lyso-phosphatidic acid [53]. Among its related pathways are metabolism and regulation of lipid metabolism by Peroxisome proliferator-activated receptor alpha *(PPARA)*.

2. The *CLCA4* gene (ENSSSCG00000006932), located in CNVR157, may be involved in mediating calcium-activated chloride conductance [54]. The porcine *CLCA4* gene has recently been shown to be duplicated into two separated genes, *CLCA4a* and *CLCA4b* [55].

3. CNVR198 contains the *PLA2G2A* gene (ENSSSCG00000003494), which encodes an enzyme that catalyzes the hydrolysis of the sn-2 FA acyl-ester bond of phosphoglycerides, releasing FAs and lysophospholipids, and could participate in the regulation of the phospholipid metabolism in biomembranes [56].

4. The *CYP4X1* gene (ENSSSCG00000024129), identified inside CNVR214, encodes a member belonging to the cytochrome P450 superfamily of enzymes. As stated before, the cytochrome P450 proteins are monooxygenases which catalyze many reactions involved in drug metabolism and synthesis of cholesterol, steroids and other lipids [44].

5. The *MOGAT2* gene (ENSSSCG00000014861), found in CNVR298, encodes a monoacylglycerol O-acyltransferase 2 enzyme. It plays a central role in absorption of dietary fat in the small intestine by catalyzing the re-synthesis of digested triacylglycerol in enterocytes. This gene may contribute to the development of the fatty-pig phenotype [57].

6. The *PRKG1* gene (ENSSSCG00000010429), located in CNVR447, has been implicated in the nitric oxide signaling pathway [58], one of the most significantly over-represented pathways found in the muscle RNA-Seq analysis of differentially-expressed genes for FA composition traits [51].

Validation of CNVRs

In order to validate the six selected CNVRs (CNVRs 112, 157, 198, 214, 298, and 447; Table 2), qPCR assays were designed. We analyzed the variation of these CNVRs in 12, 10 and 10 animals belonging to BC1_DU, BC1_LD and BC1_PI backcrosses, respectively. CNV was observed among these animals for five of the six analyzed CNVRs (112, 157, 214, 298, and 447), showing different patterns of CNV among the backcrosses (Fig 2). For CNVR112 (*GPAT2*), animals with two and three copies were observed in the three backcrosses. CNVR157 (*CLCA4*) showed the highest variability in the three backcrosses, with a CNV ranging from 0 to 6 copies among individuals from the different backcrosses. Conversely, for CNVR214 (*CYP4X1*), no variation in copy number was observed in BC1_LD animals, and it was discarded for further analyses. CNVR298 (*MOGAT2*) and CNVR447 (*PRKG1*) also showed variation in the number of copies among animals of the three backcrosses, in both cases being the individuals of the BC1_PI which presented more variation, as compared with the other two backcrosses.

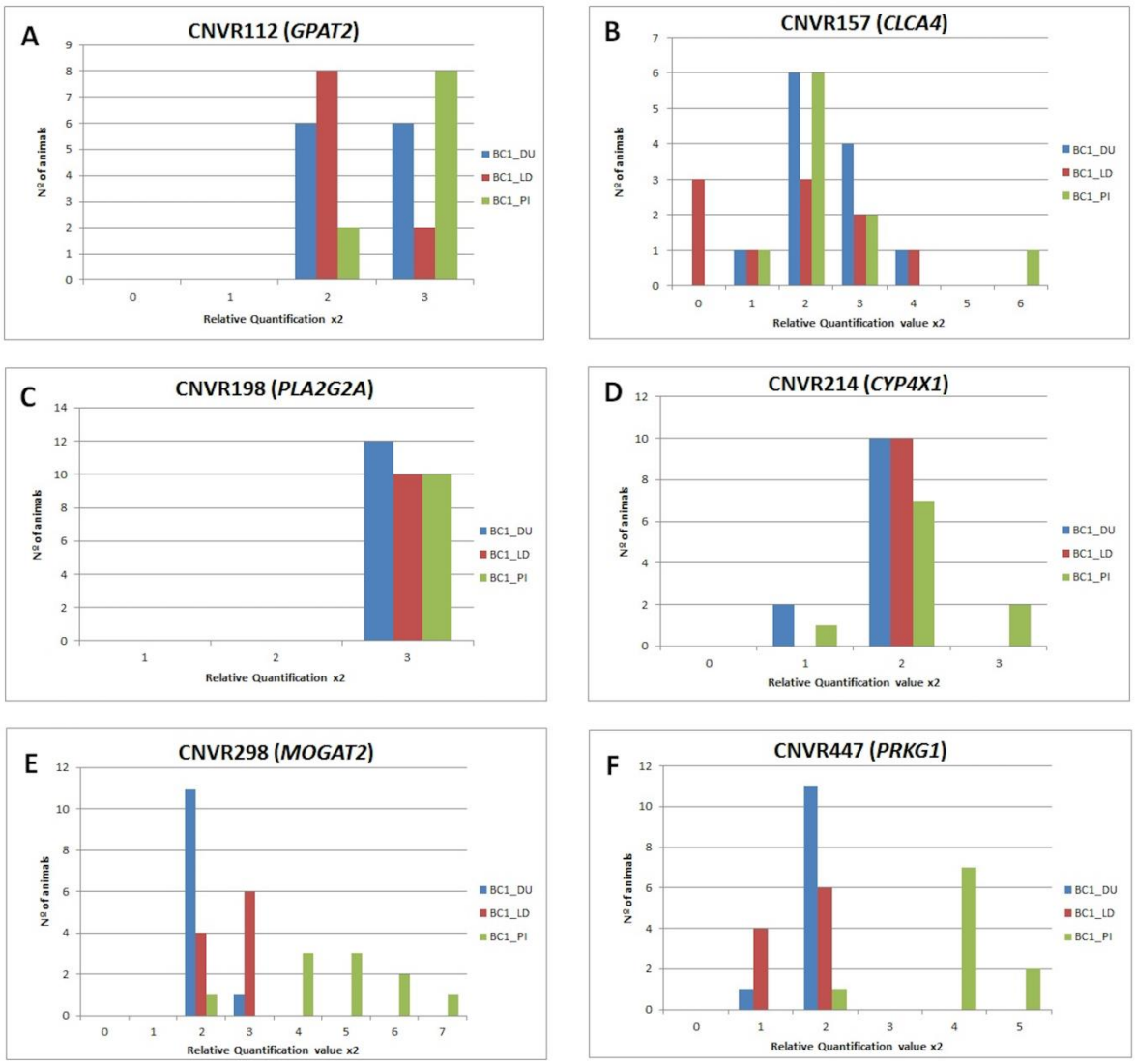

Fig 2. Validation of CNVRs detected from the WGS data using qPCR analysis. The y-axis represents the animals and the x-axis shows the relative quantification value ($2^{-\Delta\Delta Ct}$ values for qPCR; 2*(2^Sample signal) values for qPCR).

Association analysis with growth, carcass and fatty acid composition traits

With the objective to carry out association analysis between the CNVRs and growth-related and meat quality traits, 150 animals of BC1_LD were tested for CNVRs 112, 157, 298, and 447 (S1-S4 Figs). The repeatability of qPCR triplicates was highly accurate, showing a maximum standard error of 0.03. Results for CNVR157 (*CLCA4*) revealed that copy number varied greatly among the BC1_LD population (S2 Fig). The distribution of RQ values for CNVR112 (*GPAT2*) and CNVR298 (*MOGAT2*) also revealed variability and the differences between the calibrator and the sample that presented the highest value of RQ was 0.78 for CNVR112 and 0.77 for CNVR298 (S1 and S3 Figs). CNVR447 (*PRKG1*)

variation was more homogeneous, and the differences between the calibrator, and the sample that presented the highest value of RQ was 0.46 (S4 Fig).

An association analysis between the CNV estimates of CNVR112, CNVR157, CNVR298, and CNVR447 and growth-related traits and FA composition in IMF and BF of BC1_LD animals was performed using CNVassoc R package [36]. The peak intensities (CNV quantitative measurement) and densities of the four analyzed CNVRs (CNVR112, CNVR157, CNVR298 and CNVR447) are shown in Fig 3. Four latent classes, corresponding to 2, 3, 4, and 5 copies for the CNVR157, were observed. For CNVR112, CNVR298 and CNVR447, three latent classes were observed corresponding to 2, 3 and 4 copies.

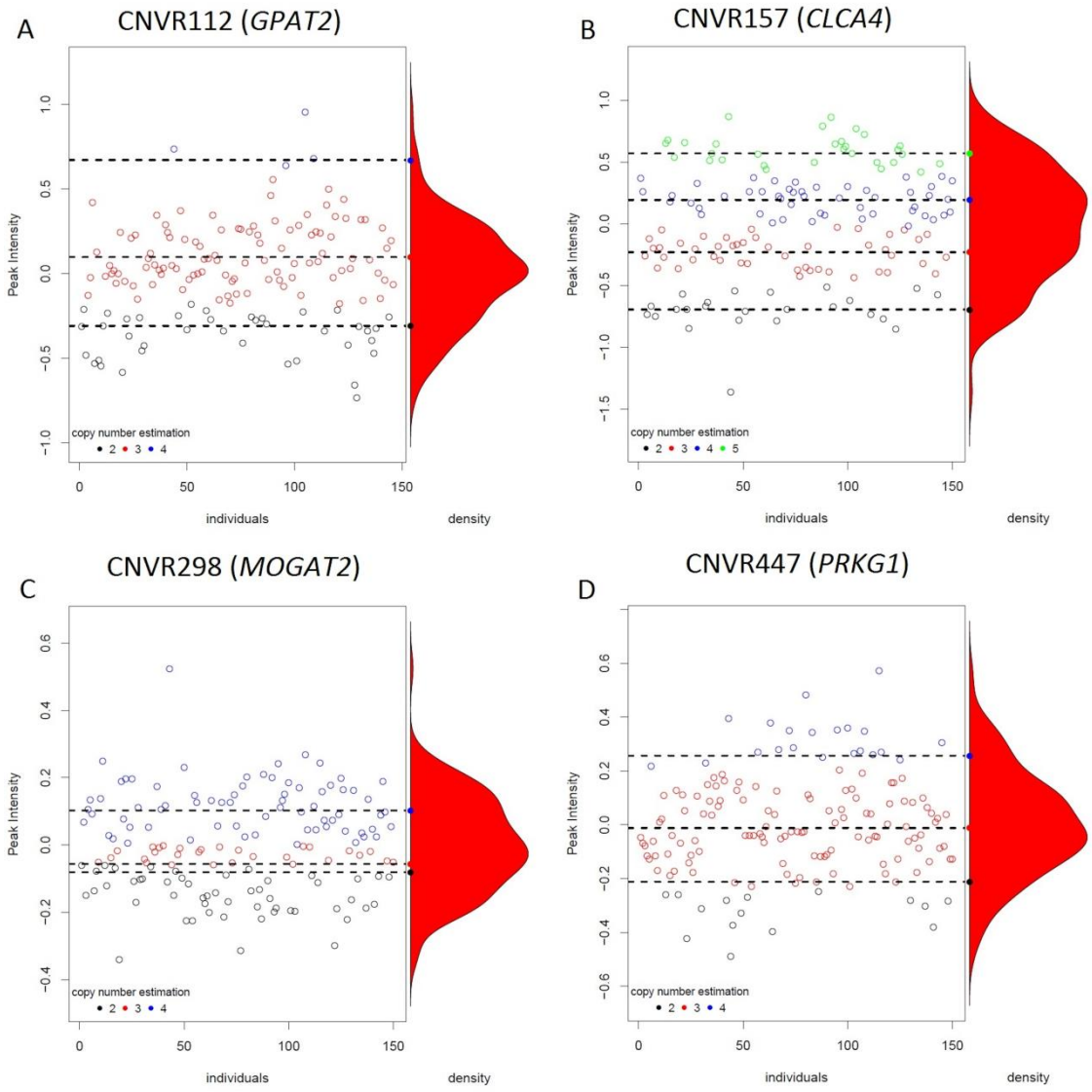

Fig 3. Plots of analyzed CNVRs generated from CNV signal-intensity data. The y-axis represents the CNV quantitative measurement (Peak Intensities) and the x-axis shows the different individuals. Each copy number estimation is shown in different colors. The density plot shows the distribution of these CNVs.

While for CNVR157, CNVR298 and CNVR447 only suggestive associations were found (S5 Table), CNVR112 (*GPAT2*) presented statistically significant associations (cut-off of *q*-value ≤ 0.05) for several traits. The strongest signal was observed for the C18:2(n-6)/C18:3(n-3) (*p*-value=9.34E-05) ratio, and cis-vaccenic acid ((C18:1(n-7)) (*p*-value=1.75E-03)) for the FA composition in BF. For FA percentages in IMF, the strongest signal was detected for oleic acid (C18:1(n-9) (*p*-value=9.16E-04)), the global percentage of MUFA (*p*-value=9.61E-04), peroxidability index (PI) (*p*-value=3.70E-03), dihomo gamma linolenic acid (C20:3(n-6) (*p*-value=5.51E-03)), the global percentage of PUFA (*p*-value=6.21E-03), eicosatrienoic acid (C20:3(n-3) (*p*-value=6.44E-03)) and the ratio of MUFA/PUFA (*p*-value=9.18E-03). For growth traits, CRCL showed statistically significant association (*p*-value=8.97E-05). These statistically significant associations and the descriptive statistics of significant phenotypic traits for CNVR112 are summarized in Table 3. A complete list of the association analyses results is shown in S5 Table, including the no significant associations observed in most of the FA composition traits measured in BF and IMF and for all the growth traits with the exception or CRCL.

Table 3. Statistically significant associations (*q*-value ≤ 0.05) between CNVR112 (*GPAT2*) and different phenotypic records in BC1_LD animals and their respective descriptive statistics

Trait	N	Mean (SEM[a])			*p*-value	*q*-value	Coefficient of determination[b]
Composition of FA in BF	147	**2 copies (n=40)**	**3 copies (n=103)**	**4 copies (n=4)**			
C18:1(n-7)		0.13 (0.01)	0.14 (0.01)	0.14 (0.01)	1.75E-03	2.12E-02	0.12
C18:2(n-6)/C18:3(n-3)		19.27 (0.37)	18.29 (0.19)	17.06 (0.25)	9.34E-05	2.26E-03	0.17
Composition of FA in IMF	142	**2 copies (n=37)**	**3 copies (n=101)**	**4 copies (n=4)**			
C18:1(n-9)		39.15 (0.49)	40.31 (0.27)	41.90 (0.81)	9.16E-04	1.01E-02	0.14
C18:2(n-6)		11.06 (0.43)	10.19 (0.23)	9.12 (0.38)	1.53E-02	2.41E-02	0.08
C20:2(n-6)		0.56 (0.02)	0.53 (0.01)	0.44 (0.03)	1.72E-02	2.41E-02	0.07
C20:3(n-3)		0.22 (0.02)	0.20 (0.02)	0.16 (0.02)	6.44E-03	2.26E-02	0.11
C20:3(n-6)		0.32 (0.02)	0.27 (0.01)	0.19 (0.04)	5.51E-03	2.26E-02	0.09
C20:4(n-6)		1.88 (0.15)	1.44 (0.06)	1.25 (0.18)	1.02E-02	2.28E-02	0.08
MUFA		46.97 (0.51)	48.18 (0.30)	49.89 (0.72)	9.61E-04	1.01E-02	0.13
PUFA		14.51 (0.62)	13.07 (0.31)	11.56 (0.56)	6.21E-03	2.26E-02	0.10
MUFA/PUFA		3.51 (0.19)	3.92 (0.10)	4.35 (0.24)	9.18E-03	2.28E-02	0.09
MUFA/SFA		1.23 (0.02)	1.25 (0.01)	1.30 (0.05)	1.21E-02	2.28E-02	0.08
PUFA/SFA		0.38 (0.02)	0.34 (0.01)	0.30 (0.02)	1.30E-02	2.28E-02	0.08
C18:1(n-9)/C18:0		2.78 (0.05)	2.85 (0.03)	3.05 (0.18)	1.05E-02	2.28E-02	0.09
C20:4(n-6)/C18:2(n-6)		0.16 (0.01)	0.14 (0.01)	0.14 (0.02)	1.65E-02	2.41E-02	0.07
PI		22.32 (1.09)	19.49 (0.49)	17.29 (1.14)	3.70E-03	2.26E-02	0.11
DBI		0.81 (0.01)	0.78 (0.01)	0.76 (0.02)	1.28E-02	2.28E-02	0.08
Growth trait	143	**2 copies (n=36)**	**3 copies (n=103)**	**4 copies (n=4)**			
CRCL		86.4 (1.37)	83.53 (0.60)	81.00 (7.78)	8.97E-05	1.51E-03	0.17

[a]Standard error of the mean.
[b]The coefficient of determination reflects the genetic variability explained by CNVR112.

Interestingly, as stated before, CNVR112 contains the *GPAT2* gene, which plays a key role in phospholipid and triacylglycerol biosynthesis [53]. Triglycerides (TG) are the main constituents of body fat in higher eukaryotes, serving as the major energy storage [59]. Very low-density lipoproteins and chylomicrons derived from the liver and diet, respectively, are important sources of FA supply to several tissues such as the BF and muscle, determining their FA composition. Essential FAs provided by the diet may be directly stored or used to synthesize highly unsaturated FAs [60]. On the other hand, FA synthase releases palmitic acid (C16:0) from acetyl-CoA and malonyl-Coa which can be, in turn, the precursor of the long-chain saturated and unsaturated FAs of n-9 family (and minor FAs of the n-7 and n-10 families) [57]. Thus, CNVR112 may play a role in the genetic determination of IMF and BF FA composition traits through the synthesis of TG in BF and muscle, using FAs provided by diet or synthesized *de novo* in the liver or adipose tissue.

Conclusions

This study is one of the first studies to investigate the association between CNVRs and economic traits in swine. We have described a map of swine CNVRs based on WGS data. A total of 540 CNVRs were identified across the autosomal chromosomes. Six selected CNVRs were validated by qPCR in three different backcrosses, and four of them were selected to study the association with FA composition in BF and IMF, and growth traits in 150 BC1_LD animals. CNVR112, which contains the *GPAT2* gene, showed associations with several of the analyzed growth-related traits and FA composition in IMF and BF.

These results indicate that CNVRs may explain a fraction of the genetic variability of FA composition, and also growth traits. These findings give novel insight into swine CNVRs and provide useful genomic information to facilitate the further identification of trait-related CNVRs.

Competing interests

The authors have declared that no competing interests exist.

Author contributions

Conceptualization: JMF MB. **Methodology:** JMF MB. **Formal analysis:** MR MB APO. JMF. **Investigation:** MR EP AC DCP. **Resources:** JMF AIF. **Writing - original draft:**

MR MB JMF. **Writing - review & editing:** MB JMF. **Visualization:** MR. **Supervision:** JMF. **Funding acquisition:** JMF AIF

Funding

This work has been funded by the MICINN AGL2014-56369-C2 and MINECO AGL2011-29821-C02. MR was funded by a Formació i Contractació de Personal Investigador Novell (FI-DGR) PhD grant from Generalitat de Catalunya (ECO/1639/2013). APO was funded by a Personal Investigador en Formación (PIF) PhD grant from the Universitat Autònoma de Barcelona (458-01-1/2011), DCP by a Formació i Contractació de Personal Investigador Novell (FI-DGR) PhD grant from Generalitat de Catalunya (ECO/1788/2014) and EP was funded by National Council of Scientific and Technological Development of Brazil (CNPq 202243/2014-1). MB was financially supported by a Ramon y Cajal contract (RYC-2013-12573) from the Spanish Ministry of Economy and Competitiveness.

Acknowledgments

We would like to thank all of the members of the INIA, IRTA, and UAB institutions who contributed to the generation of the animal material used in this work.

References

1. Redon R, Ishikawa S, Fitch KR, Feuk L, Perry GH, Andrews TD, et al. Global variation in copy number in the human genome. Nature. 2006; 44(7118): 444.
2. Freeman JL, Perry GH, Feuk L, Redon R, McCarroll SA, Altshuler DM, et al. Copy number variation: new insights in genome diversity. Genome Res. 2006; 16(8): 949-61.
3. Schiavo G, Dolezal MA, Scotti E, Bertolini F, Calò DG, Galimberti G, et al. Copy number variants in Italian Large White pigs detected using high-density single nucleotide polymorphisms and their association with back fat thickness. Anim Genet. 2014; 45(5): 745-9.
4. Vacic V, McCarthy S, Malhotra D, Murray F, Chou HH, Peoples A, et al. Duplications of the neuropeptide receptor gene VIPR2 confer significant risk for schizophrenia. Nature. 2011; 471(7339): 499-503.
5. Liu W, Sun J, Li G, Zhu Y, Zhang S, Kim ST, et al. Association of a germ-line copy number variation at 2p24.3 and risk for aggressive prostate cancer. Cancer Res. 2009; 69(6): 2176-9.

6. Jin G, Sun J, Liu W, Zhang Z, Chu LW, Kim ST, et al. Genome-wide copy-number variation analysis identifies common genetic variants at 20p13 associated with aggressiveness of prostate cancer. Carcinogenesis. 2011; 32(7): 1057-62.
7. Sailani MR, Makrythanasis P, Valsesia A, Santoni FA, Deutsch S, Popadin K, et al. The complex SNP and CNV genetic architecture of the increased risk of congenital heart defects in Down syndrome. Genome Res. 2013; 23(9): 1410-21.
8. Rubin CJ, Megens HJ, Martinez Barrio A, Maqbool K, Sayyab S, Schwochow D, et al. Strong signatures of selection in the domestic pig genome. Proc Natl Acad Sci U S A. 2012; 109(48): 19529-36.
9. Wang L, Xu L, Liu X, Zhang T, Li N, Hay el H, et al. Copy number variation-based genome wide association study reveals additional variants contributing to meat quality in Swine. Sci Rep. 2015; 5: 12535.
10. Ventanas S, Tejeda JF, Estévez M. Chemical composition and oxidative status of tissues from Iberian pigs as affected by diets: extensive feeding v. oleic acid- and tocopherol-enriched mixed diets. Animal. 2008; 2(4): 621-30.
11. Kouba M, Enser M, Whittington FM, Nute GR, Wood JD. Effect of a high-linolenic acid diet on lipogenic enzyme activities, fatty acid composition, and meat quality in the growing pig. J Anim Sci. 2003; 81(8): 1967-79.
12. Wood JD, Richardson RI, Nute GR, Fisher AV, Campo MM, Kasapidou E, et al. Effects of fatty acids on meat quality: a review. Meat Sci. 2004;66(1): 21-32.
13. Fadista J, Nygaard M, Holm LE, Thomsen B, Bendixen C. A snapshot of CNVs in the pig genome. PLoS One. 2008; 3(12): e3916.
14. Li Y, Mei S, Zhang X, Peng X, Liu G, Tao H, et al. Identification of genome-wide copy number variations among diverse pig breeds by array CGH. BMC Genomics. 2012; 13: 725.
15. Ramayo-Caldas Y, Castelló A, Pena RN, Alves E, Mercadé A, Souza CA, et al. Copy number variation in the porcine genome inferred from a 60 k SNP BeadChip. BMC Genomics. 2010; 11: 593.
16. Chen C, Qiao R, Wei R, Guo Y, Ai H, Ma J, et al. A comprehensive survey of copy number variation in 18 diverse pig populations and identification of candidate copy number variable genes associated with complex traits. BMC Genomics. 2012; 13: 733.
17. Fan Y, Xing Y, Zhang Z, Ai H, Ouyang Z, Ouyang J, et al. A further look at porcine chromosome 7 reveals VRTN variants associated with vertebral number in Chinese and Western pigs. PLoS One. 2013; 8(4): e62534.

18. Wang J, Wang H, Jiang J, Kang H, Feng X, Zhang Q, et al. Identification of genome-wide copy number variations among diverse pig breeds using SNP genotyping arrays. PLoS One. 2013; 8(7): e68683.
19. Wiedmann RT, Nonneman DJ, Rohrer GA. Genome-Wide Copy Number Variations Using SNP Genotyping in a Mixed Breed Swine Population. PLoS One. 2015; 10(7): e0133529.
20. Bickhart DM, Hou Y, Schroeder SG, Alkan C, Cardone MF, Matukumalli LK, et al. Copy number variation of individual cattle genomes using next-generation sequencing. Genome Res. 2012; 22(4): 778-90.
21. Duan J, Zhang JG, Deng HW, Wang YP. Comparative studies of copy number variation detection methods for next-generation sequencing technologies. PLoS One. 2013; 8(3): e59128.
22. Jiang J, Wang J, Wang H, Zhang Y, Kang H, Feng X, et al. Global copy number analyses by next generation sequencing provide insight into pig genome variation. BMC Genomics. 2014; 15: 593.
23. Paudel Y, Madsen O, Megens HJ, Frantz LA, Bosse M, Crooijmans RP, et al. Copy number variation in the speciation of pigs: a possible prominent role for olfactory receptors. BMC Genomics. 2015; 16: 330.
24. Fernández AI, Barragán C, Fernández A, Rodríguez MC, Villanueva B. Copy number variants in a highly inbred Iberian porcine strain. Anim Genet. 2014; 45(3): 357-66.
25. Hurd PJ, Nelson CJ. Advantages of next-generation sequencing versus the microarray in epigenetic research. Brief Funct Genomic Proteomic. 2009; 8(3): 174-83.
26. Pérez-Enciso M, Clop A, Noguera JL, Ovilo C, Coll A, Folch JM, et al. A QTL on pig chromosome 4 affects fatty acid metabolism: evidence from an Iberian by Landrace intercross. J Anim Sci. 2000; 78(10): 2525-31.
27. Sambrook J, Fritsch EE, Maniatis T. Molecular Cloning: A Laboratory Manual. 2nd Ed. Cold Spring Harbor Laboratory Press; 1989. pp. E3-E4.
28. Li H, Durbin R. Fast and accurate short read alignment with Burrows-Wheeler transform. Bioinformatics. 2009; 25(14): 1754-60.
29. Boeva V, Zinovyev A, Bleakley K, Vert JP, Janoueix-Lerosey I, Delattre O, et al. Control-free calling of copy number alterations in deep-sequencing data using GC-content normalization. Bioinformatics. 2011; 27(2): 268-9.

30. Boeva V, Popova T, Bleakley K, Chiche P, Cappo J, Schleiermacher G, et al. Control-FREEC: a tool for assessing copy number and allelic content using next-generation sequencing data. Bioinformatics. 2012; 28(3): 423-5.
31. Derrien T, Estellé J, Marco Sola S, Knowles DG, Raineri E, Guigó R, et al. Fast computation and applications of genome mappability. PLoS One. 2012; 7(1): e30377.
32. Lawrence M, Gentleman R, Carey V. rtracklayer: an R package for interfacing with genome browsers. Bioinformatics. 2009; 25(14): 1841-2.
33. Kim JH, Hu HJ, Yim SH, Bae JS, Kim SY, Chung YJ. CNVRuler: a copy number variation-based case-control association analysis tool. Bioinformatics. 2012; 28(13): 1790-2.
34. Livak KJ, Schmittgen TD. Analysis of relative gene expression data using real-time quantitative PCR and the 2(-Delta Delta C(T)) Method. Methods. 2001; 25(4): 402-8.
35. Ballester M, Cordón R, Folch JM. DAG expression: high-throughput gene expression analysis of real-time PCR data using standard curves for relative quantification. PLoS One. 2013; 8(11): e80385.
36. Subirana I, Diaz-Uriarte R, Lucas G, Gonzalez JR. CNVassoc: Association analysis of CNV data using R. BMC Med Genomics. 2011; 4: 47.
37. González JR, Subirana I, Escaramís G, Peraza S, Cáceres A, Estivill X, et al. Accounting for uncertainty when assessing association between copy number and disease: a latent class model. BMC Bioinformatics. 2009; 10: 172.
38. Hastie TJ, Pregibon D. Generalized linear models, Chapter 6 of Statistical Models in S. Chambers JM, Hastie TJ (eds.). Wadsworth & Brooks/Cole, Pacific grove; 1992.
39. Storey JD, Tibshirani R. Statistical significance for genomewide studies. Proc Natl Acad Sci U S A. 2003; 100(16): 9440-5.
40. Conrad DF, Hurles ME. The population genetics of structural variation. Nat Genet. 2007; 39(7 Suppl): S30-6.
41. Liu GE, Hou Y, Zhu B, Cardone MF, Jiang L, Cellamare A, et al. Analysis of copy number variations among diverse cattle breeds. Genome Res. 2010; 20(5): 693-703.
42. Matsuzaki H, Wang PH, Hu J, Rava R, Fu GK. High resolution discovery and confirmation of copy number variants in 90 Yoruba Nigerians. Genome Biol. 2009; 10(11): R125.
43. Eichler EE. Widening the spectrum of human genetic variation. Nat Genet. 2006; 38(1): 9-11.

44. Coon MJ, Ding XX, Pernecky SJ, Vaz AD. Cytochrome P450: progress and predictions. FASEB J. 1992; 6(2): 669-73.
45. Grindflek E, Berget I, Moe M, Oeth P, Lien S. Transcript profiling of candidate genes in testis of pigs exhibiting large differences in androstenone levels. BMC Genet. 2010; 11: 4.
46. Ramayo-Caldas Y, Mach N, Esteve-Codina A, Corominas J, Castelló A, Ballester M, et al. Liver transcriptome profile in pigs with extreme phenotypes of intramuscular fatty acid composition. BMC Genomics. 2012; 13: 547.
47. Paudel Y, Madsen O, Megens HJ, Frantz LA, Bosse M, Bastiaansen JW, et al. Evolutionary dynamics of copy number variation in pig genomes in the context of adaptation and domestication. BMC Genomics. 2013; 14:449.
48. Ramayo-Caldas Y, Mercadé A, Castelló A, Yang B, Rodríguez C, Alves E, et al. Genome-wide association study for intramuscular fatty acid composition in an Iberian x Landrace cross. J Anim Sci. 2012; 90(9): 2883-93.
49. Fernández AI, Pérez-Montarelo D, Barragán C, Ramayo-Caldas Y, Ibáñez-Escriche N, Castelló A, et al. Genome-wide linkage analysis of QTL for growth and body composition employing the PorcineSNP60 BeadChip. BMC Genet. 2012; 13: 41.
50. Muñoz M, Rodríguez MC, Alves E, Folch JM, Ibañez-Escriche N, Silió L. Genome-wide analysis of porcine backfat and intramuscular fat fatty acid composition using high-density genotyping and expression data. BMC Genomics. 2013; 14: 845.
51. Puig-Oliveras A, Ramayo-Caldas Y, Corominas J, Estellé J, Pérez-Montarelo D, Hudson NJ, et al. Differences in muscle transcriptome among pigs phenotypically extreme for fatty acid composition. PLoS One. 2014; 9(6): e99720.
52. Corominas J, Ramayo-Caldas Y, Puig-Oliveras A, Estellé J, Castelló A, Alves E, et al. Analysis of porcine adipose tissue transcriptome reveals differences in de novo fatty acid synthesis in pigs with divergent muscle fatty acid composition. BMC Genomics. 2013; 14: 843.
53. Dircks LK, Sul HS. Mammalian mitochondrial glycerol-3-phosphate acyltransferase. Biochim Biophys Acta. 1997; 1348(1-2): 17-26.
54. Plog S, Grötzsch T, Klymiuk N, Kobalz U, Gruber AD, Mundhenk L. The porcine chloride channel calcium-activated family member pCLCA4a mirrors lung expression of the human hCLCA4. J Histochem Cytochem. 2012; 60(1): 45-56.
55. Plog S, Klymiuk N, Binder S, Van Hook MJ, Thoreson WB, Gruber AD, et al. Naturally Occurring Deletion Mutants of the Pig-Specific, Intestinal Crypt Epithelial

Cell Protein CLCA4b without Apparent Phenotype. PLoS One. 2015; 10(10): e0140050.

56. Murakami M, Taketomi Y, Sato H, Yamamoto K. Secreted phospholipase A2 revisited. J Biochem. 2011; 150(3): 233-55.
57. Molnár J, Nagy T, Stéger V, Tóth G, Marincs F1, Barta E. Genome sequencing and analysis of Mangalica, a fatty local pig of Hungary. BMC Genomics. 2014; 15: 761.
58. Butt E, Abel K, Krieger M, Palm D, Hoppe V, Hoppe J, et al. cAMP- and cGMP-dependent protein kinase phosphorylation sites of the focal adhesion vasodilator-stimulated phosphoprotein (VASP) in vitro and in intact human platelets. J Biol Chem. 1994; 269(20): 14509-17.
59. Ahmadian M, Duncan RE, Jaworski K, Sarkadi-Nagy E, Sul HS. Triacylglycerol metabolism in adipose tissue. Future Lipidol. 2007; 2(2): 229-237.
60. Nakamura MT, Nara TY. Structure, function, and dietary regulation of delta6, delta5, and delta9 desaturases. Annu Rev Nutr. 2004; 24: 345-76.

Supporting Information

S1 Fig. Analysis by qPCR of CNVR112 (*GPAT2*). The y-axis represents the RQ quantitative measurement by qPCR for each sample and the x-axis shows the different samples. The baseline represents the calibrator.

S2 Fig. Analysis by qPCR of CNVR157 (*CLCA4*). The y-axis represents the RQ quantitative measurement by qPCR for each sample and the x-axis shows the different samples. The baseline represents the calibrator.

S3 Fig. Analysis by qPCR of CNVR298 (*MOGAT2*). The y-axis represents the RQ quantitative measurement by qPCR for each sample and the x-axis shows the different samples. The baseline represents the calibrator.

S4 Fig. Analysis by qPCR of CNVR447 (*PRKG1*). The y-axis represents the RQ quantitative measurement by qPCR for each sample and the x-axis shows the different samples. The baseline represents the calibrator.

S1 Table. Primers used for qPCR assays.

S2 Table. Duplication and deletion calls predicted by Control-FREEC software from all seven pigs.

S3 Table. Information of 540 identified CNVRs and gene annotation within the CNVRs retrieved from the Ensembl Genes 84 Database using the Biomart data management system.

S4 Table. Pathway analysis of genes identified in CNVRs.

S5 Table. Association analysis between CNVRs and different phenotypic records in BC1_LD animals.

PAPER III

Expression analysis in adipose tissue of candidate genes for fatty acid composition and identification of eGWAS regions

Revilla M[1,2*], Ballester M[3], Puig-Oliveras A[1,2], Crespo-Piazuelo D[1,2], Criado-Mesas L[1,2], Castelló A[1,2], Fernández AI[4], Folch JM[1,2]

[1] Departament de Ciència Animal i dels Aliments, Facultat de Veterinària, Universitat Autònoma de Barcelona (UAB), Bellaterra, Spain

[2] Plant and Animal Genomics, Centre de Recerca en Agrigenòmica (CRAG), Consorci CSIC-IRTA-UAB-UB, Campus UAB, Bellaterra, Spain

[3] Departament de Genètica i Millora Animal, Institut de Recerca i Tecnologia Agroalimentàries (IRTA), Torre Marimon, Caldes de Montbui, Spain

[4] Departamento de Genética Animal, Instituto Nacional de Investigación y Tecnología Agraria y Alimentaria (INIA), Madrid, Spain

[*] Corresponding author

Manuscript in preparation

Abstract

The aim of this work was to study the genetic basis of the backfat expression of 44 lipid-related genes associated with meat quality traits in pigs. We performed an expression genome-wide association study (eGWAS) with the backfat gene-expression measured by real-time quantitative PCR and the *PorcineSNP60 BeadChip* genotype information in 115 Iberian x Landrace backcross animals. The eGWAS identified 193 expression-associated SNPs (eSNPs) located in 19 chromosomal regions and associated with the *ACSM5, ELOVL6, FABP4, FADS2,* and *SLC27A4* genes. Three out of 19 expression quantitative trail *loci* (eQTLs) corresponding to *ACSM5, FABP4*, and *FADS2* were classified as *cis*-acting eQTLs, whereas the remaining 16 eQTLs have *trans*-regulatory effects. Remarkably, a SNP in the *ACSM5* promoter region and a SNP in the 3'UTR region of *FABP4* were identified as the most associated polymorphisms with the *ACSM5* and *FABP4* mRNA expression levels, respectively. Moreover, relevant lipid-related genes mapped in the *trans*-eQTLs regions associated with the *ACSM5, FABP4, FADS2,* and *SLC27A4*. Interestingly, a *trans*-eQTL hotspot on SSC13 at chromosome level regulating the gene expression of *ELOVL6*, *ELOLV5,* and *SCD*, three important genes implicated in the elongation and desaturation of fatty acids, was identified.

Finally, sex differences in the organization of gene-expression had been described in adipose tissue, illustrating that sex is an important factor that modifies the effects of the genetic variants that underlie complex traits in pigs. These findings provide new data to further understand the functional regulatory mechanisms implicated in the variation of meat quality traits in pigs.

Keywords: gene expression, expression QTL, eGWAS, backfat, lipogenesis, lipid metabolism, fatty acid.

Background

Pork meat is an appreciated, all-purpose lean meat, and represents one of the main sources of animal meat for humans (OECD/FAO, 2016). Fat and fatty acids (FAs), are fundamental to various aspects of meat quality and play a crucial role to meat nutritional value, both in adipose tissue (backfat, BF) and muscle (intramuscular fat; Wood *et al.*, 2008).

It is demonstrated that FA composition is dependent on physiological status, nutrition conditions (Wood *et al.*, 2004, 2008), and genetic factors (Casellas *et al.*, 2010).
In the last few years, genome-wide association studies (GWAS) have been performed in attempts to uncover the genetic basis of FA composition traits. Studies of our group and others have benefited from this approach and have identified genomic regions significantly associated with intramuscular fatty acid (IMFA) composition by using different experimental and commercial populations (Ramayo-Caldas *et al.*, 2012; Muñoz *et al.*, 2013; Yang *et al.*, 2013; Zhang *et al.*, 2016a,b). However, in most cases, the GWAS approach only allows the detection of genetic variants that explain only a modest proportion of the total heritability of the analyzed traits (Robinson *et al.*, 2014). In addition, the way from the genomic statistical association to the identification of true causal genetic variants is plagued of difficulties. Hence, it has become evident the necessity to integrate new approaches to better understand the biological significance of GWAS findings. Recently, the association between genetic variants and gene-expression levels has been described and used to identify expression quantitative trait *loci* (eQTLs). The eQTLs regulating the transcript abundance of the mRNAs can be identified systematically using high-throughput technologies and have recently been proposed as a good strategy to deepen the study of the genetic architecture of complex traits (Schadt *et al.*, 2008; Gilad *et al.*, 2008).

Liver, skeletal muscle and adipose tissue are the three most important tissues involved in FA metabolism (Frayn *et al.*, 2006). Adipose tissue, one of the main energy reserves in animals, is composed of adipocytes embedded in a matrix of connective tissue with a highly developed vascular system. The adipocytes are dynamic cells that play a relevant role in energy balance and overall body homeostasis. Their main metabolic functions are to accumulate lipids, by synthesis of triacylglycerols, and lipid mobilization, through hydrolysis of triacylglycerols (Bernlohr *et al.*, 2002).

Previous studies in our group have identified genomic regions, candidate regulators and regulatory polymorphisms in the liver and muscle tissues of individuals of an Iberian x Landrace backcross population (BC1_LD of IBMAP cross; Puig-Oliveras *et al.*, 2016; Ballester *et al.*, 2017). Furthermore, a transcriptome study using RNA-Seq of the adipose tissue of two groups of pigs with phenotypically extreme IMFA composition in the same BC1_LD identified metabolic pathways differentially modulated between groups controlling lipid and FA metabolism (Corominas *et al.*, 2013a). Taking into account the relevant role of adipose tissue in the regulation of lipid metabolism, the goals of the present article were (1) to study the expression of 44 candidate genes related with lipid metabolism in the adipose tissue of the BC1_LD population and (2) to analyze in detail the chromosomal regions significantly associated with the gene-expression levels to characterize the regulatory mechanisms influencing gene-expression phenotypes. With these results we aim to increase our knowledge of the contribution of adipose tissue in determining FA composition in the BC1_LD animals.

Materials and Methods

Ethics Statement

All animal procedures were performed according to the Spanish Policy for Animal Protection RD1201/05, which meets the European Union Directive 86/609 about the protection of animals used in experimentation. Animals were sacrificed in a commercial slaughterhouse following national and institutional guidelines for the Good Experimental Practices and approved by the Ethical Committee of the Institution (IRTA- Institut de Recerca i Tecnologia Agroalimentàries).

Animal samples

The IBMAP resource population was used in this study. This population was established by crossing 3 Iberian (Guadyerbas line) boars with 31 Landrace sows (Pérez-Enciso *et al.*, 2000), and 5 F_1 males and 25 Landrace sows were retained to propagate the BC1_LD generation (25% Iberian x 75% Landrace). Here, we reported results based on 115 BC1_LD pigs. All animals were maintained under intensive conditions and feeding was *ad libitum* with a cereal-based commercial diet. Backcross animals were slaughtered at an average age of 179.9 ± 8.9 days, and samples of BF tissue were collected, snap-frozen in liquid nitrogen and stored at -80°C until analysis. Genomic DNA was extracted from

diaphragm samples of all animals by the phenol-chloroform method (Sambrook *et al.*, 1989).

Characterization of the 3'UTR of porcine *FABP4* gene

The 3'UTR of the *FABP4* gene was amplified and sequenced in 10 animals with extreme values of *FABP4* mRNA expression in BF.

The 3'UTR variants of *FABP4* gene were characterized by 3'-RACE PCR using UAP reverse primer and, FABP4-3NC-1-Fw and FABP4-3NC-2-Fw forward primers (Table S1). The specific bands were excised from agarose gel and purified using NucleoSpin® Gel and PCR Clean-up (Macherey-Nagel GmbH & Co. KG) and sequenced in forward and reverse directions.

All primers were designed using PRIMER3 software (Rozen & Skaletsky, 2000) based on the Y16039 sequence (Gerbens *et al.*, 1998) and validated using PRIMER EXPRESS™ (Applied Biosystems). In all cases, PCR was performed in a 25 µl volume containing 2 µl of cDNA. PCR reaction contained 0.6 units of AmpliTaq Gold (Applied Biosystems), 2.5 mM $MgCl_2$, 0.2 mM of each dNTP and 0.5 µM of each primer. PCR were carried out under the following conditions: 94 ºC for 10 min, 35 cycles of 94 ºC for 1 min, 62 ºC for 1 min and 72 ºC for 1 min, with a final extension at 72 ºC for 7 min. Purification was performed using the ExoSAP-IT® method and sequenced with a Big Dye Terminator v.3.1 Cycle Sequencing Kit in an ABI 3730 analyzer (Applied Biosystems). Polymorphisms were identified using Seq scape v2.5 program (Applied Biosystems).

miRDB (Wong & Wang, 2015) program was run to find putative target miRNAs in the 3'UTR region of *FABP4*. For this purpose, the human miRNA database was used.

Detection of polymorphisms in the promoter region of the *FADS2* gene

Polymorphisms in the proximal promoter region of the *FADS2* gene were identified from the whole genome sequence data of seven founders of the IBMAP experimental population (SRA accession numbers: SRR5229970, SRR5229971, SRR5229972, SRR5229973, SRR5229974, SRR5229975, and SRR5229976) using the Integrative Genomics Viewer (IGV) software (Robinson *et al.*, 2011).

SNP Genotyping and quality control

A total of 115 animals belonging to BC1_LD were genotyped for 62,163 SNPs with the *PorcineSNP60 Beadchip* (Ramos *et al*., 2009) following the Infinium HD Assay Ultra protocol (*Illumina* Inc.; San Diego, USA). Raw data was visualized with GenomeStudio software (*Illumina* Inc.; San Diego, USA) and trimmed for high genotyping quality (call rate > 0.99). Plink software (Purcell *et al*., 2007) was used to remove markers that showed a minor allele frequency (MAF) less than 5% and SNPs with more than 5% of missing genotypes. The SNPs not mapped in the *Sscrofa10.2* assembly were also excluded. After the quality control filter, a subset of 40,460 SNPs remained.

In addition, ten polymorphisms were genotyped in the BC1_LD animals: two SNPs located in the proximal promoter region of the *ACSM5* (*g.26260422G>A*, rs331702081; Puig-Oliveras *et al*., 2016) and the *FADS2* (rs331050552) genes, and one indel and one SNP located in the intron 1 (*FABP4:g.2634_2635insC*; Mercadé *et al*., 2006) and in the 3'UTR region of the *FABP4* gene (*FABP4:g.6723*A>G), respectively. For the *ELOVL6* gene, three SNPs located in the promoter region (*ELOVL6:c.-533C>T, ELOVL6:c.-480C>T,* and *ELOVL6:c.-394G>A*; Corominas *et al*., 2013b, 2015), one in exon 4 (*ELOVL6:c.416C>T*; Corominas *et al*., 2013b) and two in the 3'UTR region (*ELOVL6:c.1408A>G* and *ELOVL6:c.1922C>T*; Corominas *et al*., 2015) were genotyped. *ACSM5* and *FADS2* SNPs were genotyped using Taqman OpenArray™ genotyping plates designed in a QuantStudio™ 12K flex Real-Time PCR System (*ThermoFisher Scientific*). The pyrosequencing protocol described by Mercadé *et al*., (2006) and the High Resolution Melting methodology (HRM, *ThermoFisher Scientific*) were used for genotyping the indel and SNP of *FABP4* gene, respectively. The SNPs belonging to *ELOVL6* gene were genotyped using the platform KASP SNP genotyping system platform (http://www.lgcgroup.com/genotyping/).

Gene-expression profiling

Total RNA was isolated from the BF of the 115 BC1_LD samples with RiboPure™ RNA Purification Kit (Ambion; Austin, TX, USA). Total RNA was quantified in a NanoDrop ND-1000 spectrophotometer (NanoDrop products; Wilmington, DE, USA). The RNA was converted to cDNA using the *High-Capacity cDNA Reverse Transcription* kit (Applied Biosystems) in 20µl of reactions, following the manufacturer's instructions. The cDNA samples were loaded into a *Dynamic Array* 48.48 chip in a BioMark system (Fluidigm; San

Francisco, CA, USA) through an integrated fluidic circuit controller following a protocol previously described (Ramayo-Caldas *et al.*, 2014).

For this experiment, the expressed levels of 48 genes were analyzed: 44 target genes and four reference genes (*ACTB*, *B2M*, *HPRT1,* and *TBP*). The *ACTB* and *TBP* were the two most stable reference genes and were used to normalize the expression levels of the target genes. Primers used for the analysis were designed using PrimerExpress 2.0 software (Applied Biosystems) and are detailed in Additional file 2: Table S2. Data was collected using the Fluidigm Real-Time PCR analysis software 3.0.2 (Fluidigm) and analyzed using the DAG expression software 1.0.5.5 (Ballester *et al.*, 2013) applying the relative standard curve method. Samples targeted in this study were analyzed in duplicate. The normalized quantity (NQ) values of each sample and assay were used to compare our data. Data obtained were normalized by performing $\log_2$ transformation of the NQ value. The sex effect was also tested by using a linear model with the *lm* function of R program (Ihaka & Gentleman, 1996).

Gene-expression association analysis

In order to detect expression-associated SNPs (eSNPs), expression GWAS (eGWAS) was performed using as phenotype the expression values of 43 genes in adipose tissue. A mixed model was employed in Qxpak 5.0 (Pérez-Enciso & Misztal, 2011):

$$Y_{ijkl} = Sex_i + Batch_j + \lambda_k a_l + u_k + e_{ijkl},$$

in which Y_{ijkl} was the k^{th} individual record, sex (two levels) and batch (five levels) were fixed effects, λ_k was a -1 (aa), 0 (Aa), +1 (AA) indicator variable depending on the k^{th} individual's genotype for the l^{th} SNP, a_l represents the additive effect associated with the l^{th} SNP, u_k is the infinitesimal genetic effect with random distribution $N(\mathbf{0}, \mathbf{A}\sigma_u^2)$ where **A** is the numerator of the pedigree-based relationship matrix and the e_{ijkl} the residual.

The association analyses of the *ACSM5* (rs331702081), *ELOVL6* (*ELOVL6:c.-533C>T, ELOVL6:c.-480C>T, ELOVL6:c.-394G>A, ELOVL6:c.416C>T, ELOVL6:c.1408A>G*, and *ELOVL6:c.1922C>T*), *FABP4* (*FABP4:g.2634_2635insC* and *FABP4:g.6723*A>G), and *FADS2* (rs331050552) polymorphisms with the *ACSM5, ELOVL6*, *FABP4*, and *FADS2* mRNA expression, respectively, were performed using the same mixed model described above.

The R package *q*-value was used to calculate the false discovery rate (FDR), and the cut-off of the significant association at the whole genome level was set at the *q*-value ≤ 0.05 (Ihaka & Gentleman, 1996; Storey & Tibshirani, 2003).

The identified eSNPs were classified as *cis* when they were at 5 Mb upstream or downstream of the gene position and as *trans* when they were located elsewhere in the genome. Significant associated eSNPs located less than 10 Mb apart were considered as belonging to the same interval.

Gene annotation and functional classification

The significantly associated eSNPs (FDR≤ 0.05) identified were mapped in the *Sscrofa10.2* assembly and were annotated with the Ensembl Genes 84 Database using Variant Effect Predictor (VEP) software (McLaren *et al.*, 2010).

The genomic eQTL intervals were annotated using Biomart software [http://www.biomart.org] considering ±1 Mb around the candidate chromosomal region for *trans*-eQTLs and only the studied candidate gene for *cis*-eQTLs.

The *Core Analysis* function included in the Ingenuity Pathway Analysis software (IPA, Ingenuity Systems Inc., http://www.ingenuity.com) was used to perform the functional analysis of genes mapped in the 19 eQTL regions. This software was used for data interpretation in the context of biological processes, pathways and networks. All information generated is derived from the Ingenuity Pathway Knowledge Base (IPKB), which is based on functions and interactions of genes published in the literature. RNA-Seq data of BF from BC1_LD individuals (Corominas *et al.*, 2013a) and Gene Expression Atlas (Kapushesky *et al.*, 2010) were used to determine which of the lipid-related genes annotated in the genomic eQTL intervals were expressed in adipose tissue. Finally, a prediction analysis of transcription factor (TF) binding sites was performed in the promoter region of the 458 annotated genes. The iRegulon Cytoscape plugin (Janky *et al.*, 2014) was used to analyze the TFs and their related target genes. iRegulon relies on the analysis of the regulatory sequences around each gene, and use a databases of nearly 10,000 TF motifs and 1,000 ChIP-seq data sets or "tracks". The normalized enrichment score (NES) >5 was considered as the threshold value for the selection of potential relationships.

Gene-expression and correlation analysis with phenotypes

A correlation analysis was performed to explore the relationship between the expressions of the 43 genes. Moreover, to analyze the relationships between gene-expression and phenotypes, correlations among gene-expression and FA composition percentages in BF (Muñoz *et al.*, 2013) were performed. If required, data was normalized applying the $\log_2$ transformation. Then, gene-expression and the composition of FA in BF were corrected both by gender (two levels) and batch effects (five levels), and the composition of FA traits was also adjusted for carcass weight, using the glm R package (Hastie & Pregibon, 1992).

Results and discussion

Selection of genes related with lipid metabolism in the adipose tissue

Using the information generated in previous studies of our group, strong candidate genes affecting FA composition of BF and intramuscular fat in the BC1_LD generation were identified by GWAS, RNA-Seq and co-association network approaches (Ramayo-Caldas *et al.*, 2012; Corominas *et al.*, 2013a,b; Puig-Oliveras *et al.*, 2014a; Ramayo-Caldas *et al.*, 2014; Ballester *et al.*, 2016) (Table S3). A total of 44 candidate genes related with lipid metabolism were selected to study their expression pattern in BF. Fourteen of them (*ARNT*, *CYP2U1*, *EGF*, *ELOVL6*, *FABP4*, *FABP5*, *FADS1*, *FADS2*, *FADS3*, *NFKB1*, *PLA2G12A*, *PLCB2*, *PLPP1,* and *USF1*) are functional and positional candidate genes related with lipid metabolism which were identified in GWAS analyses for BF and IMFA composition in the BC1_LD animals (Ramayo-Caldas *et al.*, 2012; Ballester *et al.*, 2016). We also included two candidate genes differentially-expressed (*ELOVL6* and *SCD*) in a RNA-Seq analysis of the adipose tissue of two phenotypically extreme groups of animals for IMFA composition in the BC1_LD cross (Corominas *et al.*, 2013a). Lipid metabolism genes identified in gene co-association networks for FA composition (*ACSM5, ANK2, ARNT, FABP4, FABP5, MGLL,* and *PPARG*) (Ramayo-Caldas *et al.*, 2014), two of which were also identified in gene co-association networks for fatness and growth traits (*ARNT* and *PPARG*) (Puig-Oliveras *et al.*, 2014a). In addition, in order to complete the set of genes, we included genes which have been described in the literature to play different roles in lipid metabolism such as transporters (*RBP4*, *SCAP, SLC27A1,* and *SLC27A4*), enzymes (*AGPAT2, CPT1A, CROT, DGAT1, DGAT2, ELOVL5, LIPC, LPIN1, PEX2,* and *PNPLA2*) and transcriptional factors, cofactors or nuclear receptors (*CD36*, *ESRRA, MLXIPL*, *NR1H3, POU2F1, PPARA, PPARD, PPARGC1A, RXRG,* and *SREBF1*). Finally, we added the

ADIPOQ gene, which codifies an important adipokine of white fat tissue exerting multiple biological processes on carbohydrate and lipid metabolism (review in Shehzad *et al.*, 2012). Although this gene is not mapped in the current *Sscrofa10.2* assembly, it has been mapped to the SSC13q36-41 interval (Dai *et al.*, 2006).

Four endogenous genes (*ACTB, B2M, HPRT*, and *TBP*) were also selected as reference controls.

Expression genome-wide association analysis (eGWAS)

In the present study, the adipose tissue expression of 48 genes (44 target and four reference genes previously explained) was measured by real-time quantitative PCR (qPCR) in 115 BC1_LD animals. For the *PPARGC1A* gene, a poor PCR efficiency was obtained and it was discarded for further analysis. eGWAS were performed with the gene-expression values of the 43 remaining target genes and the genotypes of 40,460 SNPs of the *PorcineSNP60 BeadChip* (Ilumina) distributed across the pig genome.

At whole genome level, significant association signals in five of the analyzed genes were detected (Table 1): *ACSM5*, *ELOVL6*, *FABP4*, *FADS2,* and *SLC27A4*. The *ACSM5, FABP4, FADS2,* and *SLC27A4* genes presented more than one associated eQTL (Table 1). Three out of 19 eQTLs were identified as *cis*-acting for the *ACSM5, FABP4,* and *FADS2* gene-expression (Fig. 1), suggesting the presence of proximal polymorphisms regulating the expression of these genes. These results showed a difference in the prevalence of *cis*- and *trans*-eQTLs. In general, studies performed in animals have identified regulatory *trans*-eQTLs in a higher ratio than those performed in humans (Gilad *et al.*, 2008; Cheung & Spielman, 2009). Our results are in concordance with this assumption, and also, previously studies of our group performed in muscle (Puig-Oliveras *et al.*, 2016) and liver (Ballester *et al.*, 2017) identified a prevalence of porcine *trans*-eQTLs compared wih the *cis*-eQTLs.

Table 1. Significant eQTL identified

Interval	Chr	Position Mb Start-End[a]	Size (Mb)	SNP Start	SNP End	No. SNPs[b]	Associated Gene	Type of eQTL
I1	2	134.99		ASGA0093797		1	*ACSM5*	*trans*
I2	3	16.47-63.25	46.78	ASGA0089930	ALGA0111911	133	*ACSM5*	*cis/trans*
I3	3	83.37		MARC0032158		1	*ACSM5*	*trans*
I4	3	100.91-101.46	0.55	ALGA0020206	ASGA0098441	3	*ACSM5*	*trans*
I5	10	0.05-0.20	0.15	H3GA0055101	ASGA0095156	8	*ACSM5*	*trans*
I6	16	19.13		ALGA0089402		1	*ACSM5*	*trans*
I7	13	6.89		ASGA0055780		1	*ELOVL6*	*trans*
I8	2	6.10-9.00	2.90	ASGA0008719	MARC0018949	2	*FABP4*	*trans*
I9	3	109.40-119.74	10.34	ASGA0015643	ASGA0016181	3	*FABP4*	*trans*
I10	4	36.73		ALGA0024527		1	*FABP4*	*trans*
I11	4	60.57-65.25	4.68	ALGA0025158	ALGA0025337	5	*FABP4*	*cis (FABP5)*
I12	9	129.18		ALGA0054847		1	*FABP4*	*trans*
I13	2	7.85-9.22	1.37	ASGA0008845	ASGA0008874	8	*FADS2*	*cis*
I14	6	74.42		ALGA0035721		1	*FADS2*	*trans*
I15	8	59.00-68.68	9.68	ASGA0100508	H3GA0024926	3	*FADS2*	*trans*
I16	10	46.93		H3GA0030086		1	*FADS2*	*trans*
I17	9	20.18-20.20	0.02	MARC0034587	ASGA0041925	2	*SLC27A4*	*trans*
I18	14	88.90-92.43	3.53	ASGA0064787	ALGA0079407	16	*SLC27A4*	*trans*
I19	15	137.05-137.37	0.32	ASGA0070790	MARC0050960	2	*SLC27A4*	*trans*

[a]Chromosomal location is given according to *Sscrofa10.2* assembly coordinates.
[b]Number of significant eSNPs within the eQTL interval.

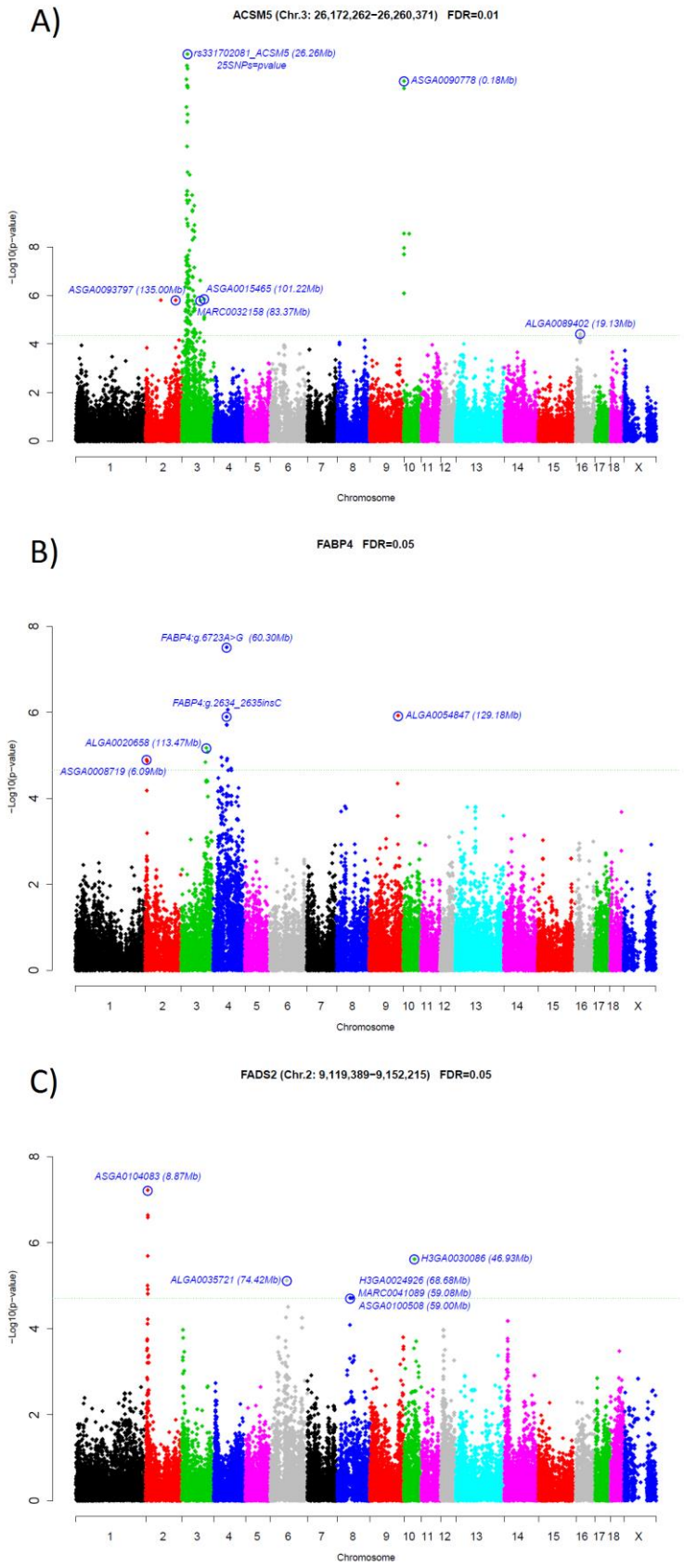

Figure 1. GWAS plot of *ACSM5, FABP4,* and *FADS2* gene-expression in adipose tissue. The X-axis represents chromosome positions in Mb relative to *Sscrofa10.2* assembly of the pig genome and the Y-axis shows the –log10 (*p*-value). Horizontal dashed lines indicate the genome-wide significance level. Plot of eGWAS for (**A**) *ACSM5*, (**B**) *FABP4,* and (**C**) *FADS2* gene-expression in backfat.

The eGWAS identified 193 eSNPs located in 19 chromosomal regions on pig chromosomes SSC2-SSC4, SSC6, SSC8-SSC10 and SSC13-SSC16 (Table 1).

From the associated eSNPs, and according to the VEP of Ensembl (*Sscrofa10.2* annotation release 84), 49.2% (95 eSNPs) were located in intergenic regions. The remaining 50.8% (98 eSNPs) mapped within a total of 68 genes: 66 in introns, 11 and 16 in 5' upstream and 3' downstream gene regions, respectively, three in the 3'UTR region, and two in the coding region of a gene determining synonymous mutations (Table S4). A total of 86 eSNPs (44.6%) were located inside the *cis*-acting eQTLs, whereas 107 eSNPs (55.4%) were in *trans* eQTLs (Table S4).

In the following sections, the eSNPs and genes mapped in the *trans*-eQTL regions associated with the expression phenotypes of *ACSM5*, *ELOVL6*, *FABP4*, *FADS2*, and *SLC27A4* are discussed in detail. Table 2 summarizes all the relevant lipid-related genes mapped in the *trans*-eQTL regions. RNA-Seq data of BF from BC1_LD individuals (Corominas *et al.*, 2013a) and Gene Expression Atlas webpage were used to confirm the expression of those genes in adipose tissue.

Table 2. Candidate genes annotated in *trans*-eQTLs related with lipid metabolism functions

Gene	Chr	Interval	Candidate gene within eQTL
ACSM5	2	I1	*ALDH7A1, MARCH3*
	3	I3	*MDH1*
	3	I4	*PIGF, PRKCE*
	10	I5	*COG7, GGA2, NDUFAB1*
FABP4	2	I8	*BSCL2, DAGLA, EHD1, FADS1, FADS2, FADS3, LGALS12, PLA2G16, SF1, TM7SF2*
	3	I9	*CYP1B1, EHD3, EPT1, GALNT14, GCKR, HADHA, HADHB, LCLAT1, PLB1, PPP1CB, RBKS, SNX17, SPAST*
	9	I12	*RFWD2*
FADS2	6	I14	*CDC42, ECE1, FUCA1, GALE, HMGCL, KDM1A*
	8	I15	*IGFBP7*
	10	I16	*CUBN*
SLC27A4	9	I17	*PRCP*
	15	I19	*FARSB, MOGAT1*

The *ACSM5* gene

One of the *cis*-eSNPs (ASGA0103234) associated with the expression of the Acyl-CoA Synthetase Medium-Chain Family Member 5 gene (*ACSM5*) mapped within an intronic region of the gene (Table S4). However, this SNP was not the most significantly associated (ASGA0103234; *p*-value= $8.18x10^{-12}$; estimated additive effect, â= -3.968), suggesting the presence of other polymorphisms within or near the *ACSM5* gene as the causative mutation affecting the expression levels of this gene. The most significant *cis*-SNPs (*p*-value= $1.11x10^{-17}$) for *ACSM5* gene-expression were located between 23.44 Mb and 27.94 Mb, covering a total of 25 SNPs, in a region with a strong linkage disequilibrium (LD) (D' = 0.99). Recently, the polymorphism *ACSM5:g.26260422G>A* (rs331702081), located at the proximal promoter region of the *ACSM5* gene, has been described as the most associated with the expression of *ACSM5* in *Longissimus dorsi* muscle of BC1_LD animals (Puig-Oliveras *et al.*, 2016). To assess the association of this polymorphism with the expression of the *ACSM5* in BF, the *ACSM5:g.26260422G>A* SNP was genotyped in the 115 BC1_LD animals and included in the eGWAS study. Remarkably, this polymorphism is one of the SNPs located in the 23.44-27.94 Mb block with the lowest *p*-value (*p*-value= $1.11x10^{-17}$; Fig. 1A). Hence, this SNP may be a strong candidate polymorphism to explain the mRNA variation of the *ACSM5* gene in BF and muscle. Even so, the correlation value between the *ACSM5* gene-expression in BF and muscle is of r= 0.60 (*p*-value= $3.0x10^{-12}$), suggesting that other factors than the SSC3 *cis*-eQTL are differentially regulating the expression of *ACSM5* in both tissues.

The effect of *ACSM5:g.26260422G>A* SNP on the binding of TFs was determined by the LASAGNA-Search version 2.0 software (Lee & Huang, 2013). Remarkably, the aryl hydrocarbon receptor nuclear translocator (*ARNT*) gene (TF ID= M00236 and M00539) and the signal transducer and activator of transcription 6 (*STAT6)* gene (TF ID= M00500) were identified to bind only when *A* allele is present. *ARNT* gene plays an important role in the regulation of hepatic lipogenesis and gluconeogenesis (Wang *et al.*, 2009; Rankin *et al.*, 2009), and was identified as one of the most central genes in a liver co-expression network analysis of IMFA composition in pigs (Ramayo-Caldas *et al.*, 2014). *STAT6* gene has been described to interact with the peroxisome proliferator activated receptor gamma gene (*PPARG*), and the cooperative binding of the two genes led to an increase response of *PPARG* (Szanto *et al.*, 2010). The importance of *PPARG* gene lies on its regulation of adipocyte differentiation and glucose homeostasis, and it was identified as a major regulator

for growth and fatness related traits in a co-association network in muscle of BC1_LD individuals (Puig-Oliveras *et al.*, 2014a). Different transcription binding sites for *PPARG* in the *ACSM5* proximal promoter region were also predicted by LASAGNA (data not shown).

Five chromosomal regions (Table 1) were also associated in *trans* with the *ACSM5* gene-expression. Interestingly, two of these regions on SSC3 (100.91-101.46 Mb) and SSC10 (0.05-0.20 Mb) have been recently associated with the mRNA expression of the *ACSM5* gene in the *Longissimus dorsi* muscle of BC1_LD animals (SSC3: 100.35 Mb; SSC10: 0.17 Mb) (Puig-Oliveras *et al.*, 2016). These results, together with the *cis*-eQTL identification for the *ACSM5* expression, further confirm the existence of common regulatory mechanisms implicated in the expression of *ACSM5* in BF and muscle. The most associated SNP was identified on SSC10 and it is an intronic polymorphism (ASGA0090778; *p*-value= $1.44x10^{-15}$; â= -4.081) in the Component of Oligomeric Golgi Complex 7 (*COG7*) gene (Table S4). In these *trans*-eQTLs regions, other lipid-related genes were identified such as the Golgi-associated, Gamma Adaptin Ear Containing, ARF Binding Protein 2 (*GGA2)* gene (H3GA0055120; *p*-value= $2.89x10^{-15}$; â= -4.072) and the NADH Dehydrogenase (Ubiquinone) 1, Alpha/Beta Subcomplex, 1, 8 kDa (*NDUFAB1*) gene (H3GA0055101 and MARC0015344; *p*-value= $8.11x10^{-07}$; â= 2.287) on SSC10, and the Phosphatidylinositol Glycan Anchor Biosynthesis Class F (*PIGF*) gene and the Protein Kinase C Epsilon (*PRKCE*) gene on SSC3 (Table S4). On SSC3, another region at 83.37 Mb was also associated in *trans* with the *ACSM5* gene-expression. In this region, the Malate Dehydrogenase 1 (*MDH1*) gene (82,603,920-82,615,099 bp) was identified. Finally, within the *trans*-eQTL for *ACSM5* at 134.99 Mb on SSC2, two genes that may affect lipid metabolism were identified: Aldehyde Dehydrogenase 7 Family Member A1 (*ALDH7A1*) and Membrane Associated Ring-CH-Type Finger 3 (*MARCH3*) (Table S5).
For the *trans*-eQTL identified on SSC16 for *ACSM5*, no strong candidate gene exerting a known lipid metabolism function was detected.

The *ELOVL6* gene

In previous studies of our group, the SNP *ELOVL6:c.-533C>T* located in the promoter region of *ELOVL6* was found to be highly associated with the *ELOVL6* expression in BF and, with the percentages of palmitic (C16:0) and palmitoleic (C16:1(n-7)) acids in BF and muscle (Corominas *et al.*, 2013b). Later on, the polymorphism *ELOVL6:c.-394G>A***,** located in a putative binding site for estrogen receptor alpha (ERα) in the *ELOVL6*

promoter, was associated with the methylation levels of the *ELOVL6* promoter and with the expression of the gene, suggesting this polymorphism as the causal mutation for the QTL on SSC8 affecting palmitic (C16:0) and palmitoleic (C16:1(n-7)) acids (Corominas *et al.*, 2015). Taking into account that a different number of BC1_LD animals and a different mRNA quantification method (microfluidic array vs conventional qPCR) was applied between studies, the previously *ELOVL6* genotyped polymorphisms (three in the promoter region, one in exon 4 and two in the 3'UTR region) (Corominas *et al.*, 2013b; Corominas *et al.*, 2015) were genotyped in the 115 BC1_LD animals and incorporated in the eGWAS. The results were consistent with those of our previous studies on SSC8 (Corominas *et al.*, 2013b), where a significant region at chromosome level associated with *ELOVL6* mRNA expression in BF was observed (Figure S1). The most significant peak was for two SNPs with the same *p*-value (ALGA0049135 and ALGA0049139; *p*-value= $4.60x10^{-05}$; â= -0.563), located in an intron of *ANK2*, very close to the *ELOVL6* gene. In addition, the *ELOVL6:c.-533C>T* and *ELOVL6:c.-394G>A* polymorphisms, which were in full LD, also showed high association (*p*-value= $6.42x10^{-04}$; â= 0.460), although in our analysis did not achieve significance after multiple testing corrections (*q*-value ≤ 0.05).

Remarkably, *ANK2* is one of the most central genes in an adipose co-expression network related with IMFA composition in the BC1_LD (Ramayo-Caldas *et al.*, 2014). In a recent study, knockin mice expressing human nonsynonymous mutations in *ANK2* showed altered glucose homeostasis contributing to increased adiposity. This phenotype was caused by the reduction in ANK2 protein levels which produce an elevation of cell surface GLUT4 and increased glucose uptake in skeletal muscle and fat (Lorenzo *et al.*, 2015). Thus, we cannot discard an association of this gene with the mRNA expression levels of *ELOVL6*. Further analyses are necessary to corroborate this hypothesis.

Regarding the *trans*-associated regions with the BF mRNA *ELOVL6* expression, Corominas *et al.* (2013b) did not identify any region at whole genome level, in contrast with the *trans*-eQTL on SSC13 identified in the present study. The observed discrepancy could be due to the different animals used between the two studies (94 samples overlapping between the two studies) and to the subtle differences observed between the two methods used for mRNA quantification (correlation coefficient, r= 0.91). No genes related to lipid metabolism function were identified in the SSC13 *trans*-eQTL. However, we have to highlight that the same region on SSC13 was associated at chromosome level with the expression of the *ELOVL5* and *SCD* genes. *ELOVLs* and *SCD* genes are implicated in

the elongation and desaturation of FAs in the endoplasmic reticulum membranes. These metabolic functions are essential to the maintenance of lipid homeostasis (reviewed in Guillou *et al.*, 2010). Interestingly, it has been reported that the expression of these genes are primarily regulated at transcriptional level (reviewed in Guillou *et al.*, 2010). In this study, highly significant correlations (*p*-value = $2.22x10^{-16}$) among the mRNA expression of these genes were obtained ($r_{ELOVL5\text{-}ELOVL6}$= 0.90; $r_{ELOVL5\text{-}SCD}$= 0.84; $r_{ELOVL6\text{-}SCD}$= 0.86), supporting the involvement of common elements regulating their mRNA expression. In addition, we found high correlations with the genes coding for the TFs SREBF1 and PPARs ($r_{ELOVL5\text{-}PPARG}$= 0.75, *p*-value= $2.22x10^{-16}$; $r_{ELOVL5\text{-}SREBF1}$= 0.74, *p*-value= $2.22x10^{-16}$; $r_{ELOVL5\text{-}PPARA}$= 0.65, *p*-value= $1.02x10^{-14}$; $r_{ELOVL6\text{-}PPARG}$= 0.68, *p*-value= $2.22x10^{-16}$; $r_{ELOVL6\text{-}SREBF1}$= 0.70, *p*-value= $2.22x10^{-16}$; $r_{ELOVL6\text{-}PPARA}$= 0.69, *p*-value= $2.22x10^{-16}$; $r_{SCD\text{-}PPARG}$= 0.59, *p*-value= $1.01x10^{-11}$; $r_{SCD\text{-}SREBF1}$= 0.63, *p*-value= $8.48x10^{-14}$; $r_{SCD\text{-}PPARA}$= 0.51, *p*-value= $1.03x10^{-08}$) which contribute to the regulation of these genes (Guillou *et al.*, 2010; Corominas *et al.*, 2013a; Estany *et al.*, 2014). High correlation values were also found between the mRNA expression of *DGAT1* and *DAGT2* genes with *ELOVLs* and *SCD* genes ($r_{DGAT1\text{-}ELOVL5}$= 0.72, *p*-value= $2.22x10^{-16}$; $r_{DGAT1\text{-}ELOVL6}$= 0.70, *p*-value= $2.22x10^{-16}$; $r_{DGAT1\text{-}SCD}$= 0.59, *p*-value= $3.89x10^{-12}$; $r_{DGAT2\text{-}ELOVL5}$= 0.81, *p*-value= $2.22x10^{-16}$; $r_{DGAT2\text{-}ELOVL6}$= 0.74, *p*-value= $2.22x10^{-16}$; $r_{DGAT2\text{-}SCD}$= 0.76, *p*-value= $2.22x10^{-16}$). This result agrees with the interrelated function of these genes which are implicated in lipogenesis (*ELOVLs* and *SCD*) and triglyceride (TG) synthesis (*DGAT1* and *DGAT2*), the main function of adipose tissue (Bernlohr *et al.*, 2002).

ELOVL6 and *SCD* genes were over-expressed in the adipose tissue transcriptome (RNA-Seq) of BC1_LD animals with higher content of intramuscular monounsaturated fatty acids (MUFA) and saturated fatty acids (SFA), when compared with animals having more polyunsaturated (PUFA) (Corominas *et al.*, 2013a) supporting the relevance of these genes in the determination of FA composition in the BC1_LD.

The *FABP4* gene

The Fatty Acid Binding Protein 4 (*FABP4*) gene is not mapped in the current *Sscrofa10.2* assembly. Nevertheless, radiation hybrid (RH) and linkage maps located *FABP4* gene close to *FABP5* on SSC4 (Gerbens *et al.*, 1998; Estellé *et al.*, 2006), in agreement with the human comparative map. For this reason, we used the known mapped *FABP5* gene (SSC4: 60.31 Mb) in order to define *cis*/*trans* eQTLs for the unmapped *FABP4* gene. This gene has been reported as a strong positional candidate gene for a QTL region associated with growth

and fatness traits in the IBMAP population (Mercadé *et al.*, 2005, 2006; Estellé *et al.*, 2006). Furthermore, Ramayo-Caldas *et al.* (2012) and Muñoz *et al.* (2013) identified an association between this position of SSC4 and fat deposition and FA composition in the BC1_LD backcross. In a previous study in the BC1_LD backcross, an indel located in the intron 1 of *FABP4* (*FABP4:g.2634_2635insC*) was identified as the most associated polymorphism with the *FABP4* mRNA levels in BF (Ballester *et al.*, submitted). In the present study, the indel, which was genotyped in the 115 BC1_LD animals and included in the eGWAS study, was one of the most significant associated polymorphisms (*p*-value= 1. 27x10^{-06}; â= -0.219) (Fig. 1B) but the most significant *cis*-SNP (ALGA0025337; *p*-value= 8.67x10^{-07}; â= 0.328) was located in an intergenic region (Table S4).

Taking into account the highly polymorphic nature of the porcine *FABP4* gene (Ojeda *et al.*, 2006) and a possible regulatory role of miRNAs in the *FABP4* gene-expression (Qi *et al.*, 2015), the 3'UTR of the *FABP4* gene was amplified and sequenced using 10 animals with extreme values of *FABP4* mRNA expression in BF. Three poly(A) signals were shown at positions 540, 1214, and 1428 bp (positions based on the GenBank Y16039 sequence counting from the first triplet code) used for mRNA poly(A) tail addition. Moreover, a polymorphism in the 3'UTR (*FABP4:g.6723*A>G) was identified and genotyped in the 115 BC1_LD animals. The association analysis with the *FABP4* mRNA expression values revealed that the SNP in the 3'UTR region has the lowest *p*-value (*p*-value= 3.07x10^{-08}; â= -0.260) (Fig. 1B).

Interestingly, *FABP4:g.6723*A>G SNP was inside a putative miRNA binding site for the putative human miRNA hsa-miR-3182 and it is predicted to bind only when *FABP4:g.6723G* allele is present. Unfortunately, we did not find the homologous *Sus scrofa* miR-3182 in the current assembly (*Sscrofa10.2*) of the pig genome. Although the 3'UTR SNP (*FABP4:g.6723*A>G) is a clear candidate to explain the differences of *FABP4* mRNA levels among animals, we cannot discard also a role of the indel (*FABP4:g.2634_2635insC)* in the *FABP4* gene regulation. Indeed, the indel polymorphism was predicted to be located in a target binding site for PPARG and NR4A2 TFs (Ballester *et al.*, submitted). In our analysis the correlation between the mRNA expression of *PPARG* and *FABP4* was r= 0.51 (*p*-value= 9.27x10^{-09}). Further functional analyses are needed to test the role of these polymorphisms in the *FABP4* gene regulation and besides in the determination of IMFA composition.

The eGWAS performed for the *FABP4* gene, revealed four *trans*-eQTLs on SSC2, SSC3, SSC4, and SSC9 (Table 1); where several genes involved in lipid metabolism were mapped. On SSC2 the Berardinelli-Seip Congenital Lipodystrophy 2 (Seipin) (*BSCL2*), Diacylglycerol Lipase Alpha (*DAGLA*), EH Domain Containing 1 (*EHD1*), Fatty Acid Desaturase 1 (*FADS1*), Fatty Acid Desaturase 2 (*FADS2*), Fatty Acid Desaturase 3 (*FADS3*), Lectin Galactoside Binding Soluble 12 (*LGALS12*), N(Alpha)-Acetyltransferase 40 Phospholipase A2 Group XVI (*PLA2G16*), Splicing Factor 1 (*SF1*), and Transmembrane 7 Superfamily Member 2 (*TM7SF2*) candidate genes were located. The function of *BSCL2* gene is still being investigated, however, its relationship with adipogenesis, with the genesis of lipid droplets and the regulation of the metabolism of phospholipids and triacylglycerides has been established (Boutet *et al*., 2009). Liu *et al*., (2014) performed an adipose-specific Seipin knockout mice with FABP-mediated *BSCL2* deletion exhibiting decreased lipolysis in response to β-adrenergic receptors agonists in vivo. We also identify some members of the fatty acid desaturase family (FADS), specifically *FADS1, FADS2,* and *FADS3* whose expression phenotypes have been also analyzed in this study. However, no significant correlations between the mRNA expression levels of the *FABP4* gene and the *FADS1, FADS2,* and *FADS3* genes were obtained. In this chromosomal region we also identified the *LGALS12* gene, an intracellular galectin preferentially expressed in adipocytes which regulates lipolysis and whole-body energy metabolism (Yang *et al.* 2011). Furthermore, *FABP4* and *LGALS12* genes were identified in the glycolysis/gluconeogenesis pathway in an expression analysis performed in human adipose-derived stem cells (Satish *et al*., 2015). *PLA2G16,* which encodes a phospholipase that catalyzes phosphatidic acid into lysophosphatidic acid and free FA, was also identified (Xiong *et al*., 2014). It is known that *FABP4* and *PLA2G16* are involucrate in the glutathione peroxidase 3 (GPX3) complex. GPX3 complex is expressed in adipose tissue (Maeda *et al*., 1997) and catalyze lipid hydroperoxides as well as hydrogen peroxide (Yamamoto & Takahashi, 1993). Other lipid-related genes identified within this *trans*-eQTL on SSC2 for *FABP4* are shown in Table 2.

The following lipid-related genes were identified within the *trans*-eQTL on SSC3 for *FABP4* gene-expression: Cytochrome P450 Family 1 Subfamily B Member 1 (*CYP1B1*), EH Domain Containing 3 (*EHD3*), Ethanolaminephosphotransferase 1 (*EPT1*), Polypeptide N-Acetylgalactosaminyltransferase 14 (*GALNT14*), Glucokinase (Hexokinase 4) Regulator (*GCKR*), Hydroxyacyl-CoA Dehydrogenase/3-Ketoacyl-CoA (*HADHA*), Hydroxyacyl-CoA Dehydrogenase/3-Ketoacyl-CoA (*HADHB*), Lysocardiolipin

Acyltransferase 1 (*LCLAT1*), Phospholipase B1 (*PLB1*), Protein Phosphatase 1 Catalytic Subunit Beta (*PPP1CB*), Ribokinase (*RBKS*), Sorting Nexin 17 (SNX17), and Spastin (*SPAST*). It has been demonstrated that *CYP1B1* extensively affects many gene responses directed by the lipid-responsive receptors. Liu *et al.*, (2015) have demonstrated that the reduction in body weight gain and white adipose tissue in *CYP1B1* deficient mice exhibited coordinate decreases in FA synthesis (regulated by *FABP4*, among others) when compared with wild type ones. The *HADHA* and *HADHB* genes encode the alpha and beta, respectively, subunits of the mitochondrial trifunctional protein, which catalyze the last three steps of mitochondrial beta-oxidation of long chain FAs. Remarkably, these two genes overlapped with QTLs previously described in the IBMAP population for palmitic (C16:0) and palmitoleic (C16:1(n-7)) acids (Ramayo-Caldas *et al.*, 2012).

For the *trans*-eQTL identified on SSC4 for *FABP4*, no strong candidate gene exerting a known lipid metabolism function was detected.

Finally, on SSC9, we identified the *RFWD2* gene (Ring Finger And WD Repeat Domain 2) associated with *FABP4* mRNA expression. Interestingly, this gene regulates lipid metabolism by targeting acetyl-CoA carboxylase, a rate-limiting enzyme in FA synthesis, for degradation *via* its interaction with the pseudokinase tribbles 3 (*TRB3*), a pseudokinase and negative regulator of the Serine/Threonine Kinase (Akt) gene in muscle and liver (Tong *et al.*, 2006; Du *et al.*, 2003).

The *FADS2* gene

The most significant *cis*-eSNP for *FADS2* gene-expression (ASGA0104083; *p*-value= 5.98 $x10^{-08}$; â= 0.466) was located less than 0.23 Mb upstream of the *FADS2* gene (Fig. 1C). Interestingly, the members belonging to the FA desaturase gene family: *FADS1, FADS2,* and *FADS3*, cluster together in a region on SSC2 significantly associated with cis-7 hexadecenoic acid (C16:1(n-9)), linoleic acid (C18:2(n-6)), α-linolenic acid (C18:3(n-3)), and PUFA in BF (Ballester *et al.*, 2016), and with palmitic acid (C16:0) and the SFA in intramuscular fat (Ramayo-Caldas *et al.*, 2012) in the BC1_LD. In addition, a high correlation has been observed between the mRNA expression levels of *FADS1* and *FADS2* in liver ($r_{FADS1\text{-}FADS2}$= 0.92; *p*-value= $1.11x10^{-17}$) which suggest common regulatory mechanisms controlling the mRNA expression of both desaturases in this tissue (Ballester *et al.*, 2017). In the present work, the correlation between the mRNA expression levels of *FADS1* and *FADS2* in BF was moderate-high ($r_{FADS1\text{-}FADS2}$= 0.63; *p*-value= $8.26x10^{-14}$).

Therefore, these results suggest that common elements could also be regulating the expression of desaturases in BF, but there are also other elements, for instance the *cis*-acting element associated with the *FADS2* mRNA expression, differentially regulating the expression of *FADS1* and *FADS2* in BF. In addition, the low correlation observed between *FADS2* mRNA levels in BF and liver (r= 0.23; *p*-value= $1.91x10^{-02}$) suggests a different mechanism of regulation in both tissues. This result agrees with the fact that *FADS2* is differentially-expressed between sexes depending on the tissue. Whereas in adipose tissue the *FADS2* gene is more expressed in males, in liver it is more expressed in females (Ballester *et al.*, 2017). Similar results have also been shown in rats, where the mRNA expression of *FADS2* is higher in the liver of females than males (Childs *et al.*, 2012). To find polymorphisms which may modulate *FADS2* expression a search of polymorphisms was performed by the analysis of whole genome sequence data from seven founders of the IBMAP population with IGV (Robinson *et al.*, 2011). Three polymorphisms were identified at positions *g9118843C>T* (rs331050552), *g9118813G>A* (rs321384923), and *g9118721G>A* (rs336076510) according the Ensembl ENSSSCG00000013072. The most proximal 5' mutation (*g9118843C>T*) was genotyped in the BC1_LD animals and included in the eGWAS analysis.

However, no significant association was found between this mutation and the *FADS2* mRNA expression. Further analyses are necessary to find new candidate *cis*-acting polymorphisms implicated in the regulation of *FADS2* gene-expression.

Three regions on SSC6, SSC8, and SSC10 were associated in *trans* with *FADS2* gene-expression. In SSC6, the Cell Division Cycle 42 (*CDC42*), Endothelin Converting Enzyme 1 (*ECE1*), Fucosidase, Alpha-L-1, Tissue (*FUCA1*), UDP-Galactose-4-Epimerase (*GALE*), 3-Hydroxymethyl-3-Methylglutaryl-CoA Lyase (*HMGCL*), and Lysine Demethylase 1A (*KDM1A*) candidate genes have been identified. Interestingly, the *KDM1A* gene, also known as *LSD1*, has been recently identified as a novel regulator of lipid metabolism as it is required for the expression of *SREBF1* and for the efficient binding of *SREBF1* to the target gene promoters (Abdulla *et al.*, 2014). Remarkably, *SREBF1* regulates the expression of desaturases (Nakamura & Nara, 2004), highlighting the *KDM1A* gene as a potential candidate regulator of *FADS2* gene-expression.

The most associated SNP for *FADS2 trans*-eQTL on SSC8 was an intronic polymorphism (MARC0041089; *p*-value= $1.93x10^{-05}$; â= 0.516) in the Insulin Like Growth Factor Binding Protein 7 (*IGFBP7*) gene (Table S4). This gene encodes a member of the insulin-like

growth factor (IGF)-binding protein and through their regulation of IGFs and insulin may influence the metabolism of adipocytes, having implications in the development of obesity and insulin resistance (Ruan *et al.*, 2010).

The last region identified in *trans* for *FADS2*, was on SSC10 where the *Cubilin* (*CUBN*) lipid-related gene was identified.

The *SLC27A4 gene*

The *SLC27A4* (Solute Carrier Family 27 (Fatty Acid Transporter), Member 4) gene-expression GWAS revealed three *trans*-eQTL on SSC9, SSC14, and SSC15. On SSC9, the Prolylcarboxypeptidase (*PRCP*) gene was located. It is an important regulator of energy and glucose homeostasis (Jeong *et al.*, 2012). For the SSC14 *trans*-eQTL, no strong candidate genes related to lipid metabolism could be detected. Finally, on SSC15, Phenylalanyl-tRNA Synthetase Beta Subunit (*FARSB*) and Monoacylglycerol O-Acyltransferase 1 (*MOGAT1*) lipid-related genes were also identified.

Sex effect on gene-expression in the adipose tissue

The control of FA homeostasis has been described to have a pronounced sexual dimorphism (Grove *et al.*, 2010). In agreement, sex differences in the control of gene-expression have been identified in different tissues like muscle, liver, adipose tissue and brain in mice (Yang *et al.*, 2006; Van Nas *et al.*, 2009). In the present work, a significant sex effect (p-value$\leq$ 0.05) on gene-expression levels was detected in 20 out of the 43 genes analyzed (47%): *ACSM5, AGPAT2, ANK2, ATGL, DGAT2, EGF, ELOVL5, ELOVL6, FADS2, MGLL, MLXIPL, NFKB1, PEX2, PLA2G12A, PLPP1, PPARA, PPARD, SCAP, SCD,* and *SREBF1* (Fig. 2). Overall, a higher number of genes were more expressed in females (*ACSM5, AGPAT2, ANK2, DGAT2, EGF, ELOVL5, ELOVL6, MGLL, MLXIPL, PLA2G12A, PNPLA2, PPARA, PPARD, PEX2, SCAP, SCD,* and *SREBF1*). Conversely, only three genes (*FADS2, NFKB1,* and *PLPP1*) showed a higher expression in males (Table S6). Among them, some key regulators of lipid metabolism such as *PPARA, SCD,* and *SREBF1* which may be determining the bias observed in the female over-expressed genes. Remarkably, lipogenic genes such as *SCD* and *SREBF1* were also more expressed in females in the *longissimus dorsi* muscle of pigs (Puig-Oliveras *et al.*, 2016), and in pig liver tissue (Ballester *et al.*, 2017). However, we observed a different pattern of expression for *PPARA*; while it was more expressed in females in liver and adipose tissue, the mRNA levels of *PPARA* were higher in males in muscle (Puig-Oliveras *et al.*, 2016;

Ballester *et al.*, 2017). Finally, for *ACSM5, AGPAT2, MLXIPL, EGF, ELOVL5*, *PEX2,* and *SCAP* the same female-biased gene-expression was observed than in pig liver tissue (Ballester *et al.*, 2017). This agree with the results observed in mice in which the analysis of sexual dimorphism in liver, adipose, muscle, and brain revealed common functionalities of steroid and lipid metabolism for the sexually dimorphic genes between liver and adipose tissues. Furthermore, the overlap of sexually dimorphic genes was higher between adipose and liver tissues (22.9%) than between adipose and muscle tissues (6.6%; Yang *et al.*, 2006). The highest rate of coincidence of female-biased gene expression among liver and adipose tissue may suggest common regulatory mechanisms in both tissues.

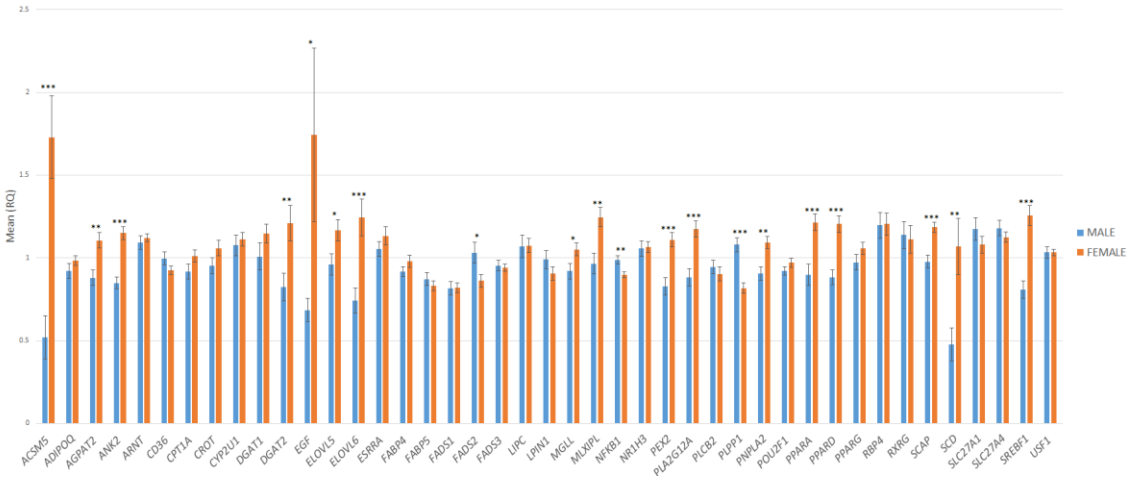

Figure 2. Comparison between males and females of gene-expression levels of 43 lipid-related genes in adipose tissue. Data represent means ± standard error of the means (SEM). Significant differences between sexes are indicated as *P≤0.05, **P≤0.01 and ***P≤0.001.

Fatty acid composition and gene-expression in the adipose tissue

To explore the relationship between gene-expression levels and FA composition percentages in BF, a correlation analysis was performed. In general moderate correlations were identified (Figure S2). The *CD36* gene, which may function as a regulator of FA transport (Bonen *et al.*, 2004), showed a negative correlation with palmitoleic acid (C16:1(n-7)) (r= -0.31; *p*-value= $9.04x10^{-04}$). Palmitoleic acid (C16:1(n-7)) has been identified as a lipokine involved in the maintenance of systemic metabolic homeostasis (Cao *et al.*, 2008). A negative correlation between *PLPP1* gene-expression and palmitic acid (C16:0) (r= -0.35; *p*-value= $1.46x10^{-04}$) was found. This gene is a member of the phosphatidic acid phosphatase (PAP) family and participates in the synthesis of glycerolipids. In addition, *PLPP1* gene-expression showed moderate correlations with the percentage of cis-7

hexadecenoic acid (C16:1(n-9)) (r= 0.32; *p*-value= $5.40x10^{-04}$) and C20:3(n-9) (r= 0.33; *p*-value= $3.40x10^{-04}$).

The cis-7 hexadecenoic acid (C16:1(n-9)) also showed negative correlation (r= -0.39; *p*-value= $2.05x10^{-05}$) with *SCD* gene-expression, which plays an important role in the regulation of the expression of genes involucrated in lipogenesis (Sampath *et al.*, 2007).

Furthermore, the octadecenoic acid (C18:1(n-7)) was negatively correlated with *CROT* (r= -0.36; *p*-value= $1.02x10^{-04}$) and *USF1* (r= -0.35; *p*-value= $1.29x10^{-04}$) gene-expressions. The *CROT* gene plays a role in the pathway of FA beta-oxidation, and provides a crucial step in the transport of medium and long-chain acyl-coA out of the mammalian peroxisome to the mitochondria (Ramsay & Gandour, 1999). Moreover, *USF1* gene is involved in the maintenance of high levels of FA synthase transcription under lipogenic conditions (Griffin & Sul, 2004).

Functional network analysis of genes mapping in eQTLs

To take a deep look at the regulatory mechanisms that are influencing the gene-expression phenotypes, gene annotation of the 19 eQTLs chromosomal regions was performed. For *trans*-eQTLs all the genes located within ±1 Mb were selected for gene annotation. Conversely, for *cis*-eQTLs only the studied candidate gene was considered for further analyses. In the 19 eQTLs, a total of 474 protein-coding genes, 2 processed transcript, 11 miRNA, 3 miscRNA, 10 pseudogenes, 6 rRNA, 17 snoRNAs, and 21 snRNA were annotated (Table S5). From the 474 protein-coding genes with Ensembl Gene ID, 393 have at least one human orthologous gene (Table S7) and were submitted to IPA to perform a functional categorization.

Several networks related to lipid metabolism were identified: (i) lipid metabolism, small molecule biochemistry, infectious diseases (score= 42; interval= 8); (ii) lipid metabolism, small molecule biochemistry, cellular assembly and organization (score= 32; interval= 8); (iii) carbohydrate metabolism, organ morphology, reproductive system development and function (score= 30; interval= 3), and (iv) amino acid metabolism, carbohydrate metabolism, molecular transport (score= 18; interval= 9) (Table S8). Interestingly, two of the identified networks have the Akt complex as central (ID= 10 and 26; Table S8). It is known that the PKB/Akt plays an important role in the insulin regulation of glucose transport (Hajduch *et al.*, 2001), and has been also identified as central in the main over-represented pathways in a muscle transcriptome study between individuals phenotypically extreme for IMFA composition (Puig-Oliveras *et al.*, 2014b), in a muscle eQTL analysis of

45 lipid-related genes (Puig-Oliveras *et al.*, 2016), and in a liver eQTL analysis of 44 candidates genes related with lipid metabolism (Ballester *et al.*, 2017). Remarkably, several of the potential regulators annotated in *trans*-eQTL for *FABP4* and *FADS2* (*BSCL2, FADS1, FADS2, KDM1A, LGALS12, PLA2G16, PLB1,* and *PPP1CB*) were identified inside the Akt pathway. These findings suggest this pathway as central in the genetic determination of FA composition traits in the BC1_LD.

Prediction analysis of transcription factor binding sites

To identify master regulators of global gene-expression in all the genes analyzed in the present study, an *in-silico* identification of the TF binding sites in the promoter region of (1) the 415 genes with human orthologous ID annotated in the *trans*-eQTL intervals and, (2) the 43 candidate lipid-related genes was performed using the iRegulon Cytoscape plugin (Janky *et al.*, 2014). The *PPARG* gene was the most enriched TF motif (NES= 5.134; 167 target genes, 30 out of the 44 analyze-related genes; Table S9). This agree with the fact that this gene is an adipogenic TF considered an important regulator of lipid and carbohydrate metabolism (Peeters & Baes, 2010). In our analysis the mRNA expression of *PPARG* was highly correlated with the mRNA expression of genes implicated in lipid transport, lipogenesis and TG synthesis (Table S10), suggesting an important role of this TF in lipid storage. Interestingly, this TF has been identified as a key regulator of FA composition in the same material using a co-association network analysis (Ramayo-Caldas *et al.*, 2014) and in a muscle eQTL analysis of 45 lipid-related genes (Puig-Oliveras *et al.*, 2016).

Conclusions

The expression pattern of forty-three lipid-related candidate genes was studied in the adipose tissue of 115 Iberian x Landrace backcrossed pigs. Furthermore, the eGWAS analysis identified the location of factors regulating the expression of these candidate genes, increasing our knowledge of the regulatory mechanisms implicated in adipose tissue lipid metabolism and its consequences in lipid-related traits.

Competing interest

The authors declare that they have no competing interests.

Author contributions

Conceptualization: JMF MB. **Methodology:** JMF MB. **Formal analysis:** MR MB APO JMF. **Investigation:** MR APO DCP LCM AC. **Resources:** JMF AIF. **Write original draft:** MR MB JMF. **Writing review & editing:** MB JMF. **Visualization:** MR MB. Supervision: JMF. **Funding acquisition:** JMF AIF.

Funding

This work has been funded by the MICINN AGL2014-56369-C2. MR was funded by a Formació i Contractació de Personal Investigador Novell (FI-DGR) PhD grant from Generalitat de Catalunya (ECO/1639/2013). MB was financially supported by a Ramon y Cajal contract (RYC-2013-12573) from the Spanish Ministry of Economy and Competitiveness, APO was funded by a Personal Investigador en Formación (PIF) PhD grant from the Universitat Autònoma de Barcelona (458-01-1/2011), DCP by a Formació i Contractació de Personal Investigador Novell (FI-DGR) PhD grant from Generalitat de Catalunya (ECO/1788/2014) and LCM was funded by a FPI PhD grant from the Spanish Ministry of Economy and Competitiveness (BES-2015-075403).

Acknowledgments

We would like to thank all of the members of the INIA, IRTA, and UAB institutions who contributed to the generation of the animal material used in this work. We acknowledge the support of the Spanish Ministry of Economy and Competitiveness for the *Centre of Excellence Severo Ochoa* 2016–2019 (SEV-2015-0533) grant awarded to the Centre for Research in Agricultural Genomics.

References

Abdulla A, Zhang Y, Hsu FN, Xiaoli AM, Zhao X, Yang ES, *et al.* (2014). Regulation of lipogenic gene expression by lysine-specific histone demethylase-1 (LSD1). *The Journal of Biological Chemistry* 289(43):29937-47.

Ballester M, Cordón R, Folch JM (2013). DAG expression: high-throughput gene expression analysis of real-time PCR data using standard curves for relative quantification. *PLoS One* 8(11):e80385.

Ballester M, Revilla M, Puig-Oliveras A, Marchesi JA, Castelló A, Corominas J, *et al.* (2016). Analysis of the porcine APOA2 gene expression in liver, polymorphism identification and association with fatty acid composition traits. *Animal Genetics* 47(5):552-9.

Ballester M, Ramayo-Caldas Y, Revilla M, Corominas J, Castelló A, Estellé J, *et al.* (2017). Integration of liver gene co-expression networks and eGWAs analyses highlighted candidate regulators implicated in lipid metabolism in pigs. *Scientific Reports* 7:46539.

Ballester M, Puig-Oliveras A, Castelló A, Revilla M, Fernández AI, Folch JM (2017). Analysis of FABP4 and FABP5 gene expression affecting pig fatness. *Animal Genetics* (*submitted*).

Bernlohr DA, Jenkins AE, Bennaars AA (2002). Chapter 10 Adipose tissue and lipid metabolism. *In New Comprehensive Biochemistry* (Vol. 36, pp. 263-289). (New Comprehensive Biochemistry; Vol. 36).

Bonen A, Campbell SE, Benton CR, Chabowski A, Coort SL, Han XX, *et al.* (2004) Regulation of fatty acid transport by fatty acid translocase/CD36. *The Proceedings of the Nutrition Society* 63(2):245-9.

Boutet E, El Mourabit H, Prot M, Nemani M, Khallouf E, Colard O, *et al.* (2009). Seipin deficiency alters fatty acid Delta9 desaturation and lipid droplet formation in Berardinelli-Seip congenital lipodystrophy. *Biochimie* 91(6):796-803.

Cao H, Gerhold K, Mayers JR, Wiest MM, Watkins SM, Hotamisligil GS (2008). Identification of a lipokine, a lipid hormone linking adipose tissue to systemic metabolism. *Cell* 134(6):933-44.

Casellas J, Noguera JL, Reixach J, Díaz I, Amills M, Quintanilla R (2010). Bayes factor analyses of heritability for serum and muscle lipid traits in Duroc pigs. *Journal of Animal Science* 88(7):2246-54.

Cheung VG, Spielman RS (2009). Genetics of human gene expression: mapping DNA variants that influence gene expression. *Nature Review Genetics* 10(9):595-604.

Childs CE, Hoile SP, Burdge GC, Calder PC (2012). Changes in rat n-3 and n-6 fatty acid composition during pregnancy are associated with progesterone concentrations and

hepatic FADS2 expression. *Prostaglandins, Leukotrienes, and Essential Fatty Acids* 86(4-5):141-7.

Corominas J, Ramayo-Caldas Y, Puig-Oliveras A, Estellé J, Castelló A, Alves E, *et al.* (2013a). Analysis of porcine adipose tissue transcriptome reveals differences in de novo fatty acid synthesis in pigs with divergent muscle fatty acid composition. *BMC Genomics* 14:843.

Corominas J, Ramayo-Caldas Y, Puig-Oliveras A, Pérez-Montarelo D, Noguera JL, Folch JM, *et al.* (2013b). Polymorphism in the ELOVL6 gene is associated with a major QTL effect on fatty acid composition in pigs. *PLoS One* 8(1):e53687.

Corominas J, Marchesi JA, Puig-Oliveras A, Revilla M, Estellé J, Alves E, *et al.* (2015): Epigenetic regulation of the ELOVL6 gene is associated with a major QTL effect on fatty acid composition in pigs. *Genetics Selection Evolution* 47:20.

Dai MH, Xia T, Zhang GD, Chen XD, Gan L, Feng SQ, *et al.* (2006). Cloning, expression and chromosome localization of porcine adiponectin and adiponectin receptors genes. *Domestic Animal Endocrinology* 30(2):117-25.

Du K, Herzig S, Kulkarni RN, Montminy M (2003). TRB3: a tribbles homolog that inhibits Akt/PKB activation by insulin in liver. *Science* 300(5625):1574-7.

Estany J, Ros-Freixedes R, Tor M, Pena RN (2014). A functional variant in the stearoyl-CoA desaturase gene promoter enhances fatty acid desaturation in pork. *PLoS One* 9(1):e86177.

Estellé J, Pérez-Enciso M, Mercadé A, Varona L, Alves E, Sánchez A, *et al.* (2006). Characterization of the porcine FABP5 gene and its association with the FAT1 QTL in an Iberian by Landrace cross. *Animal Genetics* 37(6):589-91.

Frayn KN, Arner P, Yki-Järvinen H (2006). Fatty acid metabolism in adipose tissue, muscle and liver in health and disease. *Essays in Biochemistry* 42:89-103.

Gerbens F, Jansen A, van Erp AJ, Harders F, Meuwissen TH, Rettenberger G, *et al.* (1998). The adipocyte fatty acid-binding protein locus: characterization and association with intramuscular fat content in pigs. *Mammalian Genome* 9(12):1022-6.

Gilad Y, Rifkin SA, Pritchard JK (2008). Revealing the architecture of gene regulation: the promise of eQTL studies. *Trends in Genetics* 24(8):408-15.

Griffin MJ, Sul HS (2004). Insulin regulation of fatty acid synthase gene transcription: roles of USF and SREBP-1c. *IUBMB Life* 56(10):595-600.

Grove KL, Fried SK, Greenberg AS, Xiao XQ, Clegg DJ (2010). A microarray analysis of sexual dimorphism of adipose tissues in high-fat-diet-induced obese mice. *International Journal of Obesity: Journal of the International Association for the Study of Obesity* 34(6):989-1000.

Guillou H, Zadravec D, Martin PG, Jacobsson A (2010). The key roles of elongases and desaturases in mammalian fatty acid metabolism: Insights from transgenic mi *Progress in Lipid Research* 49(2):186-99.

Hajduch E, Litherland GJ, Hundal HS (2001). Protein kinase B (PKB/Akt)--a key regulator of glucose transport? *FEBS Letters* 492(3):199-203.

Hastie TJ, Pregibon D (1992). Generalized linear models. *Chapter 6 of Statistical Models in S. Chambers JM, Hastie TJ (eds.). Wadsworth & Brooks/Cole, Pacific grove.*

Ihaka R, Gentleman R (1996). R: A language for data analysis and graphics. *Journal of Computational and Graphical Statistics* 5:299–314.

Janky R, Verfaillie A, Imrichová H, Van de Sande B, Standaert L, Christiaens V, *et al.* (2014). iRegulon: from a gene list to a gene regulatory network using large motif and track collections. *PLoS Computational Biology* 10(7):e1003731.

Jeong JK, Szabo G, Raso GM, Meli R, Diano S (2012). Deletion of prolyl carboxypeptidase attenuates the metabolic effects of diet-induced obesity. *American journal of physiology. Endocrinology and Metabolism* 302(12):E1502-10.

Kapushesky M, Emam I, Holloway E, Kurnosov P, Zorin A, Malone J, *et al.* (2010). Gene expression atlas at the European bioinformatics institute. *Nucleic Acids Research* 38:D690-8.

Lee C, Huang CH (2013). LASAGNA-Search: an integrated web tool for transcription factor binding site search and visualization. *Biotechniques* 54(3):141-53.

Liu L, Jiang Q, Wang X, Zhang Y, Lin RC, Lam SM, *et al.* (2014): Adipose-specific knockout of SEIPIN/BSCL2 results in progressive lipodystrophy. *Diabetes* 63(7):2320-31.

Liu X, Huang T, Li L, Tang Y, Tian Y, Wang S, *et al.* (2015). CYP1B1 deficiency ameliorates obesity and glucose intolerance induced by high fat diet in adult C57BL/6J mice. *American Journal of Translational Research* 7(4):761-71.

Lorenzo DN, Healy JA, Hostettler J, Davis J, Yang J, Wang C, *et al.* (2015). Ankyrin-B metabolic syndrome combines age-dependent adiposity with pancreatic β cell insufficiency. *The Journal of Clinical Investigation* 125(8):3087-102.

Maeda K, Okubo K, Shimomura I, Mizuno K, Matsuzawa Y, Matsubara K (1997). Analysis of an expression profile of genes in the human adipose tissue. *Gene* 190(2):227-35.

McLaren W, Pritchard B, Rios D, Chen Y, Flicek P, Cunningham F (2010). Deriving the consequences of genomic variants with the Ensembl API and SNP Effect Predictor. *Bioinformatics* 26(16):2069-70.

Mercadé A, Estellé J, Noguera JL, Folch JM, Varona L, Silió L, *et al.* (2005). On growth, fatness, and form: a further look at porcine chromosome 4 in an Iberian x Landrace cross. *Mammalian Genome* 16(5):374-82.

Mercadé A, Pérez-Enciso M, Varona L, Alves E, Noguera JL, Sánchez A, *et al.* (2006). Adipocyte fatty-acid binding protein is closely associated to the porcine FAT1 locus on chromosome 4. *Journal of Animal Science* 84(11):2907-13.

Muñoz M, Rodríguez MC, Alves E, Folch JM, Ibañez-Escriche N, Silió L, *et al.* (2013). Genome-wide analysis of porcine backfat and intramuscular fat fatty acid composition using high-density genotyping and expression data. *BMC Genomics* 14:845.

Nakamura MT, Nara TY (2004). Structure, function, and dietary regulation of delta6, delta5, and delta9 desaturases. *Annual Review of Nutrition* 24:345-76.

OECD/FAO (2016), "OECD-FAO Agricultural Outlook", OECD Agriculture statistics (database).

Ojeda A, Rozas J, Folch JM, Pérez-Enciso M (2006). Unexpected high polymorphism at the FABP4 gene unveils a complex history for pig populations. *Genetics* 174(4):2119-27.

Peeters A, Baes M (2010). Role of PPARα in Hepatic Carbohydrate Metabolism. *PPAR Research* pii:572405.

Pérez-Enciso M, Clop A, Noguera JL, Ovilo C, Coll A, Folch JM, *et al.* (2000). A QTL on pig chromosome 4 affects fatty acid metabolism: evidence from an Iberian by Landrace intercross. *Journal of Animal Science* 78(10):2525-31.

Pérez-Enciso M, Misztal I (2011). Qxpak.5: old mixed model solutions for new genomics problems. *BMC Bioinformatics* 12:202.

Puig-Oliveras A, Ballester M, Corominas J, Revilla M, Estellé J, Fernández AI, *et al.* (2014a). A co-association network analysis of the genetic determination of pig conformation, growth and fatness. *PLoS One* 9(12):e114862.

Puig-Oliveras A, Ramayo-Caldas Y, Corominas J, Estellé J, Pérez-Montarelo D, Hudson NJ, *et al.* (2014b). Differences in muscle transcriptome among pigs phenotypically extreme for fatty acid composition. *PLoS One* 9(6):e99720.

Puig-Oliveras A, Revilla M, Castelló A, Fernández AI, Folch JM, Ballester M (2016). Expression-based GWAS identifies variants, gene interactions and key regulators affecting intramuscular fatty acid content and composition in porcine meat. *Scientific Reports* 6:31803.

Purcell S, Neale B, Todd-Brown K, Thomas L, Ferreira MA, Bender D, *et al.* (2007). PLINK: a tool set for whole-genome association and population-based linkage analyses. *American Journal of Human Genetics* 81(3):559-75.

Qi RL, Chen Y, Huang JX, Yang FY (2015). Effects of conjugated linoleic acid on the expression levels of miR-27 and miR-143 in pig adipose tissue. *Genetics and Molecular Research* 14(2):6985-92.

Ramayo-Caldas Y, Mercadé A, Castelló A, Yang B, Rodríguez C, Alves E, *et al.* (2012). Genome-wide association study for intramuscular fatty acid composition in an Iberian × Landrace cross. *Journal of Animal Science* 90(9):2883-93.

Ramayo-Caldas Y, Ballester M, Fortes MR, Esteve-Codina A, Castelló A, Noguera JL, *et al.* (2014): From SNP co-association to RNA co-expression: novel insights into gene networks for intramuscular fatty acid composition in porcine. *BMC Genomics* 15:232.

Ramos AM, Crooijmans RP, Affara NA, Amaral AJ, Archibald AL, Beever JE, *et al.* (2009). Design of a high density SNP genotyping assay in the pig using SNPs identified and characterized by next generation sequencing technology. *PLoS One* 4(8):e6524.

Ramsay RR, Gandour RD (1999). Selective modulation of carnitine long-chain acyltransferase activities. Kinetics, inhibitors, and active sites of COT and CPT-II. *Advances in Experimental Medicine and Biology* 466:103-9.

Rankin EB, Rha J, Selak MA, Unger TL, Keith B, Liu Q, *et al.* (2009). Hypoxia-inducible factor 2 regulates hepatic lipid metabolism. *Molecular and Cellular Biology* 29(16):4527-38.

Robinson JT, Thorvaldsdóttir H, Winckler W, Guttman M, Lander ES, Getz G, *et al.* (2011) Integrative genomics viewer. *Nature Biotechnology* 29(1):24-6.

Robinson MR, Wray NR, Visscher PM (2014). Explaining additional genetic variation in complex traits. *Trends in Genetics* 30(4):124-32.

Rozen S, Skaletsky H (2000). Primer3 on the WWW for general users and for biologist programmers. *Methods in Molecular Biology* 132:365-86.

Ruan W, Lai M (2010). Insulin-like growth factor binding protein: a possible marker for the metabolic syndrome? *Acta diabetologica* 47(1):5-14.

Sambrook J, Fritsch EE, Maniatis T (1989). Molecular Cloning:A Laboratory Manual. 2nd Ed. Cold Spring Harbor Laboratory Press; pp. E3-E4.

Sampath H, Miyazaki M, Dobrzyn A, Ntambi JM (2007). Stearoyl-CoA desaturase-1 mediates the pro-lipogenic effects of dietary saturated fat. *The Journal of Biological Chemistry* 282(4):2483-93.

Satish L, Krill-Burger JM, Gallo PH, Etages SD, Liu F, Philips BJ, *et al.* (2015). Expression analysis of human adipose-derived stem cells during in vitro differentiation to an adipocyte lineage. *BMC Medical Genomics* 8:41.

Schadt EE, Molony C, Chudin E, Hao K, Yang X, Lum PY, *et al.* (2008): Mapping the genetic architecture of gene expression in human liver. *PLoS Biology* 6(5):e107.

Shehzad A, Iqbal W, Shehzad O, Lee YS (2012). Adiponectin: regulation of its production and its role in human diseases. *Hormones (Athens)* 11(1):8-20.

Storey JD, Tibshirani R (2003). Statistical significance for genomewide studies. *Proceedings of the National Academy of Sciences of the United States of America* 100:9440–9445.

Szanto A, Balint BL, Nagy ZS, Barta E, Dezso B, Pap A, *et al.* (2010). STAT6 transcription factor is a facilitator of the nuclear receptor PPARγ-regulated gene expression in macrophages and dendritic cells. *Immunity* 33(5):699-712.

Tong L, Harwood HJ Jr (2006). Acetyl-coenzyme A carboxylases: versatile targets for drug discovery. *Journal of Cellular Biochemistry* 99(6):1476-88.

Van Nas A, Guhathakurta D, Wang SS, Yehya N, Horvath S, Zhang B, *et al.* (2009). Elucidating the role of gonadal hormones in sexually dimorphic gene coexpression networks. *Endocrinology* 150(3):1235-49.

Wang XL, Suzuki R, Lee K, Tran T, Gunton JE, Saha AK, *et al.* (2009). Ablation of ARNT/HIF1beta in liver alters gluconeogenesis, lipogenic gene expression, and serum ketones. *Cell Metabolism* 9(5):428-39.

Wong N, Wang X (2015) miRDB: an online resource for microRNA target prediction and functional annotations. *Nucleic Acids Research* 43(Database issue):D146-52.

Wood JD, Nute GR, Richardson RI, Whittington FM, Southwood O, Plastow G, *et al.* (2004). Effects of breed, diet and muscle on fat deposition and eating quality in pigs. *Meat Science* 67(4):651-667.

Wood JD, Enser M, Fisher AV, Nute GR, Sheard PR, Richardson RI, *et al.* (2008). Fat deposition, fatty acid composition and meat quality: A review. *Meat Science* 78(4):343-358.

Xiong S, Tu H, Kollareddy M, Pant V, Li Q, Zhang Y, *et al.* (2014). Pla2g16 phospholipase mediates gain-of-function activities of mutant p53. *Proceedings of the National Academy of Sciences of the United States of America* 111(30):11145-50.

Yamamoto Y, Takahashi K (1993). Glutathione peroxidase isolated from plasma reduces phospholipid hydroperoxides. *Archives of Biochemistry and Biophysics* 305(2):541-5.

Yang B, Zhang W, Zhang Z, Fan Y, Xie X, Ai H, *et al.* (2013). Genome-wide association analyses for fatty acid composition in porcine muscle and abdominal fat tissues. *PLoS One* 8(6):e65554.

Yang RY, Yu L, Graham JL, Hsu DK, Lloyd KC, Havel PJ, *et al.* (2011). Ablation of a galectin preferentially expressed in adipocytes increases lipolysis, reduces adiposity, and improves insulin sensitivity in mice. *Proceedings of the National Academy of Sciences of the United States of America* 108(46):18696-701.

Yang X, Schadt EE, Wang S, Wang H, Arnold AP, Ingram-Drake L, *et al.* (2006). Tissue-specific expression and regulation of sexually dimorphic genes in mice. *Genome Research* 16(8):995-1004.

Zhang W, Zhang J, Cui L, Ma J, Chen C, Ai H, *et al.* (2016a). Genetic architecture of fatty acid composition in the longissimus dorsi muscle revealed by genome-wide association studies on diverse pig populations. *Genetics Selection Evolution* 48:5.

Zhang W, Bin Yang, Zhang J, Cui L, Ma J, Chen C, *et al.* (2016b). Genome-wide association studies for fatty acid metabolic traits in five divergent pig populations. *Scientific Reports* 6:24718.

Supporting Information

Additional file 1: Figure S1. Associations of SNPs from SSC8 and *ELOVL6* polymorphisms for *ELOVL6* gene-expression in backfat. The X-axis represents positions of SSC8 in Mb relative to *Sscrofa10.2* assembly of the pig genome and the Y-axis shows the –log10 (*p*-value). Horizontal dashed lines indicate the chromosome significance level.

Additional file 2: Figure S2. Clustered heat map to visualize correlations among gene-expression levels (NQ) of the 43 genes and fatty content in adipose tissue. Color legend was adjusted to minimal and maximal values to differentiate the differences.

Additional file 1: Table S1. Primers used for the characterization of the 3'UTR of porcine *FABP4* gene.

Additional file 2: Table S2. Primers used for the analyses of gene-expression of the 48 genes by real-time PCR.

Additional file 3: Table S3. List of 44 lipid-related genes selected to study their expression in the present study. The overlapping between categories is labelled by colors.

Additional file 4: Table S4. Description of the 193 significant expression-associated SNPs (eSNPs).

Additional file 5: Table S5. Gene annotation of genes within the eQTL intervals. Annotation was performed by considering for *trans*-eQTLs the eQTL interval ±1 Mb; whereas for *cis*-eQTLs only the studied gene was selected (*ACSM5, FABP4,* and *FADS2*).

Additional file 6: Table S6. Mean comparison between males and females of backfat gene-expression levels of 43 lipid-related genes.

Additional file 7: Table S7. Description of the 393 human orthologous genes.

Additional file 8: Table S8. Top functional networks and molecules identified with IPA from the list of annotated genes mapping within the 19 eQTLs.

Additional file 9: Table S9. Transcription factor binding sites for the *PPARG* gene.

Additional file 10: Table S10. Correlations of *PPARG* mRNA expression and analyze-related genes.

General Discussion

Chapter 4

Consumers concerns and demands have arisen as important factors determining the amount and quality of pork production, as well as the market price conditions and costs. In order to achieve success in the domestic and foreign market, producers and distributors should be aware of the consumer behaviour, and have a good command of efficient methods to influence consumers to gain benefit. In the last decades, the consumer demand for high quality pork products has grown fast due to increased consumer interest in aspects related to nutritional quality and food health in general (Grunert 2005). In recent years, the concept of food quality has received a lot of attention from food producers and retailers as well as from public authorities and health educators (Brunsø *et al.*, 2004). For the European food industry, quality is a key factor because the high quality of a product is the basis for success in this highly competitive market (Du & Sun 2006). Following Henson (2000), the translation of the quality perceptions of consumers into physical product and process attributes requires knowledge and understanding of the overall quality evaluation of consumers. For example, meat should be safe, healthy, and it should taste good (Verbeke & Viaene 1999).

The four primary measurements of meat quality that have been identified as key traits to consider in evaluation of muscle quality are color, ultimate pH, water-holding capacity, and IMF. These traits are important because they are related to attractiveness, palatability, and product loss during processing, storage and cooking, and therefore, account for a large portion of the economic loss associated with poor quality pork meat. Pig breeding programs aim to improve pigs for these important traits. Carcass quality has been successfully improved in most selection programs because phenotypes are easy to obtain on live animals via ultrasonic measurements of backfat and because these traits show a relatively high heritability. Conversely, meat quality has not been the priority in most selection programs (De Vries *et al.*, 1992; Hovenier *et al.*, 1993; Sellier 1998; Knap *et al.*, 2002) because those traits can only be measured on the relatives of selection candidates and late in life. Successful improvement of meat quality may be possible by combining molecular information and traditional measurements because marker data can be obtained on all animals at an early age (Heuven *et al.*, 2003).

In the last decades, important advances in the characterization of QTLs affecting these traits have been achieved. Furthermore, new genomics tools like high-density SNP chips and NGS technologies have allowed researchers to improve knowledge of the biological

mechanisms implicated in lipid-related traits providing new insights for the identification of causal genes and mutations.

Herewith, this PhD thesis uses different molecular genetic technologies with the aim to provide additional insight into the genetic basis of meat quality traits in pigs. Different genomic tools are used to increase the knowledge of the biological processes involved in lipid metabolism, to identify gene networks and candidate genes associate with FA composition, and to find genetic variants that can determine meat quality traits.

4.1. Global analysis of CNVs in the pig genome

Differences in the number of copies of segments of DNA between different individuals (known as CNVs) are a wide source of genetic variation in many different organisms. In humans, CNVs play a significant role in the development of complex traits. Similarly, in livestock, more and more studies evidence that CNVs may play causative effects on phenotypic variations.

Published results for detection of CNVs in pigs have commonly used two methods of detection: aCGH (Fadista *et al.*, 2008; Li *et al.*, 2012b; Wang *et al.*, 2014a) and SNP array, performed both with (Ramayo-Caldas *et al.*, 2010; Chen *et al.*, 2012; Wiedmann *et al.*, 2015) and without (Wang *et al.*, 2012b, 2013b,c, 2014b; Schiavo *et al.*, 2014; Dong *et al.*, 2015) pedigree information.

Over the last few years, NGS has been used to the comprehensive characterization of CNVs by generating hundreds of millions of short reads in a single run (Metzker 2010). The advantages of NGS approach for CNV identification include higher coverage and resolution, more precise detection of breakpoints, and higher capability to identify novel CNVs (Alkan *et al.*, 2011; Snijders *et al.*, 2001). However, there are some important limitations and challenges (Xi *et al.*, 2010; Teo *et al.*, 2012): 1) high sequencing error rate of NGS platforms, especially at the first one or two positions and increasing exponentially near the end of the read, which cause a substantial loss of reads during alignment (Dohm *et al.*, 2008), 2) given the short length of the sequenced bases, many reads do not map uniquely to the genome, 3) certain regions of the genomes are represented at a higher rate than others due to the GC bias in sequencing steps (Dohm *et al.*, 2008) and amplification errors (if used). Recently published studies used high-throughput sequencing to detect CNVs in pigs (Rubin *et al.*, 2012; Paudel *et al.*, 2013; Jiang *et al.*, 2014; Wang *et al.*, 2015a,b).

Fernández *et al.* (2014) used the SNP array method on 217 highly inbred Iberian pigs and the high-throughput sequencing on four of these pigs for validation.

These studies have provided thousands of pig CNVs with a much more refined resolution. However, the impact of CNVs on pig phenotypes is still relatively unknown. To date, a well-characterized example of a trait determined by a CNV in pigs is a copy number gain of the *KIT* gene that causes the dominant white phenotype (Giuffra *et al.*, 2002). Related to fat content and FA composition, Schiavo *et al.* (2014) identified CNVs in Italian Large White pigs using the *PorcineSNP60 BeadChip*, and tested them for association with backfat thickness. Their results indicated that CNVs might have a limited impact in determining fat deposition in this breed, but a larger number of animals would be required to reach sufficient power with these low-frequency markers. One year later, Wang *et al.* (2015b) performed a GWAS between CNVs and meat quality traits in swine and eight CNVs were significantly associated with at least one meat quality trait, and six of them were verified by qPCR. These results suggest that CNVs may contribute to the genetic variation of meat quality traits.

In this thesis, we performed a genomic analysis of porcine CNVs based on NGS data to identify CNVs segregating in the IBMAP cross and studied their association with some economically important traits related to FA composition and growth-related traits.

We have identified 1,279 CNVs, merging in 540 CNV regions (CNVRs). Although CNVRs were found on all autosomal chromosomes, the number and the total size of CNVRs per chromosome were not correlated with chromosome length, which is consistent with previous studies related to CNVRs in the porcine genome (Paudel *et al.*, 2013, 2015). There are numerous software tools available that employ very different algorithms for the identification of CNVs from NGS data. A comparative analysis of several of these has been detailed in Duan *et al.* (2013), providing guidelines to choose the most appropriate method according to the specific data set and requirements. From the tested CNV detection methods, readDepth (Miller *et al.*, 2011), CNVnator (Abyzov *et al.*, 2011) and EWT (Yoon *et al.*, 2009) achieve better break point estimation. If a high true positive rate (equivalent to sensitivity) is preferable, Control-FREEC (Boeva *et al.*, 2011, 2012), SegSeq (Chiang *et al.*, 2009) and EWT are better choices. In contrast, if the computation speed/memory usage is a priority, EWT or Control-FREEC should be taken in consideration. Furthermore, CNVnator, readDepth and CNV-seq (Xie & Tammi 2009) provide better copy number estimation compared with the rest. However, we selected the

Control-FREEC software because it uses GC-content to normalize read counts and lower mappability regions can be excluded from the analysis.

The quality of CNVRs calls was assessed by a comparison against a previously reported porcine CNV dataset identified in the IBMAP population with the *PorcineSNP60 BeadChip* (Ramayo-Caldas *et al.*, 2010), showing an overlapping of 65%. In addition, in the comparison with the work published by Fernández *et al.* (2014) using 217 Iberian pigs, seven CNVRs were identified. Different factors may limit the identification of CNVs in these studies, including marker density, non-uniform distribution of SNPs along pig chromosomes, and/or a lack of specially designed non-polymorphic probes that is necessary to identify CNVR with higher resolution (Ramos *et al.*, 2009). Furthermore, the calling algorithms to detect CNVs and the different pig assemblies used may explain the discrepancy between works. Here, the method based on NGS, resulted in a higher resolution to call CNVRs. Thus, most of the CNVRs discovered in this study are novel relative to the previous studies.

Gene annotation and functional analysis were performed for the 540 CNVRs and 245 genes were identified. Six genes were selected as potential candidate genes related to growth and FA composition traits (*CLCA4, CYP4X1, GPAT2, MOGAT2, PLA2G2A,* and *PRKG1*) for qPCR validation of the variation in the number of copies in three different backcrosses. However, CNVRs in the *CYP4X1* did not present variation in the three backcrosses and *PLA2G2A* was not validated in the BC1_LD. Several factors may account for the discrepancy: 1) polymorphisms such as SNPs and indels may influence the hybridization of the qPCR primers, changing the relative quantification values for some animals; 2) the true CNVR boundaries may be polymorphic among the analyzed animals. The four CNVRs validated by qPCR in the BC1_LD (*CLCA4, GPAT2, MOGAT2,* and *PRKG1*) were further analyzed in 150 BC1_LD animals and association analysis was performed for growth and meat quality traits. Statistically significant associations were obtained for CNVR112 (*GPAT2*). The strongest signal was observed for the C18:2(n-6)/C18:3(n-3) ratio, and cis-vaccenic acid ((C18:1(n-7)) for the FA composition in backfat. For FA percentages in IMF, the strongest signal was detected for oleic acid (C18:1(n-9)), the global percentage of MUFA, peroxidability index, dihomo gamma linolenic acid (C20:3(n-6)), the global percentage of PUFA, eicosatrienoic acid (C20:3(n-3)) and the ratio of MUFA/PUFA. In the case of growth traits, only the carcass length showed statistically significant association. These results agree with the role of this gene in phospholipid and

triacylglycerol biosynthesis (Dircks & Sul 1997). The glycerol-3-phosphate acyltransferase (*GPAT*) catalyze the acylation of glycerol-3-phosphate, which is involved in the beginning of *de novo* synthesis of glycerolipids. The lysophosphatidic acid, the product of *GPAT*, is subsequently acylated to phosphatidic acid (PA) by 1-acylglycerol-3-phospate acyltransferase (*AGPAT*). This PA is the precursor for the synthesis of triacylglycerol and glycerophospholipids. Furthermore, it has been shown that *GPAT2* gene specifically incorporates arachidonic acid to triacylglycerol (Cattaneo *et al.*, 2012), remarking the importance of this gene in lipid metabolism. These results suggest the interest of CNVR112 (*GPAT2*) in the genetic determination of IMF and backfat FA composition traits underlining the influence of CNVs in economic important traits in pigs. Further studies are required for the functional validation of the CNVR122, including the analysis of the correlation between the number of copies and the mRNA expression of the *GPAT2* gene.

4.2. From QTL to positional candidate genes for fatty acid composition

For many of the economically relevant traits in pigs major QTLs have been identified in experimental crosses or commercial populations. However, the identification of the causal genes of QTLs and their allelic variation has proven to be difficult for complex traits. Genetic markers located in QTLs are not necessarily useful in breeding schemes due to the incomplete LD between the marker and the causal mutation. Furthermore, markers may not segregate in a different population and/or the LD with the causal mutation may be different, making difficult to translate to the actual breeding population. Therefore, the identification of the causal polymorphism(s) underlying the QTL is relevant for its application in animal breeding and crucial to understand the phenotypic variation observed.

Advances in genomics provided new tools for the identification of causal polymorphisms of meat quality traits. An example, is the study of SSC8 in the IBMAP population for the palmitic (C16:0) and palmitoleic (C16:1(n-7)) FA composition in muscle and backfat. In this regard, Clop *et al.* (2003) performed the first report of a genome scan detection of QTLs directly affecting FA composition in pigs using the IBMAP cross (Pérez-Enciso *et al.*, 2000). Several regions on SSC4, SSC6, SSC8, SSC10, and SSC12 showed highly significant effects. From these regions, only SSC8, SSC10, and SSC12 were associated to FA composition independently of the covariate (carcass weight or backfat) that was used in the model. Years later, Estellé *et al.* (2009a) analyzed the Fatty acid binding protein 2

(*FABP2*) gene as a candidate for the FA composition QTL previously described on SSC8 (86 cM). Although the analyzed polymorphism (*FABP2:g.412T>C*) in *FABP2* was not associated with FA composition traits, the addition of microsatellites to the pedigree allowed to define a marker interval as the most likely QTL position, facilitating the future study of other candidate genes for this QTL. In this sense, the same year the microsomal triglyceride transfer protein (*MTTP*) gene was also tested as a positional candidate gene for this QTL on SSC8 (Estellé *et al.*, 2009b). In this case, the polymorphism analyzed (p.Phe840Leu) showed a strong association with FA composition of porcine fat, much stronger than the QTL effect. Later, Ramayo-Caldas *et al.* (2012b) using information from *PorcineSNP60 BeadChip* identified five genomic regions associated with intramuscular FA composition and indices of FA metabolism on SSC8 in the BC1_LD population. Remarkably, a strong association signal was found (92.1-96.7 Mb) with palmitic acid (C16:0), palmitoleic acid (C16:1(n-7)), SFA, and C16:1(n-7)/C16:0 and C18:1(n-7)/C16:1(n-7) ratios (Ramayo-Caldas *et al.*, 2012b). Furthermore, a positional concordance was observed between this region and QTL for palmitic (C16:0) and palmitoleic (C16:1(n-7)) acids reported in backfat in the IBMAP F_2 intercross (Clop *et al.*, 2003). In addition, Muñoz *et al.*, (2013) using a linkage QTL scan as well as GWAS revealed on SSC8 significant pleiotropic regions with effects on palmitic (C16:0) (QTL scan: 87 cM; GWAS: 83.8-130.6 Mb) and palmitoleic (C16:1(n-7)) (QTL scan: 90 cM; GWAS: 99.3-99.5 Mb and 110.9-126.9 Mb) FAs in backfat and muscle of BC1_LD animals.

With the aim to reduce the confidence interval of the SSC8 QTL for the intramuscular profile of palmitic (C16:0) and palmitoleic (C16:1(n-7)) acids in the BC1_LD, Corominas *et al.* (2013b) used a combination of haplotype-based approach and GWAS. The combined LD and linkage analysis (LDLA) method has the advantage of the high-resolution of LD mapping and the robustness to spurious associations of linkage mapping (Meuwissen & Goddard 2004). The GWAS profile was maximized at 119.7-119.9 Mb, and the profile from the haplotype-based analysis showed the association signal at 117.8-119.9 Mb for palmitic acid (C16:0). In the case of palmitoleic acid (C16:1(n-7)) the profile differs, being 119.9-120.1 Mb for the GWAS and 117.8-119.7 Mb for the haplotype-based analysis. According to the fine mapping data, Corominas *et al.* (2013b) suggested that *ELOVL6* gene is a potential positional causal gene for this QTL and underline the *ELOVL6:c.-533C>T* polymorphism as a potential mutation to explain the variation of palmitic (C16:0) and palmitoleic (C16:1(n-7)) FAs in *longissimus dorsi* muscle and adipose tissue. Later on, a new polymorphism in the *ELOVL6* promoter region (*ELOVL6:c.-394G>A*), in full LD

with *ELOVL6:c.-533C>T,* was associated with the methylation levels of the *ELOVL6* promoter and the *ELOVL6* expression (Corominas *et al.*, 2015), suggesting this polymorphism as the causal mutation for the QTL on SSC8 affecting palmitic (C16:0) and palmitoleic (C16:1(n-7)) acids (Corominas *et al.*, 2015).

In order to further study the QTL architecture for backfat FA composition on SSC8 and to identify additional positional candidate genes, in this PhD thesis we analyzed the F_2 generation of the IBMAP cross using a panel of 144 informative SNPs distributed along SSC8, mostly derived from the *PorcineSNP60 BeadChip*. Here, a combination of single-marker association and the haplotype-based approach allowed the identification of statistically significant associations for myristic acid (C14:0), palmitic acid (C16:0), stearic acid (C18:0), palmitoleic acid (C16:1(n-7)), oleic acid (C18:1(n-9)), eicosadienoic acid (C20:2(n-6)), average chain length, and C16:1(n-7)/C16:0, C18:0/C16:0, C18:1(n-7)/C16:1(n-7) and C20:2(n-6)/C18:2(n-6) ratios. Two regions that contain trait-associated SNPs (TAS) were clearly visualized at around 93 Mb and 119 Mb for all the above-mentioned FA and indices with the exception of the C20:2(n-6)/C18:2(n-6) ratio. In order to determine whether one or two QTLs were segregating on SSC8, model fitting one QTL against a model considering two different QTLs were tested. Results of the test indicated that the model with two QTLs was the most likely to explain the traits analyzed, with the 119 Mb region showing the strongest statistical signal for all traits. These results agree with Clop *et al.* (2003), who identified a high effect of SSC8 markers for palmitic acid (C16:0), palmitoleic acid (C16:1(n-7)) and average chain length.

However, the use of a panel of informative SNPs on SSC8 allowed the reduction of the confidence interval of the QTLs. Furthermore, these results were also in agreement with those reported by Ramayo-Caldas *et al.* (2012b), which identified a strong association signal covering the 92.1-96.7 Mb region for palmitic acid (C16:0), palmitoleic acid (C16:1(n-7)), SFA, and C16:1(n-7)/C16:0 and C18:1(n-7)/C16:1(n-7) ratios. For the palmitic acid (C16:0), a strong association signal was also identified at 103.8-107.5 Mb. The difference of the confidence intervals for these traits between the study reported by Ramayo-Caldas *et al.* (2012b) and the obtained here could be explained by the use of different pig assemblies, *Sscrofa9* and *Sscrofa10.2,* respectively. The positional concordance between the QTLs detected in muscle (Ramayo-Caldas *et al.,* 2012b) and adipose tissue, suggest a pleiotropic effect on both tissues.

A work of Zhang *et al.* (2016b) identified also in the 119 Mb region (119.4-129.6 Mb) associations with C16:0/C14:0, C18:0/C16:0, and C18:1(n-9)/C16:1(n-7) ratios measured on *longissimus dorsi* muscle and abdominal fat samples of White Duroc x Erhualian F_2 pigs. The same authors, in a meta-analysis of five different pig populations, detected associations in the 119.72 Mb for C16:1(n-7)/C16:0 and C18:1(n-9)/C16:1(n-7) ratios. These results overlap with the described in our work, and reflect the importance of the 119 Mb region on SSC8. GWAS on metabolic ratios can increase the power of detection of the association in comparison to individual metabolites. This hypothesis is based on the assumption that two metabolites are product of an enzyme reaction; hence, the ratios between their concentrations are representative of the enzymatic reaction rate (Petersen *et al.*, 2012). This assumption is not valid in our study, where higher significant associations were identified for the individual metabolites than the ratios of them. One explanation of this discrepancy could be that animals who consume a higher amount of a certain nutrient also exhibit higher levels of its biochemical break-down products, and therefore affect the product of the enzymatic reaction.

Gene annotation of the first TAS region allowed the identification of the mastermind-like 3 (*MAML3*) (at position 92.67 Mb) and SET domain containing lysine methyltransferase 7 (*SETD7*) (at position 93.13 Mb) genes. Both genes were reported in a predicted co-association gene network of intramuscular FA composition in pigs (Ramayo-Caldas *et al.*, 2014). Several polymorphisms related to *SETD7* and *MAML3* genes were genotyped, but the association studies showed that the genotyped polymorphisms were not the strongest signals for backfat FA composition. Conversely, the strongest signals were located within 2 Mb interval of the *SETD7* and *MAML3* genes, suggesting than other variants of these genes or other genes in this region may be determining these traits. Some factors limiting the results obtained in this analysis may be the strong linkage in the F_2 animals and the incomplete annotation of pig genome assembly on SSC8.

In the second region, the *ELOVL6* gene was identified at position 120.12 Mb and the *ELOVL6:c.-533C>T* polymorphism showed the highest association. These results are consistent with those found by Corominas *et al.* (2013b), evidencing that SSC8 is clearly associated with FA composition, with at least two QTLs related with palmitic (C16:0) and palmitoleic acid (C16:1(n-7)) content. The majority of FAs in a cell have a length of C16 to C18 carbon atoms, but the end product of FAS is palmitic acid (C16:0). Palmitic (C16:0) and palmitoleic (C16:1(n-7)) FAs can be further elongated by *ELOVL6* to stearic (C18:0)

and vaccenic FAs (C18:1(n-7)), respectively. Thus, *ELOVL6* has a pivotal role in the elongation of SFA and MUFA long chain FAs and furthermore, the results suggest *ELOVL6* as a potential causal gene for the QTL at 119 Mb.

In addition, Ballester *et al.* (2017) identified two hotspots on SSC8 (86.66-88.13 Mb and 116.2-124.0 Mb) affecting the expression of many lipid-related genes in liver. Taken together, these findings suggest a possible direct role of genes expressed in liver in the lipid metabolism, indicating the complex genetic basis of these traits.

In summary, several studies performed in our group have identified QTLs related with FA composition traits on SSC8 (Table 4.1) in the IBMAP population. The presented results identified two regions clearly associated with FA composition measured in backfat. The positional concordance observed in this study and the previously reported, regarding the QTL affecting palmitic (C16:0) and palmitoleic (C16:1(n-7)) acid, suggest a pleiotropic effect of these QTLs in backfat and muscle tissues.

Table 4.1. Summary of QTLs on SSC8 identified in the IBMAP population.

Reference	Tissue	Approach	QTL trait	QTL position	Gene
Clop *et al.*, 2003	Backfat	QTL scan	C16:0	86 cM	----
			C16:1(n-7)		
			ACL		
Estellé *et al.*, 2009a	Backfat	QTL scan	C16:0	88 cM	*FABP2*
			C16:1(n-7)	96 cM	
			ACL	95 cM	
Estellé *et al.*, 2009b	Backfat	QTL scan	C16:0	111.5 cM	*MTTP*
			C16:1(n-9)	82 cM	
			C18:1(n-9)	110 cM	
			C20:1(n-9)	111.5 cM	
Ramayo-Caldas *et al.*, 2012b	Muscle*	GWAS[1]	SFA	10.6-13.7 Mb	----
			UI		
			C16:0	68.6-71.9 Mb	----
			SFA		
			C16:1(n-7)	77.6-80.3 Mb	----
			C18:1(n-7)/C16:1(n-7)		
			C16:0	92.1-96.7 Mb	----
			C16:1(n-7)		
			SFA		
			C16:1(n-7)/C16:0		
			C18:1(n-7)/C16:1(n-7)		
			C16:0	103.8-107.5 Mb	----
Corominas *et al.* 2013b	Backfat Muscle*	GWAS[2] & LDLA	C16:0	117.8-119.9 Mb	*ELOVL6*
			C16:1(n-7)	117.8-119.7 Mb	
Muñoz *et al.*, 2013	Backfat Muscle*	QTL Scan	C16:0	87 cM	----
			C16:1(n-7)	90 cM	
	Backfat Muscle*	GWAS[2]	C16:0	83.8-130.6 Mb	----
			C16:1(n-7)	99.3-99.5 Mb 110.9-126.9 Mb	
Revilla *et al.*, 2014	Backfat	GWAS[2] & LDLA	C16:1(n-7)	93 Mb	*MAML3* *SETD7*
			C18:0/C16:0		
			C18:1(n-7)/C16:1(n-7)		
			C16:1(n-7)	119 Mb	*ELOVL6*
			C18:0/C16:0		
			C18:1(n-7)/C16:1(n-7)		

*The muscle analyzed corresponds to *Longissimus dorsi*. [1]*Sus scrofa* assembly 9. [2]*Sus scrofa* assembly 10.2.

4.3. Gene-expression and regulation of candidate genes for fatty acid metabolism

Transcript abundances of genes may be directly modified by polymorphisms in regulatory elements. Consequently, transcript abundances are treated as quantitative traits and can be mapped to genomic regions called eQTL (Schadt *et al.*, 2003; Morley *et al.*, 2004). The combination of whole genome genetic association studies and the measurement of global gene-expression allow the systematic identification of eQTLs. For genomic regions previously associated with complex traits, genome-wide eQTL mapping data can be examined to see if the same genetic markers are associated with quantitative transcript

levels of one or more genes (Figure 4.1). Such markers are known as expression-associated SNPs (eSNPs).

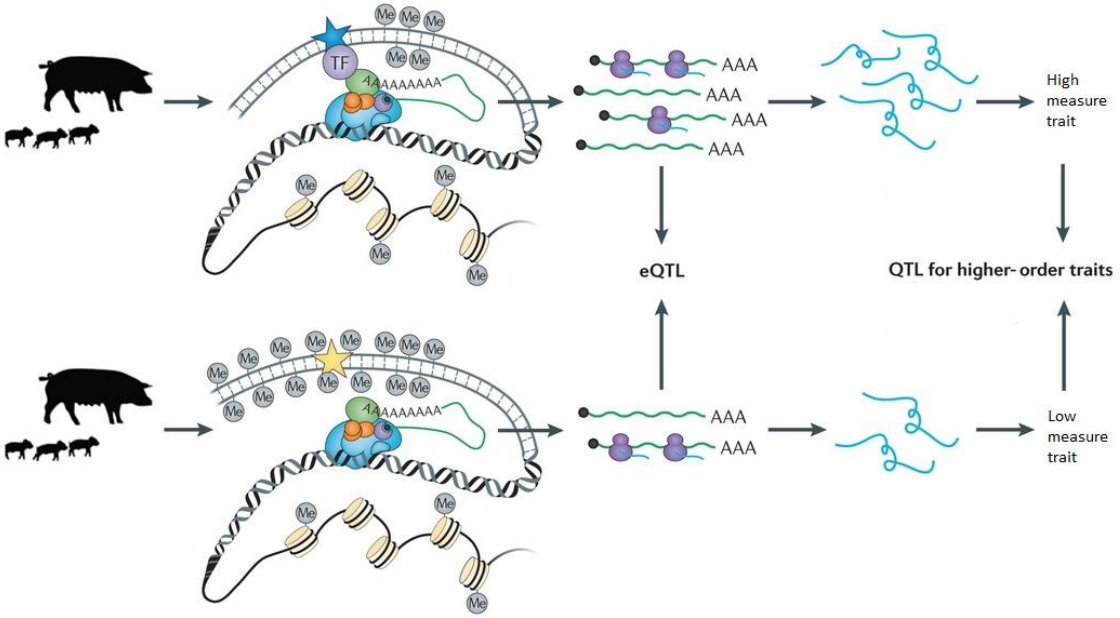

Figure 4.1. Design for genetic mapping of variation in gene-expression. The *loci* involved is marked by a star. The figure illustrates the results for two animals that differ in the expression of a certain gene. In the example, the altered protein level due to the genetic polymorphism influences a complex trait (adapted from Albert & Kruglyak 2015).

The potential of genome-wide eQTL identification has been shown in humans, animals and plants (Schadt *et al.*, 2003; Rockman & Kruglyak 2006).

In the IBMAP cross, gene-specific eQTL has been performed for some candidate genes: *ACSL4* (Corominas *et al.*, 2012), *ELOVL6* (Corominas *et al.*, 2013b), *APOA2* (Ballester *et al.*, 2016) and, *FABP4* and *FABP5* (Ballester *et al.*, submitted). In addition, taking advantage of microarray technology, Muñoz *et al.* (2013) performed an eQTL analysis to identify genes that mapped within QTLs for FA composition in *Longissimus dorsi* muscle samples of animals belonging to the IBMAP cross. Twelve eQTLs were identified at nominal *p*-value <0.005: *BGLAP, ELOVL6, MGST2, PTPN11,* and *SEC13* on SSC8; *AGPAT9, DPP4, PNPLA4, PTGR2, SGMS1,* and *THRB* on SSC11; and *RUNX1* on SSC17. However, only one eQTL reached the established false discovery ratio correction (0.2): the *MGST2* gene-expression on SSC8. Although DNA microarrays are powerful tools giving an overall picture of gene-expression behaviour, their results are often noisy or ambiguous (Editorial 2006). In contrast, qPCR is considered a "gold standard" for quantification of gene-expression and has been widely employed as a validation method for microarray studies. We have used the *Fluidigm* microfluidic technology (*Fluidigm*; San Francisco, CA, USA),

which employs integrated fluidic circuits (IFC) containing tens of thousands of microfluidic controlled valves and interconnected channels to move molecules of biological samples and reagents in a variety of patterns (Melin & Quake 2007). *Fluidigm* microfluidic technology reduce qPCR reactions from the routine 10-20 microliter volume down to the 10 nanoliter scale, making possible to perform routine qPCR analysis for thousands of reactions in a single run (Melin & Quake 2007; Spurgeon *et al*., 2008). Hence, *Fluidigm* offers rapid, cost-effective and customizable arrays for moderate number of gene-expression profiling in several animals. This technology has already been tested in our group, by performing an analysis of the *Longissimus dorsi* muscle (Puig-Oliveras *et al*., 2016) and liver (Ballester *et al*., 2017) mRNA expression of several candidate genes related with lipid metabolism in BC1_LD animals. In order to have a complete picture of the three main tissues implicated in lipid metabolism (liver, muscle and adipose tissue), in this thesis, we have studied the expression of a set of candidate genes related to lipid metabolism in the adipose tissue of pigs in order to identify genomic regions associated with the regulation of these genes. The final aim of these studies is to identify regulatory polymorphisms that may determine changes in FA composition traits. We performed an expression genome-wide association study (eGWAS) with the backfat gene-expression measured by qPCR in 43 genes and the *PorcineSNP60 BeadChip* genotype information in 115 BC1_LD animals. The eGWAS identified 193 eSNPs located in 19 chromosomal regions on SSC2-SSC4, SSC6, SSC8-SSC10, and SSC13-SSC16, and associated with the acyl-CoA synthetase medium-chain family member 5 (*ACSM5), ELOVL6,* fatty acid binding protein 4 *(FABP4), FADS2*, and solute carrier family 27 member 4 (*SLC27A4)* genes. Three out of 19 eQTLs corresponding to *ACSM5, FABP4,* and *FADS2* were classified as *cis*-acting eQTLs, whereas the remaining 16 eQTLs have *trans*-regulatory effects.

Different studies have used different definitions of *cis*-eQTLs (100 kb, 500 kb, 1 Mb), several statistical tools (linear regression, ANOVA) to analyze eQTLs and different multiple testing correction methods (Bonferroni, false discovery rate), making comparison across experiments difficult. The results here detailed are in concordance with those presented previously by our group in other tissues, which identified that porcine *trans*-eQTLs are more abundant than the *cis*-eQTLs (Table 4.2). Furthermore, it has been evidenced that genes seem to be regulated by several *trans*-acting regulators, which contributed greatly on gene-expression variation (Cheung *et al*., 2010), and only a few *cis*-acting regulators (Cheung & Spielman, 2009).

Table 4.2. Description in terms of number of chromosomal regions associated with gene-expression phenotypes.

Reference	Puig-Oliveras *et al.* (2016)	Ballester *et al.* (2017)	Data shown in this PhD thesis
Number of eQTLs	18*	7	19*
***cis*-eQTLs**	3	2	3
***trans*-eQTLs**	16	5	17
Tissue	*Longissimus dorsi* muscle	Liver	Adipose tissue

*One of the chromosomal regions showed *cis* and *trans* effects.

In the work describe here, ten polymorphisms were analyzed. Polymorphisms were identified and genotyped for the genes with *cis*-acting eQTLs in the BC1_LD animals. Two SNPs located in the proximal promoter region of *ACSM5* (*g.26260422G>A*, rs331702081; Puig-Oliveras *et al.*, 2016) and *FADS2* (*g.9118843C>T*, rs331050552), and one indel and one SNP located in the intron 1 (*FABP4:g.2634_2635insC*; Mercadé *et al.*, 2006b) and in the 3'UTR region of *FABP4* (*FABP4:g.6723*A>G), respectively. For the *ELOVL6* gene, various polymorphisms were genotyped. Three SNPs are located in the promoter region (*ELOVL6:c.-533C>T*, *ELOVL6:c.-480C>T* and *ELOVL6:c.-394G>A*; Corominas *et al.*, 2013b), one in the exon 4 (*ELOVL6:c.416C>T*; Corominas *et al.*, 2013b), and two in the 3'UTR region (*ELOVL6:c.1408A>G* and *ELOVL6:c.1922C>T*; Corominas *et al.*, 2015).

Interestingly, the strongest signal associated with *ACSM5* gene-expression was detected for the genotyped polymorphism rs331702081, which was located in a 23.44-27.94 Mb genomic region containing 25 SNPs with similar significance. This gene belongs to the acyl-coenzyme A synthetases and is involved in the initial reaction in FA metabolism by forming a thioester with CoA (Watkins *et al.*, 2007). Recently, in a previous study of our group, the same polymorphism in the *ACSM5* promoter region was the highest significant polymorphism associated with the *ACSM5* expression in *Longissimus dorsi* muscle (Puig-Oliveras *et al.*, 2016). These results reinforce rs331702081 as being the strong candidate implicated in the *cis*-regulation of *ACSM5* and suggest a common mechanism controlling *ACSM5* gene-expression in backfat and muscle. Nevertheless, the moderate correlation (r= 0.6; *p*-value= $3.0x10^{-12}$) observed between both tissues for the *ACSM5* mRNA expression suggest that other factors, most probably acting in *trans*, are also differentially regulating the expression of this gene between tissues.

Finally, the genomic region associated with the mRNA expression of *ACSM5* co-localize with several QTLs described in Pig QTLdb (Hu *et al.*, 2013) for fatness traits. These results suggest that the analyzed polymorphism is a good candidate to explain a fraction of the

genetic variability of these traits, but further studies are required to validate the functional implication of this polymorphism. Due to the strong LD of the 23.44-27.94 Mb genomic region, we are analysing the segregation of these polymorphisms in populations with different genetic backgrounds.

For *FABP4* gene-expression, the SNP in the 3'UTR region (*FABP4:g.6723*A>G) showed the lowest *p*-value and the indel (*FABP4:g.2634_2635insC*; Mercadé *et al.*, 2006b) was also one of the most significantly associated polymorphisms. This gene was previously reported by our group as a strong positional candidate gene for a QTL related with growth and fatness traits on SSC4 (Mercadé *et al.*, 2005a, 2006b; Estellé *et al.*, 2006; Ramayo-Caldas *et al.*, 2012b; Muñoz *et al.*, 2013). Furthermore, the indel (*FABP4:g.2634_2635insC*) was predicted to be located in a target-binding site for PPARG and NR4A2 (Ballester *et al.*, submitted).

In our work, we have shown that the *FABP4:g.6723*A>G SNP was inside a putative miRNA binding site. Interestingly, the human miRNA, hsa-miR-3182 is predicted to bind only when *FABP4:g.6723G* allele is present, suggesting an effect of this SNP in the RNA expression profile of *FABP4* gene. In addition, PPARG is an essential transcription factor for adipogenesis that modulates *FABP4* gene-expression (Samulin *et al.*, 2008; Lim *et al.*, 2015). In our study *FABP4* expression is correlated with the expression of the *PPARG* gene (r= 0.51; *p*-value= $9.27x10^{-09}$). Hence, the indel polymorphism (*FABP4:g.2634_2635insC*) may alter the binding of *PPARG*, modulating the differential expression of *FABP4* gene in adipose tissue.

Thus, we hypothesized that the two polymorphisms may be playing a role in the regulation of the *FABP4* gene-expression and may affect meat quality traits in the IBMAP population. Further analyses are necessary to confirm the relevant role of these polymorphisms.

For the *FADS2* gene, no significant association was found between the genotyped SNP (*g9118843C>T*; rs331050552) and the *FADS2* mRNA expression. FA desaturases play an important role in the synthesis of highly unsaturated FAs (Nakamura & Nara 2004). Interestingly, in the same animal material, Ballester *et al.* (2016) identified a chromosomal region located on SSC2 (8.60 Mb) significantly associated with cis-7 hexadecenoic acid (C16:1(n-9)), linoleic acid (C18:2(n-6)), α-linolenic acid (C18:3(n-3)), and PUFA in backfat. This genomic region are very close to the three members of the FA desaturase gene family (*FADS1*, *FADS2,* and *FADS3*). Furthermore, it has been suggested an increase conversion

of omega-3 PUFA in the liver by *FADS1* and *FADS2,* which are acting mainly in the omega-3 metabolic pathway (Szostak *et al.*, 2016). Closely related, a high correlation has been observed between the mRNA expression of *FADS1* and *FADS2* in liver ($r_{FADS1\text{-}FADS2}$= 0.92; *p*-value= $1.11x10^{-17}$) (Ballester *et al.*, 2017). In contrast, in the adipose tissue the correlation value between the expression of these genes was moderate-high ($r_{FADS1\text{-}FADS2}$= 0.63; *p*-value= $8.26x10^{-14}$). It has been demonstrated that FADS pathway is both functional in adipocytes and regulated by PUFAs (Ralston *et al.*, 2015). These results suggest that common elements could regulate the expression of FA desaturase in liver and adipose tissue, but additional regulatory elements affecting the *FADS1* and *FADS2* mRNA expression in adipose tissue may exist. However, the results obtained for the genotyped SNP suggest that other variants of this gene may be determining the expression variation of *FADS2* gene.

For the *ELOVL6* gene, a significant region at chromosome level on SSC8 was associated with *ELOVL6* mRNA expression in backfat, which is consistent with the signal identified by Corominas *et al.* (2013b). The strongest signal was identified for two SNPs (ALGA0049135 and ALGA0049139) with the same *p*-value (*p*-value= $4.60x10^{-05}$), near the *ELOVL6* gene, and located in an intron of Ankyrin 2 gene (*ANK2*). Although the *ELOVL6:c.-533C>T* and *ELOVL6:c.-394G>A* polymorphisms also showed high association (*p*-value= $6.42x10^{-04}$), in our analysis these polymorphisms did not reach significance after multiple testing correction (q-value ≤ 0.05). This discrepancy could be due to the different number of BC1_LD animals and the different mRNA quantification method (microfluidic array vs conventional qPCR) used between the studies. These results suggest that the mutation underlying the eQTL on SSC8 (117.55-117.67 Mb) would be located in a regulatory element near the *ELOVL6* gene. Interestingly, Ramayo-Caldas *et al.* (2014) identified on SSC8 the *ANK2* gene as central in an adipose co-expression network related with IMF composition in BC1_LD animals. This gene has been recently defined as an important gene for glucose homeostasis and a decrease of this gene could elevate the cell surface of glucose transporter 4 (*GLUT4*) in skeletal muscle and fat (Lorenzo *et al.*, 2015), increasing the glucose uptake and modulating the novo lipogenesis which may alter the gene expression of lipogenic genes. The assumption of an association of this gene with the mRNA expression levels of *ELOVL6* gene cannot be discarded.

Interestingly, and in agreement with previous studies where *trans*-eQTLs affecting the expression of many genes were identified (Liaubet *et al.*, 2011; Ballester *et al.*, 2017), a

chromosomal interval located on SSC13 (6.89 Mb) was associated with the expression of *ELOVL5, ELOVL6*, and *SCD* genes. The co-expression pattern of these genes showed high significant positive correlations between *ELOVLs* and *SCD* genes (r>0.84; *p*-value<$1.00x10^{-16}$) suggesting a common regulatory direction/effect (Figure 4.2). In addition, *ELOVLs* and *SCD* gene expression are regulated by insulin through activation of SREBF1 and PPARs transcription factors (Guillou *et al.*, 2010; Corominas *et al.*, 2013a; Estany *et al.*, 2014). Significant positive correlations ranking from 0.51 to 0.75 (*p*-value<$1.00x10^{-08}$) were observed among genes regulated by this eQTL and, *SREBF1* and *PPARs* (Figure 4.2). Similar results have been identified in mice, where *ELOVL5*, *ELOVL6*, and *SCD* genes are induced by activation of PPARs (Green *et al.*, 2010).

Apart for the high importance of *ELOVLs* and *SCD* genes in lipogenesis, diacylglycerol acyltransferases (DGATs) enzymes are required for triglyceride synthesis. Two of their members, *DGAT1* and *DGAT2*, showed high correlations with *ELOVLs* and *SCD* genes, ranking from 0.59 to 0.81 (*p*-value<$1.00x10^{-12}$) (Figure 4.2).

The observed interrelated functions of genes involved in lipogenesis (*ELOVLs* and *SCD*), and triglyceride synthesis (*DGAT1* and *DGAT2*), which are the main function of adipose tissue, highlight the relevance of these genes and the complex genetic architecture underlying the lipid metabolism (Figure 4.2).

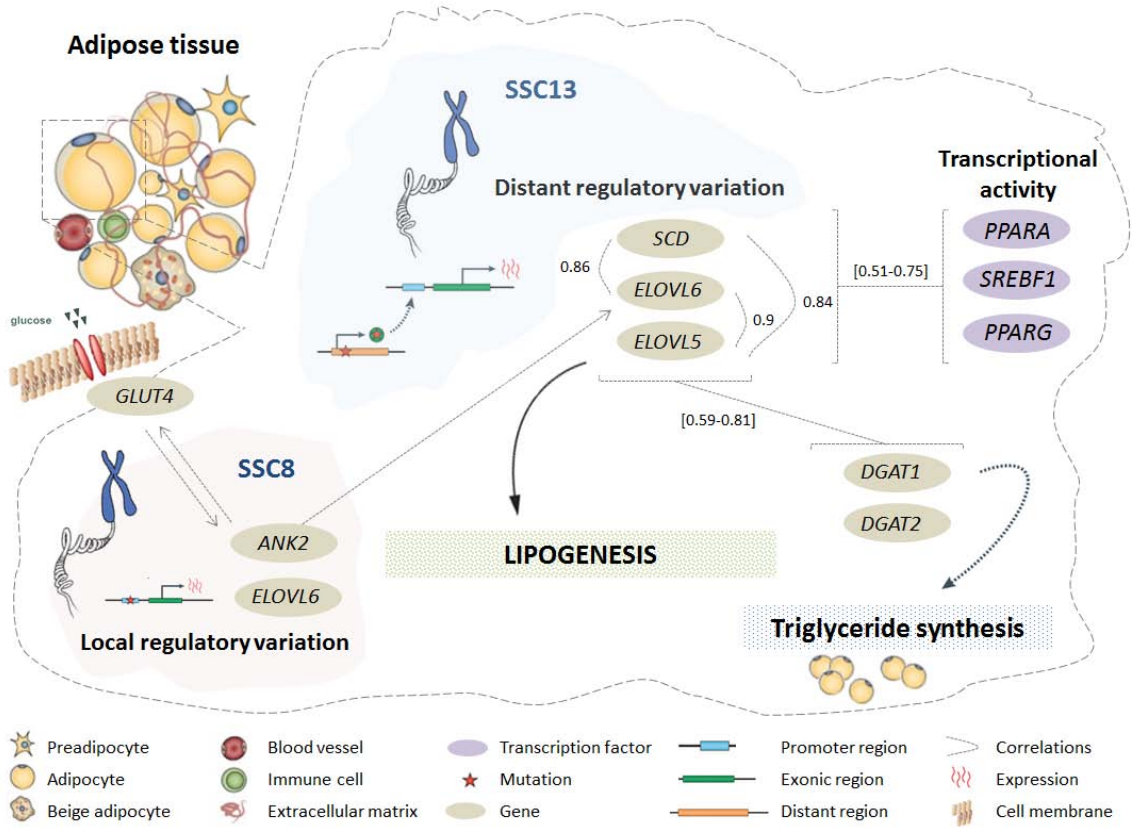

Figure 4.2. Integrative view of genes and transcription factors implicated in lipogenesis and triglyceride synthesis in adipose tissue.

4.4. Challenges in livestock genomics and future directions

In the past years, there has been a remarkable development of high-throughput omics (HTO) technologies (Table 4.3) such as genomics, epigenomics, transcriptomics, proteomics and metabolomics across all facets of biology. This has spearheaded the progress of the systems biology era, including applications in animal production. These technologies can potentially be applied to the same animal or to biological samples from the same animal but it is important to assess how these diverse datasets can be integrated to exploit the full potential of such information. Approaches that study complex traits that are measured using "omic" levels such as genome/exome arrays, gene-expression arrays, mass spectrometry and NGS are known as "Systems genomics" (Kadarmideen *et al.*, 2006).

Table 4.3. Overview of the different "omic" levels used in systems genomics.

Level	Description
Genome	Complete collection of DNA, containing all the genetic information of an organism
Epigenome	Complete collection of changes to the DNA and histone proteins
Transcriptome	Complete collection of RNA molecules in a cell or collections of cells
Proteome	Complete collection of proteins in cell, tissue or organism
Metabolome	Complete collection of small-molecule chemicals in a cell, tissue or organism
Microbiome	Complete collection of (genes of) microbes in the organism
Metagenome	Complete collection of genetic material contained in an environmental sample
Phenome	Complete collection of phenotypic traits, affected by genomic and/or environmental factor in an organism

In the last years, only a few number of articles reviewed systems genomics in an animal context (Zhu *et al.*, 2009; Woelders *et al.*, 2011; Li 2013). Furthermore, Cole *et al.* (2013) demonstrated that complex regulatory relationships exist among genotypes and phenotypes. The vast majority of the production important traits are quantitative traits, which can be explained by environmental factors and by many genes of small effect and few ones with larger effects. These genes may be controlling complex pathways with many enzymes, which determine the final phenotypes. Thus, integrative systems genomics methods may be useful in the analysis of complex traits (Cole *et al.*, 2013). However, one of the greatest difficulties presented by the multi-omic approach is the integration of the large volume of data produced across several HTO platforms.

Understandably, only one single research group cannot address all these omics. The IBMAP consortium has applied different genomic and transcriptomic approaches in the analysis of growth, carcass and meat quality traits in pigs. These approaches can be summarized in: (1) QTL and GWAS mapping experiments, (2) eQTL mapping analysis to identify expression regulatory regions, (3) analysis of positional candidate genes, (4) identification of differentially-expressed genes by microarray and RNA-Seq analysis, (5) identification of genomic variants (indels, SNPs and CNVs), and (6) network analysis to uncover key transcription factors.

The integration of all of these "omics" is a challenge to the scientific community in the next years, but we consider that integrating the heterogeneous information from the different biological levels can provide a clear understanding of the mechanisms involved in the determination of complex traits of interest. The costs to generate these HTO data are decreasing, making feasible the analysis of larger sample sizes. Remarkably, the continuous

achievements on these HTO techniques need to be followed by new computer technologies for processing, interpretation and storing data.

Furthermore, a recent addition to genome editing tools has led to a revolution in biological research. One of the most revolutionary is the genome editing technique, first introduced by Cong *et al.* (2013). This technique uses the clustered regulatory interspaced short palindromic repeats (CRISPR), which in combination with Cas9 protein (CRISPR/Cas) systems guide RNAs into a cell's genome (the nuclease) and cut the genome at desired locations (Suravajhala *et al.*, 2016). To date, it has not been thoroughly explored in livestock, but it is clearly foreseen that animal genome modification using CRISPR/Cas systems will play a key role in improving trait performances in animals.

Conclusions

Chapter 5

1. Fine mapping of QTL on SSC8 allowed the identification of two trait-associated SNP regions at around 93 Mb and 119 Mb. Effects of both regions were found for palmitoleic acid (C16:1(n-7)) content and C18:0/C16:0 and C18:1(n-7)/C16:1(n-7) elongation ratios measured in backfat.

2. *MAML3* and *SETD7* are positional candidate genes in the 93 Mb region. The characterization of these genes allowed the identification of two novel microsatellites in *MAML3* and nine SNPs in *SETD7*. Association analyses performed with the *MAML3* microsatellites and the SNP *SETD7:c.700G>T* showed that none of the analyzed polymorphisms had the strongest signal for the 93 Mb QTL region, suggesting that these polymorphisms are not the causal mutations.

3. In the 119 Mb region, the *ELOVL6:c.-533C>T* polymorphism showed a strong association with percentage of palmitic (C16:0) and palmitoleic (C16:1(n-7)) acids and C18:0/C16:0 and C18:1(n-7)/C16:1(n-7) elongation ratios. This result support the hypothesis that *ELOVL6:c.-533C>T* polymorphism has a pleiotropic effect on backfat and intramuscular fat, and has a role in the genetic determination of the 119 Mb QTL.

4. A total of 1,279 CNVs across autosomes have been identified from the whole genome sequence of Iberian and Landrace pigs, merging into 540 unique CNVRs. Six CNVRs (CNVRs 112, 157, 198, 214, 298, and 447), containing potential candidate genes for growth and fatty acid composition traits, were analyzed for segregation in three different backcrosses by qPCR. All the CNVRs with the exception of CNVR198 were validated.

5. CNVR112, CNVR157, CNVR298, and CNVR447 were selected to study their association with growth and fatty acid composition in backfat and intramuscular fat in 150 BC1_LD animals. The CNVR112, containing the *GPAT2* gene, showed association with several of the analyzed growth-related traits and fatty acid composition in backfat and intramuscular fat. The strongest signals were observed for the cis-vaccenic acid (C18:1(n-7)) and the C18:2(n-6)/C18:3(n-3) ratio in backfat, for oleic acid (C18:1(n-9)), eicosatrienoic acid (C20:3(n-3)), dihomo gamma linolenic acid (C20:3(n-6)), MUFA, PUFA, and the peroxidability index in intramuscular fat, and

carcass length for growth traits. These findings underline that CNVRs may explain a fraction of the genetic variability of fatty acid composition and growth traits.

6. The expression pattern of 44 lipid-related candidate genes was studied in the adipose tissue. eGWAS identified a total of 19 eQTLs for five genes (*ACSM5, ELOVL6, FABP4, FADS2*, and *SLC27A4*); three of them were acting in *cis* on the *ACSM5, FABP4*, and *FADS2* gene-expression, whereas the remaining 16 eQTLs had *trans*-regulatory effects.

7. A SNP in the *ACSM5* promoter region (*ACSM5:g.26260422G>A*) and a SNP in the 3'UTR region of *FABP4* (*FABP4:g.6723A>G*) were identified as the most associated polymorphisms with the *ACSM5* and *FABP4* mRNA expression levels, respectively. Hence, these SNPs may be strong candidate polymorphisms to explain the mRNA variation of these genes in adipose tissue.

8. The *trans*-eQTL on SSC13 identified for the *ELOVL6* gene was associated at chromosome level with the expression of *ELOVL5* and *SCD* genes, which are implicated in the elongation and desaturation of fatty acids, playing together an important role in the lipid homeostasis. These results support the involvement of common elements regulating their mRNA expression in adipose tissue.

References

Chapter 6

Abyzov A, Urban AE, Snyder M, Gerstein M (2011). CNVnator: an approach to discover, genotype, and characterize typical and atypical CNVs from family and population genome sequencing. *Genome Research* 21(6):974-84.

Ai H, Fang X, Yang B, Huang Z, Chen H, Mao L, *et al.* (2015). Adaptation and possible ancient interspecies introgression in pigs identified by whole-genome sequencing. *Nature Genetics* 47(3):217-25.

Albert FW, Kruglyak L (2015). The role of regulatory variation in complex traits and disease. *Nature Review. Genetics* 16(4):197-212.

Alkan C, Coe BP, Eichler EE (2011). Genome structural variation discovery and genotyping. *Nature Review. Genetics* 12(5):363-76.

Amaral AJ, Ferretti L, Megens HJ, Crooijmans RP, Nie H, Ramos-Onsins SE (2011). Genome-wide footprints of pig domestication and selection revealed through massive parallel sequencing of pooled DNA. *PLoS One* 6(4):e14782.

Andersson L, Haley CS, Ellegren H, Knott SA, Johansson M, Andersson K, *et al.* (1994). Genetic mapping of quantitative trait loci for growth and fatness in pigs. *Science* 263(5154):1771-1774.

Andersson L, Georges M (2004). Domestic-animal genomics: deciphering the genetics of complex traits. *Nature Reviews. Genetics* 2004 5(3):202-12.

Archibald AL, Bolund L, Churcher C, Fredholm M, Groenen MA, Harlizius B, *et al.* (2010). Pig genome sequence-analysis and publication strategy. *BMC Genomics* 11:438.

Aslan O, Hamill RM, Davey G, McBryan J, Mullen AM, Gispert M, *et al.* (2012). Variation in the IGF2 gene promoter region is associated with intramuscular fat content in porcine skeletal muscle. *Molecular Biology Reports* 39(4):4101-10.

Ayuso M, Fernández A, Núñez Y, Benítez R, Isabel B, Barragán C, *et al.* (2015). Comparative Analysis of Muscle Transcriptome between Pig Genotypes Identifies Genes and Regulatory Mechanisms Associated to Growth, Fatness and Metabolism. *PLoS One* 10(12):e0145162.

Ballester M, Revilla M, Puig-Oliveras A, Marchesi JA, Castelló A, Corominas J, *et al.* (2016). Analysis of the porcine APOA2 gene expression in liver, polymorphism identification and association with fatty acid composition traits. *Animal Genetics* 47(5): 552-9.

Ballester M, Ramayo-Caldas Y, Revilla M, Corominas J, Castelló A, Estellé J, *et al.* (2017). Integration of liver gene co-expression networks and eGWAs analyses highlighted candidate regulators implicated in lipid metabolism in pigs. *Scientific Reports* 7:46539.

Ballester M, Puig-Oliveras A, Castelló A, Revilla M, Fernández AI, Folch JM (2017). Analysis of FABP4 and FABP5 gene expression affecting pig fatness. *Animal Genetics* (*submitted*).

Barton-Gade PA (1990). Pork quality in genetic improvement programmes- the Danish experience. In: Proceedings of the National Swine Improvement Federation Annual Meeting. Des Moines, IA.

Bejerholm C, Barton-Gade PA (1986). Effect of intramuscular fat level on the eating quality of pig meat. Danish Meat Research Institute. Manuscript No. 720E.

Bendixen C, Hedegaard J, Horn P (2005). Functional genomics in farm animals - Microarray analysis. *Meat Science* 71(1):128-37.

Bergen WG, Mersmann HJ (2005). Comparative aspects of lipid metabolism: impact on contemporary research and use of animal models. *The Journal of Nutrition* 135(11):2499-502.

Bianco E, Nevado B, Ramos-Onsins SE, Pérez-Enciso M (2015). A deep catalog of autosomal single nucleotide variation in the pig. *PLoS One* 10(3):e0118867.

Bidner BS, Ellis M, Brewer MS, Campion D, Wilson ER, Mckeith FK (2004). Effect of ultimate ph on the quality characteristics of pork. *Journal of Muscle Foods* 15(2):139–154.

Blow N (2009). Transcriptomics: The digital generation. *Nature* 458(7235):239-42.

Boeva V, Zinovyev A, Bleakley K, Vert JP, Janoueix-Lerosey I, Delattre O, *et al.* (2011). Control-free calling of copy number alterations in deep-sequencing data using GC-content normalization. *Bioinformatics* 27(2):268-9.

Boeva V, Popova T, Bleakley K, Chiche P, Cappo J, Schleiermacher G, *et al.* (2012). Control-FREEC: a tool for assessing copy number and allelic content using next-generation sequencing data. *Bioinformatics* 28(3):423-5.

Boler DD, Dilger AC, Bidner BS, Carr SN, Eggert JM, Day JW, *et al.* (2010). Ultimate ph explains variation in pork quality traits. *Journal of Muscle Foods* 21(1):119–130.

Bosch L, Tor M, Reixach J, Estany J (2012). Age-related changes in intramuscular and subcutaneous fat content and fatty acid composition in growing pigs using longitudinal data. *Meat Science* 91(3):358-63.

Bosse M, Megens HJ, Madsen O, Paudel Y, Frantz LA, Schook LB, *et al.* (2012). Regions of homozygosity in the porcine genome: consequence of demography and the recombination landscape. *PLoS Genetics* 8(11):e1003100.

Brunsø K, Bredahl L, Grunert KG, Scholderer J (2004). Consumer perception of the quality of beef resulting from various fattening regimes. *Livestock Production Science* 94:83-93.

Bruun CS, Jørgensen CB, Nielsen VH, Andersson L, Fredholm M (2006). Evaluation of the porcine melanocortin 4 receptor (MC4R) gene as a positional candidate for a fatness QTL in a cross between Landrace and Hampshire. *Animal Genetics* 37(4):359-62.

Cameron ND (1990). Genetic and phenotypic parameters for carcass traits, meat and eating quality traits in pigs. *Livestock Production Science* 26:119-135.

Cameron ND, Enser MB (1991). Fatty acid composition of lipid in Longissimus dorsi muscle of Duroc and British Landrace pigs and its relationship with eating quality. *Meat Science* 29(4):295-307.

Cánovas A, Pena RN, Gallardo D, Ramírez O, Amills M, Quintanilla R (2012). Segregation of regulatory polymorphisms with effects on the gluteus medius transcriptome in a purebred pig population. *PLoS One* 7(4):e35583.

Casellas J, Noguera JL, Reixach J, Díaz I, Amills M, Quintanilla R (2010). Bayes factor analyses of heritability for serum and muscle lipid traits in Duroc pigs. *Journal of Animal Science* 88(7):2246-54.

Cattaneo ER, Pellon-Maison M, Rabassa ME, Lacunza E, Coleman RA, Gonzalez-Baro MR (2012). Glycerol-3-phosphate acyltransferase-2 is expressed in spermatic germ cells and incorporates arachidonic acid into triacylglycerols. *PLoS One* 7(8):e42986.

Chawla A, Repa JJ, Evans RM, Mangelsdorf DJ (2001). Chawla A1, Repa JJ, Evans RM, Mangelsdorf DJ. *Science* 294(5548):1866-70.

Chen C, Ai H, Ren J, Li W, Li P, Qiao R, *et al.* (2011). A global view of porcine transcriptome in three tissues from a full-sib pair with extreme phenotypes in growth and fat deposition by paired-end RNA sequencing. *BMC Genomics* 12:448.

Chen C, Qiao R, Wei R, Guo Y, Ai H, Ma J, *et al.* (2012). A comprehensive survey of copy number variation in 18 diverse pig populations and identification of candidate copy number variable genes associated with complex traits. *BMC Genomics* 13:733.

Chen C, Yang B, Zeng Z, Yang H, Liu C, Ren J, *et al.* (2013). Genetic dissection of blood lipid traits by integrating genome-wide association study and gene expression profiling in a porcine model. *BMC Genomics* 14:848.

Cheung VG, Spielman RS (2009). Genetics of human gene expression: mapping DNA variants that influence gene expression. *Nature Review. Genetics* 10(9):595-604.

Cheung VG, Nayak RR, Wang IX, Elwyn S, Cousins SM, Morley M, *et al.* (2010). Polymorphic cis- and trans-regulation of human gene expression. *PLoS biology* 8(9).

Chiang DY, Getz G, Jaffe DB, O'Kelly MJ, Zhao X, Carter SL, *et al.* (2009). High-resolution mapping of copy-number alterations with massively parallel sequencing. *Nature Methods* 6(1):99-103.

Chizzolini R, Zanardi E, Dorigoni V, Ghidini S (1999). Calorific value and cholesterol content of normal and low-fat meat and meat products. *Trends in Food Science & Technology* 10:119-28.

Choi JW, Chung WH, Lee KT, Cho ES, Lee SW, Choi BH, *et al.* (2015). Whole-genome resequencing analyses of five pig breeds, including Korean wild and native, and three European origin breeds. *DNA Research* 22(4):259-67.

Ciobanu D, Bastiaansen J, Malek M, Helm J, Woollard J, Plastow G, *et al.* (2001). Evidence for new alleles in the protein kinase adenosine monophosphate-activated gamma(3)-subunit gene associated with low glycogen content in pig skeletal muscle and improved meat quality. *Genetics* 159(3):1151-62.

Ciobanu DC, Bastiaansen JW, Lonergan SM, Thomsen H, Dekkers JC, Plastow GS, *et al.* (2004). New alleles in calpastatin gene are associated with meat quality traits in pigs. *Journal of Animal Science* 82(10):2829-39.

Ciobanu D, Lonergan S, Huff-Lonergan E (2011) Genetics of meat quality and carcass traits. In: Rothschild, M.F. and Ruvinsky, A. (eds) The Genetics of the Pig, 2nd Edn. (pp. 355-389). CAB International, Wallingford, UK.

Clarke J, Wu HC, Jayasinghe L, Patel A, Reid S, Bayley H (2009). Continuous base identification for single-molecule nanopore DNA sequencing. *Nature Nanotechnology* 4(4):265-70.

Clop A, Cercós A, Tomàs A, Pérez-Enciso M, Varona L, Noguera JL, *et al.* (2002). Assignment of the 2,4-dienoyl-CoA reductase (DECR) gene to porcine chromosome 4. *Animal Genetics* 33(2):164-5.

Clop A, Ovilo C, Perez-Enciso M, Cercos A, Tomas A, Fernandez A, *et al.* (2003). Detection of QTL affecting fatty acid composition in the pig. *Mammalian Genome* 14(9):650-6.

Cole JB, Lewis RM, Maltecca C, Newman S, Olson KM, Tait RG Jr (2013). Breeding and Genetics Symposium: systems biology in animal breeding: Identifying relationships among markers, genes, and phenotypes. *Journal of Animal Science* 91(2):521-2.

Cong L, Ran FA, Cox D, Lin S, Barretto R, Habib N, *et al.* (2013). Multiplex genome engineering using CRISPR/Cas systems. *Science* 339(6121):819-23.

Corominas J, Ramayo-Caldas Y, Castelló A, Muñoz M, Ibáñez-Escriche N, Folch JM, *et al.* (2012). Evaluation of the porcine ACSL4 gene as a candidate gene for meat quality traits in pigs. *Animal Genetics* 43(6):714-20.

Corominas J, Ramayo-Caldas Y, Puig-Oliveras A, Estellé J, Castelló A, Alves E, *et al.* (2013a). Analysis of porcine adipose tissue transcriptome reveals differences in de novo fatty acid synthesis in pigs with divergent muscle fatty acid composition. *BMC Genomics* 14:843.

Corominas J, Ramayo-Caldas Y, Puig-Oliveras A, Pérez-Montarelo D, Noguera JL, Folch JM, *et al.* (2013b). Polymorphism in the ELOVL6 gene is associated with a major QTL effect on fatty acid composition in pigs. *PLoS One* 8(1):e53687.

Corominas J, Marchesi J, Puig-Oliveras A, Revilla M, Estellé J, Alves E, *et al.* (2015). Epigenetic regulation of the ELOVL6 gene is associated with a major QTL effect on fatty acid composition in pigs. *Genetics Selection Evolution* 47:20.

de Oliveira Peixoto J, Facioni Guimarães SE, Sávio Lopes P, Menck Soares MA, Vieira Pires A, Gualberto Barbosa MV, *et al.* (2006). Associations of leptin gene polymorphisms with production traits in pigs. *Journal of Animal Breeding and Genetics* 123(6):378-83.

De Smet S, Raes K, Demeyer D (2004). Meat fatty acid composition as affected by fatness and genetic factors: a review. *Animal Research* 53(2):81–98.

De Vries AG, Wal van der PG, Eikelenboom G, Merks JWM (1992). Genetische variatie in varkensvleeskwaliteit. I.V.O. report B-376. I.V.O. Zeist, The Netherlands.

Dekkers JCM, Mathur PK, Knol EF (2011). Genetic improvement of the pig. In: The genetics of the pig. CAB International, UK 390-425.

DeVol DL, McKeith FK, Bechtel PJ, Novakofski J, Shanks RD, Carr TR (1988). Variation in composition and palatability traits and relationships between muscle

characteristics and palatability in a random sample of pork carcasses. *Journal of Animal Science* 66:385-395.

Dircks LK, Sul HS (1997). Mammalian mitochondrial glycerol-3-phosphate acyltransferase. *Biochimica et Biophysica Acta* 1348(1-2):17-26.

Dohm JC, Lottaz C, Borodina T, Himmelbauer H (2008). Substantial biases in ultra-short read data sets from high-throughput DNA sequencing. *Nucleic Acids Research* 36(16):e105.

Dong K, Pu Y, Yao N, Shu G, Liu X, He X, *et al.* (2015). Copy number variation detection using SNP genotyping arrays in three Chinese pig breeds. *Animal Genetics* 46(2):101-9.

Doss S, Schadt EE, Drake TA, Lusis AJ (2005). Cis-acting expression quantitative trait loci in mice. *Genome Research* 15(5):681-91.

Du CH, Sun DW (2006). Learning techniques used in computer vision for food quality evaluation: a review. *Journal of Food Engineering* 72:39–55.

Duan J, Zhang JG, Deng HW, Wang YP (2013). Comparative studies of copy number variation detection methods for next-generation sequencing technologies. *PLoS One* 8(3):e59128.

Duran-Montgé P, Theil PK, Lauridsen C, Esteve-Garcia E (2009). Fat metabolism is regulated by altered gene expression of lipogenic enzymes and regulatory factors in liver and adipose tissue but not in semimembranosus muscle of pigs during the fattening period. *Animal: an International Journal of Animal Bioscience* 3(11):1580-90.

Editorial (2006). Making the most of microarrays (Editorial). *Nature Biotechnology* 24:1039.

Ernst CW, Steibel JP (2013). Molecular advances in QTL discovery and application in pig breeding. *Trends in Genetics* 29(4):215-24.

Estany J, Ros-Freixedes R, Tor M, Pena RN (2014). A functional variant in the stearoyl-CoA desaturase gene promoter enhances fatty acid desaturation in pork. *PLoS One* 9(1):e86177.

Estellé J, Mercadé A, Noguera JL, Pérez-Enciso M, Ovilo C, Sánchez A, *et al.* (2005a). Effect of the porcine IGF2-intron3-G3072A substitution in an outbred Large White population and in an Iberian x Landrace cross. *Journal of Animal Science* 83(12):2723-8.

Estellé J, Sánchez A, Folch JM (2005b). Assignment of the microsomal triglyceride transfer protein large subunit (MTP) gene to porcine chromosome 8. *Animal Genetics* 36(4):354-5.

Estellé J, Pérez-Enciso M, Mercadé A, Varona L, Alves E, Sánchez A, *et al.* (2006). Characterization of the porcine FABP5 gene and its association with the FAT1 QTL in an Iberian by Landrace cross. *Animal Genetics* 37(6):589-91.

Estellé J, Mercadé A, Pérez-Enciso M, Pena RN, Silió L, Sánchez A, *et al.* (2009a). Evaluation of FABP2 as candidate gene for a fatty acid composition QTL in porcine chromosome 8. *Journal of Animal Breeding and Genetics* 126(1):52-8.

Estellé J, Fernández AI, Pérez-Enciso M, Fernández A, Rodríguez C, Sánchez A, *et al.* (2009b). A non-synonymous mutation in a conserved site of the MTTP gene is strongly associated with protein activity and fatty acid profile in pigs. *Animal Genetics* 40(6):813-20.

Esteve-Codina A, Paudel Y, Ferretti L, Raineri E, Megens HJ, Silió L, *et al.* (2013). Dissecting structural and nucleotide genome-wide variation in inbred Iberian pigs. *BMC Genomics* 14:148.

EuroStat (2015). Available: http://ec.europa.eu/eurostat/ [Accessed January 2017].

Fadista J, Nygaard M, Holm LE, Thomsen B, Bendixen C (2008). A snapshot of CNVs in the pig genome. *PLoS One* 3(12):e3916.

Fan B, Onteru SK, Plastow GS, Rothschild MF (2009). Detailed characterization of the porcine MC4R gene in relation to fatness and growth. *Animal Genetics* 40(4):401-9.

Fernández AI, Pérez-Montarelo D, Barragán C, Ramayo-Caldas Y, Ibáñez-Escriche N, Castelló A, *et al.* (2012). Genome-wide linkage analysis of QTL for growth and body composition employing the PorcineSNP60 BeadChip. *BMC Genetics* 13:41.

Fernández AI, Barragán C, Fernández A, Rodríguez MC, Villanueva B (2014). Copy number variants in a highly inbred Iberian porcine strain. *Animal Genetics* 45(3):357-66.

Fernandez X, Monin G, Talmant A, Mourot J, Lebret B (1999a). Influence of intramuscular fat content on the quality of pig meat - 1. Composition of the lipid fraction and sensory characteristics of m. longissimus lumborum. *Meat Science* 53(1):59-65.

Fernandez X, Monin G, Talmant A, Mourot J, Lebret B (1999b). Influence of intramuscular fat content on the quality of pig meat - 2. Consumer acceptability of m. longissimus lumborum. *Meat Science* 53(1):67-72.

Folch J, Less M, Sloane Stanley GH (1957). A simple method for the isolation and purification of total lipides from animal tissues. *The Journal of Biological Chemistry* 226(1):497-509.

Fontanesi L, Beretti F, Riggio V, Gómez González E, Dall'Olio S, Davoli R, *et al.* (2009). Copy number variation and missense mutations of the agouti signaling protein (ASIP) gene in goat breeds with different coat colors. *Cytogenetic and Genome Research* 126(4):333-47.

Font-i-Furnols M, Guerrero L (2014). Consumer preference, behavior and perception about meat and meat products: an overview. *Meat Science* 98(3):361-71.

Food and Agriculture Organization (FAO) (2014). Available: http://www.fao.org/ [Accessed January 2017].

Fortes MR, Reverter A, Zhang Y, Collis E, Nagaraj SH, Jonsson NN, *et al.* (2010). Association weight matrix for the genetic dissection of puberty in beef cattle. *Proceedings of the National Academy of Sciences of the United States of America* 107(31):13642-7.

Freeman JL, Perry GH, Feuk L, Redon R, McCarroll SA, Altshuler DM (2006). Copy number variation: new insights in genome diversity. *Genome Research* 16(8):949-61.

Fujii J, Otsu K, Zorzato F, de Leon S, Khanna VK, Weiler JE, *et al.* (1991). Identification of a mutation in porcine ryanodine receptor associated with malignant hyperthermia. *Science* 253(5018):448-51.

García-Olmo J, Corredor-Coca JI, De Pedro-Sanz E (2012) 1 H-NMR as a tool to determine the type of feeding of Iberian pigs. In: De Pedro E.J. (ed.), Cabezas A.B. (ed.). 7th International Symposium on the Mediterranean Pig. Options Méditerranéennes: Série A. Séminaires Méditerranéens. Zaragoza: CIHEAM, Vol. 101. pp. 607-610. Available: http://om.ciheam.org/om/pdf/a101/00006755.pdf

Gatlin LA, See MT, Hansen JA, Odle J (2003). Hydrogenated dietary fat improves pork quality of pigs from two lean genotypes. *Journal of Animal Science* 81(8):1989-97.

Gilad Y, Rifkin SA, Pritchard JK (2008). Revealing the architecture of gene regulation: the promise of eQTL studies. *Trends in Genetics* 24(8):408-15.

Giuffra E, Törnsten A, Marklund S, Bongcam-Rudloff E, Chardon P, Kijas JM, *et al.* (2002). A large duplication associated with dominant white color in pigs originated by homologous recombination between LINE elements flanking KIT. *Mammalian Genome* 13(10):569-77.

Goddard ME, Hayes BJ (2009). Mapping genes for complex traits in domestic animals and their use in breeding programmes. *Nature Review. Genetics* 10(6):381-91.

González-Prendes R, Quintanilla R, Cánovas A, Manunza A, Figueiredo Cardoso T, Jordana J, *et al.* (2017). Joint QTL mapping and gene expression analysis identify positional candidate genes influencing pork quality traits. *Scientific Reports* 7:39830.

Goodwin R, Burroughs S (1995). Genetic Evaluation Terminal Line Program Results. *National Pork Producers Council*; Des Moines, IA, USA.

Goodwin S, McPherson JD, McCombie WR (2016). Coming of age: ten years of next-generation sequencing technologies. *Nature reviews. Genetics* 17(6):333-51.

Green CD, Ozguden-Akkoc CG, Wang Y, Jump DB, Olson LK (2010). Role of fatty acid elongases in determination of de novo synthesized monounsaturated fatty acid species. *Journal of Lipid Research* 51(7):1871-7.

Groenen MAM, Schook LB, Archibald AL (2011). Pig genomics. In: Rothschild MF, Ruvinsky A, editors. The genetics of the pig. 2nd ed. Wallingford: CABI, p. 179–99.

Groenen MA, Archibald AL, Uenishi H, Tuggle CK, Takeuchi Y, Rothschild MF, *et al.* (2012). Analyses of pig genomes provide insight into porcine demography and evolution. *Nature* 491(7424):393-398.

Groenen MAM (2015). Development of a high-density Axiom® porcine genotyping array to meet research and commercial needs. Plant & Animal Genome XXIII Conference, San Diego, CA.

Grunert K (2005). Food quality and safety: consumer perception and demand. *European Review of Agricultural Economics* 32:369-391.

Guillou H, Zadravec D, Martin PG, Jacobsson A (2010). The key roles of elongases and desaturases in mammalian fatty acid metabolism: Insights from transgenic mice. *Progress in Lipid Research* 49(2):186-99.

Haley CS, Archibald AL, Andersson L, Bosma AA, Davies W, Fredholm M, *et al.* (1990). The pig gene mapping project – pigmap. In: 4th World Congress on Genetics Applied to Livestock Production, Edinburgh, p 67-70.

Hassen A, Wilson DE, Amin VR, Rouse GH, Hays CL (2001). Predicting percentage of intramuscular fat using two types of real-time ultrasound equipment. *Journal of Animal Science* 79(1):11-8.

Heidt H, Cinar MU, Uddin MJ, Looft C, Jüngst H, Tesfaye D, *et al.* (2013). A genetical genomics approach reveals new candidates and confirms known candidate genes for drip loss in a porcine resource population. *Mammalian Genome* 24(9-10):416-26.

Henson S (2000). The process of food quality belief formation from a consumer perspective. In: Becker T, editor. Quality policy and consumer behaviour in the European Union. Kiel, 73-89.

Heuven HCM, van Wijk HJ, van Arendonk JAM (2003). Combining traditional breeding and genomics to improve pork quality. *Outlook on Agriculture* 32:235-239.

Hocquette JF (2005). Where are we in genomics? *Journal of Physiology and Pharmacology* 56(Suppl 3):37–70.

Hocquette JF, Gondret F, Baéza E, Médale F, Jurie C, Pethick DW (2010). Intramuscular fat content in meat-producing animals: development, genetic and nutritional control, and identification of putative markers. *Animal* 4(2):303-19.

Hodgson RR, Davis GW, Smith GC, Savell JW, Cross HR (1991). Relationships between pork loin palatability traits and physical characteristics of cooked chops. *Journal of Animal Science* 69(12):4858-65.

Hovenier R, Kanis E, van Asseldonk T, Westerink NG (1993). Breeding for pig meat quality in halothane-negative populations – a review. *Pig News and Information* 14:17N-25N.

Hu ZL, Park CA, Wu XL, Reecy JM (2013). Animal QTLdb: an improved database tool for livestock animal QTL/association data dissemination in the post-genome era. *Nucleic acids research* 41(Database issue):D871-9.

Huff-Lonergan E, Baas TJ, Malek M, Dekkers JC, Prusa K, Rothschild MF (2002). Correlations among selected pork quality traits. *Journal of Animal Science* 80(3):617-27.

Humphray SJ, Scott CE, Clark R, Marron B, Bender C, Camm N, *et al.* (2007). A high utility integrated map of the pig genome. *Genome Biology* 8(7):R139.

Hurd PJ, Nelson CJ (2009). Advantages of next-generation sequencing versus the microarray in epigenetic research. *Briefings in Functional Genomics* & *Proteomics* 8(3):174-83.

Jansen RC, Nap JP (2001). Genetical genomics: the added value from segregation. *Trends in Genetics* 17(7):388-91.

Jayakumar A, Tai MH, Huang WY, al-Feel W, Hsu M, Abu-Elheiga L, *et al.* (1995). Human fatty acid synthase: properties and molecular cloning. *Proceedings of the National Academy of Sciences of the United States of America* 92(19):8695-9.

Jiang J, Wang J, Wang H, Zhang Y, Kang H, Feng X, *et al.* (2014). Global copy number analyses by next generation sequencing provide insight into pig genome variation. *BMC Genomics* 15:593.

Jiang S, Wei H, Song T, Yang Y, Peng J, Jiang S (2013). Transcriptome comparison between porcine subcutaneous and intramuscular stromal vascular cells during adipogenic differentiation. *PLoS One* 8(10):e77094.

Johansson Moller M, Chaudhary R, Hellmén E, Höyheim B, Chowdhary B, Andersson L (1996). Pigs with the dominant white coat color phenotype carry a duplication of the KIT gene encoding the mast/stem cell growth factor receptor. *Mammalian genome* 7(11):822-30.

Jump DB (2004). Fatty acid regulation of gene transcription. *Critical Reviews in Clinical Laboratory Sciences* 41(1):41-78.

Kadarmideen HN, von Rohr P, Janss LL (2006). From genetical genomics to systems genetics: potential applications in quantitative genomics and animal breeding. *Mammalian Genome* 17(6):548-64.

Kijas JM, Moller M, Plastow G, Andersson L (2001). A frameshift mutation in MC1R and a high frequency of somatic reversions cause black spotting in pigs. *Genetics* 158(2):779-85.

Kim JH, Lim HT, Park EW, Rodríguez C, Silio L, Varona L, *et al.* (2006) Polymorphisms in the promoter region of the porcine acyl-coA dehydrogenase, medium-chain (ACADM) gene have no effect on fat deposition traits in a pig Iberian x Landrace cross. *Animal Genetics* 37(4):430-1.

Kim KS, Larsen N, Short T, Plastow G, Rothschild MF (2000). A missense variant of the porcine melanocortin-4 receptor (MC4R) gene is associated with fatness, growth, and feed intake traits. *Mammalian Genome* 11(2):131-5.

Kingsmore SF, Lindquist IE, Mudge J, Gessler DD, Beavis WD (2008). Genome-wide association studies: progress and potential for drug discovery and development. *Nature Reviews. Drug Discovery* 7(3):221-30.

Kmieć M, Terman A (2006). Associations between the prolactin receptor gene polymorphism and reproductive traits of boars. *Journal of Applied Genetics* 47(2):139-41.

Knap PW, Sosnicki AA, Klont RE, Lacoste A (2002) Simultaneous improvement of meat quality and growth-and-carcass traits in pigs. *Proceedings of the 7th World Congress on Genetics Applied to Livestock Production* 31:339-346.

Kuhajda FP, Jenner K, Wood FD, Hennigar RA, Jacobs LB, Dick JD, *et al.* (1994). Fatty acid synthesis: a potential selective target for antineoplastic therapy. *Proceedings of the National Academy of Sciences of the United States of America* 91(14):6379-83.

Kurył J, Pierzchała M (2001). Association of POU1F1/RsaI genotypes with carcass traits in pigs. *Journal of Applied Genetics* 42(3):309-16.

Laliotis GP, Bizelis I, Rogdakis E (2010). Comparative Approach of the de novo Fatty Acid Synthesis (Lipogenesis) between Ruminant and Non Ruminant Mammalian Species: From Biochemical Level to the Main Regulatory Lipogenic Genes. *Current Genomics* 11(3):168-83.

Latorre P, Burgos C, Hidalgo J, Varona L, Carrodeguas JA, López-Buesa P (2016). c.A2456C-substitution in Pck1 changes the enzyme kinetic and functional properties modifying fat distribution in pigs. *Scientific Reports* 6:19617.

Leonard AE, Pereira SL, Sprecher H, Huang YS (2004). Elongation of long-chain fatty acids. *Progress in Lipid Research* 43(1):36-54.

Li H, Lu L, Manly KF, Chesler EJ, Bao L, Wang J, *et al.* (2005). Inferring gene transcriptional modulatory relations: a genetical genomics approach. *Human Molecular Genetics* 14(9):1119-25.

Li H (2013). Systems genetics in "-omics" era: current and future development. *Theory in Biosciences* 132(1):1-16.

Li XJ, Yang H, Li GX, Zhang GH, Cheng J, Guan H, *et al.* (2012a). Transcriptome profile analysis of porcine adipose tissue by high-throughput sequencing. *Animal Genetics* 43(2):144-52.

Li Y, Mei S, Zhang X, Peng X, Liu G, Tao H, *et al.* (2012b). Identification of genome-wide copy number variations among diverse pig breeds by array CGH. *BMC Genomics* 13:725.

Liaubet L, Lobjois V, Faraut T, Tircazes A, Benne F, Iannuccelli N, *et al.* (2011). Genetic variability of transcript abundance in pig peri-mortem skeletal muscle: eQTL localized genes involved in stress response, cell death, muscle disorders and metabolism. *BMC Genomics* 12:548.

Lim D, Chai HH, Lee SH, Cho YM, Choi JW, Kim NK (2015). Gene Expression Patterns Associated with Peroxisome Proliferator-activated Receptor (PPAR) Signaling in the Longissimus dorsi of Hanwoo (Korean Cattle). *Asian-Australasian Journal of Animal Sciences* 28(8):1075-83.

Lonergan SM, Stalder KJ, Huff-Lonergan E, Knight TJ, Goodwin RN, Prusa KJ, *et al.* (2007). Influence of lipid content on pork sensory quality within pH classification. *Journal of Animal Science* 85(4):1074-9.

Lorenzo DN, Healy JA, Hostettler J, Davis J, Yang J, Wang C, *et al.* (2015). Ankyrin-B metabolic syndrome combines age-dependent adiposity with pancreatic β cell insufficiency. *The Journal of Clinical Investigation* 125(8):3087-102.

Manunza A, Casellas J, Quintanilla R, González-Prendes R, Pena RN, Tibau J, *et al.* (2014). A genome-wide association analysis for porcine serum lipid traits reveals the existence of age-specific genetic determinants. *BMC Genomics* 15:758.

Margulies M, Egholm M, Altman WE, Attiya S, Bader JS, Bemben LA, *et al.* (2005) Genome sequencing in microfabricated high-density picolitre reactors. *Nature* 437(7057): 376-80.

Martínez-Montes AM, Fernández A, Pérez-Montarelo D, Alves E, Benítez RM, Nuñez Y, *et al.* (2017a). Using RNA-Seq SNP data to reveal potential causal mutations related to pig production traits and RNA editing. *Animal Genetics* 48(2):151-165.

Martínez-Montes AM, Muiños-Bühl A, Fernández A, Folch JM, Ibáñez-Escriche N, Fernández AI (2017b). Deciphering the regulation of porcine genes influencing

growth, fatness and yield-related traits through genetical genomics. *Mammalian Genome* 28(3-4):130-142.

Melin J, Quake SR (2007). Microfluidic large-scale integration: the evolution of design rules for biological automation. *Annual Review of Biophysics and Biomolecular Structure* 36:213-31.

Mercadé A, Estellé J, Noguera JL, Folch JM, Varona L, Silió L, *et al.* (2005a). On growth, fatness, and form: a further look at porcine chromosome 4 in an Iberian x Landrace cross. *Mammalian Genome* 16(5):374-82.

Mercadé A, Sánchez A, Folch JM (2005b). Exclusion of the acyl CoA:diacylglycerol acyltransferase 1 gene (DGAT1) as a candidate for a fatty acid composition QTL on porcine chromosome 4. *Journal of Animal Breeding and Genetics* 122(3):161-4.

Mercadé A, Estellé J, Pérez-Enciso M, Varona L, Silió L, Noguera JL, *et al.* (2006a). Characterization of the porcine acyl-CoA synthetase long-chain 4 gene and its association with growth and meat quality traits. *Animal Genetics* 37(3):219-24.

Mercadé A, Pérez-Enciso M, Varona L, Alves E, Noguera JL, Sánchez A, *et al.* (2006b). Adipocyte fatty-acid binding protein is closely associated to the porcine FAT1 locus on chromosome 4. *Journal of Animal Science* 84(11):2907-13.

Mercadé A, Sánchez A, Folch JM (2007). Characterization and physical mapping of the porcine CDS1 and CDS2 genes. *Animal Biotechnology* 18(1):23-35.

Metzker ML (2010). Sequencing technologies - the next generation. *Nature Review. Genetics* 11(1):31-46.

Meuwissen TH, Goddard ME (2000). Fine mapping of quantitative trait loci using linkage disequilibria with closely linked marker loci. *Genetics* 155(1):421-30.

Meuwissen TH, Goddard ME (2004). Mapping multiple QTL using linkage disequilibrium and linkage analysis information and multitrait data. *Genetics Selection Evolution* 36(3):261-79.

Michaelson JJ, Loguercio S, Beyer A (2009). Detection and interpretation of expression quantitative trait loci (eQTL). *Methods : a Companion to Methods in Enzymology* 48(3):265-76.

Milan D, Jeon JT, Looft C, Amarger V, Robic A, Thelander M, *et al.* (2000). A mutation in PRKAG3 associated with excess glycogen content in pig skeletal muscle. *Science* 288(5469):1248-51.

Miller CA, Hampton O, Coarfa C, Milosavljevic A (2011). ReadDepth: a parallel R package for detecting copy number alterations from short sequencing reads. *PLoS One* 6(1):e16327.

Moon S, Kim TH, Lee KT, Kwak W, Lee T, Lee SW, *et al.* (2015). A genome-wide scan for signatures of directional selection in domesticated pigs. *BMC Genomics* 16:130.

Morley M, Molony CM, Weber TM, Devlin JL, Ewens KG, Spielman RS, *et al.* (2004). Genetic analysis of genome-wide variation in human gene expression. *Nature* 430(7001):743-7.

Morozova O, Marra MA (2008). Applications of next-generation sequencing technologies in functional genomics. *Genomics* 92(5):255-64.

Mortazavi A, Williams BA, McCue K, Schaeffer L, Wold B (2008). Mapping and quantifying mammalian transcriptomes by RNA-Seq. *Nature Methods* 5(7):621-8.

Muñoz G, Alves E, Fernández A, Ovilo C, Barragán C, Estellé J, *et al.* (2007). QTL detection on porcine chromosome 12 for fatty-acid composition and association analyses of the fatty acid synthase, gastric inhibitory polypeptide and acetyl-coenzyme A carboxylase alpha genes. *Animal Genetics* 38(6):639-46.

Muñoz G, Ovilo C, Silió L, Tomás A, Noguera JL, Rodríguez MC (2009). Single- and joint-population analyses of two experimental pig crosses to confirm quantitative trait loci on Sus scrofa chromosome 6 and leptin receptor effects on fatness and growth traits. *Journal of Animal Science* 87(2):459-68.

Muñoz M, Fernández AI, Ovilo C, Muñoz G, Rodriguez C, Fernández A, *et al.* (2010). Non-additive effects of RBP4, ESR1 and IGF2 polymorphisms on litter size at

different parities in a Chinese-European porcine line. *Genetics Selection Evolution* 42:23.

Muñoz M, Rodríguez MC, Alves E, Folch JM, Ibañez-Escriche N, Silió L, *et al.* (2013). Genome-wide analysis of porcine backfat and intramuscular fat fatty acid composition using high-density genotyping and expression data. *BMC Genomics* 14:845.

Nafikov RA, Beitz DC (2007). Carbohydrate and lipid metabolism in farm animals. *The Journal of Nutrition* 137(3):702-5.

Nakamura MT, Nara TY (2004). Structure, function, and dietary regulation of delta6, delta5, and delta9 desaturases. *Annual Review of Nutrition* 24:345-76

Newcom DW, Baas TJ, Lampe JF (2002). Prediction of intramuscular fat percentage in live swine using real-time ultrasound. *Journal of Animal Science* 80(12):3046-3052.

Noguera JL, Varona L, Gómez-Raya L, Sánchez A, Babot D, Estany J, *et al.* (2003). Estrogen receptor polymorphism in Landrace pigs and its association with litter size performance. *Livestock Production Science* 82:53-59.

Nonneman D, Lindholm-Perry AK, Shackelford SD, King DA, Wheeler TL, Rohrer GA, *et al.* (2011). Predictive markers in calpastatin for tenderness in commercial pig populations. *Journal of Animal Science* 89(9):2663-72.

Ntawubizi M, Colman E, Janssens S, Raes K, Buys N, De Smet S (2010). Genetic parameters for intramuscular fatty acid composition and metabolism in pigs. *Journal of Animal Science* 88(4):1286-94.

Nürnberg K, Wegner J, Ender K (1998). Factors influencing fat composition in muscle and adipose tissue of farm animals. *Livestock Production Science* 56:145–156.

O'Brien PJ, MacLennan DH (1992). Application in the swine industry of a DNA-based test for porcine stress syndrome. *Proceedings* 23:433–435.

O'Hea EK, Leveille GA (1969). Significance of adipose tissue and liver as sites of fatty acid synthesis in the pig and the efficiency of utilization of various substrates for lipogenesis. *The Journal of Nutrition* 99(3):338-44.

Ojeda A, Rozas J, Folch JM, Pérez-Enciso M (2006). Unexpected high polymorphism at the FABP4 gene unveils a complex history for pig populations. *Genetics* 174(4):2119-27.

Onteru SK, Ross JW, Rothschild MF (2009). The role of gene discovery, QTL analyses and gene expression in reproductive traits in the pig. *Society of Reproduction and Fertility Supplement* 66:87-102.

Ovilo C, Pérez-Enciso M, Barragán C, Clop A, Rodríquez C, Oliver MA, *et al.* (2000). A QTL for intramuscular fat and backfat thickness is located on porcine chromosome 6. *Mammalian Genome* 11(4):344-6.

Ovilo C, Clop A, Noguera JL, Oliver MA, Barragán C, Rodriguez C, *et al.* (2002). Quantitative trait locus mapping for meat quality traits in an Iberian x Landrace F2 pig population. *Journal of Animal Science* 80(11):2801-8.

Ovilo C, Fernández A, Noguera JL, Barragán C, Letón R, Rodríguez C, *et al.* (2005). Fine mapping of porcine chromosome 6 QTL and LEPR effects on body composition in multiple generations of an Iberian by Landrace intercross. *Genetics Research* 85(1):57-67.

Paton CM, Ntambi JM (2009). Biochemical and physiological function of stearoyl-CoA desaturase. *American journal of physiology. Endocrinology and Metabolism* 297(1):E28-37.

Paudel Y, Madsen O, Megens HJ, Frantz LA, Bosse M, Bastiaansen JW, *et al.* (2013). Evolutionary dynamics of copy number variation in pig genomes in the context of adaptation and domestication. *BMC Genomics* 14:449.

Paudel Y, Madsen O, Megens HJ, Frantz LA, Bosse M, Crooijmans RP, *et al.* (2015). Copy number variation in the speciation of pigs: a possible prominent role for olfactory receptors. *BMC Genomics* 16:330.

Pena RN, Noguera JL, Casellas J, Díaz I, Fernández AI, Folch JM, *et al.* (2013). Transcriptional analysis of intramuscular fatty acid composition in the longissimus thoracis muscle of Iberian × Landrace back-crossed pigs. *Animal Genetics* 44(6):648-60.

Pérez-Enciso M, Clop A, Noguera JL, Ovilo C, Coll A, Folch JM, *et al.* (2000). A QTL on pig chromosome 4 affects fatty acid metabolism: evidence from an Iberian by Landrace intercross. *Journal of Animal Science* 78(10):2525-31.

Pérez-Enciso M, Clop A, Folch JM, Sánchez A, Oliver MA, Ovilo C, *et al.* (2002). Exploring alternative models for sex-linked quantitative trait loci in outbred populations: application to an iberian x landrace pig intercross. *Genetics* 161(4):1625-32.

Pérez-Enciso M, Mercadé A, Bidanel JP, Geldermann H, Cepica S, Bartenschlager H, *et al.* (2005). Large-scale, multibreed, multitrait analyses of quantitative trait loci experiments: the case of porcine X chromosome. *Journal of Animal Science* 83(10):2289-96.

Pérez-Montarelo D, Madsen O, Alves E, Rodríguez MC, Folch JM, Noguera JL, *et al.* (2014). Identification of genes regulating growth and fatness traits in pig through hypothalamic transcriptome analysis. *Physiological Genomics* 46(6):195-206.

Petersen AK, Krumsiek J, Wägele B, Theis FJ, Wichmann HE, Gieger C, *et al.* (2012). On the hypothesis-free testing of metabolite ratios in genome-wide and metabolome-wide association studies. *BMC Bioinformatics* 13:120.

Petretto E, Mangion J, Dickens NJ, Cook SA, Kumaran MK, Lu H, *et al.* (2006). Heritability and tissue specificity of expression quantitative trait loci. *PLoS Genetics* 2(10):e172.

Pitchford WS, Deland MP, Siebert BD, Malau-Aduli AE, Bottema CD (2002). Genetic variation in fatness and fatty acid composition of crossbred cattle. *Journal of Animal Science* 80(11):2825-32.

Plastow GS, Carrión D, Gil M, García-Regueiro JA, I Furnols MF, Gispert M, *et al.* (2005). Quality pork genes and meat production. *Meat Science* 70(3):409-21.

Ponsuksili S, Jonas E, Murani E, Phatsara C, Srikanchai T, Walz C, *et al.* (2008). Trait correlated expression combined with expression QTL analysis reveals biological pathways and candidate genes affecting water holding capacity of muscle. *BMC Genomics* 9:367.

Ponsuksili S, Murani E, Schwerin M, Schellander K, Wimmers K (2010). Identification of expression QTL (eQTL) of genes expressed in porcine M. longissimus dorsi and associated with meat quality traits. *BMC Genomics* 11:572.

Ponsuksili S, Murani E, Brand B, Schwerin M, Wimmers K (2011). Integrating expression profiling and whole-genome association for dissection of fat traits in a porcine model. *Journal of Lipid Research* 52(4):668-78.

Ponsuksili S, Du Y, Murani E, Schwerin M, Wimmers K (2012). Elucidating molecular networks that either affect or respond to plasma cortisol concentration in target tissues of liver and muscle. *Genetics* 192(3):1109-22.

Ponsuksili S, Murani E, Trakooljul N, Schwerin M, Wimmers K (2014). Discovery of candidate genes for muscle traits based on GWAS supported by eQTL-analysis. *International Journal of Biological Sciences* 10(3):327-37.

Porter V (1993). Pigs: A Handbook to the Breeds of the World. Mountfield, East Sussex: Helm Information, Ltd.

Poudyal H, Panchal SK, Diwan V, Brown L (2011). Omega-3 fatty acids and metabolic syndrome: effects and emerging mechanisms of action. *Progress in Lipid Research* 50(4):372-87.

Puig-Oliveras A, Ramayo-Caldas Y, Corominas J, Estellé J, Pérez-Montarelo D, Hudson NJ, *et al.* (2014a). Differences in muscle transcriptome among pigs phenotypically extreme for fatty acid composition. *PLoS One* 9(6):e99720.

Puig-Oliveras A, Ballester M, Corominas J, Revilla M, Estellé J, Fernández AI, *et al.* (2014b). A co-association network analysis of the genetic determination of pig conformation, growth and fatness. *PLoS One* 9(12):e114862.

Puig-Oliveras A, Revilla M, Castelló A, Fernández AI, Folch JM, Ballester M (2016). Expression-based GWAS identifies variants, gene interactions and key regulators

affecting intramuscular fatty acid content and composition in porcine meat. *Scientific Reports* 6:31803.

Raj S, Skiba G, Weremko D, Fandrejewski H, Migdał W, Borowiec F, *et al.* (2010) The relationship between the chemical composition of the carcass and the fatty acid composition of intramuscular fat and backfat of several pig breeds slaughtered at different weights. *Meat Science* 86(2):324-30.

Ralston JC, Matravadia S, Gaudio N, Holloway GP, Mutch DM (2015). Polyunsaturated fatty acid regulation of adipocyte FADS1 and FADS2 expression and function. *Obesity* 23(4):725-8.

Ramayo-Caldas Y, Castelló A, Pena RN, Alves E, Mercadé A, Souza CA, *et al.* (2010). Copy number variation in the porcine genome inferred from a 60 k SNP BeadChip. *BMC Genomics* 11:593.

Ramayo-Caldas Y, Mach N, Esteve-Codina A, Corominas J, Castelló A, Ballester M, *et al.* (2012a). Liver transcriptome profile in pigs with extreme phenotypes of intramuscular fatty acid composition. *BMC Genomics* 13:547.

Ramayo-Caldas Y, Mercadé A, Castelló A, Yang B, Rodríguez C, Alves E, *et al.* (2012b). Genome-wide association study for intramuscular fatty acid composition in an Iberian × Landrace cross. *Journal of Animal Science* 90(9):2883-93.

Ramayo-Caldas Y, Ballester M, Fortes MR, Esteve-Codina A, Castelló A, Noguera JL, *et al.* (2014). From SNP co-association to RNA co-expression: novel insights into gene networks for intramuscular fatty acid composition in porcine. *BMC Genomics* 15:232.

Ramírez O, Burgos-Paz W, Casas E, Ballester M, Bianco E, Olalde I, *et al.* (2015). Genome data from a sixteenth century pig illuminate modern breed relationships. *Heredity* 114(2):175-84.

Ramos AM, Crooijmans RP, Affara NA, Amaral AJ, Archibald AL, Beever JE, *et al.* (2009). Design of a high density SNP genotyping assay in the pig using SNPs identified and characterized by next generation sequencing technology. *PLoS One* 4(8):e6524.

Raudsepp T, Chowdhary BP (2011). Cytogenetics and chromosome maps. In: Rothschild MF, Ruvinsky A, editors. The genetics of the pig. 2nd ed. Wallingford: CABI, p. 134–78.

Reiner G, Dreher F, Drungowski M, Hoeltig D, Bertsch N, Selke M, *et al.* (2014). Pathway deregulation and expression QTLs in response to Actinobacillus pleuropneumoniae infection in swine. *Mammalian Genome* 25(11-12):600-17.

Reverter A, Fortes MR (2013). Association weight matrix: a network-based approach towards functional genome-wide association studies. *Methods in Molecular Biology* 1019:437-47.

Revilla M, Ramayo-Caldas Y, Castelló A, Corominas J, Puig-Oliveras A, Ibáñez-Escriche N, *et al.* (2014). New insight into the SSC8 genetic determination of fatty acid composition in pigs. *Genetics Selection Evolution* 46:28.

Ritchie MD, Holzinger ER, Li R, Pendergrass SA, Kim D (2015). Methods of integrating data to uncover genotype-phenotype interactions. *Nature Reviews. Genetics* 16(2):85-97.

Roberts A, Pimentel H, Trapnell C, Pachter L (2011). Identification of novel transcripts in annotated genomes using RNA-Seq. *Bioinformatics* 27(17):2325-9.

Rockman MV, Kruglyak L (2006). Genetics of global gene expression. *Nature Review. Genetics* 7(11):862-72.

Rosen ED, Walkey CJ, Puigserver P, Spiegelman BM (2000). Transcriptional regulation of adipogenesis. *Genes* & *Development* 14(11):1293-307.

Rothschild M, Jacobson C, Vaske D, Tuggle C, Wang L, Short T, *et al.* (1996). The estrogen receptor locus is associated with a major gene influencing litter size in pigs. *Proceedings of the National Academy of Sciences of the United States of America* 93(1):201-5.

Rothschild MF, Messer L, Day A, Wales R, Short T, Southwood O, *et al.* (2000). Investigation of the retinol-binding protein 4 (RBP4) gene as a candidate gene for increased litter size in pigs. *Mammalian Genome* 11(1):75-7.

Rubin CJ, Megens HJ, Martinez Barrio A, Maqbool K, Sayyab S, Schwochow D, *et al.* (2012). Strong signatures of selection in the domestic pig genome. *Proceedings of the National Academy of Sciences of the United States of America* 109(48):19529-36.

Rudel LL, Parks JS, Sawyer JK (1995). Compared with dietary monounsaturated and saturated fat, polyunsaturated fat protects African green monkeys from coronary artery atherosclerosis. *Arteriosclerosis, Thrombosis, and Vascular Biology* 15(12):2101-10.

Salmon Hillbertz NH, Isaksson M, Karlsson EK, Hellmén E, Pielberg GR, Savolainen P, *et al.* (2007). Duplication of FGF3, FGF4, FGF19 and ORAOV1 causes hair ridge and predisposition to dermoid sinus in Ridgeback dogs. *Nature Genetics* 39(11):1318-20.

Samorè AB, Fontanesi L (2016). Genomic selection in pigs: state of the art and perspectives, *Italian Journal of Animal Science* 15:211-232.

Samulin J, Berget I, Lien S, Sundvold H (2008). Differential gene expression of fatty acid binding proteins during porcine adipogenesis. *Comparative Biochemistry and Physiology. Part B, Biochemistry* & *Molecular Biology* 151(2):147-52.

Schadt EE, Monks SA, Drake TA, Lusis AJ, Che N, Colinayo V, *et al.* (2003). Genetics of gene expression surveyed in maize, mouse and man. *Nature* 422(6929):297-302.

Schena M, Shalon D, Davis RW, Brown PO (1995). Quantitative monitoring of gene expression patterns with a complementary DNA microarray. *Science* 270(5235):467-70.

Schiavo G, Dolezal MA, Scotti E, Bertolini F, Calò DG, Galimberti G, *et al.* (2014). Copy number variants in Italian Large White pigs detected using high-density single nucleotide polymorphisms and their association with back fat thickness. *Animal Genetics* 45(5):745-9.

Schook LB, Beever JE, Rogers J, Humphray S, Archibald A, Chardon P, *et al.* (2005). Swine Genome Sequencing Consortium (SGSC): a strategic roadmap for sequencing the pig genome. *Comparative and Functional Genomics* 6(4):251-5.

Sellier P (1998). Genetics of meat and carcass traits. The genetics of the pig. Rothschild MF, Ruvinsky A, editors. Oxon, UK: CAB International, 463-510.

Seroussi E, Glick G, Shirak A, Yakobson E, Weller JI, Ezra E, *et al.* (2010). Analysis of copy loss and gain variations in Holstein cattle autosomes using BeadChip SNPs. *BMC Genomics* 11:673.

Serra X, Gil F, Pérez-Enciso M, Oliver MA, Vázquez JM, Gispert M, *et al.* (1998). A comparison of carcass, meat quality and histochemical characteristics of Iberian (Guadyerbas line) and Landrace pigs. *Livestock Production Science* 56:215–223.

Snijders AM, Nowak N, Segraves R, Blackwood S, Brown N, Conroy J, *et al.* (2001). Assembly of microarrays for genome-wide measurement of DNA copy number. *Nature Genetics* 29(3):263-4.

Sodhi SS, Park WC, Ghosh M, Kim JN, Sharma N, Shin KY, *et al.* (2014). Comparative transcriptomic analysis to identify differentially expressed genes in fat tissue of adult Berkshire and Jeju Native Pig using RNA-seq. *Molecular Biology Reports* 41(9):6305-15.

Song CY, Gao B, Teng SH, Wang XY, Xie F, Chen GH, *et al.* (2007). Polymorphisms in intron 1 of the porcine POU1F1 gene. *Journal of Applied Genetics* 48(4):371-4.

Spurgeon SL, Jones RC, Ramakrishnan R (2008). High throughput gene expression measurement with real time PCR in a microfluidic dynamic array. *PLoS One* 3(2):e1662.

Steibel JP, Bates RO, Rosa GJ, Tempelman RJ, Rilington VD, Ragavendran A, *et al.* (2011). Genome-wide linkage analysis of global gene expression in loin muscle tissue identifies candidate genes in pigs. *PLoS One* 6(2):e16766.

Su Z, Li Z, Chen T, Li QZ, Fang H, Ding D, *et al.* (2011). Comparing next-generation sequencing and microarray technologies in a toxicological study of the effects of aristolochic acid on rat kidneys. *Chemical Research in Toxicology* 24(9):1486-93.

Suravajhala P, Kogelman LJ, Kadarmideen HN (2016). Multi-omic data integration and analysis using systems genomics approaches: methods and applications in animal production, health and welfare. *Genetics Selection Evolution* 48(1):38.

Suzuki K, Irie M, Kadowaki H, Shibata T, Kumagai M, Nishida A (2005). Genetic parameter estimates of meat quality traits in Duroc pigs selected for average daily gain, longissimus muscle area, backfat thickness, and intramuscular fat content. *Journal of Animal Science* 83(9):2058-65.

Szostak A, Ogłuszka M, Te Pas MF, Poławska E, Urbański P, Juszczuk-Kubiak E, *et al.* (2016). Effect of a diet enriched with omega-6 and omega-3 fatty acids on the pig liver transcriptome. *Genes* & *Nutrition* 11:9.

Tarling E, Salter A, Bennett A (2004). Transcriptional regulation of human SREBP-1c (sterol-regulatory-element-binding protein-1c): a key regulator of lipogenesis. *Biochemical Society Transactions* 32(Pt 1):107-9.

Teo SM, Pawitan Y, Ku CS, Chia KS, Salim A (2012). Statistical challenges associated with detecting copy number variations with next-generation sequencing. *Bioinformatics* 28(21):2711-8.

Tomás A, Casellas J, Ramírez O, Muñoz G, Noguera JL, Sánchez A (2006). High amino acid variation in the intracellular domain of the pig prolactin receptor (PRLR) and its relation to ovulation rate and piglet survival traits. *Journal of Animal Science* 84(8):1991-8.

Toro MA, Rodrigañez J, Silió L, Rodríguez C (2000). Genealogical analysis of a closed herd of black hairless Iberian pigs. *Conservation Biology* 14:1743-1851.

Tuggle CK, Dekkers JC, Reecy JM (2006). Integration of structural and functional genomics. *Animal Genetics* 37 Suppl 1:1-6.

Van Laere AS, Nguyen M, Braunschweig M, Nezer C, Collette C, Moreau L, *et al.* (2003). A regulatory mutation in IGF2 causes a major QTL effect on muscle growth in the pig. *Nature* 425(6960):832-6.

Varona L, Ovilo C, Clop A, Noguera JL, Pérez-Enciso M, Coll A, *et al.* (2002). QTL mapping for growth and carcass traits in an Iberian by Landrace pig intercross: additive, dominant and epistatic effects. *Genetic Research* 80(2):145-54.

Verbeke W, Viaene J (1999). Beliefs, attitude and behaviour towards fresh meat consumption in Belgium: empirical evidence from a consumer survey. *Food Quality and Preference* 10:437-445.

Veroneze R, Lopes PS, Guimarães SE, Silva FF, Lopes MS, Harlizius B, *et al.* (2013). Linkage disequilibrium and haplotype block structure in six commercial pig lines. *Journal of Animal Science* 91(8):3493-501.

Vitti JJ, Grossman SR, Sabeti PC (2013). Detecting natural selection in genomic data. *Annual Review of Genetics* 47:97-120.

Volpe JJ, Vagelos PR (1976). Mechanisms and regulation of biosynthesis of saturated fatty acids. *Physiological Reviews* 56(2):339-417.

Wang Z, Gerstein M, Snyder M (2009). RNA-Seq: a revolutionary tool for transcriptomics. *Nature Reviews. Genetics* 10(1):57-63.

Wang SJ, Liu WJ, Yang LG, Sargent CA, Liu HB, Wang C, *et al.* (2012a). Effects of FUT1 gene mutation on resistance to infectious disease. *Molecular Biology Reports* 39(3):2805-10.

Wang J, Jiang J, Fu W, Jiang L, Ding X, Liu JF, *et al.* (2012b). A genome-wide detection of copy number variations using SNP genotyping arrays in swine. *BMC Genomics* 13:273.

Wang T, Jiang A, Guo Y, Tan Y, Tang G, Mai M, *et al.* (2013a). Deep sequencing of the transcriptome reveals inflammatory features of porcine visceral adipose tissue. *International Journal of Biological Sciences* 9(6):550-6.

Wang J, Wang H, Jiang J, Kang H, Feng X, Zhang Q, *et al.* (2013b). Identification of genome-wide copy number variations among diverse pig breeds using SNP genotyping arrays. *PLoS One* 8(7):e68683.

Wang L, Liu X, Zhang L, Yan H, Luo W, Liang J, *et al.* (2013c). Genome-wide copy number variations inferred from SNP genotyping arrays using a Large White and Minzhu intercross population. *PLoS One* 8(10):e74879.

Wang J, Jiang J, Wang H, Kang H, Zhang Q, Liu JF (2014a). Enhancing genome-wide copy number variation identification by high density array CGH using diverse resources of pig breeds. *PLoS One* 9(1):e87571.

Wang Y, Tang Z, Sun Y, Wang H, Wang C, Yu S, *et al.* (2014b). Analysis of genome-wide copy number variations in Chinese indigenous and western pig breeds by 60 K SNP genotyping arrays. *PLoS One* 9(9):e106780.

Wang H, Wang C, Yang K, Liu J, Zhang Y, Wang Y, *et al.* (2015a). Genome Wide Distributions and Functional Characterization of Copy Number Variations between Chinese and Western Pigs. *PLoS One* 10(7):e0131522.

Wang L, Xu L, Liu X, Zhang T, Li N, Hay el H, *et al.* (2015b). Copy number variation-based genome wide association study reveals additional variants contributing to meat quality in Swine. *Scientific Reports* 2015 5:12535.

Watkins PA, Maiguel D, Jia Z, Pevsner J (2007). Evidence for 26 distinct acyl-coenzyme A synthetase genes in the human genome. *Journal of Lipid Research* 48(12):2736-50.

Weis BK (2005). Standardizing global gene expression analysis between laboratories and across platforms. *Nature Methods* 2:351–6.

Wiedmann RT, Nonneman DJ, Rohrer GA (2015). Genome-Wide Copy Number Variations Using SNP Genotyping in a Mixed Breed Swine Population. *PLoS One* 10(7):e0133529.

Wimmers K, Murani E, Te Pas MF, Chang KC, Davoli R, Merks JW, *et al.* (2007). Associations of functional candidate genes derived from gene-expression profiles of prenatal porcine muscle tissue with meat quality and muscle deposition. *Animal Genetics* 38(5):474-84.

Wimmers K, Murani E, Ponsuksili S (2010). Functional genomics and genetical genomics approaches towards elucidating networks of genes affecting meat performance in pigs. *Briefings in Functional Genomics* 9(3):251-8.

Woelders H, Te Pas MF, Bannink A, Veerkamp RF, Smits MA (2011). Systems biology in animal sciences. *Animal* 5(7):1036-47.

Wood JD, Nute GR, Richardson RI, Whittington FM, Southwood O, Plastow G, *et al.* (2004). Effects of breed, diet and muscle on fat deposition and eating quality in pigs. *Meat Science* 67(4):651-67.

Wood J, Whittemore C (2007). Pig Meat and Carcass Quality. In: Whittemore's Science and Practise of Pig Production (pp.4-64). Blackwell Publishing Ltd.

Xi R, Kim TM, Park PJ (2010). Detecting structural variations in the human genome using next generation sequencing. *Briefings in Functional Genomics* 9(5-6):405-15.

Xie C, Tammi MT (2009). CNV-seq, a new method to detect copy number variation using high-throughput sequencing. *BMC Bioinformatics* 10:80.

Xing K, Zhu F, Zhai L, Liu H, Wang Y, Wang Z, *et al.* (2015). Integration of transcriptome and whole genomic resequencing data to identify key genes affecting swine fat deposition. *PLoS One* 10(4):e0122396.

Xing K, Zhu F, Zhai L, Chen S, Tan Z, Sun Y, *et al.* (2016). Identification of genes for controlling swine adipose deposition by integrating transcriptome, whole-genome resequencing, and quantitative trait loci data. *Scientific Reports* 6:23219.

Yang B, Zhang W, Zhang Z, Fan Y, Xie X, Ai H, *et al.* (2013). Genome-wide association analyses for fatty acid composition in porcine muscle and abdominal fat tissues. *PLoS One* 8(6):e65554.

Yoon S, Xuan Z, Makarov V, Ye K, Sebat J (2009). Sensitive and accurate detection of copy number variants using read depth of coverage. *Genome Research* 19(9):1586-92.

Yvert G, Brem RB, Whittle J, Akey JM, Foss E, Smith EN, *et al.* (2003). Trans-acting regulatory variation in Saccharomyces cerevisiae and the role of transcription factors. *Nature Genetics* 35(1):57-64.

Zhang W, Zhang J, Cui L, Ma J, Chen C, Ai H, *et al.* (2016a). Genetic architecture of fatty acid composition in the longissimus dorsi muscle revealed by genome-wide association studies on diverse pig populations. *Genetics Selection Evolution* 48:5.

Zhang W, Bin Yang, Zhang J, Cui L, Ma J, Chen C, *et al.* (2016b). Genome-wide association studies for fatty acid metabolic traits in five divergent pig populations. *Scientific Reports* 6:24718.

Zhao M, Wang Q, Wang Q, Jia P, Zhao Z (2013). Computational tools for copy number variation (CNV) detection using next-generation sequencing data: features and perspectives. *BMC Bioinformatics* 14 Suppl 11:S1.

Zhu M, Yu M, Zhao S (2009). Understanding quantitative genetics in the systems biology era. *International Journal of Biological Sciences* 5(2):161-70.

Annexes

Chapter 7

7.1. Supplementary material Paper I: "New insight into the SSC8 genetic determination of fatty acid composition in pigs"

Paper I. Table S1: List of SNPs genotyped. List of 144 SNPs located on SCC8 genotyped and genotyping statistics.

SNP	Position (bp) in *Sscrofa10.2*	Call Rate	MAF[1]	HWE[2]	Used[3]
ALGA0046149	5 172 632	1.000	0.434	0.7588	Yes
ASGA0037565	5 201 344	1.000	0.405	0.9446	Yes
ALGA0046317	6 295 586	1.000	0.382	0.7487	Yes
ALGA0107380	6 904 797	1.000	0.332	0.0077	Yes
ASGA0037637	7 207 103	0.983	0.403	0.9916	Yes
H3GA0024211	7 517 818	1.000	0.341	0.4600	Yes
ALGA0046233	7 551 522	1.000	0.323	0.3732	Yes
ALGA0046202	7 749 484	0.998	0.311	0.4007	Yes
ASGA0094688	8 840 160	1.000	0.489	0.9624	Yes
M1GA0011801	11 263 172	1.000	0.226	0.5501	Yes
MARC0043725	16 904 240	1.000	0.250	0.5419	Yes
ALGA0046694	17 889 049	0.998	0.301	0.4536	Yes
ASGA0038079	19 500 165	1.000	0.462	0.8768	Yes
DRGA0008376	20 845 249	0.989	0.282	0.6021	Yes
MARC0021747	24 600 093	1.000	0.054	0.5783	No
ALGA0119566	25 020 120	1.000	0.113	0.6745	Yes
DRGA0008477	28 972 036	0.998	0.176	0.3382	Yes
H3GA0024605	30 605 538	1.000	0.414	0.6937	Yes
M1GA0011887	31 525 187	0.998	0.317	0.6920	Yes
ASGA0038470	31 593 446	0.000	0.000	0.0000	No
ALGA0047421	32 984 498	1.000	0.317	0.0587	Yes
MARC0075877	33 365 922	1.000	0.340	0.8151	Yes
ALGA0047564	35 526 849	1.000	0.182	0.0727	Yes
ASGA0096723	37 029 609	1.000	0.429	0.2819	Yes
ALGA0047653	38 715 913	1.000	0.090	0.6344	Yes
ASGA0103358	38 771 285	1.000	0.102	0.5013	Yes
ALGA0047663	38 781 175	1.000	0.376	0.1396	Yes
ALGA0047689	39 851 468	1.000	0.376	0.1656	Yes
DRGA0008696	93 820 555	0.000	0.000	0.0000	No
ALGA0047829	47 560 329	1.000	0.300	0.7381	Yes
ASGA0038791	47 539 360	1.000	0.303	0.6720	Yes
M1GA0011935	47 434 157	0.989	0.305	0.6582	Yes
MARC0093074	50 223 543	0.994	0.099	0.7124	Yes
H3GA0024868	50 479 231	1.000	0.102	0.6594	Yes
DRGA0008588	51 580 681	1.000	0.156	0.1708	Yes
MARC0077695	53 929 233	0.994	0.163	0.1410	Yes

SNP	Position (bp) in *Sscrofa10.2*	Call Rate	MAF[1]	HWE[2]	Used[3]
H3GA0024879	55 749 069	1.000	0.162	0.1449	Yes
ALGA0047923	58 000 986	1.000	0.171	0.1059	Yes
MARC0035425	58 302 878	1.000	0.171	0.1059	Yes
ALGA0047927	58 426 682	1.000	0.245	0.8957	Yes
ALGA0047962	63 000 451	1.000	0.245	0.8957	Yes
ALGA0047982	64 602 131	0.998	0.152	0.1024	Yes
ALGA0048001	66 072 630	1.000	0.152	0.1033	Yes
MARC0000554	67 026 060	1.000	0.152	0.1033	Yes
MARC0050311	67 597 907	0.998	0.341	0.1975	Yes
ALGA0048032	67 669 269	0.000	0.000	0.0000	No
ASGA0092219	76 673 290	0.998	0.170	0.9425	Yes
INRA0029891	72 390 046	0.000	0.000	0.0000	No
MARC0021611	72 567 179	1.000	0.065	0.7347	Yes
MARC0059165	72 678 010	1.000	0.065	0.7347	Yes
MARC0107119	73 117 361	1.000	0.089	0.4728	Yes
CASI0009910	73 108 818	0.998	0.090	0.4714	Yes
ALGA0048092	73 810 886	1.000	0.380	0.4815	Yes
H3GA0024944	74 188 735	1.000	0.248	0.5588	Yes
MARC0043064	74 934 147	1.000	0.394	0.0000	Yes
DIAS0000521	78 168 017	1.000	0.361	0.5717	Yes
ASGA0039041	78 964 955	1.000	0.089	0.4728	Yes
ASGA0101844	81 243 428	0.000	0.000	0.0000	No
ALGA0048355	84 439 484	1.000	0.348	0.2272	Yes
ALGA0048452	89 396 415	1.000	0.437	0.6562	Yes
H3GA0025111	91 556 991	1.000	0.327	0.3770	Yes
ALGA0048513	91 571 647	1.000	0.306	0.2250	Yes
ALGA0048521	91 798 086	1.000	0.278	0.0413	Yes
M1GA0011992	91 991 327	1.000	0.420	0.9994	Yes
ALGA0048544	91 931 519	1.000	0.267	0.0339	Yes
ALGA0113197	92 641 183	1.000	0.480	0.8518	Yes
ASGA0089555	92 715 025	0.957	0.318	0.0214	Yes
H3GA0025137	92 803 868	1.000	0.350	0.3705	Yes
ALGA0048572	92 816 525	1.000	0.398	0.4555	Yes
H3GA0025135	92 870 605	0.957	0.136	0.0004	Yes
ALGA0048583	93 209 866	0.998	0.187	0.3035	Yes
MARC0061487	93 320 380	1.000	0.214	0.3432	Yes
MARC0024098	93 295 329	1.000	0.214	0.3432	Yes
MARC0029000	93 494 016	1.000	0.214	0.3432	Yes
ALGA0115296	93 496 083	1.000	0.214	0.3432	Yes
MARC0005229	93 618 063	1.000	0.216	0.4570	Yes
ALGA0048589	93 655 838	0.998	0.187	0.3035	Yes

SNP	Position (bp) in *Sscrofa10.2*	Call Rate	MAF[1]	HWE[2]	Used[3]
ALGA0048594	93 721 504	1.000	0.190	0.4043	Yes
MARC0020530	93 772 525	1.000	0.217	0.4423	Yes
ALGA0048597	93 787 649	0.998	0.229	0.2447	Yes
ASGA0039312	93 799 252	0.998	0.435	0.7113	Yes
H3GA0025162	93 865 285	1.000	0.268	0.7269	Yes
MARC0097057	94 731 152	0.996	0.471	0.8713	Yes
H3GA0025172	95 696 734	1.000	0.268	0.8946	Yes
ASGA0039343	95 856 199	1.000	0.268	0.8946	Yes
ALGA0048654	96 775 500	1.000	0.273	0.7588	Yes
ASGA0039349	97 708 951	1.000	0.212	0.6158	Yes
ASGA0039362	98 985 483	0.000	0.000	0.0000	No
ALGA0048684	99 240 536	1.000	0.365	0.7535	Yes
ALGA0048697	99 519 250	0.998	0.264	0.8940	Yes
ALGA0048708	99 899 949	1.000	0.273	0.7588	Yes
ALGA0048717	100 629 167	1.000	0.198	0.4690	Yes
MARC0035880	100 725 819	0.985	0.089	0.3327	Yes
ASGA0039382	100 850 517	1.000	0.272	0.8182	Yes
ALGA0048753	103 445 870	1.000	0.000	10,000	No
ALGA0048755	103 584 645	0.998	0.423	0.7924	Yes
FABP2	Unknown	0.983	0.000	10,000	No
H3GA0025264	111 567 232	1.000	0.382	0.6167	Yes
ALGA0049011	112 856 026	0.000	0.000	0.0000	No
ALGA0049074	114 238 093	1.000	0.148	0.0828	Yes
ASGA0039595	117 438 656	1.000	0.270	0.5662	Yes
ALGA0049130	117 485 685	1.000	0.270	0.5662	Yes
ALGA0049122	117 456 463	1.000	0.270	0.5662	Yes
ALGA0049135	117 548 144	0.998	0.271	0.5606	Yes
ALGA0049139	117 666 087	1.000	0.261	0.6645	Yes
ASGA0039614	117 902 625	0.983	0.390	0.7939	Yes
MARC0008579	118 421 256	0.998	0.318	0.8182	Yes
SIRI0000509	119 727 822	1.000	0.269	0.4459	Yes
INRA0030422	119 851 321	1.000	0.269	0.4459	Yes
H3GA0025321	119 887 525	1.000	0.269	0.4459	Yes
DIAS0003532	120 567 215	0.998	0.388	0.4522	Yes
ALGA0049233	120 608 511	1.000	0.419	0.8221	Yes
ASGA0039670	121 038 694	1.000	0.267	0.6239	Yes
ALGA0049249	120 972 820	0.981	0.303	0.7412	Yes
ALGA0049254	120 996 107	0.998	0.307	0.8245	Yes
MARC0069612	122 226 942	1.000	0.024	0.8103	No
ALGA0049276	122 249 328	1.000	0.087	0.3407	Yes
MARC0037703	122 288 920	1.000	0.424	0.5606	Yes

SNP	Position (bp) in *Sscrofa10.2*	Call Rate	MAF[1]	HWE[2]	Used[3]
MARC0022520	124 248 464	1.000	0.184	0.0913	Yes
MARC0023377	124 214 989	1.000	0.431	0.5878	Yes
MARC0087394	127 777 989	0.998	0.208	0.1445	Yes
ALGA0049404	128 842 533	1.000	0.253	0.7247	Yes
MTTP	Unknown	0.998	0.390	0.7473	Yes
ASGA0039821	130 710 470	0.998	0.431	0.6636	Yes
ALGA0107284	131 690 829	1.000	0.284	0.1453	Yes
ASGA0092434	135 960 757	1.000	0.263	0.6249	Yes
MARC0052565	137 114 772	1.000	0.216	0.0455	Yes
ALGA0120603	139 458 060	1.000	0.265	0.0003	Yes
MARC0073511	140 966 269	1.000	0.305	0.1987	Yes
ALGA0106925	142 232 561	1.000	0.211	0.1649	Yes
ASGA0040343	143 633 633	0.998	0.437	0.4669	Yes
ALGA0050117	144 383 303	1.000	0.402	0.3302	Yes
ASGA0102835	145 098 780	1.000	0.317	0.9815	Yes
ALGA0050175	145 451 027	1.000	0.185	0.8995	Yes
MARC0054376	145 853 404	1.000	0.328	0.1119	Yes
ALGA0107742	146 341 093	1.000	0.434	0.0752	Yes
ALGA0050227	146 293 844	1.000	0.313	0.1665	Yes
MARC0073087	146 413 339	1.000	0.433	0.0814	Yes
MARC0072304	146 423 420	1.000	0.433	0.0814	Yes
ALGA0122878	146 829 727	0.996	0.420	0.1477	Yes
MARC0011508	147 363 214	1.000	0.437	0.2665	Yes
H3GA0025831	147 385 039	1.000	0.438	0.2508	Yes
DRGA0009028	147 583 976	1.000	0.422	0.3020	Yes
MARC0042613	147 800 024	0.998	0.446	0.0822	Yes

[1]MAF= Minor Allele Frequency
[2]HWE= *p*-value of the Hardy-Weinberg Equilibrium test calculated by GenomeStudio software (*Illumina*)
[3]Used= Used in association analyses

Paper I. Table S2: Primers for SETD7 and MAML3 promoter sequencing (P), promoter and exon 1 sequencing (PE), microsatellite study (MS), and RT-qPCR (RT) study.

Gene[1]	Primer	Sequence	Amplicon length (bp)	Tm	[$MgCl_2$]
SETD7	SETD7-Fw1 (P)	5'-ACAACTTTCTCTTGCTCCCTTCTA-3'	473	62ºC	1.5mM
SETD7	SETD7-Rv1 (P)	5'-ATTCAGAAATTCACCAGATCCAAA-3'			
SETD7	SETD7-Fw2 (PE)	5'-GTTCCTTTTCCGTTACCACAAC-3'	478	62ºC	1.5mM
SETD7	SETD7-Rv2 (PE)	5'-GCTCAGAACTCCCGACCTC-3'			
SETD7	SETD7-Fw (RT)	5'-TGCTGGATATACTACCCAGATGGA-3'	71	60ºC	np
SETD7	SETD7-Rv (RT)	5'-TCTCCTGTCATCTCCCCATCTT-3'			
MAML3	MAML3-Fw1 (P)	5'-GTACCGCGCATTAAATAATATTCC-3'	517	56ºC	2.5mM
MAML3	MAML3-Rv1 (P)	5'-GCCAGAAAACAGAGAAAGAAAGAT-3'			
MAML3	MAML3-Fw2 (PE)	5'-TGTATAACAACAACTTGGGCTCTC-3'	663	58ºC	*GC-Rich PCR System
MAML3	MAML3-Rv2 (PE)	5'-GACTGCAAAAGTAGATCGGTGA -3'			
MAML3	MAML3_HEX-Fw (MS)	5'- TGTATAACAACAACTTGGGCTCTC-3'	249	58ºC	2.5mM
MAML3	MAML3-Rv1 (MS)	5'-GCCAGAAAACAGAGAAAGAAAGAT-3'			
MAML3	MAML3_FAM-Fw (MS)	5'-GCTGCCGTGTTTACTGAGCT-3'	135	58ºC	2.5mM
MAML3	MAML3-Rv3 (MS)	5'-ACCATCACAATGATCAACTGCT-3'			
MAML3	MAML3-Fw (RT)	5'-GGTCAACCAGTTTCAAGGGTCT-3'	102	60ºC	np
MAML3	MAML3-Rv (RT)	5'-CCTGCATTCTGTGCCATCAA-3'			
ACTB	ACTB-Fw (RT)	5'-CAAGGACCTCTACGCCAACAC-3'	130	60ºC	np
ACTB	ACTB-Rv (RT)	5'-TGGAGGCGCGATGATCTT-3'			
B2M	B2M-Fw (RT)	5'-ACCTTCTGGTCCACACTGAGTTC-3'	108	60ºC	np
B2M	B2M-Rv (RT)	5'-GGTCTCGATCCCACTTAACTATCTTG-3'			
HPRT1	HPRT1-Fw (RT)	5'-TCATTATGCCGAGGATTTGGA-3'	91	60ºC	np
HPRT1	HPRT1-Rv (RT)	5'-CTCTTTCATCACATCTCGAGCAA-3'			
TBP	TBP-Fw (RT)	5'-CAGAATGATCAAACCGAGAATTGT-3'	80	60ºC	np
TBP	TBP-Rv (RT)	5'-CTGCTCTGACTTTAGCACCTGTTAA-3'			

[1]The genes analyzed were: SET domain containing lysine methyltransferase 7 (*SETD7*) and mastermind-like 3 (*MAML3*).
np: not provided by the manufacturer.

Paper I. Table S3: Significant SNPs affecting BF FA composition (FDR=0.05) in LDLA analyses in the F_2 generation.

Trait	Chromosomal region (Mb)	SNP	LR	*P*-value	*a* (SE)
C16:1(n-7)	93.87	H3GA0025162	35.9228	2.05E-09	0.164 (0.085)
	119.85[1]	INRA0030422	45.4291	1.58E-11	0.223 (0.082)
ACL	93.72	ALGA0048594	40.5341	1.93E-10	-0.020 (0.001)
	117.66	ALGA0049139	45.2997	1.69E-11	-0.021 (0.001)
C18:0/C16:0	93.87	H3GA0025162	39.8781	2.70E-10	-0.022 (0.002)
	119.73	SIRI0000509	55.9362	7.48E-14	-0.032 (0.002)
C18:1(n-7)/ C16:1(n-7)	93.87	H3GA0025162	35.4047	2.68E-09	-0.058 (0.016)
	117.66	ALGA0049139	46.6404	8.53E-12	-0.088 (0.015)

LR. Likehood ratio test values; *a* (SE): additive effect (standard error).
[1]SNP H3GA0025321 (119.89 Mb) showed the same *P*-value.

Paper I. Table S4: Analysis of a two QTL model on SCC8 for the most significant regions affecting BF FA composition.

Trait	Chromosomal region (Mb)	SNP	LR	*P*-value
C14:0	91.57	ALGA0048513	21.0699	4.43E-06
	117.66	ALGA0049139		
C16:0	91.57	ALGA0048513	47.4716	5.58E-12
	117.66	ALGA0049139		
C18:0	91.56	H3GA0025111	19.1441	1.21E-05
	119.73	SIRI0000509		
C16:1(n-7)	91.56	H3GA0025111	68.9761	1.11E-16
	119.73	SIRI0000509		
C18:1(n-9)	91.57	ALGA0048513	35.9079	2.07E-09
	117.66	ALGA0049139		
C20:2(n-6)	91.56	H3GA0025111	23.3687	1.34E-06
	117.55	ALGA0049135		
ACL	91.57	ALGA0048513	69.2893	1.11E-16
	117.66	ALGA0049139		
C16:1(n-7)/C16:0	91.57	H3GA0025111	37.5734	8.80E-10
	119.73	SIRI0000509		
C18:0/C16:0	91.56	H3GA0025111	66.7598	3.33E-16
	119.73	SIRI0000509		
C18:1(n-7)/C16:1(n-7)	91.57	ALGA0048513	66.3888	3.33E-16
	119.73	SIRI0000509		

LR. Likehood ratio test values.

Paper I. Table S5: Additive value affecting BF FA composition in 168 F_2 animals for the *SETD7:c.700G>T* and *ELOVL6:c.533C>T* SNPs.

Trait	***SETD7:c.700G>T***	***ELOVL6:c.533C>T***
C16:0	0.421	0.652
C16:1(n-7)	0.169	0.221
C18:1(n-9)	-0.465	-0.714
C18:1(n-7)	0.068	0.081
ACL	-0.015	-0.022
MUFA	-0.266	-0.457
C16:1(n-7)/C16:0	0.006	0.007
C18:0/C16:0	-0.022	-0.032
C18:1(n-7)/C16:1(n-7)	-0.062	-0.101
C20:2(n-6)/C18:2(n-6)	-0.003	-0.005

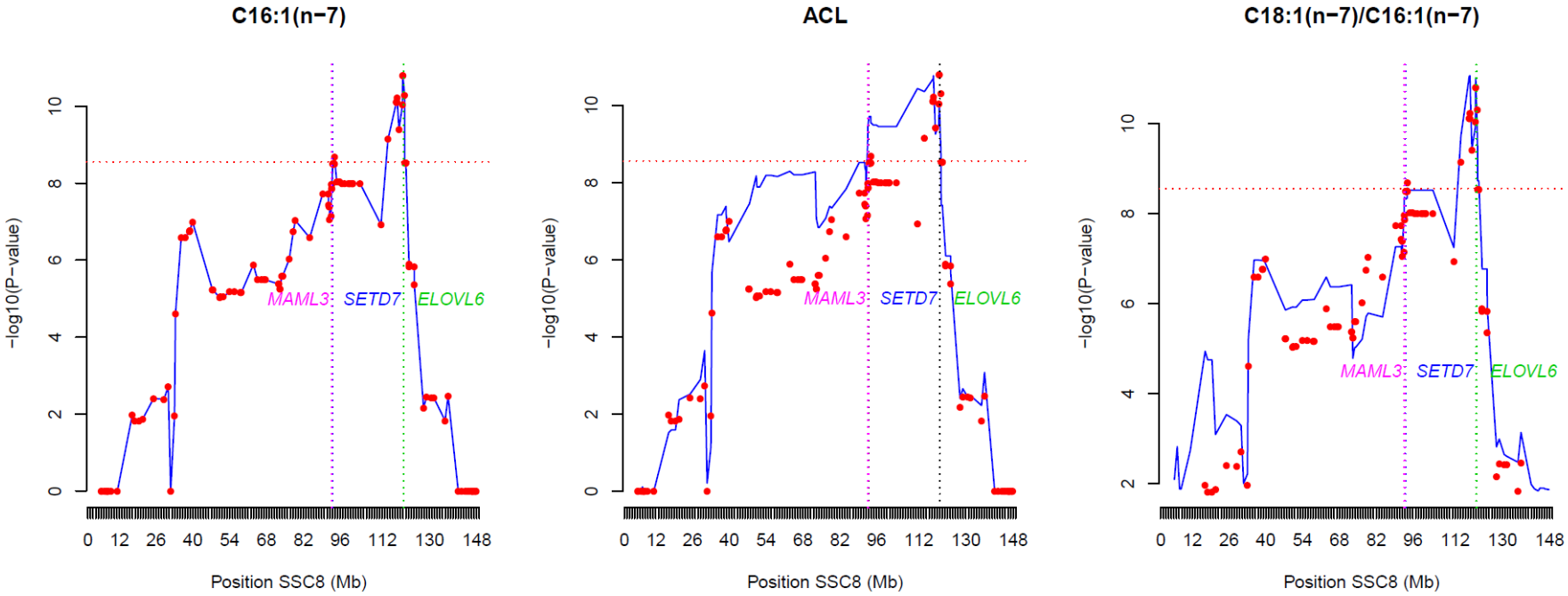

Paper I. Figure S1: Association study and LDLA of the C16:1(n-7), ACL and C18:1(n-7)/C16:1(n-7) elongation ratio in BF. Plot of association study (red points) and LDLA patterns (blue line) for palmitoleic acid, ACL and vaccenic/palmitoleic ratio; the X-axis represents positions in Mb on SSC8, and the Y-axis shows the –log10 (*p*-value); vertical, the pink line represents the position of the *MAML3* gene, the blue line represents the position of the *SETD7* gene and the green line represents the position of the *ELOVL6* gene on SSC8; horizontal, dashed lines mark the association study significance level (FDR-based *q*-value ≤ 0.05); positions in Mb are relative to the *Sscrofa10.2* assembly of the pig genome.

7.2. Supplementary material Paper II: "A global analysis of CNVs in swine using whole genome sequence data and association analysis with fatty acid composition and growth traits"

Paper II. Table S1: Primers used for qPCR assays.

CNVR ID	Chr	Gene	No. of tested animals	Forward primer (5'-3')	Reverse primer (5'-3')
112	3	*GPAT2*	182	AGGTTTGGTCCTTTCATCCTTTG	GGTCCACTCCTGCTCCTTCTC
92	4	*CLCA4*	182	AGCACGGCAACAGGTAAAATG	TGAGTTGTCTGTCGCCCTGTAC
125	6	*CYP4X1*	182	ATCCTGGGTGACGGGTCTTC	AAAATCCCGTGGAGCAAACTT
198	6	*PLA2G2A*	32	CCTGCTATTGGCAGTGATCATG	GCTTCCCTCCCTGCACTGT
160	9	*MOGAT2*	182	CTGGGTCTTGGAACTTTCTAAACAC	GAGTGCCTAATTCTTCACCATAAGC
217	14	*PRKG1*	32	GGCATGAACATTCGTCAAATCTC	AGACAGCTGCAATCTCACTAAAGC
Control	15	*GCG*	-	AACATTGCCAAACGTCACGATG	GCCTTCCTCGGCCTTTCA

Paper II. Table S2: Duplication and deletion calls predicted by Control-FREEC software from all seven pigs. (too large to be attached, not included in the present thesis).

See table at:
https://doi.org/10.1371/journal.pone.0177014.s006 (XLSX)

Paper II. Table S3: Information of 540 identified CNVRs and gene annotation within the CNVRs retrieved from the Ensembl Genes 84 Database using the Biomart data management system. (too large to be attached, not included in the present thesis).

See table at:
https://doi.org/10.1371/journal.pone.0177014.s007 (XLSX)

Paper II. Table S4: Pathway analysis of genes identified in CNVRs. (too large to be attached, not included in the present thesis).

See table at:
https://doi.org/10.1371/journal.pone.0177014.s008 (XLSX)

Paper II. Table S5: Association analysis between CNVRs and different phenotypic records in BC1_LD animals. (too large to be attached, not included in the present thesis).

See table at:
https://doi.org/10.1371/journal.pone.0177014.s009 (XLSX)

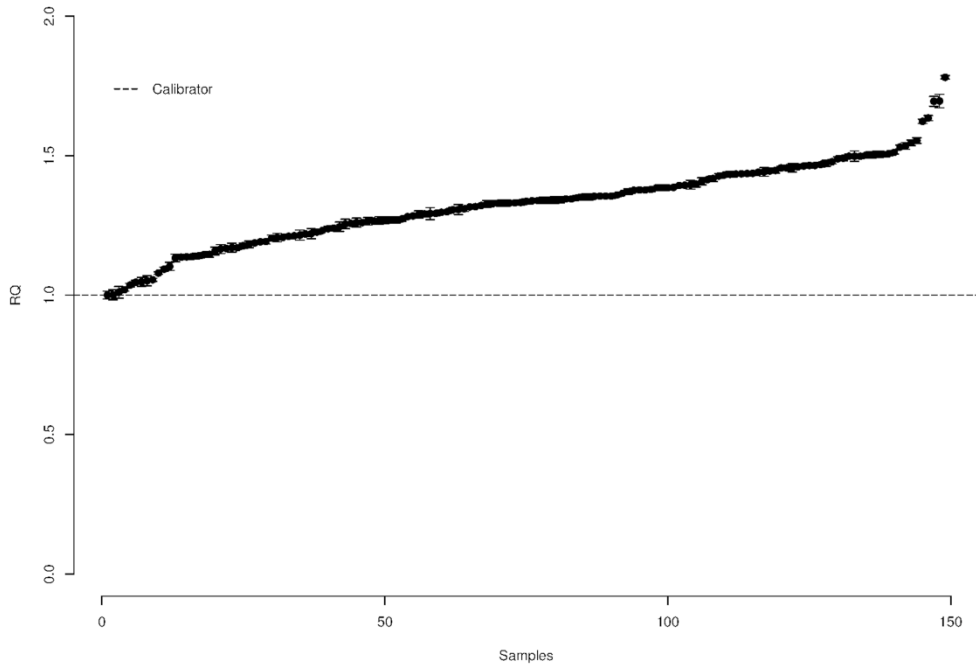

Paper II. Figure S1: Analysis by qPCR of CNVR112 (*GPAT2*). The y-axis represents the RQ quantitative measurement by qPCR for each sample and the x-axis shows the different samples. The baseline represents the calibrator.

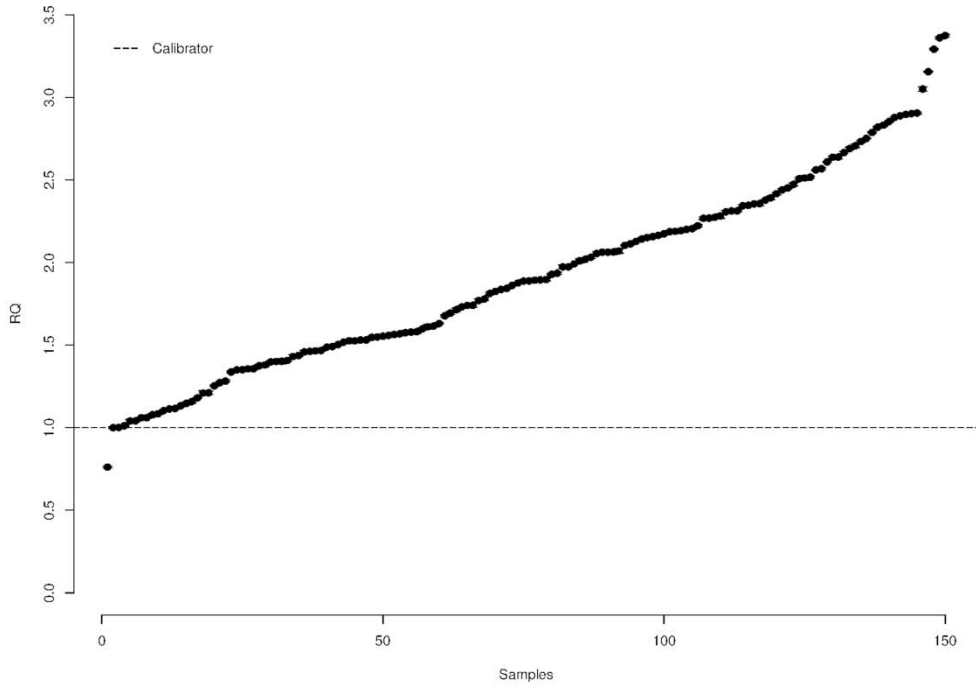

Paper II. Figure S2: Analysis by qPCR of CNVR157 (*CLCA4*). The y-axis represents the RQ quantitative measurement by qPCR for each sample and the x-axis shows the different samples. The baseline represents the calibrator.

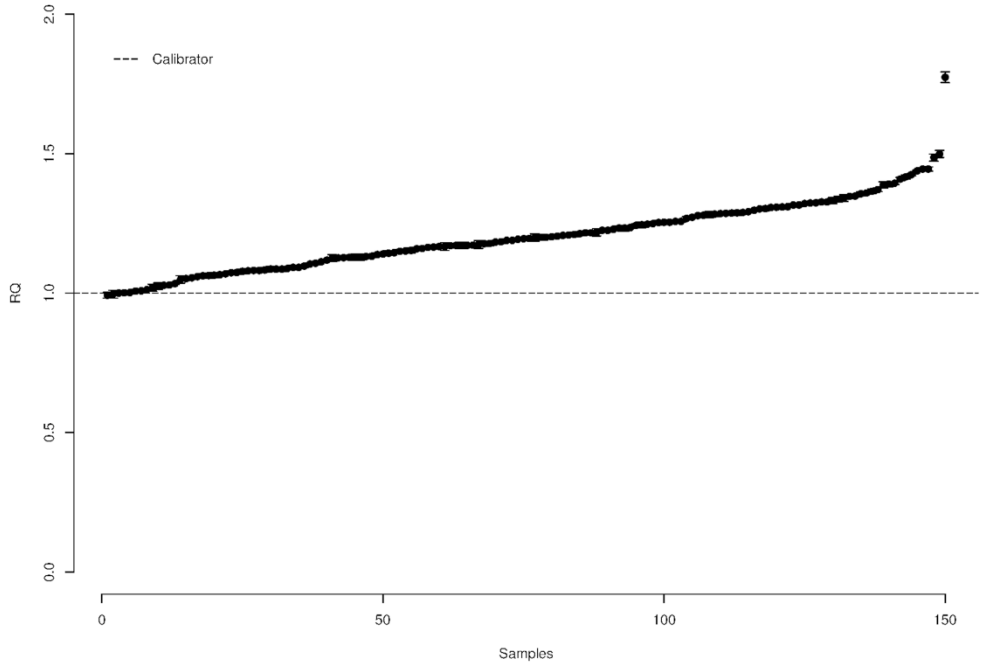

Paper II. Figure S3: Analysis by qPCR of CNVR298 (*MOGAT2*). The y-axis represents the RQ quantitative measurement by qPCR for each sample and the x-axis shows the different samples. The baseline represents the calibrator.

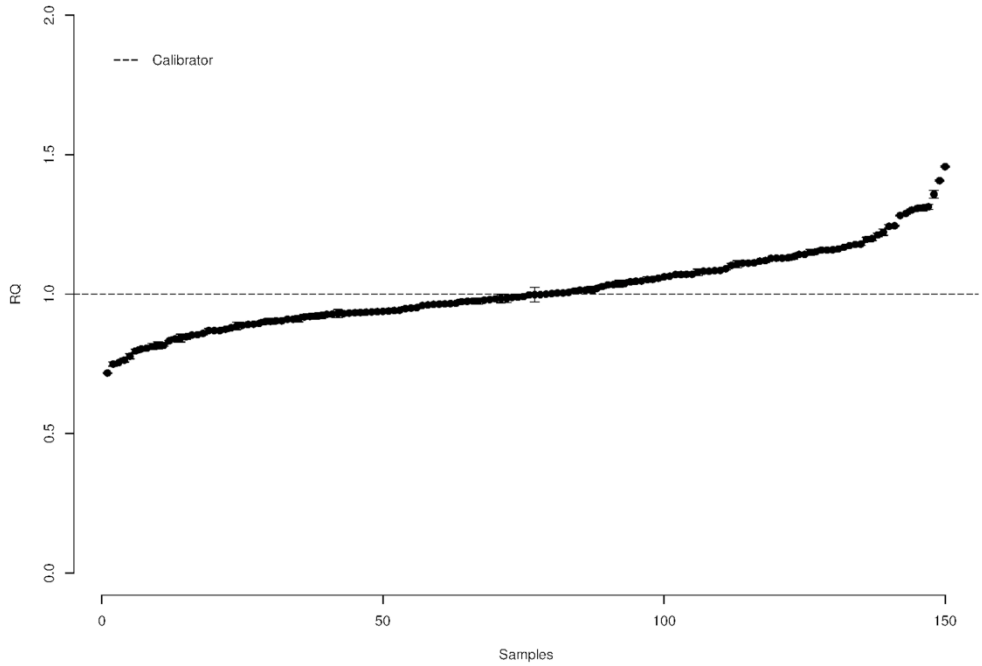

Paper II. Figure S4: Analysis by qPCR of CNVR447 (*PRKG1*). The y-axis represents the RQ quantitative measurement by qPCR for each sample and the x-axis shows the different samples. The baseline represents the calibrator.

7.3. Supplementary material Paper III: "Expression analysis in adipose tissue of candidate genes for fatty acid composition and identification of eGWAS regions"

Paper III. Table S1: Primers used for the characterization of the 3'UTR of porcine *FABP4* gene.

Gene	Full name	Primer Name	Type	Primer Sequence[1]
FABP4	*Fatty acid binding protein 4*	oligo(dT)-UAP	mRNA 3' UTR amplification	5'-GGCCACGCGTCGACTAGTAC(T)30VN-3'
FABP4	*Fatty acid binding protein 4*	UAP	mRNA 3' UTR amplification	5'-GGCCACGCGTCGACTAGTAC-3'
FABP4	*Fatty acid binding protein 4*	FABP4-3NC-1-Fw	mRNA 3' UTR sequencing	5'-TTGGATCGAACTCTACAACACTCTG-3'
FABP4	*Fatty acid binding protein 4*	FABP4-3NC-2-Fw	mRNA 3' UTR sequencing	5'-TGTTTATGGATCTTCCATTATCTTAGG-3'

[1]Primers were designed from the GenBank Y16039 sequence

Paper III. Table S2: Primers used for the analyses of gene-expression of the 48 genes by real-time PCR.

Gene	Full name	Type	Primer sequence	
			Forward	Reverse
ACSM5	Acyl-CoA synthetase medium-chain family member 5	Target	5'-TGTAATCTGTGCCAATCCCAAA-3'	5'-CATCATCTACGATCTGCACCTCAT-3'
ACTB	Actin, Beta	Reference	5'-CAAGGACCTCTACGCCAACAC-3'	5'-TGGAGGCGCGATGATCTT-3'
ADIPOQ	Adiponectin, C1Q and collagen domain containing	Target	5'-GTACCCCAGGCCGTGATG-3'	5'- CCCTTAGGACCAGTAAGACCTGTATCT-3'
AGPAT2	1-acylglycerol-3-phosphate O-acyltransferase 2	Target	5'-CATGGTCAGGGAGAAGCTCAA-3'	5'-GCCAGGTAGAAGGCACCTTTC-3'
ANK2	Ankyrin 2	Target	5'-GTGGATTCTGCTACGAAGAAAGG-3'	5'-AAGGACTTTGACAACTTCTGCTTGT-3'
ARNT	Aryl hydrocarbon receptor nuclear translocator	Target	5'-TCTAATGATAAGGAGCGGTTTGC-3'	5'-TATGATTTTCCCTGGCGAGTCT-3'
B2M	Beta-2-microglobulin	Reference	5'- ACCTTCTGGTCCACACTGAGTTC-3'	5'- GGTCTCGATCCCACTTAACTATCTTG-3'
CD36	CD36 molecule	Target	5'-GGTCCTTACACGTACAGAGTTCGTT-3'	5'-CCATTGGGCTGTAGGAAAGAGA-3'
CPT1A	Carnitine palmitoyltransferase 1A	Target	5'-CCTGAAGGTGCTGCTCTCCTA-3'	5'-CTCACCATCATCATCCAGATCTTG-3'
CROT	Carnitine O-octanoyltransferase	Target	5'-GGGAAACGAAATTGGTTGGA-3'	5'-CGCAAAGTTGACATTCAGTTGTG-3'
CYP2U1	Cytochrome P450, family 2, subfamily U, member 1	Target	5'-AGAGAAAACAGTGCTCCAAGGGTAT-3'	5'-TGGCTGGGTCTCTGTGTACTGA-3'
DGAT1	Diacylglycerol O-acyltransferase 1	Target	5'-CCTGAATTGGTGTGTGGTCATG-3'	5'-GATGCCGTACTTGATGAGGTTCTC-3'
DGAT2	Diacylglycerol O-acyltransferase 2	Target	5'-GGAACACGCCCAAGAAAGGT-3'	5'-GGATGGGAAAGTAGTCTCGAAAGTAG-3'
EGF	Epidermal growth factor	Target	5'-AACGGGAATGCCACTTGTGT-3'	5'-CCTTCCAAGTCAATCCTAAAGATACTG-3'
ELOVL5	ELOVL fatty acid elongase 5	Target	5'-CCTCTCGGCTGGCTGTACTT-3'	5'-CCTTCTTGTTGTAGGTCTGGATGTAG-3'
ELOVL6	ELOVL fatty acid elongase 6	Target	5'-AGCAGTTCAACGAGAACGAAGCC-3'	5'-TGCCGACCGCCAAAGATAAAG-3'
ESRRA	Estrogen-related receptor alpha	Target	5'-CAAGAGCATCCCAGGCTTCTC-3'	5'-CACCCAACACCAATACCTCCAT-3'
FABP4	Fatty acid binding protein 4	Target	5'-TAAGTTGGTGGTGGAATGTATCATG-3'	5'-AGAGTGTTGTAGAGTTCGATCCAAAC-3'
FABP5	Fatty acid binding protein 5	Target	5'-CCAATGGAGAATTGGTTCAACA-3'	5'-GTTCATGACGCATACCACCACTA-3'
FADS1	Fatty acid desaturase 1	Target	5'-CCTTGTGAGGAAGTATATGAGCTCTCT-3'	5'-TCATCTGTCAGCTCTTTATTCTTAGTCG-3'
FADS2	Fatty acid desaturase 2	Target	5'-TCCACCGCGACCTTGATTTA-3'	5'-TCGGTGATCTCAGAGTTCTTGGT-3'
FADS3	Fatty acid desaturase 3	Target	5'-CCAGCACCTCTACTTCTTCCTGAT-3'	5'-CATGTATGCCAGATTTTCCACTTC-3'
HPRT1	Hypoxanthine phosphoribosyltransferase 1	Reference	5'- TCATTATGCCGAGGATTTGGA-3'	5'- CTCTTTCATCACATCTCGAGCAA-3'
LIPC	Lipase C, hepatic type	Target	5'- CGTTACAGCAGTGTGGCTTCA-3'	5'- CCAGCAAGCCATCCATCAA-3'

Gene	Full name	Type	Primer sequence	
			Forward	Reverse
LPIN1	Lipin 1	Target	5'- CCGAGAGAAGGTGGTGGACAT-3'	5'- CTCTCCATTGTCTCCCAGTTTCA-3'
MGLL	Monoglyceride lipase	Target	5'-GTGTTCGCCCACGACCAT-3'	5'-CCTGACGAACACCTGGAAGTC-3'
MLXIPL	MLX Interacting Protein-Like	Target	5'-CCCAAGTGGAAGAATTTCAAAGG-3'	5'-CTTCCTCCGCTCCACATACTG-3'
NFKB1	Nuclear factor kappa B subunit 1	Target	5'-CCCACAGACGTTCATAGACAATTT-3'	5'-GAGGCTGGTTTTGTAATGTTGACA-3'
NR1H3	Nuclear Receptor Subfamily 1, Group H, Member 3	Target	5'-CTGGGCATGATCGAGAAGCT-3'	5'-TGGGCCAAGGCGTGACT-3'
PEX2	Peroxisomal biogenesis factor 2	Target	5'-CTCAGACTCCTAAGAAACCTTCAGAGA-3'	5'-ACTGATTCTGAGCACTCTGTTTGC-3'
PLA2G12A	Phospholipase A2, group XIIA	Target	5'-CCCACTCTTTGGTGTTCATCTTAA-3'	5'-ATAGCACCTGTCGTGCTGGTT-3'
PLCB2	Phospholipase C, beta 2	Target	5'- AGATCTTCACTTCCTACCACTCCAA-3'	5'- GCGCTGTTTCTGGTTGATGA-3'
PLPP1	Phospholipid phosphatase 1	Target	5'-GGCCACTCTTCATTCTCCATGTAC-3'	5'-AGGCCCACGTAAATGGATACAG-3'
PNPLA2	Patatin-like phospholipase domain containing 2	Target	5'-CTTCACCGTCCGCTTGCT-3'	5'-GCATCACCAGGTACTGGCAGAT-3'
POU2F1	POU class 2 homeobox 1	Target	5'- CCCATACAGATCGCACAGGAT-3'	5'- GATGATAAACTGTGCTGGTTGCA-3'
PPARA	Peroxisome proliferator-activated receptor alpha	Target	5'-GGCACTGAACATCGAATGTAGAATC-3'	5'-CCGAAAGAAGCCCTTGCAA-3'
PPARD	Peroxisome proliferator-activated receptor delta	Target	5'-GCATGTCTCA CAACGCCATT-3'	5'-GCTGACTCCCCTCGTTTGC-3'
PPARG	Peroxisome proliferator-activated receptor gamma	Target	5'-TTGTGAAGGATGCAAGGGTTT-3'	5'-ATCCGACAGTTAAGATCGCACCTA-3'
PPARGC1A	Peroxisome proliferator-activated receptor gamma, coactivator 1 alpha	Target	5'-CTCTGGAACTGCAGGCCTAA-3'	5'-TGGAGAAGCCCTAAAAGGGTTAT-3'
RBP4	Retinol binding protein 4	Target	5'-GGGTCGAGTCCGTCTTTTAAATAACT-3'	5'-GGTCCTCGGTGTCTGTAAAGGT-3'
RXRG	Retinoid X receptor, gamma	Target	5'-GAGGATTCTGGAAGCTGAACTTG-3'	5'-TCATTCGTCGAATTCTCCATGT-3'
SCAP	SREBF chaperone	Target	5'- AGATATCTCAGGCCTTCTACAACCA-3'	5'- AGTTTCAACAGTGGGTAGCAGC-3'
SCD	Stearoyl-CoA Desaturase	Target	5'- GGTGATGTTCCAGAGGAGGTACTAC-3'	5'- CAGCAATACCAGGGCACGAT-3'
SLC27A1	Solute carrier family 27, member 1	Target	5'-TCACTCGGCAGGGAACATC-3'	5'-CGGCTGGCTGAAAACTTCTT-3'
SLC27A4	Solute carrier family 27, member 4	Target	5'-GCTGCATAAAACAGGGACTTTCA-3'	5'-AACAGCGGGTCTTTCACGACT-3'
SREBF1	Sterol Regulatory Element Binding Transcription Factor 1	Target	5'-CACGGAGGCGAAGCTGAATA-3'	5'-GCTTCTGGTTGCTCTGCTGAA-3'
TBP	TATA-Box Binding Protein	Reference	5'-CAGAATGATCAAACCGAGAATTGT-3'	5'-CTGCTCTGACTTTAGCACCTGTTAA-3'
USF1	Upstream transcription factor 1	Target	5'- CCCTTATTCCCCGAAGTCAGA-3'	5'- GCGGCGTTCCACTTCATTAT-3'

Paper III. Table S3: List of 44 lipid-related genes selected to study their expression in the present study. The overlapping between categories is labelled by colors.

Description	Article	Genes
Candidate functional and positional genes identified in a GWAS study for intramuscular FA composition in the BC1_LD backcross	Ramayo-Caldas *et al.*, 2012	*ARNT*, *CYP2U1*, *EGF*, *ELOVL6*, *FABP4*, *FABP5*, *FADS1*, *FADS2*, *FADS3*, *NFKB1*, *PLA2G12A*, *PLCB2*, *PLPP1*, and *USF1*
Genes differentially expressed by RNA-Seq in the adipose tissue of two phenotypically extreme groups of animals for intramuscular FA composition in the BC1_LD backcross	Corominas *et al.*, 2013a	*ELOVL6* and *SCD*
Candidate positional gene affecting palmitic and palmitoleic FA in pigs	Corominas *et al.*, 2013b	*ELOVL6*
Genes related to lipid metabolism identified in gene co-association networks for FA composition in the BC1_LD backcross	Ramayo-Caldas *et al.*, 2014	*ACSM5*, *ANK2*, *ARNT*, *FABP4*, *FABP5*, *MGLL*, and *PPARG*
Genes related to lipid metabolism identified in gene co-association networks for fatness and growth related traits in the IBMAP cross	Puig-Oliveras *et al.*, 2014	*ARNT* and *PPARG*
Candidate positional genes identified in a GWAS study for backfat FA composition in the BC1_LD backcross	Ballester *et al.*, 2016	*FADS1*, *FADS2*, and *FADS3*
Transporters involved in lipid metabolism		*RBP4*, *SCAP*, *SLC27A1*, and *SLC27A4*
Enzymes involved in lipid metabolism		*AGPAT2*, *CPT1A*, *CROT*, *DGAT1*, *DGAT2*, *ELOVL5*, *LIPC*, *LPIN1*, *PEX2*, and *PNPLA2*
Transcriptional factors, cofactors or nuclear receptors involved in lipid metabolism		*ADIPOQ*, *CD36*, *ESRRA*, *MLXIPL*, *NR1H3*, *POU2F1*, *PPARA*, *PPARD*, *PPARGC1A*, *RXRG*, and *SREBF1*
Adipokine of white fat tissue	Shehzad *et al.*, 2012	*ADIPOQ*

Paper III. Table S4: Description of the 193 significant expression-associated SNPs (eSNPs).

Interval	Chr	SNP	Position (bp)	fA1	fA2	*p*-value	*q*-value	Associated Gene	Consequence	Ensembl_GeneId	Gene Id	*Cis/Trans*-eSNPs
I1	2	ASGA0093797	134992155	0.94	0.06	1.55E-06	5.48E-04	*ACSM5*	intergenic	-	-	*trans*
I2	3	ASGA0089930	16473829	0.74	0.26	4.45E-06	1.30E-03	*ACSM5*	intergenic	-	-	*trans*
I2	3	H3GA0053939	18724340	0.90	0.10	3.75E-06	1.17E-03	*ACSM5*	intronic	ENSSSCG00000007804	*SH2B1*	*trans*
I2	3	ASGA0101457	18742778	0.90	0.10	3.03E-07	1.22E-04	*ACSM5*	intronic	ENSSSCG00000007805	*ATP2A1*	*trans*
I2	3	ALGA0112844	19373384	0.67	0.33	3.66E-08	1.84E-05	*ACSM5*	intronic	ENSSSCG00000022785	*GSG1L*	*trans*
I2	3	ASGA0098276	21286903	0.82	0.18	1.69E-14	1.70E-11	*ACSM5*	intergenic	-	-	*cis*
I2	3	ALGA0017974	21309417	0.77	0.23	1.22E-15	1.51E-12	*ACSM5*	intergenic	-	-	*cis*
I2	3	ASGA0013836	21387300	0.77	0.23	6.97E-10	4.76E-07	*ACSM5*	intergenic	-	-	*cis*
I2	3	ALGA0017987	21528275	0.53	0.47	2.68E-05	6.75E-03	*ACSM5*	intergenic	-	-	*cis*
I2	3	ASGA0013852	21562254	0.73	0.27	5.69E-08	2.79E-05	*ACSM5*	intergenic	-	-	*cis*
I2	3	ALGA0123606	21777886	0.63	0.37	7.13E-11	5.66E-08	*ACSM5*	intergenic	-	-	*cis*
I2	3	ASGA0089383	22771385	0.50	0.50	1.19E-10	8.93E-08	*ACSM5*	intronic	ENSSSCG00000007831	*CACNG3*	*cis*
I2	3	MARC0101247	22772065	0.88	0.12	1.96E-06	6.52E-04	*ACSM5*	intronic	ENSSSCG00000007831	*CACNG3*	*cis*
I2	3	ASGA0094123	22794781	0.84	0.16	7.97E-06	2.23E-03	*ACSM5*	intronic	ENSSSCG00000007831	*CACNG3*	*cis*
I2	3	ALGA0018006	23015607	0.70	0.30	1.08E-07	4.86E-05	*ACSM5*	intergenic	-	-	*cis*
I2	3	ALGA0018040	23224453	0.66	0.34	3.33E-16	4.39E-13	*ACSM5*	intergenic	-	-	*cis*
I2	3	ASGA0098738	23442184	0.73	0.27	1.11E-17	1.57E-14	*ACSM5*	downstream	ENSSSCG00000007836	*SCNN1G*	*cis*
I2	3	ALGA0103397	23522898	0.73	0.27	1.11E-17	1.57E-14	*ACSM5*	upstream	ENSSSCG00000030424	-	*cis*
I2	3	ALGA0123533	23592793	0.60	0.40	7.20E-11	5.66E-08	*ACSM5*	intergenic	-	-	*cis*
I2	3	MARC0041570	23603118	0.73	0.27	1.11E-17	1.57E-14	*ACSM5*	downstream	ENSSSCG00000026544	*USP31*	*cis*
I2	3	ASGA0093175	23778733	0.80	0.20	1.11E-17	1.57E-14	*ACSM5*	intronic	ENSSSCG00000007837	*HS3ST2*	*cis*
I2	3	MARC0003844	23802761	0.80	0.20	1.11E-17	1.57E-14	*ACSM5*	intronic	ENSSSCG00000007837	*HS3ST2*	*cis*
I2	3	MARC0047020	23961903	0.73	0.27	1.11E-17	1.57E-14	*ACSM5*	intergenic	-	-	*cis*

Interval	Chr	SNP	Position (bp)	fA1	fA2	*p*-value	*q*-value	Associated Gene	Consequence	Ensembl_GeneId	Gene Id	*Cis/Trans*-eSNPs
I2	3	ASGA0103399	24010664	0.75	0.25	1.11E-17	1.57E-14	*ACSM5*	downstream	ENSSSCG00000007838	*OTOA*	*cis*
I2	3	ALGA0112358	24025177	0.80	0.20	4.93E-11	4.10E-08	*ACSM5*	intronic	ENSSSCG00000007838	*OTOA*	*cis*
I2	3	ALGA0123020	24042892	0.78	0.22	7.14E-13	6.50E-10	*ACSM5*	intronic	ENSSSCG00000007838	*OTOA*	*cis*
I2	3	ASGA0094818	24086731	0.33	0.67	2.69E-05	6.75E-03	*ACSM5*	intergenic	-	-	*cis*
I2	3	ALGA0115152	24218664	0.53	0.47	2.08E-07	8.84E-05	*ACSM5*	intergenic	-	-	*cis*
I2	3	ASGA0094620	24288043	0.71	0.29	2.22E-15	2.43E-12	*ACSM5*	3_prime_UTR_variant	ENSSSCG00000007839	*EEF2K*	*cis*
I2	3	ASGA0089883	24297157	0.71	0.29	2.22E-15	2.43E-12	*ACSM5*	intronic	ENSSSCG00000007839	*EEF2K*	*cis*
I2	3	ASGA0099261	24299990	0.84	0.16	6.93E-14	6.47E-11	*ACSM5*	intronic	ENSSSCG00000007839	*EEF2K*	*cis*
I2	3	ALGA0103433	24365103	0.40	0.60	4.04E-05	9.20E-03	*ACSM5*	intronic	ENSSSCG00000007839	*EEF2K*	*cis*
I2	3	MARC0006151	24387052	0.47	0.53	2.70E-05	6.75E-03	*ACSM5*	intronic	ENSSSCG00000007839	*EEF2K*	*cis*
I2	3	ASGA0101242	24418411	0.77	0.23	1.11E-17	1.57E-14	*ACSM5*	downstream	ENSSSCG00000007842	*SDR42E2*	*cis*
I2	3	ASGA0013894	24602938	0.53	0.47	4.46E-08	2.22E-05	*ACSM5*	upstream	ENSSSCG00000027510	-	*cis*
I2	3	MARC0110831	25162049	0.84	0.16	6.93E-14	6.47E-11	*ACSM5*	intronic	ENSSSCG00000007847	-	*cis*
I2	3	MARC0115165	25531453	0.80	0.20	4.93E-11	4.10E-08	*ACSM5*	upstream	ENSSSCG00000007849	*CRYM*	*cis*
I2	3	ASGA0085542	25695049	0.73	0.27	1.11E-17	1.57E-14	*ACSM5*	intergenic	-	-	*cis*
I2	3	MARC0060700	25794656	0.67	0.33	1.11E-16	1.57E-13	*ACSM5*	intergenic	-	-	*cis*
I2	3	ASGA0013904	25862724	0.74	0.26	1.11E-17	1.57E-14	*ACSM5*	intergenic	-	-	*cis*
I2	3	ASGA0013906	25939787	0.73	0.27	1.11E-17	1.57E-14	*ACSM5*	upstream	ENSSSCG00000007853	*LYRM1*	*cis*
I2	3	ALGA0018079	25957412	0.73	0.27	1.11E-17	1.57E-14	*ACSM5*	intergenic	-	-	*cis*
I2	3	ASGA0095840	25990903	0.74	0.26	1.11E-17	1.57E-14	*ACSM5*	intronic	ENSSSCG00000007855	-	*cis*
I2	3	MARC0108510	26002460	0.74	0.26	1.11E-17	1.57E-14	*ACSM5*	intronic	ENSSSCG00000007855	-	*cis*
I2	3	ALGA0108097	26045382	0.74	0.26	1.11E-17	1.57E-14	*ACSM5*	intronic	ENSSSCG00000007857	*ACSM3*	*cis*
I2	3	ASGA0103234	26183486	0.66	0.34	8.18E-12	7.28E-09	*ACSM5*	intronic	ENSSSCG00000026453	*ACSM5*	*cis*
I2	3	ASGA0085560	26316304	0.76	0.24	1.11E-17	1.57E-14	*ACSM5*	intergenic	-	-	*cis*
I2	3	H3GA0053928	26392557	0.71	0.29	3.40E-14	3.34E-11	*ACSM5*	intergenic	-	-	*cis*

Interval	Chr	SNP	Position (bp)	fA1	fA2	*p*-value	*q*-value	Associated Gene	Consequence	Ensembl_GeneId	Gene Id	*Cis/Trans*-eSNPs
I2	3	MARC0101263	26425965	0.83	0.17	1.11E-17	1.57E-14	*ACSM5*	intergenic	-	-	*cis*
I2	3	MARC0050331	26428824	0.79	0.21	4.44E-16	5.66E-13	*ACSM5*	intergenic	-	-	*cis*
I2	3	MARC0019934	26488381	0.34	0.66	1.36E-05	3.61E-03	*ACSM5*	intergenic	-	-	*cis*
I2	3	MARC0007734	26517625	0.66	0.34	1.56E-10	1.15E-07	*ACSM5*	intergenic	-	-	*cis*
I2	3	MARC0052941	26537702	0.73	0.27	1.11E-17	1.57E-14	*ACSM5*	downstream	ENSSSCG00000007862	*GPR139*	*cis*
I2	3	ALGA0018104	26631496	0.49	0.51	1.89E-06	6.34E-04	*ACSM5*	intergenic	-	-	*cis*
I2	3	M1GA0004189	26724456	0.40	0.60	3.53E-05	8.24E-03	*ACSM5*	intergenic	-	-	*cis*
I2	3	MARC0001269	26822485	0.72	0.28	1.11E-17	1.57E-14	*ACSM5*	intergenic	-	-	*cis*
I2	3	ALGA0106209	26913735	0.43	0.57	3.16E-08	1.61E-05	*ACSM5*	intronic	ENSSSCG00000029212	*GDE1*	*cis*
I2	3	ALGA0121590	26978899	0.52	0.48	2.66E-15	2.83E-12	*ACSM5*	intronic	ENSSSCG00000007866	*TMC7*	*cis*
I2	3	ASGA0090088	27058670	0.77	0.23	1.11E-17	1.57E-14	*ACSM5*	intronic	ENSSSCG00000007868	*TMC5*	*cis*
I2	3	MARC0094635	27083041	0.47	0.53	1.13E-06	4.12E-04	*ACSM5*	intergenic	-	-	*cis*
I2	3	ASGA0105223	27200658	0.77	0.23	1.11E-17	1.57E-14	*ACSM5*	intronic	ENSSSCG00000022200	-	*cis*
I2	3	ALGA0124353	27208947	0.53	0.47	9.98E-06	2.75E-03	*ACSM5*	intronic	ENSSSCG00000022200	-	*cis*
I2	3	SIRI0001454	27254477	0.77	0.23	1.11E-17	1.57E-14	*ACSM5*	intronic	ENSSSCG00000022200	-	*cis*
I2	3	MARC0010219	27473051	0.44	0.56	1.56E-06	5.48E-04	*ACSM5*	intergenic	-	-	*cis*
I2	3	ASGA0090426	27551099	0.56	0.44	2.20E-08	1.17E-05	*ACSM5*	intergenic	-	-	*cis*
I2	3	ALGA0018136	27799603	0.47	0.53	4.95E-06	1.42E-03	*ACSM5*	intronic	ENSSSCG00000007872	-	*cis*
I2	3	ALGA0018138	27839633	0.71	0.29	1.11E-17	1.57E-14	*ACSM5*	intronic	ENSSSCG00000007872	-	*cis*
I2	3	MARC0000263	27855477	0.59	0.41	3.32E-07	1.32E-04	*ACSM5*	intronic	ENSSSCG00000007872	-	*cis*
I2	3	MARC0046257	27878993	0.79	0.21	1.11E-17	1.57E-14	*ACSM5*	intronic	ENSSSCG00000007872	-	*cis*
I2	3	ALGA0018155	27912117	0.66	0.34	1.37E-07	6.10E-05	*ACSM5*	upstream	ENSSSCG00000007872	-	*cis*
I2	3	ALGA0018160	27925965	0.66	0.34	2.36E-07	9.92E-05	*ACSM5*	intergenic	-	-	*cis*
I2	3	ASGA0013982	27941321	0.71	0.29	1.11E-17	1.57E-14	*ACSM5*	intergenic	-	-	*cis*
I2	3	ASGA0013988	27988181	0.65	0.35	1.01E-05	2.76E-03	*ACSM5*	intergenic	-	-	*cis*

Interval	Chr	SNP	Position (bp)	fA1	fA2	*p*-value	*q*-value	Associated Gene	Consequence	Ensembl_GeneId	Gene Id	*Cis/Trans*-eSNPs
I2	3	ALGA0018199	28346892	0.66	0.34	9.35E-07	3.47E-04	*ACSM5*	intergenic	-	-	*cis*
I2	3	ASGA0014014	28373428	0.65	0.35	2.85E-07	1.17E-04	*ACSM5*	upstream	ENSSSCG00000019735	*5S_rRNA*	*cis*
I2	3	ASGA0014023	28786813	0.67	0.33	2.59E-06	8.47E-04	*ACSM5*	intergenic	-	-	*cis*
I2	3	ASGA0104499	28886788	0.54	0.46	4.94E-07	1.93E-04	*ACSM5*	downstream	ENSSSCG00000019945	*U6*	*cis*
I2	3	ASGA0014039	29752690	0.61	0.39	2.89E-05	7.18E-03	*ACSM5*	intronic	ENSSSCG00000007878	*PARN*	*cis*
I2	3	H3GA0009179	30781487	0.63	0.37	4.30E-06	1.27E-03	*ACSM5*	intergenic	-	-	*cis*
I2	3	CASI0006297	32293788	0.54	0.46	2.90E-07	1.18E-04	*ACSM5*	intergenic	-	-	*trans*
I2	3	M1GA0024387	32474314	0.55	0.45	6.00E-08	2.83E-05	*ACSM5*	intergenic	-	-	*trans*
I2	3	ALGA0119050	32501522	0.55	0.45	6.00E-08	2.83E-05	*ACSM5*	intergenic	-	-	*trans*
I2	3	MARC0015229	32509563	0.55	0.45	6.00E-08	2.83E-05	*ACSM5*	upstream	ENSSSCG00000007899	-	*trans*
I2	3	MARC0031378	32543630	0.55	0.45	1.63E-07	7.09E-05	*ACSM5*	intergenic	-	-	*trans*
I2	3	MARC0004212	34672106	0.44	0.56	1.18E-10	8.93E-08	*ACSM5*	synonymous	ENSSSCG00000007909	*ABAT*	*trans*
I2	3	M1GA0004280	34875865	0.62	0.38	1.60E-06	5.52E-04	*ACSM5*	intergenic	-	-	*trans*
I2	3	ASGA0014213	34921528	0.50	0.50	1.39E-08	7.71E-06	*ACSM5*	intronic	ENSSSCG00000007914	-	*trans*
I2	3	ALGA0115191	34936811	0.30	0.70	1.16E-05	3.13E-03	*ACSM5*	intronic	ENSSSCG00000007914	-	*trans*
I2	3	ALGA0107071	35759334	0.69	0.31	1.06E-11	9.22E-09	*ACSM5*	intergenic	-	-	*trans*
I2	3	ALGA0102473	37034994	0.76	0.24	8.97E-08	4.14E-05	*ACSM5*	intergenic	-	-	*trans*
I2	3	MARC0020793	37234505	0.77	0.23	5.05E-07	1.95E-04	*ACSM5*	intergenic	-	-	*trans*
I2	3	ASGA0105173	39375927	0.37	0.63	1.52E-05	3.93E-03	*ACSM5*	intergenic	-	-	*trans*
I2	3	ALGA0105074	39433703	0.37	0.63	1.52E-05	3.93E-03	*ACSM5*	intergenic	-	-	*trans*
I2	3	ALGA0114510	39644923	0.37	0.63	1.52E-05	3.93E-03	*ACSM5*	intronic	ENSSSCG00000007951	*CREBBP*	*trans*
I2	3	H3GA0009309	39858459	0.37	0.63	1.52E-05	3.93E-03	*ACSM5*	downstream	ENSSSCG00000007953	*DNASE1*	*trans*
I2	3	ALGA0018568	39881683	0.53	0.47	6.11E-06	1.73E-03	*ACSM5*	intergenic	-	-	*trans*
I2	3	M1GA0004302	39992614	0.53	0.47	6.11E-06	1.73E-03	*ACSM5*	downstream	ENSSSCG00000007954	*SLX4*	*trans*
I2	3	ASGA0093403	46893143	0.75	0.25	7.25E-11	5.66E-08	*ACSM5*	intergenic	-	-	*trans*

Interval	Chr	SNP	Position (bp)	fA1	fA2	*p*-value	*q*-value	Associated Gene	Consequence	Ensembl_GeneId	Gene Id	*Cis/Trans*-eSNPs
I2	3	H3GA0009347	47890224	0.53	0.47	3.38E-10	2.35E-07	*ACSM5*	intergenic	-	-	*trans*
I2	3	ALGA0018674	47957752	0.69	0.31	1.63E-06	5.52E-04	*ACSM5*	intronic	ENSSSCG00000008111	*NPHP1*	*trans*
I2	3	ALGA0018683	47979489	0.69	0.31	1.63E-06	5.52E-04	*ACSM5*	intronic	ENSSSCG00000008111	*NPHP1*	*trans*
I2	3	H3GA0009368	48216866	0.81	0.19	3.26E-05	7.75E-03	*ACSM5*	intergenic	-	-	*trans*
I2	3	MARC0071874	48324056	0.86	0.14	5.07E-09	2.90E-06	*ACSM5*	intergenic	-	-	*trans*
I2	3	MARC0041994	48345565	0.86	0.14	2.00E-09	1.23E-06	*ACSM5*	downstream	ENSSSCG00000022826	-	*trans*
I2	3	ALGA0018791	48500096	0.77	0.23	3.02E-10	2.14E-07	*ACSM5*	upstream	ENSSSCG00000008121	*GPAT2*	*trans*
I2	3	ALGA0114161	48855083	0.81	0.19	3.26E-05	7.75E-03	*ACSM5*	intronic	ENSSSCG00000008123	*ARID5A*	*trans*
I2	3	ASGA0104566	48856852	0.81	0.19	3.26E-05	7.75E-03	*ACSM5*	intronic	ENSSSCG00000008123	*ARID5A*	*trans*
I2	3	ALGA0018800	49041576	0.81	0.19	3.26E-05	7.75E-03	*ACSM5*	intronic	ENSSSCG00000008127	-	*trans*
I2	3	ASGA0014426	49104674	0.81	0.19	3.26E-05	7.75E-03	*ACSM5*	downstream	ENSSSCG00000008129	-	*trans*
I2	3	ASGA0103041	49443426	0.86	0.14	2.00E-09	1.23E-06	*ACSM5*	intergenic	-	-	*trans*
I2	3	ASGA0090160	49528314	0.86	0.14	2.00E-09	1.23E-06	*ACSM5*	intergenic	-	-	*trans*
I2	3	ALGA0018859	49555848	0.78	0.22	1.80E-07	7.74E-05	*ACSM5*	intergenic	-	-	*trans*
I2	3	H3GA0009485	50180162	0.85	0.15	6.17E-07	2.36E-04	*ACSM5*	intronic	ENSSSCG00000008140	*SLC5A7*	*trans*
I2	3	MARC0024281	50793814	0.43	0.57	4.60E-06	1.33E-03	*ACSM5*	intergenic	-	-	*trans*
I2	3	ASGA0014649	56289772	0.65	0.35	2.41E-05	6.19E-03	*ACSM5*	intergenic	-	-	*trans*
I2	3	M1GA0004378	56459296	0.62	0.38	1.97E-10	1.42E-07	*ACSM5*	intronic	ENSSSCG00000008175	*CHST10*	*trans*
I2	3	M1GA0004379	56484282	0.73	0.27	2.29E-06	7.55E-04	*ACSM5*	3_prime_UTR_variant	ENSSSCG00000008175	*CHST10*	*trans*
I2	3	INRA0010621	56668305	0.86	0.14	3.41E-06	1.07E-03	*ACSM5*	intergenic	-	-	*trans*
I2	3	DRGA0003897	56709945	0.86	0.14	3.41E-06	1.07E-03	*ACSM5*	intergenic	-	-	*trans*
I2	3	ALGA0019110	56746317	0.86	0.14	3.41E-06	1.07E-03	*ACSM5*	intergenic	-	-	*trans*
I2	3	ASGA0014688	56833842	0.67	0.33	4.03E-09	2.34E-06	*ACSM5*	intronic	ENSSSCG00000008177	*AFF3*	*trans*
I2	3	ASGA0014690	56857721	0.73	0.27	4.09E-06	1.22E-03	*ACSM5*	intronic	ENSSSCG00000008177	*AFF3*	*trans*
I2	3	ALGA0019116	56885984	0.86	0.14	3.41E-06	1.07E-03	*ACSM5*	intronic	ENSSSCG00000008177	*AFF3*	*trans*

Interval	Chr	SNP	Position (bp)	fA1	fA2	*p*-value	*q*-value	Associated Gene	Consequence	Ensembl_GeneId	Gene Id	*Cis/Trans*-eSNPs
I2	3	ALGA0019121	57129085	0.73	0.27	4.09E-06	1.22E-03	*ACSM5*	intronic	ENSSSCG00000008177	*AFF3*	*trans*
I2	3	ALGA0108239	57170110	0.73	0.27	4.09E-06	1.22E-03	*ACSM5*	intronic	ENSSSCG00000008177	*AFF3*	*trans*
I2	3	MARC0001937	57187517	0.54	0.46	1.25E-09	8.25E-07	*ACSM5*	intronic	ENSSSCG00000008177	*AFF3*	*trans*
I2	3	MARC0034058	57211150	0.40	0.60	2.27E-09	1.38E-06	*ACSM5*	intergenic	-	-	*trans*
I2	3	ASGA0094631	57219021	0.56	0.44	1.06E-06	3.90E-04	*ACSM5*	intergenic	-	-	*trans*
I2	3	ALGA0019125	57431333	0.73	0.27	4.09E-06	1.22E-03	*ACSM5*	intronic	ENSSSCG00000008179	*REV1*	*trans*
I2	3	ASGA0082387	57704441	0.73	0.27	4.09E-06	1.22E-03	*ACSM5*	downstream	ENSSSCG00000008185	*MITD1*	*trans*
I2	3	ASGA0014810	60580301	0.18	0.82	3.14E-05	7.75E-03	*ACSM5*	upstream	ENSSSCG00000008213	*CD8B*	*trans*
I2	3	MARC0017871	60850148	0.81	0.19	3.97E-05	9.10E-03	*ACSM5*	downstream	ENSSSCG00000008217	*CD8A*	*trans*
I2	3	ASGA0014871	62719672	0.21	0.79	3.86E-05	8.90E-03	*ACSM5*	intergenic	-	-	*trans*
I2	3	ALGA0111911	63248078	0.19	0.81	3.42E-05	8.03E-03	*ACSM5*	intergenic	-	-	*trans*
I3	3	MARC0032158	83365626	0.35	0.65	1.63E-06	5.52E-04	*ACSM5*	intergenic	-	-	*trans*
I4	3	ALGA0020206	100905327	0.70	0.30	9.34E-06	2.59E-03	*ACSM5*	intergenic	-	-	*trans*
I4	3	ASGA0015465	101222209	0.68	0.32	1.41E-06	5.09E-04	*ACSM5*	intergenic	-	-	*trans*
I4	3	ASGA0098441	101461883	0.70	0.30	7.63E-06	2.15E-03	*ACSM5*	intergenic	-	-	*trans*
I5	10	H3GA0055101	54839	0.47	0.53	8.11E-07	3.04E-04	*ACSM5*	intronic	ENSSSCG00000010795	*NDUFAB1*	*trans*
I5	10	MARC0015344	65922	0.47	0.53	8.11E-07	3.04E-04	*ACSM5*	downstream	ENSSSCG00000010795	*NDUFAB1*	*trans*
I5	10	ASGA0082591	120016	0.74	0.26	2.00E-08	1.08E-05	*ACSM5*	downstream	ENSSSCG00000010797	*EARS2*	*trans*
I5	10	ASGA0092761	150115	0.65	0.35	2.78E-09	1.66E-06	*ACSM5*	intronic	ENSSSCG00000010798	*GGA2*	*trans*
I5	10	H3GA0055120	167126	0.70	0.30	2.89E-15	2.99E-12	*ACSM5*	downstream	ENSSSCG00000010798	*GGA2*	*trans*
I5	10	ASGA0090778	175359	0.76	0.24	1.44E-15	1.72E-12	*ACSM5*	intronic	ENSSSCG00000010799	*COG7*	*trans*
I5	10	ASGA0094144	184863	0.71	0.29	1.09E-08	6.13E-06	*ACSM5*	intronic	ENSSSCG00000010799	*COG7*	*trans*
I5	10	ASGA0095156	202837	0.74	0.26	2.00E-08	1.08E-05	*ACSM5*	intronic	ENSSSCG00000010799	*COG7*	*trans*
I6	16	ALGA0089402	19133382	0.66	0.34	3.83E-05	8.88E-03	*ACSM5*	intronic	ENSSSCG00000016810	*PDZD2*	*trans*
I7	13	ASGA0055780	6891435	0.55	0.45	1.20E-07	4.74E-03	*ELOVL6*	intergenic	-	-	*trans*

Interval	Chr	SNP	Position (bp)	fA1	fA2	*p*-value	*q*-value	Associated Gene	Consequence	Ensembl_GeneId	Gene Id	*Cis/Trans*-eSNPs
I8	2	ASGA0008719	6094116	0.48	0.52	1.26E-05	4.75E-02	*FABP4*	intergenic	-	-	*trans*
I8	2	MARC0018949	8997005	0.59	0.41	1.38E-05	4.75E-02	*FABP4*	upstream	ENSSSCG00000023090	*BEST1*	*trans*
I9	3	ASGA0015643	109404009	0.69	0.31	1.44E-05	4.75E-02	*FABP4*	3_prime_UTR_variant	ENSSSCG00000020689	*CEBPZOS*	*trans*
I9	3	ALGA0020658	113469226	0.91	0.09	6.70E-06	4.75E-02	*FABP4*	intronic	ENSSSCG00000008510	*LTBP1*	*trans*
I9	3	ASGA0016181	119739502	0.66	0.34	8.31E-06	4.75E-02	*FABP4*	synonymous	ENSSSCG00000008568	*DRC1*	*trans*
I10	4	ALGA0024527	36727180	0.57	0.43	1.11E-05	4.75E-02	*FABP4*	intergenic	-	-	*trans*
I11	4	ALGA0025158	60566866	0.48	0.52	1.93E-06	1.95E-02	*FABP4*	intergenic	-	-	*cis (FABP5)*
I11	4	ALGA0025162	60844160	0.68	0.32	1.32E-05	4.75E-02	*FABP4*	intergenic	-	-	*cis (FABP5)*
I11	4	MARC0115316	61059205	0.52	0.48	1.97E-06	1.95E-02	*FABP4*	intronic	ENSSSCG00000022989	*ZNF704*	*cis (FABP5)*
I11	4	INRA0014244	63090979	0.59	0.41	1.19E-05	4.75E-02	*FABP4*	intronic	ENSSSCG00000006163	PKIA	*cis (FABP5)*
I11	4	ALGA0025337	65252780	0.77	0.23	8.67E-07	1.95E-02	*FABP4*	intergenic	-	-	*cis (FABP5)*
I12	9	ALGA0054847	129178729	0.88	0.12	1.19E-06	1.95E-02	*FABP4*	intronic	ENSSSCG00000015508	*TNR*	*trans*
I13	2	ASGA0008845	7850065	0.61	0.39	9.88E-06	3.93E-02	*FADS2*	intronic	ENSSSCG00000013056	*LGALS12*	*trans*
I13	2	ASGA0104083	8867970	0.78	0.22	5.98E-08	5.94E-04	*FADS2*	intronic	ENSSSCG00000013066	-	*cis*
I13	2	ASGA0090054	8943379	0.86	0.14	2.03E-06	1.15E-02	*FADS2*	intergenic	-	-	*cis*
I13	2	ALGA0011764	9098547	0.89	0.11	1.54E-05	4.71E-02	*FADS2*	intergenic	-	-	*cis*
I13	2	ASGA0008884	9139348	0.92	0.08	1.54E-05	4.71E-02	*FADS2*	intronic	ENSSSCG00000013072	*FADS2*	*cis*
I13	2	ASGA0008896	9171685	0.66	0.34	2.58E-07	1.71E-03	*FADS2*	intronic	ENSSSCG00000013073	*FADS3*	*cis*
I13	2	ALGA0011760	9198141	0.86	0.14	1.21E-05	4.37E-02	*FADS2*	upstream	ENSSSCG00000013074	*RAB3IL1*	*cis*
I13	2	ASGA0008874	9218889	0.79	0.21	2.28E-07	1.71E-03	*FADS2*	intergenic	-	-	*cis*
I14	6	ALGA0035721	74418977	0.74	0.26	7.50E-06	3.31E-02	*FADS2*	intergenic	-	-	*trans*
I15	8	ASGA0100508	59002816	0.35	0.65	1.93E-05	4.80E-02	*FADS2*	intronic	ENSSSCG00000025792	-	*trans*
I15	8	MARC0041089	59080961	0.65	0.35	1.93E-05	4.80E-02	*FADS2*	intronic	ENSSSCG00000008913	*IGFBP7*	*trans*
I15	8	H3GA0024926	68676342	0.65	0.35	1.93E-05	4.80E-02	*FADS2*	intergenic	-	-	*trans*
I16	10	H3GA0030086	46933533	0.66	0.34	2.40E-06	1.19E-02	*FADS2*	intergenic	-	-	*trans*

Interval	Chr	SNP	Position (bp)	fA1	fA2	*p*-value	*q*-value	Associated Gene	Consequence	Ensembl_GeneId	Gene Id	*Cis/Trans*-eSNPs
I17	9	MARC0034587	20183865	0.76	0.24	2.15E-05	3.42E-02	*SLC27A4*	intergenic	-	-	*trans*
I17	9	ASGA0041925	20196539	0.79	0.21	1.69E-05	2.92E-02	*SLC27A4*	intergenic	-	-	*trans*
I18	14	ASGA0064787	88898693	0.95	0.05	2.51E-06	4.76E-03	*SLC27A4*	intergenic	-	-	*trans*
I18	14	MARC0057510	89058255	0.95	0.05	2.51E-06	4.76E-03	*SLC27A4*	intronic	ENSSSCG00000010342	*SH2D4B*	*trans*
I18	14	MARC0029597	89073094	0.95	0.05	2.51E-06	4.76E-03	*SLC27A4*	downstream	ENSSSCG00000010342	*SH2D4B*	*trans*
I18	14	ALGA0079330	89521045	0.95	0.05	2.51E-06	4.76E-03	*SLC27A4*	intergenic	-	-	*trans*
I18	14	MARC0041088	90286262	0.95	0.05	2.51E-06	4.76E-03	*SLC27A4*	intergenic	-	-	*trans*
I18	14	ASGA0064841	90338701	0.95	0.05	2.51E-06	4.76E-03	*SLC27A4*	intergenic	-	-	*trans*
I18	14	ASGA0064844	90362764	0.95	0.05	2.51E-06	4.76E-03	*SLC27A4*	intergenic	-	-	*trans*
I18	14	MARC0088303	90797721	0.95	0.05	2.51E-06	4.76E-03	*SLC27A4*	intergenic	-	-	*trans*
I18	14	ALGA0079375	90925232	0.95	0.05	2.51E-06	4.76E-03	*SLC27A4*	intergenic	-	-	*trans*
I18	14	MARC0010015	91126881	0.95	0.05	2.51E-06	4.76E-03	*SLC27A4*	intergenic	-	-	*trans*
I18	14	MARC0003938	91360798	0.91	0.09	6.84E-06	1.24E-02	*SLC27A4*	intergenic	-	-	*trans*
I18	14	ALGA0079393	91666877	0.95	0.05	2.51E-06	4.76E-03	*SLC27A4*	intergenic	-	-	*trans*
I18	14	MARC0056155	91685430	0.95	0.05	2.51E-06	4.76E-03	*SLC27A4*	intergenic	-	-	*trans*
I18	14	ALGA0079399	92014581	0.95	0.05	2.51E-06	4.76E-03	*SLC27A4*	intergenic	-	-	*trans*
I18	14	MARC0014799	92290727	0.95	0.05	2.51E-06	4.76E-03	*SLC27A4*	intronic	ENSSSCG00000010350	*RGR*	*trans*
I18	14	ALGA0079407	92432834	0.95	0.05	2.51E-06	4.76E-03	*SLC27A4*	intronic	ENSSSCG00000010351	*CCSER2*	*trans*
I19	15	ASGA0070790	137054337	0.93	0.07	3.39E-05	5.00E-02	*SLC27A4*	intergenic	-	-	*trans*
I19	15	MARC0050960	137365338	0.93	0.07	3.39E-05	5.00E-02	*SLC27A4*	intergenic	-	-	*trans*

Paper III. Table S5: Gene annotation of genes within the eQTL intervals. Annotation was performed by considering for *trans*-eQTLs the eQTL interval ±1 Mb; whereas for *cis*-eQTLs only the studied gene was selected (*ACSM5, FABP4,* and *FADS2*). (too large to be attached, not included in the present thesis).

See table at:
https://drive.google.com/open?id=0B6AO_ypOnvVONUprdEFGaExmS3c

Paper III. Table S6: Mean comparison between males and females of backfat gene-expression levels of 43 lipid-related genes.

Gene	Mean in Male	Mean in Female	*P*-value
ACSM5	0.51817697	1.72852438	3.13E-04
ADIPOQ	0.92164360	0.98284488	2.36E-01
AGPAT2	0.87918084	1.10464597	1.37E-03
ANK2	0.84801896	1.14951534	2.29E-07
ARNT	1.09244595	1.12042622	5.19E-01
CD36	0.99617293	0.92619269	1.19E-01
CPT1A	0.91728879	1.01130066	1.12E-01
CROT	0.95256618	1.05867480	1.22E-01
CYP2U1	1.07606492	1.11208908	6.16E-01
DGAT1	1.00775545	1.14631721	1.60E-01
DGAT2	0.82390245	1.20770872	9.35E-03
EGF	0.68500959	1.74315974	8.85E-02
ELOVL5	0.95955732	1.16724091	2.98E-02
ELOVL6	0.74078130	1.24349924	7.89E-04
ESRRA	1.05230240	1.13238052	2.85E-01
FABP4	0.91716259	0.97833632	2.20E-01
FABP5	0.87094802	0.83276296	4.29E-01
FADS1	0.81510182	0.81918792	9.35E-01
FADS2	1.03167992	0.86056221	1.79E-02
FADS3	0.95338485	0.94140547	7.46E-01
LIPC	1.06810700	1.07355133	9.44E-01
LPIN1	0.98953571	0.90460040	2.09E-01
MGLL	0.91940037	1.05084173	2.84E-02
MLXIPL	0.96472806	1.24568591	1.65E-03
NFKB1	0.98551744	0.89685752	4.24E-03
NR1H3	1.05627984	1.06637889	8.59E-01
PEX2	0.82736047	1.10936741	7.24E-05
PLA2G12A	0.88319601	1.17250484	1.19E-04
PLCB2	0.94496027	0.90234026	4.85E-01
PLPP1	1.07868017	0.81758309	1.47E-06
PNPLA2	0.90634158	1.09133116	1.21E-03
POU2F1	0.91960235	0.97001854	1.84E-01
PPARA	0.89844266	1.21347231	2.13E-04
PPARD	0.88021205	1.20349846	1.15E-05
PPARG	0.97231705	1.05651618	1.51E-01
RBP4	1.19587676	1.20421240	9.36E-01
RXRG	1.13725219	1.11110297	8.30E-01
SCAP	0.97647064	1.18466371	7.55E-05
SCD	0.47626940	1.06854340	7.40E-03
SLC27A1	1.17366254	1.07916161	2.65E-01
SLC27A4	1.17979415	1.12465775	3.09E-01
SREBF1	0.80739118	1.25519900	5.86E-07
USF1	1.03241102	1.03328212	9.82E-01

Paper III. Table S7: Description of the 393 human orthologous genes.

Interval	Human associated gene name
I1	*ALDH7A1, C5orf63, CTXN3, LMNB1, MARCH3, MEGF10, PHAX, PRRC1, TEX43, GRAMD3*
I2	*ACSM5*
I3	*B3GNT2, CCT4, COMMD1, EHBP1, FAM161A, NUP54, OTX1, USP34, XPO1, MDH1*
I4	*ATP6V1E2, CAMKMT, EPAS1, PPM1B, PREPL, PRKCE, RHOQ, SIX2, SLC3A1, SRBD1, TMEM247, PIGF*
I5	*COG7, EARS2, GGA2, NDUFAB1, PALB2, UBFD1, DCTN*
I6	*C5orf22, DROSHA, PDZD2, CDH6*
I7	*EFHB, KCNH8, SATB1*
I8	*AHNAK, AP000721.4, AP5B1, ARL2, ASRGL1, ATG2A, ATL3, B3GAT3, B4GAT1, BAD, BANF1, BATF2, BEST1, BRMS1, BSCL2, C11orf68, C11orf84, C11orf95, C11orf98, CAPN1, CATSPER1, CCDC85B, CCDC88B, CD248, CDC42BPG, CDC42EP2, CDCA5, CFL1, CHRM1, CNIH2, CPSF7, CST6, CTSW, CYB561A3, DAGLA, DDB1, DNAJC4, DPF2, DRAP1, EEF1G, EFEMP2, EHD1, EIF1AD, EML3, ESRRA, FADS1, FADS2, FADS3, FAU, FEN1, FERMT3, FIBP, FKBP2, FLRT1, FOSL1, FRMD8, GAL3ST3, GANAB, GPHA2, GPR137, HNRNPUL2, HRASLS5, INCENP, INTS5, KAT5, KCNK4, KCNK7, KLC2, LGALS12, LRRC10B, LTBP3, MACROD1, MAP4K2, MARK2, MEN1, METTL12, MRPL49, MTA2, MUS81, MYRF, NAA40, NAALADL1, NRXN2, NUDT22, NXF1, OTUB1, OVOL1, PACS1, PCNXL3, PGA4, PLA2G16, PLCB3, POLA2, POLR2G, PPP1R14B, PPP1R32, PPP2R5B, PRDX5, PYGM, RAB3IL1, RASGRP2, RCOR2, RELA, RIN1, RNASEH2C, ROM1, RPL13A, RPL22, RPS6KA4, RTN3, SAC3D1, SART1, SCGB1A1, SCGB1D2, SCYL1, SDHAF2, SF1, SF3B2, SIPA1, SLC22A10, SLC22A11, SLC22A12, SLC22A6, SLC22A8, SLC25A45, SLC3A2, SNX15, SNX32, SSSCA1, STIP1, STX5, SYT7, SYVN1, TAF6L, TEX40, TIGD3, TKFC, TM7SF2, TMEM138, TMEM151A, TMEM216, TMEM223, TMEM258, TMEM262, TRMT112, TRPT1, TSGA10IP, TTC9C, TUT1, UBXN1, UQCC3, VEGFB, VPS51, VWCE, WDR74, YIF1A, ZBTB3, ZFPL1, ZNHIT2, SCGB2A1, SLC29A2*
I9	*ABHD1, ADGRF3, AGBL5, ALK, ASXL2, ATRAID, BIRC6, BRE, C2orf16, C2orf70, C2orf71, CAPN14, CCDC121, CDC42EP3, CEBPZ, CEBPZOS, CENPA, CGREF1, CIB4, CLIP4, CRIM1, DNMT3A, DPY30, DPYSL5, DRC1, DTNB, EHD3, EIF2B4, EMILIN1, EPT1, FAM179A, FAM98A, FEZ2, FNDC4, FOSL2, GAREM2, GCKR, GPATCH11, GPN1, HADHA, HADHB, HEATR5B, IFT172, KHK, KIF3C, KRTCAP3, LBH, LCLAT1, LTBP1, MAPRE3, MEMO1, NDUFAF7, NLRC4, NRBP1, PLB1, PPM1G, PPP1CB, PREB, PRKD3, PRR30, QPCT, RAB10, RASGRP3, RBKS, RMDN2, SLC30A6, SLC35F6, SLC4A1AP, SLC5A6, SNX17, SPAST, SPDYA, SRD5A2, STRN, SUPT7L, TCF23, TMEM214, TRMT61B, TTC27, VTI, WDR43, XDH, YPEL5, YWHAE, ZNF512, CYP1B1, GALNT14*
I10	*ATP6V1C1, AZIN1, BAALC, CTHRC1, DCAF13, FZD6, KLF10, ODF1, RRM2B, SLC25A32, UBR5, RIMS2*
I11	*FABP5*
I12	*CACYBP, GPR52, KIAA0040, MRPS14, PAPPA2, RABGAP1L, RFWD2, TNN, TNR, NXPE2*
I14	*C1orf234, C1QA, C1QB, C1QC, CDC42, CNR2, ECE1, EPHA8, EPHB2, FUCA1, GALE, HMGCL, HSPG2, HTR1D, KDM1A, LACTBL1, LUZP1, ZBTB40*
I15	*ADGRL3, CENPC, CEP135, CLOCK, EPHA5, EXOC1, IGFBP7, NOA1, PDCL2, POLR2B, PPIC, REST, TECRL, TMEM165, TMSB4X*
I16	*ARHGAP12, CUBN, EPC1, ERV3-1, KIF5B, PTCHD3, SVIL, ZEB1, ZNF438*
I17	*ANKRD42, CCDC90B, DLG2, PCF11, PRCP, RAB30*
I18	*ANXA11, C10orf99, CCSER2, CDHR1, DYDC1, DYDC2, FAM213A, GHITM, GRID1, LRIT1, LRIT2, MAT1A, NRG3, PLAC9, PPIF, RGR, SFTPA1, SFTPD, SH2D4B, TMEM254, TSPAN14, ZMIZ1*
I19	*EPHA4, FARSB, MOGAT1, PAX3, SGPP2*

Paper III. Table S8: Top functional networks and molecules identified with IPA from the list of annotated genes mapping within the 19 eQTLs.

ID	Interval	Top Diseases and Functions	Score	Focus Molecules	Molecules in Network
1	I1	Cell-To-Cell Signaling and Interaction, Hematological System Development and Function, Immune Cell Trafficking	21	7	ALDH4A1,ALDH7A1,ALDH8A1,APBB3,APP,ARHGAP24,C3orf62,C9orf78,CASC4,CCL26,CREBBP,CXCL12,DPY19L3,EVI2A,Fcr,FRMD8,GIMAP4,GIMAP5,GIMAP8,GPR85,GRAMD3,GRAMD1C,LMNB1,MARCH3,MEGF10,NMNAT2,Oas1b,PHAX,PRRC1,RGL1,RTP4,SYK,TMOD4,VAV1,ZCCHC12
2	I3	Carbohydrate Metabolism, Organ Morphology, Reproductive System Development and Function	30	10	B3GNT2,B3GNT7,B4GAT1,BRCA1,C16orf62,CCT4,COMMD1,DBR1,EHBP1,EXD2,FAM161A,FAM173A,FAM83A,GAREM1,Hd-neuronal intranuclear inclusions,HEATR5B,HTT,LSM14B,MAGEB18,MDH1,MFAP4,NTRK1,NUP54,OTX1,PLEKHA6,POU5F1,PRRT4,Ptprv,RWDD4,TP53,USP29,USP34,WDR91,XPO1,ZC3H7A
3	I4	Connective Tissue Disorders, Organismal Injury and Abnormalities, Cell Death and Survival	29	10	ALKBH7,APP,C11orf52,C11orf71,C2orf49,C9orf64,CAMKMT,CD40LG,CYB561D2,DTWD1,EPAS1,HNF4A,HPF1,Insulin,MCEE,MPV17L,NBPF3,NFkB (complex),NTRK1,omega-muricholic acid,PI3K (complex),PIGF,PPIP5K2,PPM1B,PREPL,PRKCE,PURG,RHOQ,RSPH3,SIX2,SLC3A1,SRBD1,THYN1,TP53,TP53TG5
4	I4	Molecular Transport, Hereditary Disorder, Metabolic Disease	3	1	ATP6V1B1,ATP6V1C2,ATP6V1E2,ATP6V1G1,C9orf16,H+-exporting ATPase,RICTOR,Vacuolar H+ ATPase
5	I5	Cancer, Organismal Injury and Abnormalities, Reproductive System Disease	21	7	ACOT1,AIM1,ANGPTL2,CDC42SE1,CHST2,CNNM4,COG7,CUL3,DCTN5,DDX10,EARS2,ERBB2,ESR1,FAM98B,GGA2,LCN1,MAN1A1,NDUFAB1,NTRK1,PALB2,PCDH8,PCNA,PGM3,PRR15L,PTPRT,RHOBTB2,RTN4RL1,SPAG1,SPAG4,SUPV3L1,THADA,UBAP2,UBFD1,WDR81,ZSWIM8
6	I6	Cellular Development, Embryonic Development, Hair and Skin Development and Function	12	4	BCL9,Bcl9-Cbp/p300-Ctnnb1-Lef/Tcf,C12orf49,C5orf22,CASC4,CDH6,CDH7,CDH8,CDH9,CDH10,CDH15,CDH18,CNMD,CTBS,CTDSPL,CTNNB1,CTNNβ-LEF1,DACT3,DROSHA,DUSP7,ELAVL1,FBXO8,GLIPR1,GPX2,MUM1,MYBPH,MYC,PDZD2,RPL41,TCF4-CTNNβ,TMEM2,Trp53cor1,UST,VEZT,ZXDB
7	I7	Immunological Disease, Inflammatory Disease, Inflammatory Response	4	1	IL1B,KCNH8,PTGER3
8	I7	Cell Cycle, Organ Morphology, Visual System Development and Function	3	1	ABTB1,BTLA,CLEC2B,CORO6,Cux1,ENOSF1,EPSTI1,EVI2A,FAM110A,FAM129A,FAM65B,FOXJ3,Foxp2,GPR18,GPT2,HELZ2,HLA-DOB,HSF5,HVCN1,Ighen,LAG3,LPIN2,LRRN3,MT1A,MYCL,PIK3IP1,POU3F4,QSER1,SATB1,TBX6,TMEM2,TMEM117,TMEM241,ZKSCAN8,ZNF287

ID	Interval	Top Diseases and Functions	Score	Focus Molecules	Molecules in Network
9	I8	Cell Cycle, DNA Replication, Recombination, and Repair, Developmental Disorder	52	26	26sProteasome,Actin,BANF1,CAPN1,caspase,CD3,CTSW,DDB1,DPF2,EEF1G,ESRRA,FEN1,FERMT3,FKBP2,HISTONE,Histone h3,Histone h4,INCENP,INTS5,KAT5,KCNK4,MAP4K2,MTA2,MUS81,NFkB (complex),OTUB1,POLA2,POLR2G,PRDX5,RNA polymerase II,RPL13A,SF1,SF3B2,TAF6L,UBXN1
10	I8	Lipid Metabolism, Small Molecule Biochemistry, Infectious Diseases	42	22	Akt,BSCL2,Calmodulin,CDCA5,CHRM1,Ck2,ERK,estrogen receptor,FADS1,FADS2,FAU,FIBP,FSH,GANAB,Hsp90,Insulin,LGALS12,Lh,Mapk,MYRF,PLA2,PLA2G16,PLC,PLCB3,PPP2R5B,RELA,SCGB1A1,SLC22A8,SLC3A2,STAT5a/b,STIP1,STX5,SYT7,SYVN1,TMEM216
11	I8	Lipid Metabolism, Small Molecule Biochemistry, Cellular Assembly and Organization	32	18	AES,AHNAK,ARL2,C11orf68,C20orf194,CCT3,CDC37,CPSF7,DAGLA,DUS3L,EIF1AD,EML3,GPR137,GPR174,HSP90AA1,KCNK7,KLF3,MAP3K1,MAP3K15,MRPL49,MYLK4,NUDT22,NXF1,PDIK1L,PSKH1,RAB3IL1,SSSCA1,STAT4,SUPT5H,TRMT112,TTC9C,TUBB,TUT1,YWHAQ,ZBTB3
12	I8	Cellular Assembly and Organization, Cell-To-Cell Signaling and Interaction, Nervous System Development and Function	25	15	14-3-3,Alp,Ap1,BAD,BRMS1,CDC42EP2,CFL1,Creb,ERK1/2,F Actin,Fibrinogen,FOSL1,Igg3,IgG2a,Igm,Immunoglobulin,KLC2,LDL,LTBP3,MARK2,MEN1,PACS1,PDGF BB,Pka,Pka catalytic subunit,PP2A,Rap1,Ras,RASGRP2,RIN1,Rock,RPS6KA4,Rsk,SIPA1,VEGFB
13	I8	Cellular Compromise, Gastrointestinal Disease, Hepatic System Disease	25	15	ABHD2,ATG2A,BRCA1,C11orf84,C11orf98,CDC42BPG,Cyp2d1/Cyp2d5,DNAJB1,Dnajb1-Hsp70,DNAJC4,DNAJC16,EGFR,EHD1,Esr1-Estrogen-Sp1,FAM153A/FAM153B,HLA-C,HNRNPUL2,HSCB,HSPA9,HSPB1,lipid,MACROD1,MDC1,NAA40,PGA5 (includes others),RCOR2,RPL22,SDHAF2,SP1,SUMO2,TMCO3,TMEM223,tretinoin,TSGA10IP,XRCC5
14	I8	Nutritional Disease, Cell Morphology, Cell-To-Cell Signaling and Interaction	21	13	APP,ATL3,C15orf39,CACNG2,CACNG3,CACNG8,CNIH2,DRAP1,FRMD8,GORAB,GRIA1,HIST1H2AD,HRASLS5,INIP,MAD2L1,N-acetyl-L-aspartic acid,OLFM1,OLFM3,PDCD7,PPP1R32,RABL3,REEP6,RTN3,SAC3D1,SCYL1,SLC22A6,SLC30A3,SNX1,SNX14,SNX15,SNX32,SP140L,TCP11L1,TRPT1,ZCCHC6
15	I8	Cancer, Cell Death and Survival, Organismal Injury and Abnormalities	21	13	ADIRF,AP5B1,ASRGL1,B3GAT3,BCL2,beta-estradiol,CAMK2B,CD248,FADS3,GSK3B,IFNB1,JUNB,PELP1,PHACTR3,PP1 protein complex group,PPP1R11,PPP1R17,PPP1R14B,PPP1R14C,PPP1R14D,PPP2CA,Ppp2r3d,PSMC3,PXYLP1,PYGM,REM1,RNASEH2C,SCGB2A1,TGFB2,TKFC,TMEM44,TMEM258,VPS51,WDR74,YAP/TAZ
16	I8	Cellular Function and Maintenance, Organ Development, Reproductive System Development and Function	19	12	adenosine,AIFM2,CACNA1I,CATSPER,CATSPER1,CATSPER2,CATSPER3,CATSPER4,CYB561A3,EFEMP2,EGF,KCTD11,LSM14A,NRXN2,PPARD,PRPF8,RNU4-1,RNU5A-1,ROM1,SART1,SLC29A2,SLC30A6,SNRNP27,TMED7,TMEM17,TMEM138,TMEM151A,TP53,UBIAD1,UBL5,USO1,voltage-gated calcium channel,YIF1A,ZFPL1,ZNHIT2

ID	Interval	Top Diseases and Functions	Score	Focus Molecules	Molecules in Network
17	I8	Cell Death and Survival, Gastrointestinal Disease, Organismal Injury and Abnormalities	17	11	ADGRA1,ADGRG6,Akr1c19,B4GAT1,BEST1,Ca2+,CCDC85B,CPQ,CST6,FLRT1,FPR3,GAL3ST3,GPHA2,GPHB5,GPR19,GPR21,GPR85,GPR108,GPR146,GPR156,HNF1A,NPFFR2,NPS,OSM,P2RY10,PCNX3,PTH1R,SLC22A11,SLC22A12,SOX9,TGFB1,TM7SF2,TRPM5,TSHR,UGT2A3
18	I8	Organ Morphology, Organismal Injury and Abnormalities, Reproductive System Development and Function	6	5	BATF2,CCDC88B,Ctla2a/Ctla2b,CYP4Z1,Egfr-Erbb2,ESR2,Granzyme,IkB-NfkB,IKK (complex),IL12 (complex),IL12 (family),IL22R1-IL10R2,IRS1/2,isoleucine,Jnk,MIP1,miR-146a-5p (and other miRNAs w/seed GAGAACU),N-arachidonylglycine,OVOL1,P38 MAPK,p85 (pik3r),PI3K (complex),Pkc(s),POU6F1,Rap1-gp91-p22 phox-p40 phox-p47 phox-p67 phox,Sh2b3,SHISA2,TCR,TIGD3,TLR2/TLR4,TPST1,TRAF1-TRAF2-TRAF3,Vegf,Vegfr dimer,VWCE
19	I8	Developmental Disorder, Hereditary Disorder, Metabolic Disease	2	1	PHLDA3,UQCC3
20	I8	Cancer, Organismal Injury and Abnormalities, Reproductive System Disease	2	1	SCGB1D2,SCGB2A2
21	I8	Hereditary Disorder, Nephrosis, Organismal Injury and Abnormalities	2	1	METTL12,NT5DC2,XPNPEP3
22	I9	Developmental Disorder, Hereditary Disorder, Metabolic Disease	58	25	26sProteasome,ALK,BIRC6,BRE,caspase,CENPA,Cg,CGREF1,CYP1B1,DNMT3A,DPY30,EMILIN1,ERK1/2,FOSL2,GCKR,GPN1,HADHA,HADHB,Histone h3,Jnk,KHK,mediator,MEMO1,NFkB (complex),NLRC4,Pkc(s),PRKD3,RASGRP3,RNA polymerase II,SPAST,SPDYA,SRD5A2,SUPT7L,XDH,YWHAE
23	I9	Auditory and Vestibular System Development and Function, Cell Death and Survival, Nervous System Development and Function	32	16	APP,ASXL2,ATRAID,CEBPZ,CIART,CLIP4,CREB1,CRIM1,DPY19L3,FBXO6,FNDC4,GIMAP8,GPR85,IGSF10,KCNC4,MT-ND5,NAGA,NDUFAF7,NMNAT2,NPM1,OCIAD2,PPM1G,PRKACA,QPCT,RAB10,RMDN2,SLC4A1AP,SLC9A6,SNX17,TMEM214,TTC27,WARS2,ZDHHC23,ZNF35,ZNF512
24	I9	Cellular Assembly and Organization, Cancer, Cell Morphology	30	15	24R,25-dihydroxyvitamin D3,ABCA1,AGPAT5,ANGPT4,C3orf52,CYP4Z1,DTNB,ELAVL1,ERBB2,FAM20B,FAM98A,GALNT4,GALNT14,HEATR5B,IFT172,LBH,LCLAT1,LPCAT4,MAPK3,norepinephrine,NRBP1,NUDC,PDE7B,PREB,PRKCD,SELENOI,SLC35F6,STRN,TAS1R1,TC2N,TCF23,Vegf,VHL,WDR43,YPEL5
25	I9	Cell Morphology, Cellular Assembly and Organization, Nervous System Development and Function	20	11	ACTB,ADGRA1,ADGRF3,AGBL5,CDC42EP3,Clip1,DLG4,DPYSL5,EHD3,FEZ2,FOS,GPR63,GPR137,GPR146,GPR160,HNF4A,KBTBD4,KIF3C,MAPRE3,MSRB2,NGF,NUDT11,ornithine decarboxylase,PCNX1,PTEN,Ptprt,QRFPR,RBKS,SLC30A6,SORCS3,SSTR4,SSU72,TRMT61B,Uba52,VN1R1

ID	Interval	Top Diseases and Functions	Score	Focus Molecules	Molecules in Network
26	I9	Amino Acid Metabolism, Carbohydrate Metabolism, Molecular Transport	18	10	Akt,ANGPTL1,ARTN,BMP3,CCDC121,CD38,CLEC4A,CLEC4C,Cyp2j9,DEFB1,DRC1,EIF2B4,ERK,GAREM2,GPATCH11,IFNA2,Insulin,KDM1A,LTBP1,Na+,NANOG,NMN,NMUR2,NRG4,PLB1,PPP1CB,PRR30,S100a7a,SCD5,SLC2A9,SLC5A6,SLC8B1,SLC9A5,THEMIS2,VTCN1
27	I9	Cell Cycle, DNA Replication, Recombination, and Repair, Cellular Development	2	1	ABHD1,CCDC155
28	I9	Neurological Disease, Organismal Injury and Abnormalities, Psychological Disorders	2	1	CIB4,UBB,ZNHIT2
29	I10	Cell Morphology, Cellular Function and Maintenance, Cardiovascular Disease	36	12	ADAT1,ATMIN,ATP6V1C1,AZIN1,BAALC,C9orf64,CA5B,CDK5,CHEK2,CTHRC1,D-glucose,DCAF13,DZANK1,EED,ELAVL1,FZD6,GPR137,GPR180,GUF1,HCN3,HNF4A,KIAA0895,KLF10,ODF1,RIMS2,RRM2B,SLC16A5,SLC25A32,SLC43A2,SMIM7,SMIM12,TMEM101,TNF,UBR5,VN1R1
30	I12	Cell Cycle, Cellular Growth and Proliferation, Tissue Morphology	22	8	ADGRD1,ADGRD2,ADGRF2,ADGRF3,ADGRF4,ADGRG5,CACYBP,DEFB114,ERK1/2,Gpcr,GPR52,GPR61,GPR62,GPR82,GPR149,GPR150,GPR152,GPR157,GPR162,GPR137C,MAS1L,MRPS14,NPFFR1,PAPPA2,RABGAP1L,RB1,RFWD2,RRH,TNF,TNN,TNR,TP53,tretinoin,VN1R1,VN1R2
31	I12	Connective Tissue Development and Function, Connective Tissue Disorders, Nervous System Development and Function	3	1	KIAA0040,KRTAP10-3,MDFI
32	I12	Infectious Diseases, Immunological Disease, Hematological System Development and Function	3	1	AHR,IL10RA,NXPE2
33	I14	Developmental Disorder, Hereditary Disorder, Immunological Disease	26	10	5-oxo-6-8-11-14-(e,z,z,z)-eicosatetraenoic acid,ADGRG6,ALK3-BMPR2,C1q,C1QA,C1QB,C1QC,CDC42,CNR2,CR,CYP4Z1,ECE1,EPHA8,EPHB2,ERK,ERK1/2,Focal adhesion kinase,ganglioside GD2,GPR171,HSPG2,KDM1A,LAIR2,Mapk,N-arachidonylglycine,NMUR1,noladin ether,P38 MAPK,PI3K (complex),PIK3R6,Pka,RXFP3,SCARF1,STYX,TAS1R1,tetraiodothyroacetic acid
34	I14	Cell Signaling, Nucleic Acid Metabolism, Small Molecule Biochemistry	11	5	ADCY4,ADRA2C,ADRB2,APP,BACE2,CPLX1,Dstn/Dstnl1,endocannabinoid,F2RL3,FUCA1,FZD3,GALE,GPR3,GPR6,GPR12,GPR15,GPR61,GPR78,GPR85,GPRC5B,HMGCL,HTR1B,HTR1D,LPAR3,LUZP1,MRAP2,PIK3R5,PTGDR,RXFP3,S1PR1,SCTR,SLC52A2,SNURF,SP1,VIPR2

ID	Interval	Top Diseases and Functions	Score	Focus Molecules	Molecules in Network
35	I14	Cellular Assembly and Organization, Developmental Disorder, Hereditary Disorder	2	1	CDC37,DLG4,FHL1,FOXB1,IER2,ZBTB40
36	I15	Cellular Development, Cellular Growth and Proliferation, Cell Death and Survival	27	10	BCL2,CENPC,CLOCK,DCTPP1,Defb8,EPHA5,ERMAP,HRAS,IGDCC3,IGF1,Igf1-Igfbp,IGFBP7,Il1bos,miR-1195 (miRNAs w/seed GAGUUCG),miR-153-3p (miRNAs w/seed UGCAUAG),Mucl1/Mucl2,NOA1,PCDHAC2,POLR2B,POLR2J2/POLR2J3,PPIC,RDM1,REST,RNA Pol-II-TFIIA-TFIIB-TFIID-TFIIF,RNA polymerase II,SCG3,SLC9A8,SNORD118,SPAG7,SPP1,STAT3,TMEM165,TMSB10/TMSB4X,tretinoin,ZNF74
37	I15	Cell Cycle, Cellular Assembly and Organization, DNA Replication, Recombination, and Repair	6	3	ADGRL3,CCDC14,CCDC18,CCDC61,CCDC77,CENPJ,CEP72,CEP120,CEP131,CEP135,CEP162,CEP290,CEP295,CEP350,CTNND1,CYLD,EXOC1,FGFR1OP,FOPNL,GYS1,KIAA0753,LUZP1,MAPRE1,MIB1,MTNR1A,NEDD1,PIBF1,PRKAR2A,PRKD1,RALA,SIPA1L1,SIPA1L2,SPATA2,TBC1D31,TMEFF1
38	I15	Cancer, Endocrine System Disorders, Neurological Disease	3	1	CXorf56,GOLGA1,PDCL2
39	I16	Cancer, Hematological Disease, Immunological Disease	17	6	ARHGAP12,beta-estradiol,Crip2,CUBN,CUL7,DNPH1,EPC1,ER-α-Estradiol,FMO1,Gm13194,GPX2,Hmgn2 (includes others),Jnk dimer,JUN,KIF5B,Magea3 (includes others),mir-383,mir-99,MYC,PADI1,PGLYRP2,Ppp1r15a,PRDM2,SCPEP1,SDK1,Snrpc,Sprr2b,Sprr2g,SVIL,TP53,TRIM6,TSKU,UBL3,YY2,ZEB1
40	I16	Cell Cycle, Cancer, Developmental Disorder	3	1	ERV3-1,HECW2
41	I17	Hair and Skin Development and Function, Cellular Compromise, Cell Morphology	18	6	ADGRG6,ANKRD42,B4GALT6,C10orf10,CCDC90B,DEFB114,DLG2,EMCN,FAM132A,FUT3,goralatide,GPR37L1,GUF1,HNF4A,MAPK3,NUDT6,NUDT11,ORM2,PAFAH2,PCF11,PFKFB4,PPP1CA,PPP1R11,PPP1R14D,PRCP,RAB30,RASGRP4,SSTR4,TMEM176B,TNF,ULBP3,UTP11,ZBTB11,ZCCHC9,ZNF300
42	I18	Drug Metabolism, Molecular Transport, Cellular Function and Maintenance	28	11	ADAM10,AFM,ANGPTL7,ANXA11,APP,C2orf57,CALML4,CCSER2,CDHR1,DEF6,DEFA4,DYDC1,DYDC2,ethanol,EZH2,FAM213A,Fcna,FLRT1,GIMAP6,GPR21,GRID1,KIAA0513,MAT1A,MPV17L,NME5,NRG3,OARD1,SLC13A3,TGFB1,THSD4,tretinoin,TSPAN14,TSPAN33,VAT1L,ZMIZ1
43	I18	Cell Morphology, Cellular Function and Maintenance, Organismal Development	13	6	ADGRD1,ADGRD2,ADGRF2,ADGRF3,ADGRF4,ADGRG5,EPO,GHITM,Gpcr,GPR27,GPR61,GPR62,GPR75,GPR82,GPR139,GPR148,GPR149,GPR150,GPR152,GPR157,GPR162,GPR137C,HNF4A,LRIT1,MAS1L,NFkB (complex),NPFFR1,OXGR1,PPIF,RGR,RRH,SFTPA1,SFTPD,VN1R1,VN1R2

ID	Interval	Top Diseases and Functions	Score	Focus Molecules	Molecules in Network
44	I18	Cardiovascular Disease, Hereditary Disorder, Neurological Disease	2	1	CCDC14,EMILIN1,PLAC9,RAPGEF5,RNF213
45	I19	Post-Translational Modification, Gene Expression, Cellular Development	11	4	Calcineurin B,CD6,DUSP2,DUSP8,DUSP16,EPHA1,EPHA4,EYA2,FARSB,FZD10,G0S2,glycochenodeoxycholate,GSTA2,GSTM2,HNF4α dimer,IL36B,Jnk,mir-101,MKP2/5,NUDT1,PAX3,PPP1R16B,PPP2R5B,PRAM1,PTPRH,RLBP1,S1PR4,S1PR5,SGPP2,SH2D3C,sphingosine-1-phosphate,sphingosine-1-phosphate phosphatase,SRGN,TFF2,tretinoin
46	I19	Cell-mediated Immune Response, Cellular Movement, Hematological System Development and Function	3	1	2-acylglycerol O-acyltransferase,AGPAT2,BSCL2,Ccl2,CD44,CXCL10,diacylglycerol O-acyltransferase,MOGAT1,TIMP1,triacylglycerol

Paper III. Table S9: Transcription factor binding sites for the *PPARG* gene.

ID	Target Name	Interval	*Cis/Trans*-eQTL	Associated Gene
1	ABHD1	I9	*trans*	*FABP4*
2	ADIPOQ			
3	AGPAT2			
4	AHNAK	I8	*trans*	*FABP4*
5	ALK	I9	*trans*	*FABP4*
6	ATL3	I8	*trans*	*FABP4*
7	ATP6V1C1	I10	*trans*	*FABP4*
8	AZIN1	I10	*trans*	*FABP4*
9	B3GNT2	I3	*trans*	*ACSM5*
10	BAD	I8	*trans*	*FABP4*
11	BATF2	I8	*trans*	*FABP4*
12	BEST1	I8	*trans*	*FABP4*
13	C1QA	I14	*trans*	*FADS2*
14	C2orf16	I9	*trans*	*FABP4*
15	C2orf71	I9	*trans*	*FABP4*
16	CAPN14	I9	*trans*	*FABP4*
17	CD248	I8	*trans*	*FABP4*
18	CD36			
19	CDC42BPG	I8	*trans*	*FABP4*
20	CDC42EP2	I8	*trans*	*FABP4*
21	CDC42EP3	I9	*trans*	*FABP4*
22	CDH6	I6	*trans*	*ACSM5*
23	CDHR1	I18	*trans*	*SLC27A4*
24	CENPA	I9	*trans*	*FABP4*
25	CEP135	I15	*trans*	*FADS2*
26	CHRM1	I8	*trans*	*FABP4*
27	CIB4	I9	*trans*	*FABP4*
28	CLOCK	I15	*trans*	*FADS2*
29	CPSF7	I8	*trans*	*FABP4*
30	CPT1A			
31	CRIM1	I9	*trans*	*FABP4*
32	CST6	I8	*trans*	*FABP4*
33	CTHRC1	I10	*trans*	*FABP4*
34	CTXN3	I1	*trans*	*ACSM5*
35	CUBN	I16	*trans*	*FADS2*
36	CYP2U1			
37	DAGLA	I8	*trans*	*FABP4*
38	DDB1	I8	*trans*	*FABP4*
39	DGAT1			
40	DGAT2			

ID	Target Name	Interval	*Cis/Trans*-eQTL	Associated Gene
41	*DLG2*	I17	*trans*	*SLC27A4*
42	*DNMT3A*	I9	*trans*	*FABP4*
43	*ECE1*	I14	*trans*	*FADS2*
44	*EHBP1*	I3	*trans*	*ACSM5*
45	*EHD3*	I9	*trans*	*FABP4*
46	*ELOVL5*			
47	*EMILIN1*	I9	*trans*	*FABP4*
48	*EML3*	I8	*trans*	*FABP4*
49	*EPAS1*	I4	*trans*	*ACSM5*
50	*EPC1*	I16	*trans*	*FADS2*
51	*EPHA8*	I14	*trans*	*FADS2*
52	*EPT1*	I9	*trans*	*FABP4*
53	*ESRRA*	I8	*trans*	*FABP4*
54	*FABP4*			
55	*FADS1*	I8	*trans*	*FABP4*
56	*FADS2*	I8.I13	*trans/cis*	*FABP4/FADS2*
57	*FADS3*	I8	*trans*	*FABP4*
58	*FAM179A*	I9	*trans*	*FABP4*
59	*FKBP2*	I8	*trans*	*FABP4*
60	*FLRT1*	I8	*trans*	*FABP4*
61	*FNDC4*	I9	*trans*	*FABP4*
62	*FOSL1*	I8	*trans*	*FABP4*
63	*FOSL2*	I9	*trans*	*FABP4*
64	*FRMD8*	I8	*trans*	*FABP4*
65	*GAL3ST3*	I8	*trans*	*FABP4*
66	*GALNT14*	I9	*trans*	*FABP4*
67	*GCKR*	I9	*trans*	*FABP4*
68	*GGA2*	I5	*trans*	*ACSM5*
69	*GPR52*	I12	*trans*	*FABP4*
70	*GRID1*	I18	*trans*	*SLC27A4*
71	*HADHA*	I9	*trans*	*FABP4*
72	*HSPG2*	I14	*trans*	*FADS2*
73	*IGFBP7*	I15	*trans*	*FADS2*
74	*KCNH8*	I7	*trans*	*ELOVL6*
75	*KHK*	I9	*trans*	*FABP4*
76	*KIAA0040*	I12	*trans*	*FABP4*
77	*KIF5B*	I16	*trans*	*FADS2*
78	*KLC2*	I8	*trans*	*FABP4*
79	*KLF10*	I10	*trans*	*FABP4*
80	*LBH*	I9	*trans*	*FABP4*

ID	Target Name	Interval	*Cis/Trans*-eQTL	Associated Gene
81	*LCLAT1*	I9	*trans*	*FABP4*
82	*LIPC*			
83	*LMNB1*	I1	*trans*	*ACSM5*
84	*LPIN1*			
85	*LRRC10B*	I8	*trans*	*FABP4*
86	*LTBP1*	I9	*trans*	*FABP4*
87	*LTBP3*	I8	*trans*	*FABP4*
88	*LUZP1*	I14	*trans*	*FADS2*
89	*MACROD1*	I8	*trans*	*FABP4*
90	*MAP4K2*	I8	*trans*	*FABP4*
91	*MAPRE3*	I9	*trans*	*FABP4*
92	*MARCH3*	I1	*trans*	*ACSM5*
93	*MARK2*	I8	*trans*	*FABP4*
94	*MDH1*	I3	*trans*	*ACSM5*
95	*MEGF10*	I1	*trans*	*ACSM5*
96	*MGLL*			
97	*MIR194-2*	I8	*trans*	*FABP4*
98	*MLXIPL*			
99	*MOGAT1*	I19	*trans*	*SLC27A4*
100	*MRPL49*	I8	*trans*	*FABP4*
101	*NR1H3*			
102	*NRXN2*	I8	*trans*	*FABP4*
103	*NUDT22*	I8	*trans*	*FABP4*
104	*OVOL1*	I8	*trans*	*FABP4*
105	*PAPPA2*	I12	*trans*	*FABP4*
106	*PCNXL3*	I8	*trans*	*FABP4*
107	*PDZD2*	I6	*trans*	*ACSM5*
108	*PEX2*			
109	*PLA2G16*	I8	*trans*	*FABP4*
110	*PLAC9*	I18	*trans*	*SLC27A4*
111	*PLCB2*			
112	*PLCB3*	I8	*trans*	*FABP4*
113	*PNPLA2*			
114	*POU2F1*			
115	*PPARA*			
116	*PPARG*			
117	*PPIF*	I18	*trans*	*SLC27A4*
118	*PPM1B*	I4	*trans*	*ACSM5*
119	*PPP1R14B*	I8	*trans*	*FABP4*
120	*PRKCE*	I4	*trans*	*ACSM5*

ID	Target Name	Interval	*Cis/Trans*-eQTL	Associated Gene
121	*PRKD3*	I9	*trans*	*FABP4*
122	*PRRC1*	I1	*trans*	*ACSM5*
123	*PYGM*	I8	*trans*	*FABP4*
124	*RAB30*	I17	*trans*	*SLC27A4*
125	*RAB3IL1*	I8	*trans*	*FABP4*
126	*RABGAP1L*	I12	*trans*	*FABP4*
127	*RASGRP2*	I8	*trans*	*FABP4*
128	*RASGRP3*	I9	*trans*	*FABP4*
129	*RBP4*			
130	*RCOR2*	I8	*trans*	*FABP4*
131	*REST*	I15	*trans*	*FADS2*
132	*RHOQ*	I4	*trans*	*ACSM5*
133	*RIMS2*	I10	*trans*	*FABP4*
134	*RTN3*	I8	*trans*	*FABP4*
135	*RXRG*			
136	*SATB1*	I7	*trans*	*ELOVL6*
137	*SCD*			
138	*SF3B2*	I8	*trans*	*FABP4*
139	*SH2D4B*	I18	*trans*	*SLC27A4*
140	*SLC22A11*	I8	*trans*	*FABP4*
141	*SLC22A12*	I8	*trans*	*FABP4*
142	*SLC25A45*	I8	*trans*	*FABP4*
143	*SLC27A1*			
144	*SLC27A4*			
145	*SLC5A6*	I9	*trans*	*FABP4*
146	*SNX15*	I8	*trans*	*FABP4*
147	*SNX17*	I9	*trans*	*FABP4*
148	*SREBF1*			
149	*STRN*	I9	*trans*	*FABP4*
150	*SYT7*	I8	*trans*	*FABP4*
151	*TAF6L*	I8	*trans*	*FABP4*
152	*TCF23*	I9	*trans*	*FABP4*
153	*TMEM138*	I8	*trans*	*FABP4*
154	*TMEM165*	I15	*trans*	*FADS2*
155	*TNN*	I12	*trans*	*FABP4*
156	*TNR*	I12	*trans*	*FABP4*
157	*TRPT1*	I8	*trans*	*FABP4*
158	*TSPAN14*	I18	*trans*	*SLC27A4*
159	*TUT1*	I8	*trans*	*FABP4*
160	*UBR5*	I10	*trans*	*FABP4*

ID	Target Name	Interval	*Cis/Trans*-eQTL	Associated Gene
161	*VIT*	I9	*trans*	*FABP4*
162	*VWCE*	I8	*trans*	*FABP4*
163	*XDH*	I9	*trans*	*FABP4*
164	*ZBTB40*	I14	*trans*	*FADS2*
165	*ZEB1*	I16	*trans*	*FADS2*
166	*ZMIZ1*	I18	*trans*	*SLC27A4*
167	*ZNF438*	I16	*trans*	*FADS2*

Paper III. Table S10: Correlations of *PPARG* mRNA expression and analyze-related genes.

Gene	Correlation	*p*-value
ACSM5	0.08	3.86E-01
ADIPOQ	0.66	1.78E-15
AGPAT2	0.54	6.98E-10
ANK2	0.27	3.93E-03
ARNT	0.30	1.42E-03
CD36	0.70	2.22E-16
CPT1A	0.03	7.33E-01
CROT	0.50	1.71E-08
CYP2U1	0.54	6.01E-10
DGAT1	0.62	2.53E-13
DGAT2	0.61	1.09E-12
EGF	0.08	4.00E-01
ELOVL5	0.75	2.22E-16
ELOVL6	0.68	2.22E-16
ESRRA	0.43	2.41E-06
FABP4	0.51	9.27E-09
FABP5	0.40	1.27E-05
FADS1	0.12	1.95E-01
FADS2	0.18	5.92E-02
FADS3	0.17	7.71E-02
LIPC	0.27	3.55E-03
LPIN1	0.69	2.22E-16
MGLL	0.43	1.90E-06
MLXIPL	0.61	5.55E-13
NFKB1	0.58	2.49E-11
NR1H3	0.56	1.56E-10
PEX2	0.60	1.69E-12
PLA2G12A	0.61	9.13E-13
PLCB2	0.13	1.71E-01
PLPP1	0.27	4.16E-03
PNPLA2	0.55	3.09E-10
POU2F1	0.25	7.75E-03
PPARA	0.63	1.01E-13
PPARD	0.48	8.61E-08
RBP4	0.36	1.11E-04
RXRG	0.41	7.83E-06
SCAP	0.45	4.59E-07
SCD	0.59	1.01E-11
SLC27A1	0.23	1.23E-02
SLC27A4	0.23	1.60E-02
SREBF1	0.55	2.63E-10
USF1	0.33	4.15E-04

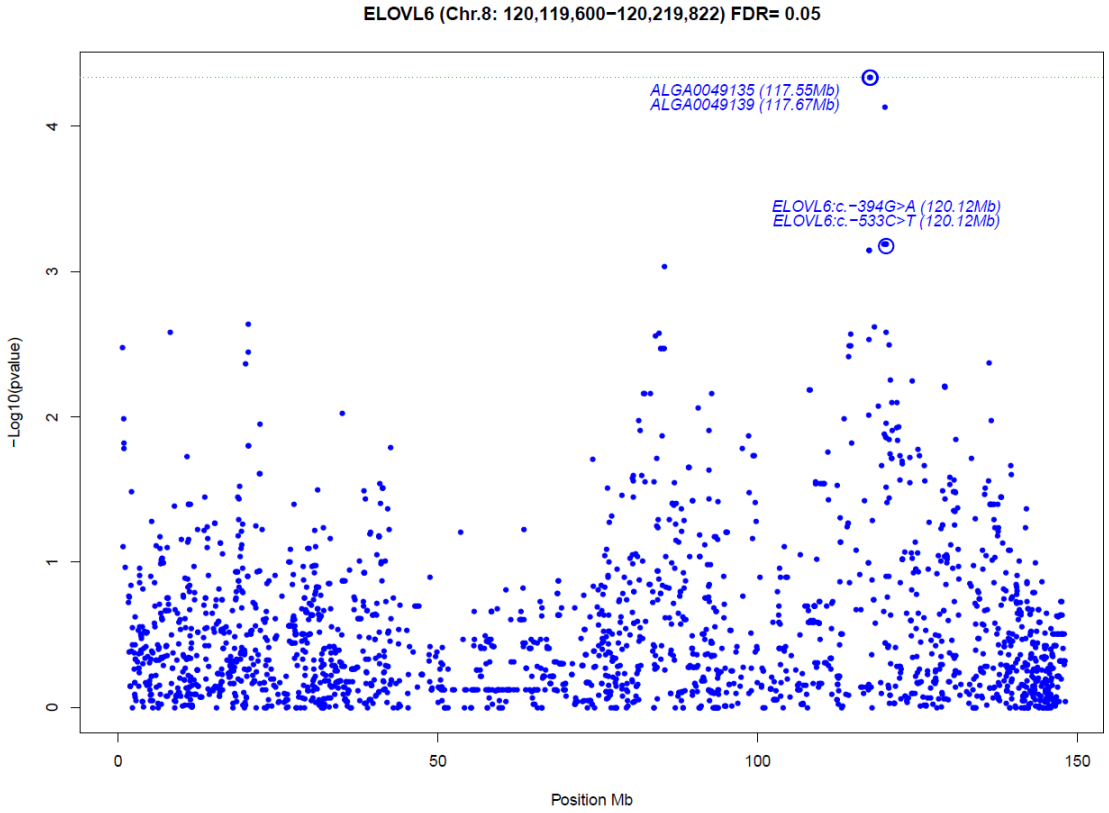

Paper III. Figure S1: Associations of SNPs from SSC8 and *ELOVL6* polymorphisms for *ELOVL6* gene-expression in backfat. The X-axis represents positions of SSC8 in Mb relative to *Sscrofa10.2* assembly of the pig genome and the Y-axis shows the –log10 (*p*-value). Horizontal dashed lines indicate the chromosome significance level.

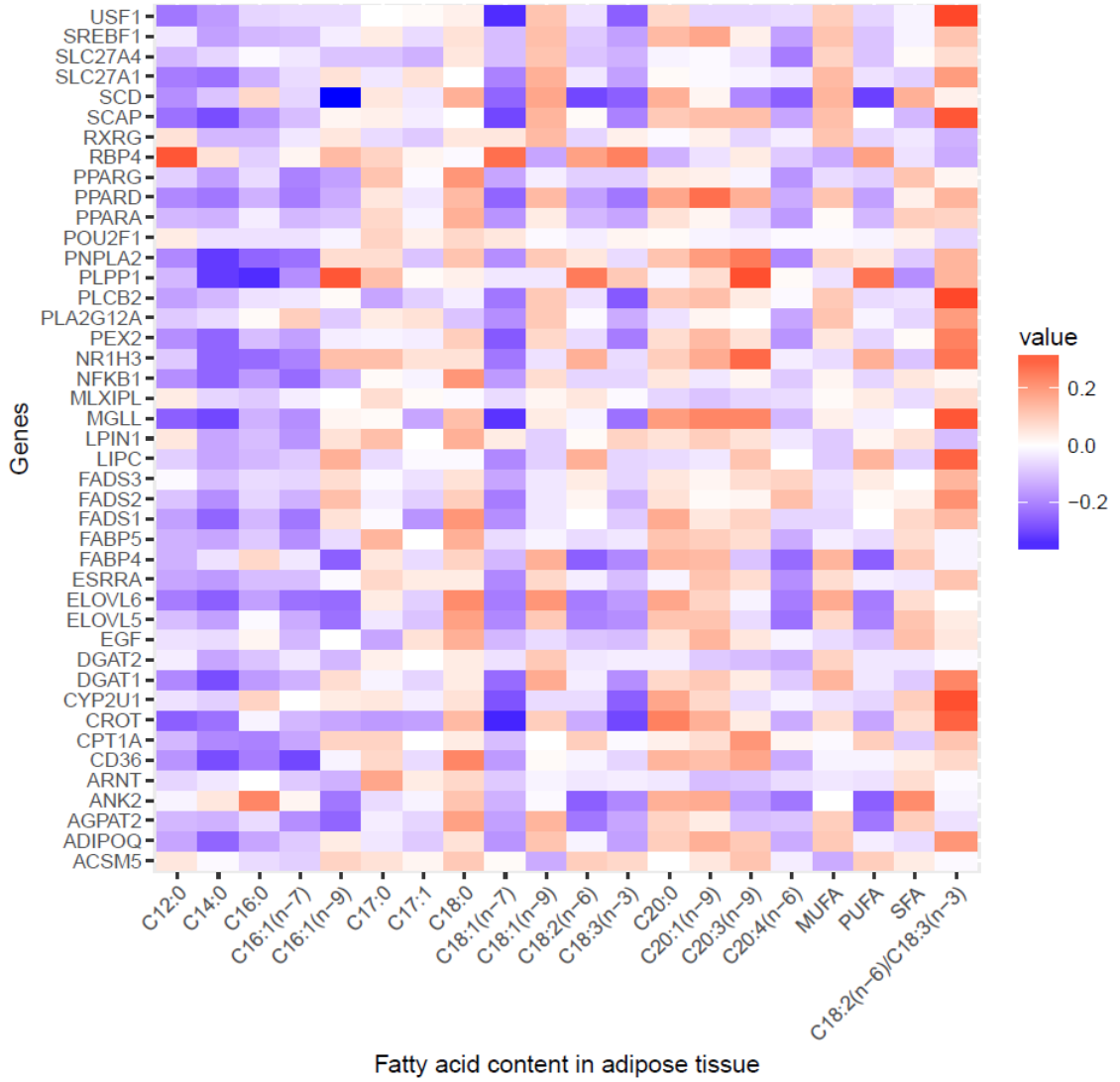

Paper III. Figure S2: Clustered heat map to visualize correlations among gene-expression levels (NQ) of the 43 genes and fatty content in adipose tissue. Color legend was adjusted to minimal and maximal values to differentiate the differences.

Acknowledgements

Chapter 8

Suele decirse que ningún éxito sabe mejor que el que viene de nuestros esfuerzos y determinación. Esta tesis doctoral, si bien ha requerido de esfuerzo y dedicación, no hubiese sido posible su finalización sin la cooperación desinteresada de todas y cada una de las personas que me han acompañado a lo largo de estos años y a las que me gustaría mostrar mi más profundo y sincero agradecimiento.

En primer lugar agradecer a la *Universitat Autònoma de Barcelona* (UAB) y en especial al personal investigador del *Centre de Recerca en Agrigènomica* (CRAG), por abrirme las puertas y permitir iniciar mi formación investigadora.

Debo a su vez un especial agradecimiento a mi Director de Tesis, el **Dr. Josep M Folch** por su generosidad al brindarme la oportunidad de recurrir a su capacidad y experiencia científica en un marco de confianza, afecto y amistad, fundamentales para la concreción de este proyecto.

Del mismo modo merece un agradecimiento especial mi Directora de Tesis, la **Dra. Maria Ballester** quien me guió por la ruta de la genética molecular y el mejoramiento genético, quien siempre estuvo allí a la hora de cualquier duda y asesoramiento en aspectos moleculares. Por su generosidad en la explicación y valiosos comentarios realizados en todo el proceso de elaboración del trabajo y sus atinadas correcciones. Sin la cual la elaboración de este proyecto no hubiera sido viable.

Quiero agradecer a mis compañeros de proyecto. Tanto los que marcharon y marcaron el camino a seguir, como los que continúan. **Dr. Yuliaxis Ramayo**, por su presencia incondicional, quien nos enseñó que no es incompatible el éxito profesional con la honestidad, pocas personas conozco con tanto amor a su profesión como la que él irradia. **Dr. Jordi Corominas**, por sus apreciados y relevantes comentarios, y por su enorme sensatez. **Dra. Anna Puig**, ejemplo de entrega y sacrificio, cada día compartido a su lado era un aprendizaje continuo en un entorno de diversión, le debo mucho. **Daniel Crespo**, por su predisposición y generosidad. **Lourdes Criado**, por su tiempo. Y a aquellos que aunque su paso fuese más o menos breve, dejaron gratos recuerdos: **Jorge Petroli**, **Ediane Paludo**, **Natalia Blay**, **Eduardo Sambache**, **Odei Barreñada**, **Iván Martos**, **Wiktoria Torbé** y **Roi Rodríguez**.

A los investigadores que forman parte de la *Unidad de Genómica animal* del CRAG, **Dr. Alex Clop** por los constantes ánimos, **Dr. Armand Sánchez** por su capacidad de liderazgo, **Dr. Marcel Amills** por las tan amenas conversaciones mantenidas, **Dr. Miguel Pérez-Enciso**

por compartir afición más allá de la científica, y **Dr. Sebastián Ramos** por sus constantes y divertidas visitas al despacho. A todos vosotros gracias por compartir la vocación de la docencia y sobre todo de la investigación, tan poco valorada a veces.

A todos y cada uno de los compañeros de trabajo con los que he compartido vivencias en el CRAG durante estos años. Al **Dr. Rayner González**, por haber crecido profesionalmente a mi lado y por todas las reflexiones compartidas. A **Marta Gòdia**, porque cualquier línea está de más si se trata de agradecer todo el apoyo y cariño recibido. A la **Dra. Antonia Noce**, por su carisma especial y sonrisa contagiosa. A la **Dra. Erica Bianco**, por su disposición de brindar ayuda espontáneamente. A la **Dra. Sarai Córdoba**, por su constante espíritu servicial. A la **Dra. Arianna Manunza**, por su responsabilidad. A la **Dra. Verónica Martínez**, por su versatilidad. Al **Dr. Oriol Tiomoneda**, por los momentos compartidos. A **Paulina García**, por enseñarnos que en viajar reside la auténtica riqueza. A la **Dra. Fabiana Quoos**, por su pasión y alegría. A **Julieta Nafissi**, por contagiar su optimismo. A **Tainã Cardoso**, por su simpatía. A **Jordi Leno**, por contribuir en la "cultureta general" que tango nos gusta. A **Joan Jené**, por su discreción y sencillez. A **Emilio Mármol**, por liderar las riendas burocráticas del centro. A la **Dra. Sara Guirao**, por su entusiasmo en el trabajo. A la **Dra. Natalia Forneris**, por enseñarnos las costumbres argentinas. A **Lino César**, por enseñarnos que con un poco de tereré todo es más sencillo. A **Betlem Cabrera**, por su permanente disposición y desinteresada ayuda. A la **Dra. Maria Corujo** y **Sara Martínez**, por nuestras charlas científicas y no tan científicas. A los compañeros con los que he compartido despacho, **Dra. Cèlia Guiu**, **Dra. María Urrutia**, **Dr. Pablo Ríos**, **Yu Zhang**, **Elena Navas**, **Pol Rey**, por todos los momentos vividos.

Así como a los compañeros de la *Facultat de Veterinària* de la UAB. Al **Dr. Joaquim Casellas**, por compartir su visión de la ciencia. A la **Dra. Olga Francino**, por su profesionalidad. A la **Dr. Natàlia Sastre**, por su vitalidad. Al **Dr. David Gallardo**, por aportarnos su constante visión comercial. A **Anna Cuscó**, por hacer que los seguimientos valgan la pena. A **Sara d'Andreano**, por los ánimos aportados.

A las **Dra. Anna Castelló** y **Dra. Anna Mercadé** por siempre haber sido un ejemplo a la ética, profesionalismo y por su continuo asesoramiento.

A **Julia Lacuesta** y **Tania Guil** por vuestra implicación y complicidad.

Todos ellos han conseguido crear un ambiente de trabajo excepcional.

Thanks to all the people of the *Génétique Animale et Biologie Intégrative* department (GABI) at *Institut National de la Recherche Agronomique* (INRA), who hosted me during my stay in France. In particular I thank to **Dr. Andrea Rau** for giving me the opportunity to work with her. I am grateful for her patience, support and helpful suggestions. Thanks to **Dr. Dominique Rocha** for his enthusiastic support. Thanks to **Clémentine Escouflaire**, **Dr. David Pérez**, **Dr. Hector Argüello**, **Dr. Marco Moroldo**, **Maurice Konkobo**, **Michiel Van Niekerk**, **Dr. Núria Mach**, **Rabia Letaief**, **Dr. Rebeca Martin**, **Dr. Parsaoran Silalahi**, **Dr. Yoel Rodríguez**, and the rest of the group for letting me feel at home during my stay. I also would like to thank the **Thaon family** for their hospitality and friendship.

Agradecimiento especial merece el **Dr. Jordi Estellé**, por el aprendizaje y el crecimiento profesional y personal que he tenido la oportunidad de desarrollar a su lado, y por toda la confianza depositada.

A todo el grupo de *Mejora Genética Animal* del *Instituto Nacional de Investigación y Tecnología Agraria y Alimentaria* (INIA) de Madrid con el que he tenido la oportunidad de colaborar durante estos años. **Dra. Ana I Fernández**, **Dr. Luis Silió**, **Dra. Carmen Rodríguez**, **Dra. Cristina Óvilo**, **Dra. Estefania Alves**, **Dra. María Muñoz**, **Dra. Almudena Fernández**, **Ángel Martínez** y **Rita Benítez**.

A todos los profesores de la *Universidad de Extremadura* (UNEX), de los cuales he aprendido mi profesión y a los que les debo bastante de mi recorrido académico y profesional. Merecen un reconocimiento especial la **Dra. Araceli Rabasco**, la **Dra. Margarita Martínez** y la **Dra. Esther Sansinforiano**, quienes despertaron mi interés hacia la genética.

A todos los profesores que he tenido a lo largo de mi vida académica, por su dedicación, entrega y transmisión de conocimientos.

A mis compañeros de Máster, de los cuales me llevo gratas experiencias, en especial a vosotros **Marcia Ferraz**, la **Dra. Marina Martínez** y **Ximena Quintero**.

A mi familia en Barcelona, quienes han compartido conmigo los "ires y venires" en el plano personal durante estos años en la ciudad Condal. Por los buenos momentos vividos en Aribau: **Dr. Javier Arranz**, **Dr. Luis Manuel Molinos** y **Marta Fernández**. Y las risas de Balmes: **Dra. Laura Pérez**, **Juan Azcárate**, **Dr. Sebastián Agramunt**, **Anna Jané**, **Laia Quintá**, **Selma Casals, Pablo Mediavilla**, **Irean Navas** y **Alba Soler**. Por nuestras

peculiares jornadas gastronómicas: **Dr. Álvaro Hernáez**, **Laura Mariño**, **Dr. Pablo Pérez**, **Paula Santa Barbara** y **Ricardo Moure**. Sin olvidar también los días de vermut que tantos momentos de felicidad nos han aportado: **Albert Viel**, **Ananda Marina**, **Biotza del Campo**, **Cristian Casorrán**, **Leonor Ayala**, **Marta Valle**, **Sara Sarroca** y **Dr. Xavier Roa**.

Tampoco puedo olvidarme de esos amigos con los que tanto he compartido y tantos años han estado apoyando cada una de mis decisiones. Los amigos: una familia cuyos individuos se eligen a voluntad. Los que aprendimos a andar juntos: **Javier García**, **Jose Antonio Parra** y **Luis Gómez**. Los que me enseñasteis que cualquier persona que te motiva a ser mejor, es alguien a quien merece la pena mantener cerca: **Adrián de Dios**, **Álvaro del Castillo**, **Álvaro García**, **Ignacio Benito**, **Jaime de la Cuesta**, **Jose M Benito**, **Julio Pérez-Tabernero**, **Marcos Areces** y **Michel Rodilla.** A los compañeros de carrera que continúan demostrando que son amigos para siempre: **Álvaro García**, **Beatriz Bigeriego**, **Francisco Fernández**, **Javier García**, **José Vaquero**, **Lope Sánchez**, **Manuel Romero**, **María Suárez** y **Tamara Matos**.

Al *Club Ciclista Gràcia* (CCG) por enseñarme que sólo aquellos que arriesgan con ir más lejos pueden descubrir lo lejos que son capaces de llegar. Reconocimiento especial merecen la **familia Domènech**, **Eloi Cuevas**, **Joan Coromina**, **LLuìs Martí**, **Miguel Chiva** y **Pedro Toledo**.

A mis padres, **Manuel** y **Asunción**, porque todo lo que soy se lo debo a ellos. Gracias por vuestras enseñanzas, por ser un ejemplo, por creer en mí, por apoyarme, por estar siempre a mí lado, por comprenderme, y sobretodo, gracias por brindarme todo vuestro amor y por otorgarme mi educación, la mejor herencia que todo hijo pueda recibir. A mi hermana, **Cristina**, por ser un ejemplo de valentía, capacidad y superación; el espejo donde mirarme, el ejemplo a seguir. ¡Os quiero!

A las personas que, aunque no aparecen aquí con nombres y apellidos, han estado presentes durante el desarrollo de este trabajo y han hecho posible que hoy vea la luz.

A todos vosotros os podría seguir dedicando bonitas palabras que al leerlas os llenasen de emoción. Pero considero que lo más gratificante es dedicar tiempo, eso sí que es un bonito regalo. Y con todos vosotros he compartido mucho de este último.

A todos mi eterno agradecimiento.